Modelling of batch dextransucrase production

MODELLING OF BATCH DEXTRANSUCRASE PRODUCTION

by

Yuzhao Lü

A Doctoral Thesis

Submitted in partial fulfilment of the requirements

for the award of

Dotor of Philosophy of the Loughborough University of Technology

March 1989

To my parents

To my motherland

ACKNOWLEDGEMENTS

I would like to express sincere thanks and appreciation to my supervisor Dr. D. W. Drott for his valuable guidance and discussions throughout the course of this study. I am also most grateful to his encouragement, inspiration, careful reading of the draft and helpful comments.

During this work I am deeply indebted to the staff and my colleagues in the Chemical Engineering Department of Loughborough University of Technology for their kindly help and encouragement, in particular to Professor J. Mann and Dr. R. B. Wilcokson for their understanding and support, and also to Mr. D. L. Smith, Mr. A. Milne, Ms. A. Mendoza, Mr. T. M. Neale, Mr. H. Clayton and Mr. G. Boyden for technical assistance.

Thanks are due also to Dr. P. D. G. Wilson of AFRC Food Research Institute, Norwich, for making available of his computer program which performs data transformations.

This work is sponsored in part by a studentship from the Technical Co-operation Training Department of the British Council. I wish to express my special thanks to Mr. S. S. Dhillon of the British Council Regional Office for his help.

Finally, I would like to extend my heartfelt gratitude to all friends for their help during my stay in Loughborough.

CONTENTS

INDEX TO FIGURES

INDEX TO TABLES

INDEX TO PLATES

Chapter 1 Introduction

Biotechnology is undoubtedly emerging as one of the rapidly developing areas of major importance in science and technology and will certainly benefit us in the future. Progress in this area has already had a great impact on human activity in recent years. Remarkable achievements have been accomplished in industrial scale production of insulin, vaccines and growth hormones.

Biotechnology is a comprehensive interdisciplinary field involving at least microbiology, biochemistry and engineering. It spans fields from basic concepts to practical industrial applications, from enzyme production to waste water treatment, energy production, oil recovery and nitrogen fixation. The scientific basis of biotechnology is microbiology which is the study of living microorganisms. Although the ubiquitous microbe has a longstanding relationship with mankind (e.g. in wine-making process, preparation of bread, cheese and soy, and as the cause of many human diseases), it was not until the end of last century, that the work of Pasteur and Tyndall established the critical role of microorganisms in fermentation processes and initiated the emergence of microbiology as a science. Since then, new microbial processes were developed for production of ethanol, glycerol, and other important chemicals in the early 20th century.

Of the engineering disciplines concerned, there is no argument that the traditional chemical-engineering-based biochemical engineering is in a strong position to apply the new discoveries in biotechnology. In the 1940s complementary developments in biochemistry, microbial genetics and process engineering led to the production of penicillin and other antibiotics with immense relief of mankind's suffering. This was the beginning of biochemical engineering. The basic strategy of biochemical engineering is to

scale up biological processes to industrial dimensions by adapting methods of process and control engineering to biological processes. Further improvements involve design of new bioreactors, better techniques for measurement and process control and even optimization of the process.

In general, biological processes are unusually complicated in every aspect and general concepts and relationships are not readily perceived. To achieve the goal of optimization of a complex system such as biological process, it is crucial that our qualitative knowledge of the system is extended to quantitative mathematical representations. The more complex the system, the more necessary it becomes to resort to mathematical models. Mathematical models are of extreme importance in process engineering and will be widely utilized in biological systems.

Practical mathematical models deal with the mathematical relations among the measurable quantities associated with a process. Models initially serve to correlate data and so provide a concise way of characterizing the system. Apart from this, models can be used to predict quantitatively the performance of the system, thus reducing the amount of laborious experimental work in system design. Another use of mathematical models is to guide the design of experiments needed to determine important parameters and elucidate the nature of the system.

Depending upon the system being considered and the intended application, mathematical models can be expressed as simple algebraic equations or complex nonlinear differential equations or integrodifferential equations. For most biological processes, the mathematical models will often be extremely simplified and idealized, since even a single microorganism is a tremendously complicated system involving hundreds of enzymatically catalyzed reactions. Also simple models of biological systems can ease the task of implementing process control. This study attempts to build and make

use of simple mathematical models in predicting and simulating a fermentation process.

1.1 Modelling for Fermentation Processes

The development of a mathematical model involves many aspects of the process to be considered. The first important thing is to choose those quantities or variables of significance that reflect the state of the process and the purpose of the model. After this, the model can be formulated in accordance with existing knowledge and assumptions. Mathematical models for fermentation processes concerning microbial growth and product formation are generated in part by application of well-established physical, chemical and biological principles. The ubiquitous physical principles of conservation, thermodynamics and physiochemical constitutive principles are fundamental to any modelling process. Although some ecological and physiological principles describing the state of an organism and its interaction with the organism's environment have long been universally recognized in fermentation processes, these specific biological principles are often not incorporated in models explicitly because of substantial mathematical difficulties.

To construct a useful process model, some simplifying hypotheses or assumptions must be made. In a fermentation system, the growing individual microbial cells of a population are not only different in physiological and morphological states, i.e. different in structure, but also different in sizes and generation times. The model equations derived on the basis of such differences are most likely impractical in the sense that these equations require extensive numerical computation for their solutions, or even become mathematically intractable in some cases. Also these equations often require parameters which cannot be determined from overall system response. However, it is usually reasonable in fermentation processes to ignore all the

internal differences between individual organisms and regard them as an integral, structureless single entity of the system. In addition, microbial activities on the surface of the fermentation vessel will be neglected. The fermentation broth is assumed to be perfectly mixed. Temperature, pressure, and other thermodynamic variables are usually considered to be time-independent and uniform throughout the culture. The process equations based on such assumptions will form an unsegregated, unstructured deterministic model.

Although a mathematical model can never be definitely proved to be the one which describes the system, the model must be subjected to experimental testing. Clearly, any mathematical model of a fermentation process contains physical or biological parameters with unknown numerical values. These parameters should be able to be evaluated by fitting the model's prediction to experimental data. As a result, the model must be rejected or modified if it does not reproduce the experimental data or if the estimated parameters have unreasonable values. It is important to note in the testing process the model should be applied to more than one case. If a good fit to other data from independent experiments is obtained using the same set of parameters, confidence in the model is improved.

1.2 Objective of the Study

Because of the obvious importance of mathematical models in the application of process and control engineering principles, it is important to develop mathematical models of industrial fermentation processes. This study concerns an industrial enzyme-producing fermentation process. The bacterium *Leuconostoc mesenteroides* grows in a sucrose-containing medium to produce dextransucrase, an extracellular enzyme used to convert sucrose to dextran. This microbially produced biopolymer has unique properties of medicinal use.

Although the industrial fermentation process for producing dextransucrase has been used for a long time, very little is known about the kinetics of microbial growth and enzyme-formation kinetics. This study first looks at cell growth under aerobic conditions on a medium similar to that employed in an industrial procedure which is claimed to be optimum for enzyme production. A series of experiments to determine the initial growth rate are carried out. From the results obtained, it is found that the growth of the organism follows the Monod kinetics. The parameters in the model (i.e. maximum specific growth rate and saturation coefficient) are estimated by the nonlinear curve fitting method implemented in a computer program. The data transformation method developed for evaluating these parameters is also used in determination of such constants. The significance of the parameters obtained is discussed. Some of the experiments are then repeated in order to test the validity of the model.

Oxygen plays an important role in aerobic cell metabolism. It could be the substrate which limits cell growth other than the carbon source, or both substrates are limiting the growth simultaneously. Three experiments are performed to investigate the dynamic effect of oxygen on cell growth. The effect is quantified by determining the saturation coefficient for oxygen in an

extension of the Monod model. Computer simulations are used throughout these analyses.

The ultimate objective of this study is to develop a model describing enzyme production accompanied by cell growth. Several enzyme-producing experiments are carried out to examine the kinetics of enzyme biosynthesis. On the basis of these experimental results and data presented in the literature, a simple relationship between the enzyme concentration (enzyme activity) and cell growth is proposed.

As a final testing and an application of the model, it is used to simulate a fed-batch procedure for enzyme production. The model's predictions are compared with experimental results. The implications of the differences between the model prediction and the experimental data are discussed.

All the necessary experiments are carried out on a bench-top fermentation system using a microcomputer for the control of temperature, pH and other environmental variables. The system is modified to meet the needs of some experiments.

Chapter 2 Literature Review

Dextran is the collective name of a large class of hydrocolloid homopolysaccharides composed almost exclusively of the monomeric unit α-D-glucopyranose linked mainly by 1-6 bonds. The term "dextran" was first used by Scheibler in 1874 when he found that the mysterious thickening or solidification of cane and beet sugar juices was caused by a glucan having positive optical rotation and noticed that this material was closely related to starch and dextrin. Previously Pasteur in 1861 explained that these viscous slimes resulted from microbial action. In 1878, Van Tieghem named the causative bacteria *Leuconostoc mesenteroides* because its growth in colourless flocs resembled that of the green algae of the genus Nostoc.

Most of the work with dextran has been conducted with various strains of *Leuconostoc mesenteroides* and in particular the strain NRRL B-512F first isolated at the Northern Regional Research Laboratory (currently N.R.R.C., Peoria, Ill., U.S.). This strain produces a dextran containing 95% 1,6- and 5% 1,3- α-D-glucopyranosidic linkage (Robyt *et al.*, 1974) and is the main strain in common use for commercial dextran production. The reason for the choice of this strain is related to the use of dextran as a blood plasma extender. Extensive trials conducted in the U.S.A. demonstrated that the dextran from this strain of *L. mesenteroides* caused fewer antigenic reactions than other strains. Other reasons for the commercial production of dextran from *L. mesenteroides* NRRL B-512F are that it excretes relatively large amounts of the enzyme dextransucrase into the fermentation medium, produces a minimum number and quantity of contaminating enzymes (i.e. invertase and levensucrase) and it forms a high-molecular weight, soluble dextran (Jeanes, 1966, 1977).

2.1 Dextran Production and Application

The literature relating to dextran and its production is well documented in a number of reviews (Neely, 1960; Jeanes, 1966; Murphy & Whistler, 1973; Alsop, 1983).

Two basic methods have been employed in commercial dextran production, a whole-cell method and an enzymic method. In both cases, the dextran is formed by the polymerization of the glucose moiety of sucrose with the resulting liberation of fructose. This polymerization is catalyzed by the enzyme dextransucrase, produced by *L. mesenteroides*. However, the primary product is usually native or high-molecular-weight dextran. The low-molecular-weight pharmaceutical dextran is then conventionally produced by hydrolysis or solvent fractionation procedures using native dextran.

In the whole-cell method, the bacteria are grown in a medium containing excess sucrose and limited other nutrients, and release the enzyme into the culture broth. Near the end of the growth phase, the conditions are altered to favour polymerization. The excess sucrose is converted to dextran, which is extracted by subsequent processing.

In the enzymic method, the cells are grown in a balanced medium to produce the enzyme. The enzyme-containing fermentation broth is then separated from the cells and the filtrate is used to polymerize a sucrose solution to dextran.

As stated by Jeanes (1965), enzymic synthesis of dextran has the following advantages : better control of the product produced, more uniform and purer product. There is therefore an economic advantage in synthesis of dextran by this method.

For more than a century, dextran was known mainly as industrial nuisances and laboratory curiosities. In recent times, dextran has become the first microbial polysaccharide to be produced and extensively used on the industrial scale. Dextran produced by *Leuconostoc mesenteroides* has found use as a blood volume extender and a blood flow improver because of its biological role of a protective coat against predators. Other uses are the manufacture of molecular seives, iron-dextran complexes for treatment of iron deficiency anaemia, production of photographic film, water-loss inhibitors in oil-well drilling muds and food use.

2.2 Cultural Characteristics of *Leuconostoc mesenteroides*

2.2.1 The Organism

Leuconostoc mesenteroides NRRL B-512F (or NCDO 553 or NCIB 8710) belongs to the genus *Leuconostoc*, tribe *Streptococceae* of the family *Lactobacillaceae*. The cells may be spherical but often lenticular in shape, and typically 0.5 - 0.7 by 0.7 - 1.2 microns in size. The cells usually occur in pairs or short chains. The colonies formed on sucrose agar are small, usually less than 1 mm in diameter, smooth, round and greyish white. The cells are Gram positive facultative anaerobes, are non-motile and do not form spores. Strains of *Leuconostoc. mesenteroides* are non-pathogenic non-proteolytic chemoheterotrophs which require rich media for growth. The growth factors include nicotinic acid, thiamine, pantothenic acid and biotin. The amino acids, valine and glutamic acid are also required for growth.

Growth is dependent on the presence of a suitable carbohydrate such as glucose which is metabolized in the Pentose Phosphoketolase Pathway yielding 1 mole each of lactic acid, carbon dioxide and ethanol. This strain also has an aerobic oxidative metabolism using 1 mole oxygen/mole glucose and yielding equimolar quantities of carbon dioxide, lactate and acetate. This strain also has peroxidase activity (Bergey, 1974).

2.2.2 The Effect of Nutrient Type and Concentration on Growth

The growth medium is formulated to supply the nutritional needs for the organism to support growth and product synthesis. Nutrients should therefore, be supplied in sufficient quantities and proper proportions in the fermentation medium for energy, product formation and cell maintenance

during growth. The nutritional requirements for *Leuconostoc mesenteroides* thus consist of substrate providing energy and structural elements and those minor growth factors.

2.2.2.1 Carbon Sources

Leuconostoc mesenteroides will utilize a large number of carbohydrates. Acetate, lactate and tartrate are not used as sole sources of carbon for growth (Bergey, 1974). However, sucrose seems to be the only suitable carbohydrate inducer for the production of enzyme and dextran. Several of the sugars were poor carbon sources and growth was consequently slow.

In the whole-cell process for the production of dextran, high concentrations of sucrose are used. It was noted that high sucrose concentration in a batch fermentation inhibited the growth of the organism. Experiments were carried out using different initial concentrations of sucrose to observe the effects on the growth of the organism in batch cultures (Hollo & Laszlo, 1971). The results are shown in Figure 2.1.

Fermentation medium used in these experiments :

Peptone	1 %
KCl	0.1 %
Na_2HPO_4	0.55 %
Na_3PO_4	0.075 %
Yeast Extract	0.33 %
Sucrose	variable

Growth was determined by optical density
Temperature : 28 °C
Initial pH : not given
Not aerated

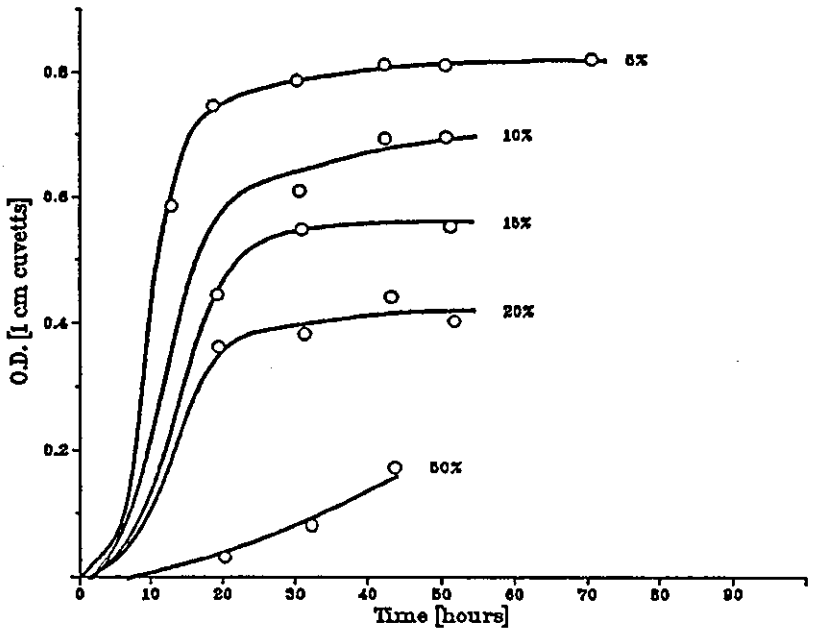

Fig. 2.1 Growth of *L. mesenteroides* on Sucrose (Hollo & Laszlo , 1971)

The figure clearly proves that both the growth rate and the attainable maximum of microbial growth depend mainly on the sucrose concentration, optima being at 5% sucrose concentration. Accordingly, the relative rate of dextran formation is the greatest at this concentration.

2.2.2.2 Nitrogen and Other Nutrient Sources

2.2.2.2.1 Nitrogen

Since nitrogen constitutes about 7.5% of the dry weight of bacterial cells it is an important constituent of any growth medium. The main nitrogen sources used in the growth of *L. mesenteroides* are corn-steep liquor (CSL) or yeast extract. These complex nitrogen sources provide amino acids and biotin described before. The bacteria are non-proteolytic and do not reduce nitrogen (Bergey, 1974). *L. mesenteroides* requirements of nitrogen and

other related nutrients for the production of dextransucrase are higher than those needed in the whole-cell process for the production of dextran. Only 0.25 per cent corn-steep liquor solids sufficed for the whole-cell process compared with 2.0 per cent required for the production of dextransucrase (Jeanes, 1966). Higher concentrations of nitrogen only result in increased growth and enzyme production rates when high levels of phosphate are also present in the fermentation medium (Tsuchiya *et al.*, 1952).

2.2.2.2.2 Phosphate

The main sources of phosphate for both dextran formation and production of dextransucrase are the inorganic salts K_2HPO_4 and KH_2PO_4.

Some experiments were carried out to find the effect of phosphate concentration on dextransucrase production by Tsuchiya *et al.* (1952). It was discovered that production of dextransucrase was optimal at 3.5% phosphate, but on increasing the concentration of the nitrogen source, as corn-steep liquor, the phosphate concentration in the medium also has to be increased to gain any beneficial effects in dextransucrase yields. The possibility that phosphate concentration may be having a direct influence on the growth and enzyme production of the organism has not been considered.

2.2.2.2.3 Trace Elements

No major studies have, as yet, been carried out into the effects of trace elements on the growth and enzyme production of *L. mesenteroides* NRRL B-512F. It is possible that the elusive stimulatory factors in raw sugar and other similar substances could be trace elements (Whiteside-Carlson & Carlson, 1949).

The use of yeast extract or corn-steep liquor should supply all the

necessary trace elements for the growth and production of dextransucrase by the bacteria. However, in nearly all the fermentation media reported in the literature for the production of dextransucrase, a supplement of trace elements has been added. This supplement, however, is not used in the whole-cell process for the production of dextran.

This supplement was first used by Koepsell and Tsuchiya (1952) and termed R salts. It consists of a stock solution of salts prepared as follows :

$MgSO_4.7H_2O$	4.0 %
NaCl	0.2 %
$FeSO_4.7H_2O$	0.2 %
$MnSO_4.H_2O$	0.2 %

An amount of 0.5 per cent (by volume, i.e. 5 mL per litre of medium) R salts solution was used for each fermentation.

2.2.3 The Effect of Some Environmental Factors on Growth

2.2.3.1 pH

L. mesenteroides NRRL B-512F will initiate growth between pH 5.5 and pH 6.5 or greater. However, the cells can grow on a suitable medium with glucose as carbohydrate source at pH 4.5.

During the production of dextran from growing cultures of *Leuconostoc mesenteroides* B-512F the initial pH is 7.2 which on completion of dextran production becomes about 4.8. In the cell-free enzymic process, the initial pH is 7.0 to 7.2 which is allowed to decrease to pH 6.7 ± 0.1 at which point it is controlled by the addition of alkali (Jeanes, 1966). Sodium hydroxide or potassium hydroxide are recommended

for use in the control of pH. Ammonium hydroxide should not be used to control the pH because the ammonium ion exerts a detrimental effect on the organism and the formation of enzyme dextransucrase (Tsuchiya *et al.*, 1952).

2.2.3.2 Temperature

Temperature range for the growth of *L. mesenteroides* extends from 10 °C to 37 °C. Dextran formation from sucrose is favoured by a temperature of 20 to 25 °C (Bergey, 1974). The optimal temperature for the growth of this strain is stated by N.R.R.L. to be 30 °C.

2.2.3.3 Aeration

Leuconostoc mesenteroides B-512F is a facultative anaerobe, i.e. it can grow anaerobically or aerobically. Production of dextran using the whole-cell process does not require aeration although agitation is provided in large vessels to aid temperature control (Jeanes, 1966). The review by Foster (1968) also states that the aeration of the culture gives a lower yield of dextran.

It had been noticed as early as 1952 that enzyme yields were higher in shaken flasks than in still flasks (Koepsell & Tsuchiya, 1952; Tsuchiya *et al.*, 1952). No reasons have been given for an increase in the yield of dextransucrase due to aeration. The uptake of oxygen and the effect on growth have been investigated (Johnson & McCleskey, 1957; Neely & Nott, 1962). The results of these experiments show that aeration greatly increases the growth rate of *L. mesenteroides*. Experiments carried out by Battelle also indicate that the specific growth rate is dependent on the aeration conditions (Schneider *et al.*, 1980). The highest specific growth rate is obtained when the dissolved oxygen concentration is maintained at a high

constant level.

2.3 Metabolic Processes

Leuconostoc mesenteroides NRRL B-512F is a facultative anaerobe and can therefore carry out either of two metabolic processes, aerobic respiration or fermentation. A change-over from aerobiosis to anaeriosis usually incurs a reduction of the cell yield, the growth rate, the glucose uptake and is reflected in the type of fermentation end-products. This phenomenon is known as the "Pasteur Effect". (Barker *et al.*, 1964).

Leuconostoc mesenteroides breaks down one mole of glucose anaerobically to yield one mole each of D(-) lactic acid, ethanol and carbon dioxide. There are some strains which possess an aerobical oxidative metabolism using one mole of oxygen and one mole of glucose yielding equimolar quantities of carbon dioxide, lactate and acetate. These strains also have peroxidase activity (Bergey, 1974; Johnson & McCleskey, 1957).

L. mesenteroides B-512F is a member of the strains possessing this aerobic oxidative metabolism since it has been observed that they grow aerobically (Neely & Nott, 1962). Phosphoketolase has been shown to be present in *L. mesenteroides* as a constitutive enzyme. *L. mesenteroides* B-512F appears to metabolize glucose and other sugars via the Pentose Phosphoketolase Pathway (PK) which is outlined in the next section.

No information as to the biosynthesis of the dextransucrase molecule has been presented in the literature.

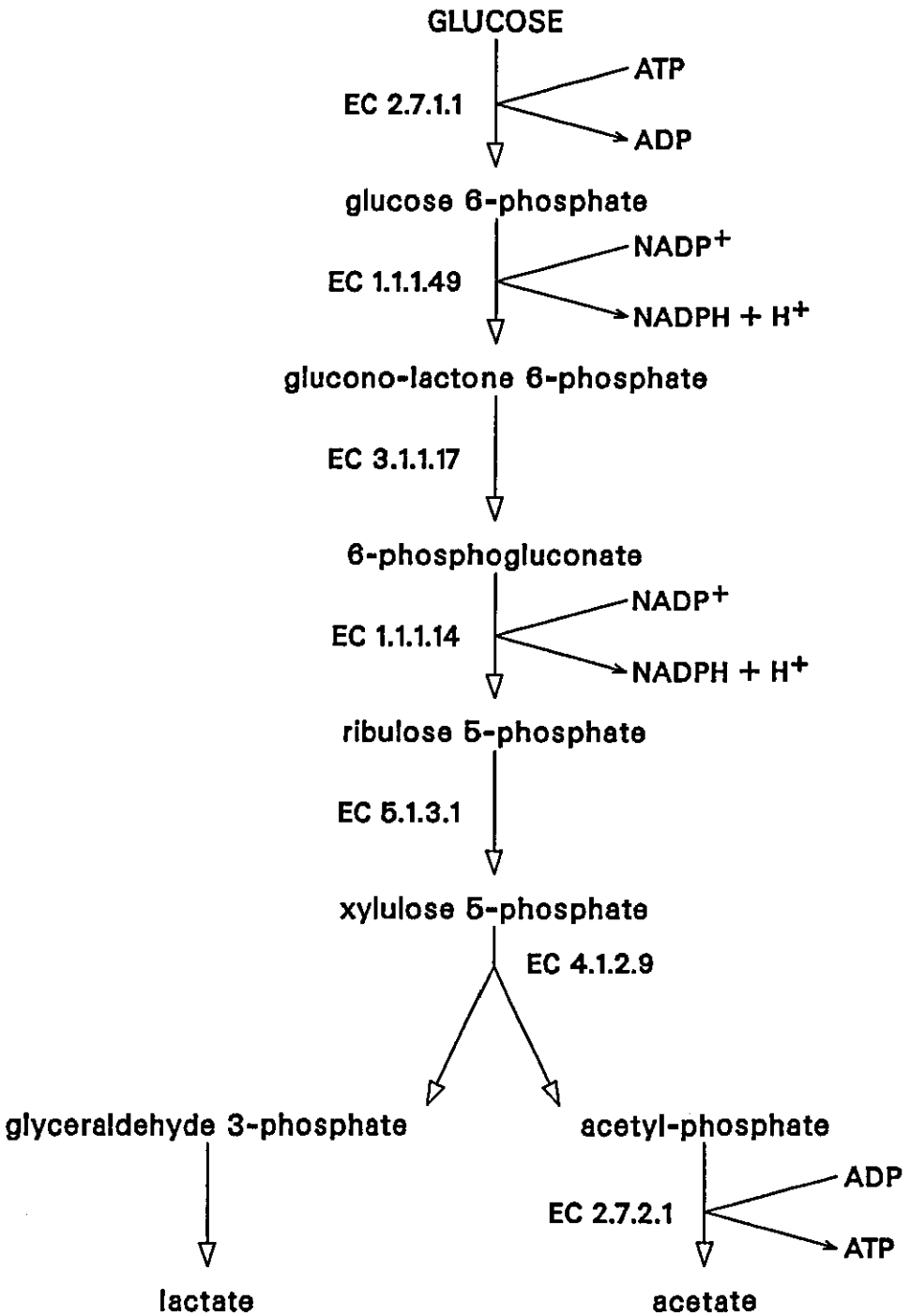

Figure 2.2 Schematic Representation of
the Phosphoketolase Pathway of Glucose Utilization

2.3.1 Carbohydrate Metabolism

Leuconostoc mesenteroides cannot utilize the EMP (Embden-Meyerhof-Parnas) pathway since it lacks the key enzyme fructose 1 - 6 diphosphate aldolase. The Pentose Phosphoketolase Pathway is possessed by only a small group of bacteria, the heterofermentative lactobacilli. The process produces only 1 mole of ATP/mole of glucose, as compared with the 2 mole of ATP/mole of glucose produced by the EMP pathway. This pathway can be regarded as a branch or a variation of the Hexose Monophosphate (HMP) or Warburg-Dickens pathway, as these bacteria lack the enzyme aldolase, which converts fructose 1,6-bisphosphate into the two triosephosphates, glyceraldehyde 3-phosphate and dihydroxyacetonephosphate, as well as the enzymes transaldolase and transketolase of the HMP pathway. The first three steps of glucose metabolism, oxidation of glucose including the decarboxylation of 6-phosphogluconate, are identical to the HMP pathway. The so formed ribulose 5-phosphate is isomerized to phosphate ester D-xylulose 5-phosphate which is then cleaved in a reaction requiring inorganic phosphate for the formation of the high energy phosphate compound, acetyl-phosphate. The second part of the xylulose 5-phosphate molecule forms glyceraldehyde 3-phosphate, which is further metabolized using the enzymes of the EMP pathway (Doelle, 1975, 1981). The schematic representation of this process is illustrated in Figure 2.2. This reaction has been shown to take place in *Leuconostoc mesenteroides* (Heath *et al.*, 1956).

If acetyl-phosphate is converted to ethanol, the high energy bond is lost and the net energy gain would be one mole of ATP (adenosine triphosphate) per mole of glucose. If, however, the conversion leads to acetate production by the enzyme acetokinase, the high energy bond is conserved and a net gain of two moles of ATP is the result, the same energy gain as in the EMP pathway.

According to Bergey (1974), acetate is formed when bacteria are grown aerobically, but there is no mention of a requirement of oxygen for this conversion to proceed. Rose (1976) also does not mention a requirement for oxygen, but acetyl-phosphate is reported to be converted to ethanol with no ATP gain. Although there appears to be no information in the literature on this topic, oxygen apparently induces the formation of acetate with a gain of one ATP molecule, whereas anaerobic metabolism converts acetyl phosphate to ethanol with no ATP gain. Therefore, aerobically grown *L. mesenteroides* would have gained two moles of ATP from one mole of glucose against one mole of ATP from one mole of glucose if anaerobically grown.

2.3.2 Electron Transport System

Strains of *Leuconostoc mesenteroides* which are able to grow aerobically, display peroxidase activity but do not have any cytochromes (Bergey, 1974).

Lactic acid bacteria have been shown to effect the following reduction of oxygen to water :

$$NADH + H^+ + O_2 \longrightarrow NAD^+ + H_2O_2$$
$$NADH + H^+ + H_2O_2 \longrightarrow NAD^+ + H_2O$$

$$2(NADH + H^+) + O_2 \longrightarrow 2NAD^+ + 2H_2O$$

These steps are brought about by the combined action of two enzymes, flavoprotein-linked NAD dehydrogenase and flavoprotein-linked NAD peroxidase. The organic compound nicotinamide adenine dinucleotide (NAD) is one of the most common coenzymes (prosthetic group of enzymes) occurring in metabolic catalysis, as it transfers hydrogen from one compound to another.

Strains of *L. mesenteroides* have been shown to employ flavoprotein-linked peroxidase, although no work on this topic has been completed on *L. mesenteroides* B-512F. There have been identified two types of flavoprotein-linked peroxidases, typical and atypical, both of which have been isolated from strains of *Leuconostoc mesenteroides.*

Typical peroxidases have an FAD (flavin adenine dinucleotide) prosthetic group but no heme or metal group and are specific for reduced NAD.

Atypical peroxidases catalyze the reduction of hydrogen to water with oxidisable substrates as electron donors. The oxidisable substrate can be alcohol, glucose, glycerol, lactate or fructose.

Anaerobic metabolism of *Leuconostoc mesenteroides* employs the enzyme diaphorase, which has been shown to couple the oxidation of reduced NAD to the reduction of artificial electron acceptors :

$$NADH + H^+ + A \longrightarrow NAD^+ + AH_2$$

Many of these enzymes are flavoproteins and their significance to the cell is questionable (Doelle, 1975).

2.4 The Enzyme

Dextransucrase (E.C. 2.4.1.5 ; sucrose : α-1,6 D-glucan : D-fructose 2-glucosyltransferase) is produced by *Leuconostoc mesenteroides* (and some other bacteria of the genus *Leuconostoc* and *Streptococcus*) and secreted into the culture broth during growth. The enzyme was given the name dextransucrase in 1944 by Hestrin. It was shown by Itaya and Yamamoto (1975) and confirmed by Robyt and Walseth that it is a calcium metallo-enzyme. Treatment with EDTA (ethlenediamintetraacetic acid) decreases the enzyme activity, which may be restored completely by the addition of calcium ions.

The extracellular dextransucrase elaborated by *L. mesenteroides* B-512F catalyzes the formation of dextran linked predominantly by α-1,6 bonds by transfer of glucosyl residues to growing polymer chains. This enzyme is one of the very few synthesizing enzymes which do not require the presence of cofactors or of high energy phosphorylated intermediates. To date, only three substrates have been discovered : sucrose (Hehre, 1941), D-glucopyranosylfluoride (Genghof & Hehre, 1972; Figures & Edwards, 1976), and Lactulosucrose (Hehre & Suzuki, 1966). With the first substrate, the following reaction occurs :

$$(C_6H_{10}O_5)_n + C_{12}H_{22}O_{11} \rightarrow (C_6H_{10}O_5)_{n+1} + C_6H_{12}O_6$$

$$[\alpha\text{-1,6-glucosyl}]_n + \text{Sucrose} \rightarrow [\alpha\text{-1,6-glucosyl}]_{n+1} + \text{fructose}$$

Hehre (1946) showed that the reaction approaches well within 1% of completion and is essentially irreversible. This lack of reversibility might be explained by the rapid conversion of the liberated D-fructofuranose to the more stable fructopyranose form (Neely, 1960).

After many years of controversy, it now appears that the

polymerization reaction takes place by an insertion mechanism proposed by Ebert and Schenk (1968), with a glucosyl unit from sucrose (or presumably one of the other two donors) forming a covalent intermediate with dextransucrase and being inserted between the enzyme and the reducing end of the growing dextran chain (acceptor). The latter is transferred to the site holding its newest residue, and a new glucosyl unit occupies the site vacated by the chain (Robyt *et al.*, 1974). Dextran molecules of varying sizes may displace glucosyl and dextranosyl units from dextransucrase by nucleophilic attack on the link between them, forming branches one or more glucosyl units in length and terminating chain growth. Other sugar acceptors also attack by the same mechanism, yielding oligosaccharides and dextran chains capped at the reducing end (Robyt & Walseth, 1979).

The proposed mechanism for dextran formation can be presented in a simple form :

$$EP_n + S \underset{K_{-1}}{\overset{K_1}{\rightleftharpoons}} ESP_n$$

$$ESP_n \xrightarrow{K_2} EP_{n+1} + F$$

where E is enzyme, P is growing polymer chain, S is sucrose, F is fructose and ESP is a complex. The formation of dextran terminates only when the dextran molecule is detached from the enzyme.

Polymer growth can be terminated by the action of various acceptors (A) which detach polymer from enzyme.

$$SEP_n + A \longrightarrow ES + AP_n$$

Glucose, fructose, maltose and sucrose can act as acceptors. Many

other acceptors, which act with varying degrees of effectiveness, are reported in the literature (Robyt & Walseth, 1978).

2.4.1 Enzymatic Properties of Dextransucrase

The purified enzyme has been shown to have a molecular weight of 64000 to 65000, pI (isoelectric point) value of pH 4.1, and 17% carbohydrate in a molecule. The major component of the carbohydrate has been identified as mannose; this also indicates the possibility of the enzyme being a glycoprotein (Robyt & Walseth, 1979 ; Kobayashi & Matsuda, 1980).

One of the main characteristics of dextransucrase is the unique role played by sucrose as the donor substrate. The Michaelis constant for the dextransucrase/sucrose system was determined by various workers. Their results are presented in Table 2.1.

Table 2.1 The Michaelis Constant for Dextransucrase/Sucrose

Michaelis Constant K_m (mM Sucrose)	Strain	Reference
18	NRRL B-512F	Monsan and Lopez (1981)
16.6	NRRL B-512F	Greulich & Ludwig (1979)
20.0	NRRL B-512F	Lawford *et al.* (1979)
12	NRRL B-512F	Paul *et al.* (1986)
12 - 16	NRRL B-512F	Miller and Robyt (1986)
5.4 ♣	NRRL B1416	Kobayashi *et al.* (1984)
36.6 ♠	NRRL B1416	Kobayashi *et al.* (1984)
13.4	IAM 1046	Tsumaraya (1976)

♣ without dextran
♠ with dextran

It is seen from the above table that the estimates for strain NRRL

B-512F seem to be consistent, and lie in the region of 16 mM sucrose.

Activation energy for dextransucrase action was estimated from the Arrhenius equation to be 5.3 kcal/mole from measurements between 20 °C and 30 °C (Tsumaraya, 1976), whereas from 15 °C to 30 °C the activation energy obtained by Kaboli and Reilly (1980) was 8.57 ± 1.23 kcal/mole, where this interval indicates the 95% confidence limits.

2.4.2 Some Effects on Enzyme Activity and Stability

In common with other enzymes, the concentration of dextransucrase is expressed in terms of its activity under defined conditions. The most common unit used is the dextransucrase unit (DSU). One DSU is defined as the amount of enzyme which will convert 1 mg of sucrose to dextran in 1 hour (thus releasing 0.5263 mg of fructose) at 30 °C in acetate buffered sucrose at pH 5.2 (Hehre, 1946, 1955; Koepsell & Tsuchiya, 1952; Tsuchiya *et al.*, 1952; Jeanes, 1966). The standard unit (U or IU) is defined by the International Committee on Enzymes as the amount of enzyme which will catalyze the transformation of one micromole of the substrate per minute at 25 °C, pH 5.2 for dextransucrase. The specific activity of dextransucrase is expressed as enzyme activity units per mg of enzyme protein.

2.4.2.1 Effect of pH

Figure 2.3 demonstrates that the enzyme is most active at pH 5.2 ± 0.1. It is also most stable in the same pH range. The enzyme activity is high over the pH range 4.8 to 5.6 (Kaboli & Reilly, 1980). This is in agreement with work carried out by others (Tsuchiya *et al.*, 1952; Bailey *et al.*, 1957; Itaya & Yamamoto, 1975; Kobayashi & Matsuda, 1975; Tsumaraya *et al.*, 1976).

2.4.2.2 Effect of Temperature

As can be seen from Figure 2.4 the optimal temperature for enzyme activity is 30 °C. This is also in agreement with numerous other results presented in the literature (Bailey *et al.*, 1957; Itaya & Yamamoto, 1975; Koepsell & Tsuchiya, 1952).

Figure 2.5 indicates that enzyme decay deviates from first order kinetics at all temperatures below 35 °C (half-lives during first-order decay segments were 13.5 min at 30 °C, 7.02 min at 32.5 °C, and 3.28 min at 35 °C), the deviation occurring at successively higher values of enzyme activity as the incubation temperature decreased. The variance of decay rates from first order kinetics is attributed to the various states of aggregation found in dextransucrase (Kaboli & Reilly, 1980).

2.4.2.3 Effect of Metallic Ions and Other Reagents

Effects of metallic salts and other reagents were tested on dextransucrase activity by measuring the activity after incubating the enzyme with these substances for some time at certain temperature. It was found that dextransucrase activity was markedly inhibited by EDTA. As previously mentioned, the EDTA-inactivated enzyme could be recovered by adding Ca^{2+}, but hardly by other divalent-metal ions (Tsumuraya *et al.*, 1976). Complete loss of activity of low concentration (mM) of mercury, copper, and lead was expected because these ions are general enzyme poisons, but the complete inhibition by 5 mM zinc ions when added to the EDTA-treated enzyme is unusual (Robyt & Walseth, 1979).

Figure 2.6 gives results of work completed by Kaboli and Reilly (1980) showing that the addition of calcium ions significantly stabilizes the dextransucrase. Lawford *et al.* (1979) reported that dextransucrase is

irreversibly denatured by prolonged incubation in the absence of calcium ions. More recently, however, Miller and Robyt (1986) showed that above one mM, Ca^{2+} was a weak competitive inhibitor (K_i = 59 mM). Below one mM, Ca^{2+} activated the enzyme by increasing V_{max} and decreasing K_m for sucrose. These results, coupled with the 2-fold increase in dextransucrase activity in the culture medium supplemented with 0.05% of calcium chloride, suggest that dextransucrase is a calcium-metallo enzyme (Robyt & Walseth, 1979).

Dextransucrase has been noted to be strongly linked to dextran forming an enzyme-dextran complex (Kobayashi & Matsuda, 1980). Robyt and Walseth (1979) observed that addition of dextran (0.08 - 4 mg/mL) had no effect on the activity of the purified enzyme, but at 4 mg/mL, dextran stabilized the enzyme against losses of activity on storage. Miller and Robyt (1984) investigated the stabilization of dextransucrase from *L. mesenteroides* NRRL B-512F by three classes of stabilizer. The enzyme could be stabilized by low levels of high-molecular-weight dextran (2 μg/mL), poly(ethylene glycol) (e.g. 10 μg/mL PEG 20000), or nonionic detergents (e.g. 10 μg/mL Tween 80) at or slightly below their critical micellae concentrations. The mechanisms of stabilization, which may be different for different classes of stabilizer, remain unknown, as do the mechanisms of inactivation.

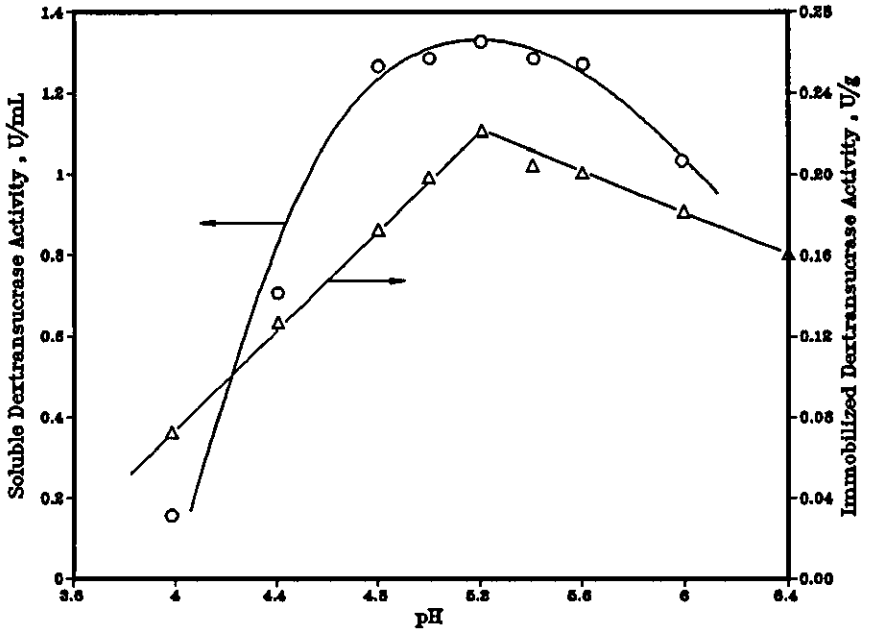

Fig. 2.3 Effect of pH on Activity of Dextransucrase at 30 °C
(Kaboli & Reilly , 1980)

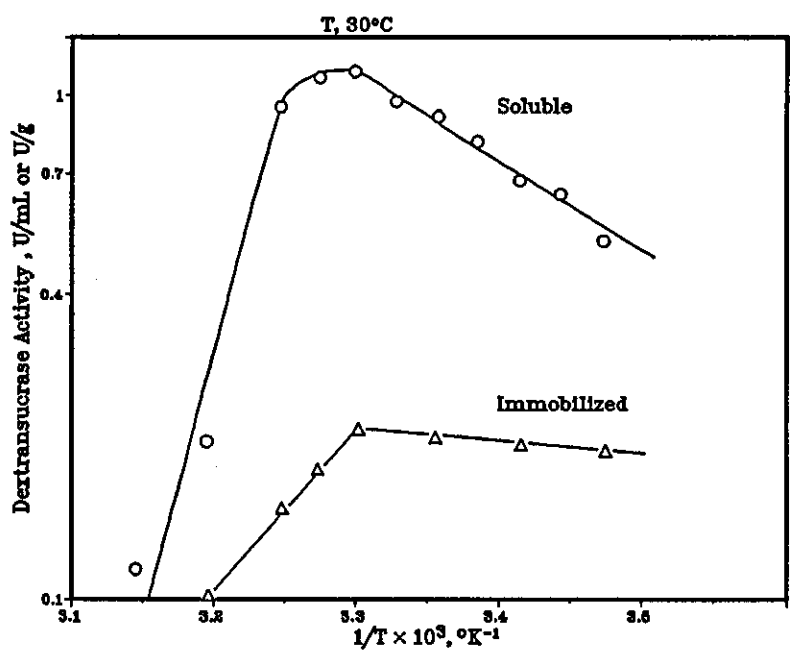

Fig. 2.4 Effect of Temperature on Dextransucrase Activity at pH 5.2
(Kaboli & Reilly , 1980)

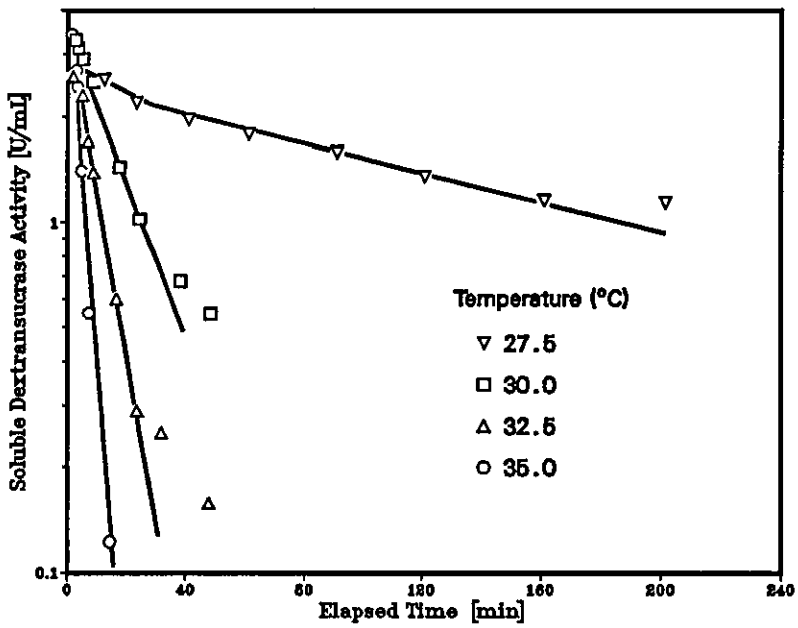

Fig. 2.5 Effect of Temperature on Stability of Dextransucrase at pH 4.9 (Kaboli & Reilly , 1980)

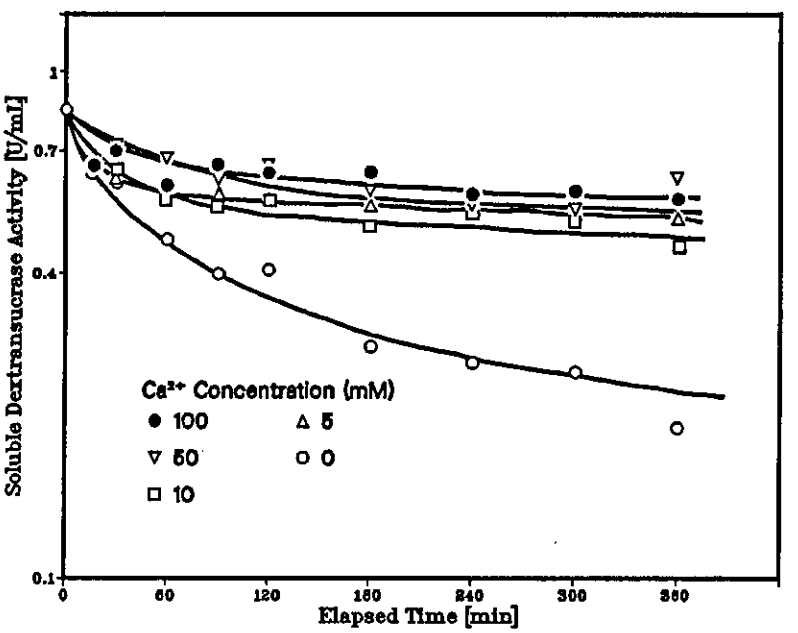

Fig. 2.6 Effect of Ca^{2+} on Stability of Dextransucrase at pH 4.5 and 27.5 °C (Kaboli & Reilly , 1980)

2.4.3 Enzyme Producing Fermentation

2.4.3.1 Cultural Characteristics for Enzyme Production

The research on dextransucrase from *L. mesenteroides* was initiated by Hehre (1941). In 1952 Koepsell, Tsuchiya and co-workers first established the conditions for production of dextransucrase and these were further described by Jeanes (1965). Tsuchiya (1952) described the effect of certain cultural factors on production of dextransucrase by *Leuconostoc mesenteroides* NRRL B-512F. In the first place it was re-confirmed that sucrose is essential for the production of the enzyme. The organism may be grown on glucose-, fructose-, or maltose-containing media but no dextransucrase is formed. This first discovery, together with other results, supports the conclusion that dextransucrase is an inducible enzyme. Its substrate, sucrose, is the only known inducer of enzyme synthesis. The absence of enzyme activity in either glucose, fructose or maltose cultures is a consequence of the lack of the requisite inducer, sucrose. It has been suggested that the enzyme induction process may be triggered by the D-fructofuranosyl group of the sucrose molecule (Neely & Nott, 1962).

The most important factors affecting enzyme productivity are temperature, pH, and sucrose concentration. Tsuchiya (1952) found that increasing the levels of sucrose progressively from 0.5% to 5% resulted in increased enzyme yields (Table 2.2) but that at sucrose concentrations greater than 2% the solution was too viscous for cell removal and further processing. Accordingly, it was concluded that 2 per cent sucrose was the optimum level for production of dextransucrase with this strain of *L. mesenteroides.* As noted previously, higher yields of dextransucrase were progressively obtained as CSL (corn-steep liquor) levels were raised to 2 per cent but only if phosphate levels were raised concomitantly.

Table 2.2 Effect of Sucrose Concentration on Production of Dextransucrase by *L. mesenteroides*

Sucrose (%)	Dextransucrase (DSU/mL)
0.5	6
1.0	17
2.0	86
3.0	99
4.0	110
5.0	120

Medium Composition :	Sucrose	variable
	Corn-steep liquor	2 % (dry basis)
	KH_2PO_4	2 %
	R salts	0.5 % (v/v)

Initial pH 7.2

In studying the effect of pH on enzyme production, Koepsell and Tsuchiya (1952) stated the optimal pH for enzyme production is 6.5 - 7.0, and the maximum yield could be obtained at pH 6.7 (Figure 2.7) although at this pH the enzyme is relatively unstable and is rapidly inactivated even at 25 °C.

Temperature regulation of the fermentation is also a critical parameter and interdependent with pH. Thus although pH 6.7 has been shown to be an optimum value this only applies at a temperature of 23 °C. Higher temperature accentuates markedly the deleterious effect of pH on the enzyme. Thus at higher temperature inactivation at pH 6.7 is extremely rapid and lower yields are obtained. Consequently, the optimal temperature for growth at 30 °C is too high for maximal enzyme production. Enzymatic activities in experiments carried out at 19, 23, and 27 °C are shown in

Figure 2.8 (Alsop, 1983).

Although growth rate is faster and maximum enzyme yield achieved sooner at 27 °C than 23 °C and 19 °C it can be seen that the highest enzyme yield is achieved at 23 °C.

Obtaining the right combination of temperature and pH is, therefore, extremely critical to maximize enzyme yield.

Fig. 2.7 Effect of pH on Yields of Dextransucrase by *L. mesenteroides* (Tsuchiya *et al.*, 1952)

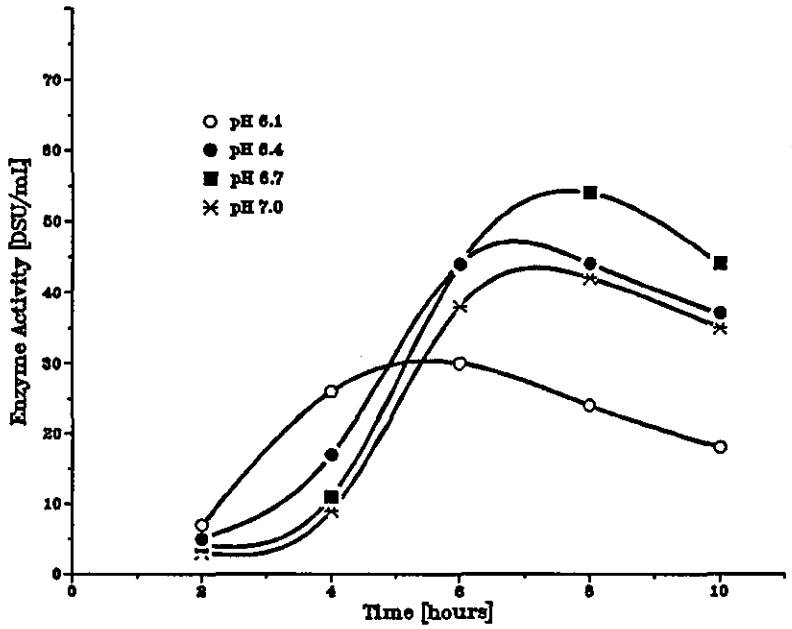

Fig. 2.8 Enzyme Production vs Time at Various Temperatures, pH 6.7 (Alsop, 1983)

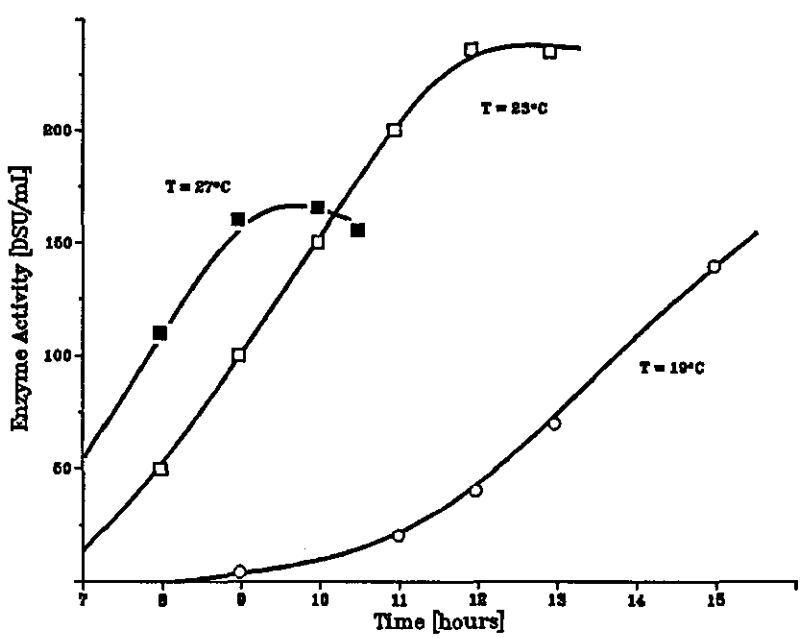

2.4.3.2 Fed-Batch and Continuous Culture

The conditions described above were established initially for enzyme production by batch culture. Attempts have been made to improve the yield of dextransucrase by careful optimization of the process conditions and in particular by control of the sucrose level in the fermentation.

2.4.3.2.1 Fed-Batch Culture

Illustrated in Figure 2.9, Experiments carried out by Monsan and Lopez (1980, 1981) showed a 6-fold increase in final dextransucrase activity by continuous addition of a concentrated sucrose solution (1 kg/L) to the fermentation broth of *L. mesenteroides* NRRL B-512F during exponential growth at a rate of 20 $gL^{-1}hr^{-1}$ for approximately 4 hours, when compared with the production of dextransucrase in batch culture without sucrose addition. Work completed by Battelle (Schneider, 1980) has also resulted in much higher yields of dextransucrase being obtained by maintaining sucrose level in the fermentation at around 0.5 - 1.0% by continuous sucrose addition particularly during the active growth phase when enzyme production is induced.

A pH-linked substrate feed system utilizing sucrose and sodium hydroxide in a specified ratio was investigated by McAvoy (1981). A very high enzyme yield was achieved with an initial background sucrose concentration of approximately 6 gL^{-1}.

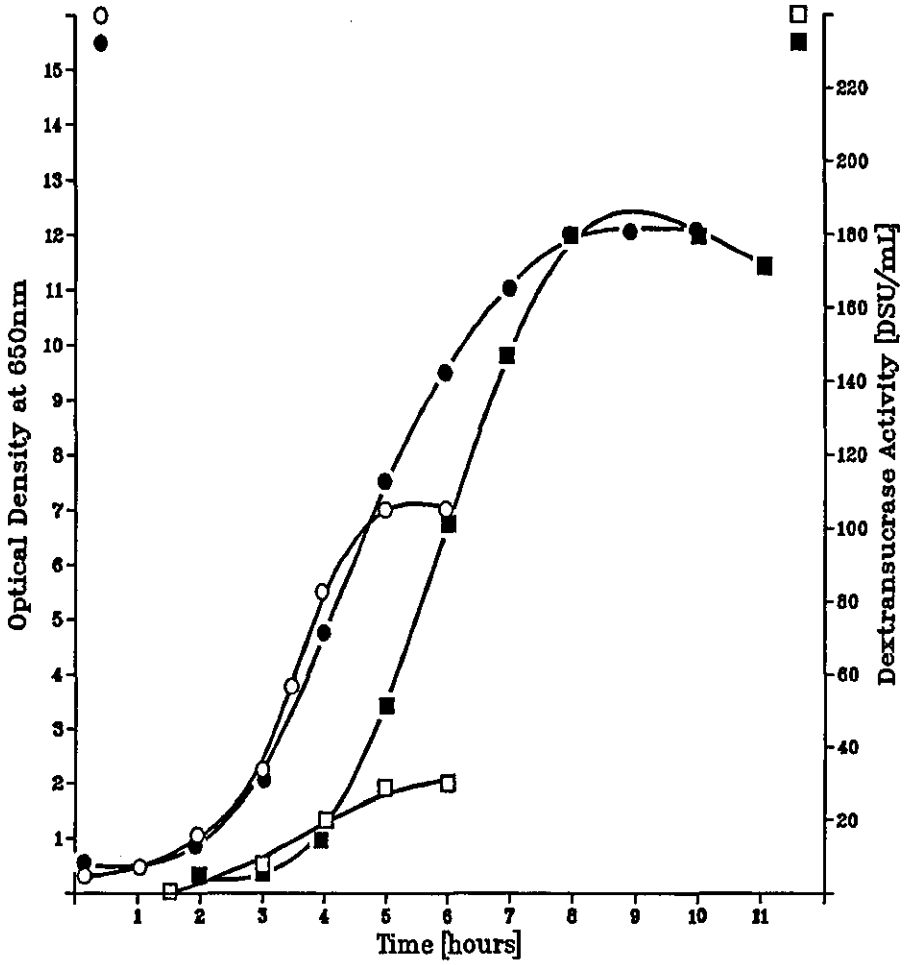

Fig. 2.9 Dextransucrase Production by Cultures of *L. mesenteroides* NRRL B-512F (Monsan & Lopez, 1981)

Culture conditions :

batch fermentation (°, □) using 20 g/L sucrose as carbon source;
fed-batch fermentation (•, ■) using 20 g/L sucrose as carbon source, with continuous addition of sucrose at a rate of 20 $gL^{-1}hr^{-1}$ during growth.

2.4.3.2.2 Continuous Culture

Only a limited amount of work has been published on the continuous culture of *L. mesenteroides* to produce dextransucrase.

Ringfeil and Selenia (1964) theoretically calculated from batch culture experiments that the maximum yield of dextransucrase would be obtained from a sucrose-limited continuous culture at low dilution rates.

Lawford *et al.* (1979) presented results on the production of dextransucrase in comparative batch and continuous culture of *Leuconostoc mesenteroides* NRRL B-512F. Both batch and continuous cultures were maintained at 25 °C, pH 6.7 and aerated. In batch culture at 1% sucrose they varied the media composition with respect to phosphate. Greater losses of dextransucrase occurred in the higher phosphate levels which was attributed to the ability of phosphate to remove calcium ions from solution at pH 6.7. Only low yields of enzyme (9.2 DSU/mL) were achieved.

In continuous culture with either glucose or sucrose as the energy source they calculated the theoretical critical dilution rate to be 0.67 hr^{-1} based on the maximum specific growth rate of a midexponential-phase batch culture. No enzyme activity was recorded even at very low dilution rates under glucose-limited condition. Dextransucrase could not be detected at dilution rates less than 0.2 hr^{-1} and the maximum production (16 DSU/mL) was achieved at 0.53 hr^{-1} (cf. 9.2 DSU/mL batch culture). It was therefore concluded that the enzyme was synthesized and the enzyme activity increased with increasing dilution rate only after a critical concentration of the inducer (sucrose) in the chemostat had been reached.

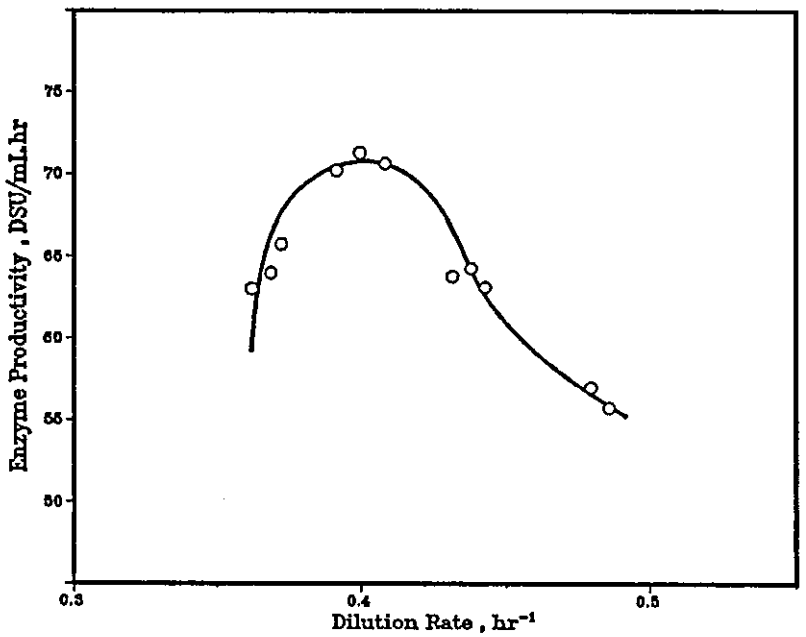

Fig. 2.10 Dextransucrase Productivity vs Dilution Rate in Continuous Culture of *Leuconostoc mesenteroides* NRRL B–512F (Paul , Auriol , Oril , & Monsan , 1984)

Paul *et al.* (1984) continued Monsan's work trying to improve enzyme production using continuous culture of *L. mesenteroides* NRRL B-512F. The experimental results showed that enzyme productivity in continuous culture is three times greater than in usual fed-batch culture. Dextransucrase is produced during the exponential growth phase of the cells. It may be seen from Figure 2.10, in the continuous culture, enzyme productivity depends directly on the dilution rate; optimum enzyme productivity (70 hr^{-1}DSU/mL) is achieved at a 0.4 hr^{-1} dilution rate.

2.4.4 Enzyme Purification and Immobilization

Recent research on dextransucrase from *L. mesenteroides* has been concentrating on the methods and procedures of enzyme purification and immobilization because the immobilized dextransucrase looks promising for low-molecular-weight clinical dextran production.

In the early studies on *L. mesenteroides* NRRL B-512F dextransucrase relatively crude enzymes were produced by precipitation of the enzyme from the culture medium using ethanol (Tsuchiya, 1955). The enzymes were purified by adsorption onto calcium phosphate gels, by separation based on precipitation with ammonium sulphate or by ultra-centrifugation.

Kaboli and Reilly (1980) first reported a 300 fold purification of the enzyme in 56% yield by ultrafiltration and gel permeation chromatograph procedure similar to that of Robyt and Walseth (1979). This technique was then adopted by other workers (Chang, 1981; Monsan & Lopez,1980), but different purification yields were achieved. Schneider (1980) in contrast purified dextransucrase from high yield fermentation by firstly precipitating the enzyme with alcohol followed by chromatograph on DEAE 2.5 (Pharmacia).

Dextransucrase is an extraordinarily difficult enzyme to immobilize. Most of the above groups of workers have attempted to immobilize their purified enzymes and significant progress has been made. The enzyme has been immobilized ionically to DEAE-Sephadex A-50, covalently to Bio-Gel P-2, and covalently to Polyacrylamide gel, cellulose acetate membranes, and polysulfone hollow fibres. A deviation from the Michaelis behaviour followed by the free enzyme is then observed by Monsan and Lopez (1981). This may be attributed to the viscosity gradient resulting from dextran synthesis in the immobilized enzyme microenvironment.

2.4.5 Process Kinetics of Enzyme Production

Although dextran has been produced commercially from *L. mesenteroides* either by conventional fermentation process or by enzymatic synthesis for many years, and much is known about the mechanism of the polymerization reaction, there is a great lack of knowledge about the kinetics of cell growth and no kinetic models of enzyme production are presented in the literature. Only qualitative description of the enzyme synthesis was given by various workers in this field until recently.

Wilson (1985) presented an anaerobic growth model of *L. mesenteroides* in his thesis. A simple Monod model was found to be suitable although a non-competitively inhibited Monod model was used to analyze the experimental data. No information was given about the enzyme biosynthesis. However, Lawford *et al.* (1979) mentioned that the dextransucrase activity of the cell-free supernatant parallels growth in batch culture. In fed-batch experiments maintaining a constant sucrose concentration, McAvoy's results (1981) also indicate that the production of enzyme is linearly related to the growth of cells although the proportionality varies under different growth conditions.

A comprehensive model of dextran production and dextransucrase synthesis by *L. mesenteroides* growing on sucrose under anaerobic conditions was considered by Dussap and Gros (1985). Results based on experiments of Lawford (1979), Kaboli and Reilly (1980) in batch and continuous cultures under anaerobic condition, and simulation of the growth model were presented. The model of enzyme synthesis is a simple growth-associated product kinetics :

$$\frac{dp}{dt} = k_p \frac{dx}{dt} \qquad [2.1]$$

where x is the cell concentration, p denotes enzyme concentration expressed in DSU/mL, and k_p is the product formation rate constant.

In the field of enzyme biosynthesis, particularly dextransucrase production by *L. mesenteroides*, modelling or kinetic study has to be pursued further so that the whole system could be fully understood.

Chapter 3 Experimental Apparatus

Theories are established on the basis of experimental findings. Experiments test and decide the theory. To model the process of enzyme synthesis from *Leuconostoc mesenteroides*, an appropriate fermentation system was needed to perform the necessary experiments. At the beginning of the study, a laboratory-scale bench-top fermentation system (L.H. FERMENTATION 500 Series) was available for use. This system was built up in modules based on the culture vessel, stirrer and heater unit. Process monitoring and control modules were provided for dissolved oxygen measurement, pH, temperature and foam control. In view of the experiments needed to be done, the whole system must be reliable and easy to control with precision. The system must be flexible enough so that changes can be made to perform different types of experiments. Thus this fermenter system was modified to use a microcomputer as the central display and control unit. A schematic representation of the fermentation system is shown in Figure 3.1. A photograph of the system is included in Plate 1. Details of the system are described in this chapter.

3.1 Fermenter System

Biochemical processes, especially fermentations, are generally much more complex than chemical processes. Therefore, some special equipment is required and special operational procedures must be followed. The unique feature of fermentation is the requirement of sterility which is crucial in unicellular culture. The fermenter system must be designed to enable transfers of fluid in and out of the reaction vessel, for example aeration in aerobic culture, the addition of media supplements, inoculation and sampling, to be carried out without risk of contamination.

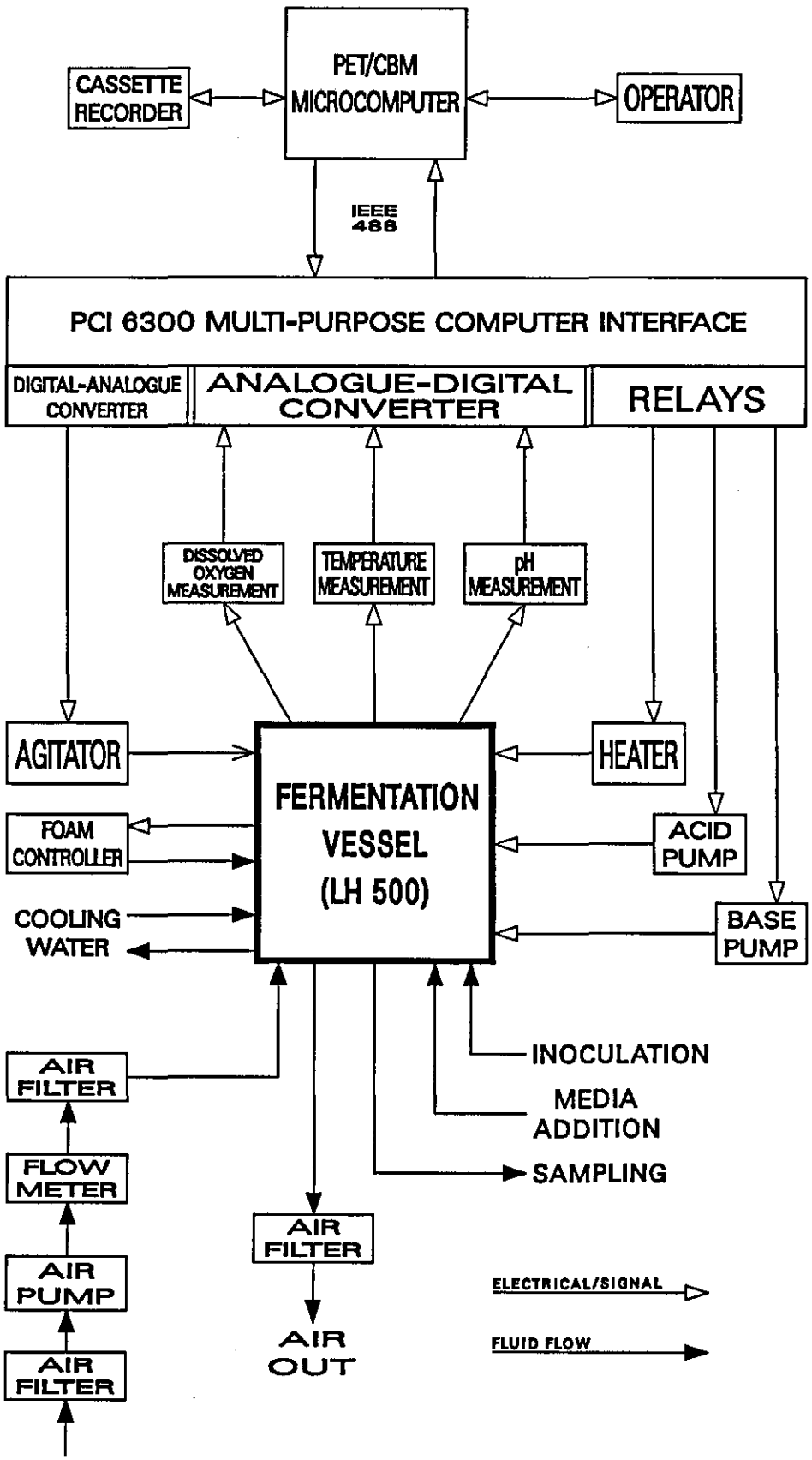

Figure 3.1 Schematic Diagram of the Fermentation System

3.1.1 The Vessel

The fermenter vessel (L.H. FERMENTATION 500) comprises a two litre Borosilicate glass jar (QUICKFIT FV2L) with a circular stainless steel top plate which is firmly held on to the vessel by three stainless steel clamps and sealed with a silicone rubber 'O' ring. The capacity of this vessel allows a 1 - 1.5 litre culture volume when operated aerobically. A sterile bearing for the agitator shaft is located centrally on the top plate. The bearing housing incorporates two stainless steel ball races and two single lipped rotary seals. Two Rushton type impellers are fitted on the shaft and their positions can be adjusted. The bottom impeller is located 3 cm up from the vessel base, and the upper impeller 6 cm below the liquid level. Aeration is through the hollow agitation shaft with the gas released from the air sparger below the bottom impeller. Stainless steel ports with silicone rubber 'O' ring seals are set into the top plate for mounting temperature measurement, heating and cooling probes, as well as pH and dissolved oxygen measurement electrodes. There are also ports for inoculation, acid, alkali and antifoam addition, medium addition, sampling and air out. A PTFE sampling hood is fitted to the outside end of a long stainless steel sampling tube for use with screw-necked glass Bijou bottles, and allows repeated sampling without contamination. The vessel with associated probes and connections are suitable for autoclave sterilization.

3.1.2 Agitation

The fundamental function of agitation is to mix the culture and so maintain homogeneous chemical and physical conditions in the culture. Agitation also assists mass transfer between different phases present in the culture. Agitation of this system is provided by a direct drive stirrer unit (L.H. FERMENTATION 502D). The agitator uses a brushless motor with tacho feedback control and has an infinitely variable speed from 100 rpm to over

2000 rpm. The speed may be varied either by a potentiometer on the agitator or by a 0 - 10 Volt external signal which can be generated by the microcomputer through D/A converter interface. The agitator shaft is connected to the vessel by means of a split coupling. A four-bladed stainless steel baffle is fitted in the vessel to prevent vortex formation and increase turbulence in the culture. This unit when used at high agitation rate is capable of providing adequate oxygen transfer for aerobic cultures.

3.1.3 Aeration

Aeration is provided by a diaphragm pump (CHARLES AUSTEN PUMP Ltd, CAPEX 2D-C). The air flow rate is measured by a rotameter (PLATON FLOW CONTROL, GAPMETER GB/B6/D) and regulated by a pinch-clamp and bleed arrangement. The air is prefiltered before entering the pump unit and then passed through a sterilizing miniature line filter (MICROFLOW PATHFINDER Ltd, LF22) so that the air is sterilized before introduction to the vessel. Silicone tubing is used to join air pump outlet to flow meter, to the filter and to the gas inlet nipple of the culture vessel on the agitation shaft. The effluent gas is passed through an air outlet condenser mounted through the top plate and finally enters into the atmosphere through a gas filter attached to the top of the condenser.

3.1.4 Temperature Measurement and Control

Temperature is a crucial parameter in biochemical processes, especially with regard to reaction rate. An efficient temperature control is therefore indispensable for most biochemical processes as enzyme production from growing cells. Temperature measurement is performed by means of a platinum resistance thermometer probe (L.H. FERMENTATION R1-01-01A) inserted into the culture vessel through the top plate. The thermometer sensor has a stainless steel sheath with PTFE insulated

screened lead suitable for autoclave sterilization. The resistance signal is converted to a voltage signal by a bridge circuit interface unit. This voltage signal is then fed into the analogue to digital converter (A/D). The digital signal thus generated is manipulated by the microcomputer and displayed on the monitor screen.

Temperature of the culture medium is controlled by a combination of a 24 Volt, 50 Watt electric heater (WALTON EUROPE) mounted through the top plate and a stainless steel cooling finger which is permanently fitted to the top plate and supplied with mains cooling water. The heater and cooling finger are in direct contact with the culture medium. The cooling finger is needed because the optimum cultivation temperature for dextransucrase production from *Leuconostoc mesenteroides* is near ambient temperature. The inlet center connection of the cooling finger is joined to the top connection of the gas outlet condenser with silicone tubing, the outlet connection of the cooling finger being extended to the sink by rubber tubing. A flow of cold water is maintained through the condenser and the cooling finger. The power to the heater is turned on and off by a custom-built switching unit which is joined to the relays of the computer interface.

3.1.5 Dissolved Oxygen Measurement and Control

The dissolved oxygen concentration is measured by a sterilizable galvanic oxygen electrode (UNIPROBE, TYPE G-2) mounted through the top plate. This electrode has been specially developed for measuring dissolved oxygen in fermenters. It can be repeatedly sterilized by autoclave or *in-situ* steaming at temperature up to 130 °C and is unaffected by suspensions of microorganisms, complex nutrient media and antifoam. The electrode works on the galvanic principle. It measures the partial pressure (pO_2) or activity of the dissolved oxygen and not the dissolved oxygen concentration. The body of the electrode is a toughened glass tube which supports the silver disc

cathode and spiral lead anode. The oxygen permeable membrane is sealed to the body and held in place by a silicone rubber retaining sleeve to separate the electrode internals from the liquid medium. The electrode is vented in order to withstand repeated autoclaving. The electrode output signal is sent to an oxygen monitoring unit (L.H. FERMENTATION 507) via a detachable cable. The unit has zero, fine and coarse span controls for calibration. The output is displayed on a dual-scale meter (low oxygen tension 0 - 20% and high oxygen tension 0 - 100%). A proportional voltage signal of 0 - 1 V generated by this unit is sent directly to the analogue to digital converter (A/D) and then displayed on the microcomputer monitor screen.

The dissolved oxygen level in the fermenter is manually controlled by varying agitation speed and adjusting aeration flow rate.

3.1.6 pH Measurement and Regulation

The pH value is an important indicator of the state of a fermentation and therefore the physical significance of a pH measurement is straightforward. pH is determined by means of an Ingold steam-sterilizable combined reference and measurement glass electrode (PYE-UNICAM 465-35-ka) mounted through the top plate. The voltage signal developed from the electrode is sent to a portable pH meter (WALDEN PRECISION APPARATUS C120). This signal is proportional to the pH being measured according to the Nernst equation. The C120 pH meter has manual temperature adjustment, zero and span controls for calibration. The measured pH value is displayed on a multi-range meter and the voltage signal from the chart recorder output is sent directly to the A/D converter in the computer interface and the corresponding digital signal is manipulated by the control program as pH measurement.

In order to achieve high growth rates and optimum product formation in fermentation processes, the pH must be kept constant within a narrow range depending upon the individual type of organism and upon the actual phase of the culture. Control of the pH is realized by addition of sterile acid or alkali solutions through the corresponding ports in the top plate of the vessel. Flow of acid and alkali is controlled by means of two Delta peristaltic pumps (WATSON MARLOW) switched on and off directly by the relays in the computer interface according to the deviation between the pH value measured and the set-point.

A variable speed peristaltic pump (WATSON MARLOW 501U/R) is also available for pH control. This versatile pump provides manual, remote or automatic control operations. The pump can be programmed to respond to both voltage and current control signals, and can be set to provide a rising flow rate against rising or falling signals. In any of the speed control modes, the pump may be started and stopped remotely from the footswitch. Apart from this on/off operation, a sophisticated control algorithm can be employed to drive the pump for more accurate control.

3.1.7 Foaming Control

Foaming is a nuisance occurring in most aerobic and many anaerobic fermentations. It may be caused by surface-active metabolites such as proteins and polysaccharides, by components of the media or by the growing cells. In certain circumstances, slight foaming is considered favourable because it minimizes entrainment of the medium with the gas and also prevents growth of organisms on the fermenter wall. However, excessive foaming must be suppressed in order to prevent possible contamination of the culture due to wetted outlet filters caused by overflowing foam. Foam destruction can be achieved by mechanical devices or chemically by adding sterile antifoaming agents to the culture vessel either manually as required or by means of a controlling device. A foam control unit (L.H. FERMENTATION 506) with manual and automatic control operation modes is available for this purpose. The controller monitors the formation of foam by a dedicated conductivity probe situated at a suitable position above the liquid surface inside the fermenter. The presence of foam triggers a small peristaltic pump in the antifoam feeding line for a limited period, thus delivering a predetermined amount of sterile antifoaming agent to the vessel. Sporadic splashing of droplets carried in the effluent gas onto the foam sensor may also produce control signals. A time delay in the control circuit will prevent these false signals causing control action.

The underlying operation principle of this foam control unit is that when foam reaches the probe, an electrical circuit is closed between the probe and the top plate via the foam and the fermentation broth. The controller detects this closed circuit and switches on the peristaltic pump which acts as a control valve in the antifoam line. This approach of foam control, however, lacks intrinsic reliability. It was found that in certain circumstances, foam gathered together may form an electrical connection between the detection sensor and an adjacent metal probe causing

antifoaming agent to be added continuously into the vessel. Quite often, the foam built up unevenly, not touching the detection probe and was expelled from the vessel via the air outlet port causing clogging of the exhaust system including the air outlet filter.

Another disadvantage of using this foam control unit, particularly with the opaque silicone-based antifoaming agent, is that the presence of the antifoaming agent contributed significantly to the optical density of the fermentation broth. Therefore, when optical density measurements are used to determine cell growth, the unpredictable dosing of antifoaming agent into the vessel prevents accurate interpretation of the experimental data.

To overcome these difficulties, a small dose of transparent polypropylene glycol was used as antifoaming agent and added to the vessel before inoculation. One great advantage of this antifoaming agent is its high activity at very low concentration. It was found that very little foam was produced during aerobic fermentation of *Leuconostoc mesenteroides*. Thus, a single dose of only 0.1% - 0.2% V/V polypropylene glycol will suffice for foaming suppression in each experiment.

3.1.8 Substrate Feeding

In fed-batch fermentations, fresh sterile nutrient medium is added to the vessel aseptically according to a pre-defined feeding strategy or the level of substrate in the fermenter. This operation is carried out through a fixed port in the top plate of the vessel by means of a variable speed peristaltic pump (WATSON MARLOW 501U/R). The flow rate of the medium addition is controlled by varying the rotor speed of the pump either manually by the potentiometer on the pump or by a 0 - 10 Volt external signal produced in the microcomputer interface.

3.2 Calibration of Instruments

As is common knowledge, some of the measuring devices are designed for use under defined conditions; therefore, calibration is essential for successful operation of the system.

3.2.1 Calibration of pH Meter

For long time pH measurement with a sterilized glass electrode, repeated calibration is necessary because the glass membrane might be blocked by decomposition of proteinaceous material or silver compounds. The Ingold pH electrode used for this fermenter has a nominal **Eo** (equilibrium output) value of pH 7.0, that is to say, the electrode produces a zero voltage signal at pH 7.0. Calibration is accomplished by first standardizing the electrode, i.e. setting the zero ("Buffer") control with the electrode dipped in pH 7.0 buffer, and then adjusting the span ("Slope") control with the electrode in another buffer at a different pH as close as possible to the pH range being investigated (pH 4 and pH 9.2 are commonly available buffer solutions). For very high accuracy fermentation, these steps are repeated until no further adjustment is required. The detail of the calibration procedure is given in the manufacturer's instruction manuals.

For employment under aseptic conditions, the pH electrode is sterilized together with the fermenter vessel. In order to maintain the sterile environment in the vessel, the calibration procedure could only be carried out prior to sterilization. To check the reliability of the calibration after sterilization, parallel samples of the fermentation broth were removed aseptically from the vessel and analyzed on another pre-calibrated pH meter. The pH values thus measured were then checked against the pH instrument on the fermenter. It was found that the calibration setting of the pH meter used varied very little between fermentation runs, but could vary

considerably between different electrodes. Therefore the pre-fermentation calibration step could be omitted if the electrode was in good condition and unchanged. The parallel cross-checking was, however, always carried out during the course of fermentation. If the cross-check revealed a considerable discrepancy between the readings on the two pH meters, a single point calibration could be carried out at, or near, the desired set point pH during the fermentation. On completion of the culture run the electrode was checked for signs of mechanical damage, and the level of electrolyte in the reference chamber also checked. The electrode was replenished to the required level with fresh electrolyte should the need arise.

To ensure reliable performance of the pH measurement unit, especially the pH electrode, the glass electrode should be stored with its measuring tip in 3M potassium chloride solution or distilled water when not in use.

3.2.2 Calibration of Dissolved Oxygen Indicator

The galvanic oxygen electrode used in the fermenter is designed for use under conditions of constant temperature and should be calibrated at the operating temperature of the culture. The electrode output as microamperes current is directly proportional to the oxygen partial pressure (pO_2) over the range of 0 - 0.21 atmospheres O_2 and is essentially zero at zero oxygen tension. This linear relationship thus indicates that a simple point calibration is usually sufficient for the instrument. With the electrode immersed in culture medium saturated with air the span potentiometer of the oxygen indicator is adjusted to read 100% full scale. The error introduced by this method of calibration is 1% at air saturation and 10% at one tenth air saturation.

However, for more accurate observation of the dissolved oxygen concentration, especially at low oxygen tension in study of oxygen effect on

cell growth, a two point calibration was required. The culture medium was first brought to the desired operating temperature and then deoxygenated by bubbling the vessel with oxygen-free nitrogen at a high agitation speed. When the reading on the oxygen meter was at its lowest and steady (after about 30 minutes), the meter was set to zero whilst the range was switched to 0 - 20% scale. Air was then sparged into the vessel for at least 30 minutes at exactly the intended culture temperature whilst the range switch was set to 0 - 100% scale. When the steady highest reading of the meter was obtained, the coarse and fine span controls on the oxygen indicator were adjusted to bring to 100% air saturation.

3.2.3 Calibration of Air Flow Meter

The small bench flow meter used to measure the air flow rate is a rotameter type. It consists essentially of a duralumin float and a slightly tapered glass tube mounted vertically in a frame with the small end down. The meter is uncalibrated but the transparent glass tube is graduated in a nearly linear scale (1:10 UNIT SCALE). This range corresponds to 0.4 - 5 L/min air flow rate at room temperature and 1 atmosphere. There is no need to perform a detailed calibration with air because the precision of the flow meter is not critical.

3.2.4 Calibration of Peristaltic Pump

The speed-variable peristaltic pump (WATSON MARLOW 501U/R) used to feed sterile substrate into the vessel was calibrated against distilled water at room temperature with negligible suction and delivery pressures. The actual flow rate depends not only on the rotor speed, but also on the operating conditions. The important factors affecting flow rate include temperature, liquid viscosity and tubing material. With the appropriate tubing size chosen for experimental use, the amount of water or substrate delivered in certain time (e.g. 5 minutes) by the pump at preset speed was measured so the flow rate can be obtained. The relationship between the resulting flow rates and rotor speed was proved to be linear.

3.3 Control System

Microbial processes are regulated by the biochemical activities of the microbes and by the conditions of their environment. The objective of process control in the fermentation system is, therefore, to create the most favourable environment for the culture in order to produce an optimum of the desired metabolic activity. As in chemical processes, control of the fermentation processes can be performed by conventional techniques or by computer-aided methods. The control task on this experimental fermentation system was to keep such environmental variables as pH and temperature at defined values. This regulator control was carried out, as mentioned earlier, by a combination of conventional control units and a microcomputer control system, details of which are described below.

3.3.1 The Microcomputer and Control Program

There are many advantages to be gained by coupling process instruments to digital computers. In the first place, the computer can enhance reliability and accuracy of data acquisition from various kinds of sensors by using statistical methods and digital filtering. With a computer, simple signal conditioning and correcting operations such as linearization are readily accomplished without the need for additional specific hardware. Another advantage of using computers is the inherent ability of computers to store large quantities of measured values on a suitable medium in digital form which may be accessed conveniently, analyzed, and displayed later on.

In contrast to the conventional control techniques, computer-aided process control offers additional and more advanced possibilities. One computer can replace many conventional analogue controllers and control many individual variables such as pH and temperature using standard feedback methods. For example, operation of a batch process requires a

carefully controlled and coordinated sequence of pump starts and stops. While these switching operations have been done by various timers and relays, they may be managed efficiently by a computer. Furthermore, a computer can employ highly sophisticated multivariable control algorithms adapted specifically to the response behaviour of a system. Thus, the computer provides the memory and computational capability to implement the optimization strategies of complex processes.

To take the advantage of computer-aided control and take into consideration the availability of machines, a PET/CBM microcomputer (COMMODORE BUSINESS MACHINES Model 4032) was employed in this fermentation system to control selected environmental variables. This computer is equipped with a cassette interface designed specifically for an external cassette tape unit. The cassette tape recorder is used to store or load control programs. However, the long access time of tape storage makes this medium unsuitable for online storage of measured results. The CBM computer also has a built-in IEEE 488 interface which allows the computer to communicate with external peripherals. Optionally, a printer can be connected to the computer via the IEEE 488 bus to enable data to be printed during a fermentation experiment.

The control program was written in high-level language BASIC because the speed of data acquisition was not critical here. The BASIC interpreter enables quick direct access to the program parts so corrections and changes can be performed quickly without time consuming assembly run of changed program. The high resolution CRT monitor was used to display measured variables and parameter changes such as agitation speed, temperature and pH set points can be made easily via the keyboard. The whole control program is not to be listed here, only the program parts concerning temperature and pH control are described below.

3.3.1.1 Temperature Control Algorithm

As shown earlier, the temperature of the culture broth was measured by a platinum resistance thermometer sending a signal to the microcomputer via a signal conversion unit and analogue to digital (A/D) converter. This signal was found to contain high frequency noise which made the thermometer output unsuitable for use as an accurate measurement. In order to obtain a reliable temperature value from the output signal, a digital filter was incorporated into the control program. Since the dominant frequency of the fluctuation noise was much greater than the sampling rate attainable on the computer, an empirical recursive exponential filter was employed. In discrete-time form, such a filter is given by :

$$w_k = \alpha w_{k-1} + (1 - \alpha) g_k \qquad [3.1]$$

where w is the filtered output, g is the filter input (noisy signal), and subscripts k and k-1 denote the current and the previous discrete sampling times. The sampling interval for signals entering this filter was estimated to be between 1.5 and 2.0 seconds. The parameter α determines the filter characteristics. It takes values between zero and one, and represents the relative weighting to the current and previous sampling values of the signal. A value of 0.9 was found to be suitable for the parameter α by trial-and-error method. To further attenuate input fluctuations, the signal g_k was taken as the average of five of the sequence of measurements from the platinum resistance probe. The sampling time for this pre-filtering was approximately 0.03 seconds. With these values, such an exponential filter reduced the fluctuations in the smoothed temperature at steady state to less than 0.005 °C.

The actuating device available for temperature control was an electric heater inserted into the vessel through the top plate. The heater was used in

an ON/OFF fashion because equipment was not available to vary the magnitude of power input and output. In order to prevent rapid switching of the heater unit, a deadband was introduced into the control algorithm around the set point. The switching algorithm for the heater can be expressed by a logical function as follows:

$$H_k = [T<(T_{st}-T_{db})] \text{ OR } [(T<(T_{st}+T_{db})) \text{ AND } H_{k-1}] \qquad [3.2]$$

where **H** stands for the heater status, "TRUE" representing "ON" and "FALSE" representing "OFF". H_k is the present heater status and H_{k-1} is the previous status, **T** is the measured temperature value. T_{st} is the temperature set point and T_{db} the deadband.

The signal H_k was used to turn the power to the heater on and off by means of one of the relays in the computer peripheral interface and a power switching unit. A temperature deadband of ±0.05 °C was found suitable and used throughout the experiments. This deadband prevented erratic switching of the heater, thus preventing excessive wear of the relay contacts and the switching unit, whilst maintaining the temperature of fermentation medium constant to within ±0.1 °C.

3.3.1.2 pH Control Algorithm

The pH of the fermentation broth was measured by using a steam-sterilizable Ingold glass electrode. The voltage signal from the electrode was sent directly to a pH meter C120 which was used on an expanded scale (pH 5 - 9). The amplified signal (± 2V) from the chart recorder output of the pH meter was sent directly to the analogue to digital (A/D) converter in the computer interface (q.v. section 3.1.6). No filtering was performed by the control program because of the high quality of the signal.

The pH was controlled by adding sterile acid (3M H_2SO_4) and base (4M NaOH) solutions to the vessel depending on the measured pH value. Addition of these reagents was effected by the switching of peristaltic pumps. The switching algorithm used can be expressed as simple logical functions:

$$A = (P_m > P_{high}) \text{ AND } (\text{NOT } B) \quad [3.3]$$

$$B = (P_m < P_{low}) \text{ AND } (\text{NOT } B) \quad [3.4]$$

where **A** and **B** represents status of the acid and base pumps respectively, "TRUE" being equivalent to "ON". $\mathbf{P_m}$ is the measured pH value and $\mathbf{P_{low}}$ and $\mathbf{P_{high}}$ the low and high limits of the required pH. The deadband (P_{high} - P_{low}) was used to prevent successive additions of acid and base due to measurement lag. A deadband of 0.02 pH units was found to be sufficient for stable pH regulation.

Since *Leuconostoc mesenteroides* produces acetic acid and lactic acid during fermentation when grown on sucrose, the steady state pH should be centred around the lower limit. It was found that after the initial control action to bring the sterilized broth to the desired pH, only the alkali addition was needed to maintain the pH constant as the overshoot of the control action was practically less than the deadband imposed.

Consequently, the Delta pump used for base addition was replaced by a variable speed peristaltic pump (WATSON MARLOW 501U/R) in later experiments. Similar to the Delta pump, the switching algorithm [3.4] was used to perform the on/off operation. An incremental proportional plus integral (PI) control algorithm with appropriate parameters was incorporated in the program to vary the voltage signal sent to the pump. The utilization of this pump improved the pH control.

3.3.2 Computer Process Interface

Analogue signals originating from various sensors must be converted into digital form by an analogue to digital (A/D) converter before being input to the computer for analysis. Similarly, digital output control signals generated by the computer usually need to be transformed into analogue form by a digital to analogue (D/A) converter before being sent to actuators for execution. In the experimental fermentation system, these tasks are performed by an interface unit (C.I.L Microsystems PCI 6300) which enables communication between the fermenter system and the CBM microcomputer. This unit has a built-in microprocessor and comprises 8 analogue to digital (A/D) converters, 4 digital to analogue (D/A) converters and 4 change-over silver contact relays. The analogue to digital converters are of successive approximation type and give conversion times of the order of 1 ms. The A/D converters accept voltage inputs in three gain ranges (±100 mv, ±1 V, ±10 V) which are settable in control programs. The output voltage of the D/A converters is in the range .:.26110 Volts. Both the A/D and D/A converters work to a resolution of 12 bits (the most significant bit is the sign bit), i.e. 1 in 4096, and are linear over the whole range of voltages. The change-over relays are capable of switching load directly up to a current of 1 A. Communication between the interface and the CBM microcomputer is by means of IEEE 488 bus. Low-loss coaxial cables are provided for electrical connections between the interface and various control units.

Chapter 4 Materials and Experimental Methods

Experimental work is an important part of this study during which various experiments have been carried out to investigate cell growth and enzyme production. There are many technical details involved in the experiments and aseptic fermentation is usually a time-consuming proposition. The apparatus used for the fermentation experiments was described in the previous chapter. This system was, like all the fermentation systems, very complicated in nature. Therefore, strict procedures must be followed in order to obtain reliable results with a minimum of experimental effort.

4.1 Materials Preparation

4.1.1 Culture Maintenance and Inoculum Preparation

The strain *Leuconostoc mesenteroides* NRRL B-512F was obtained from Fisons plc in lyophilized (freeze-dried) form (ref. Fisons C31 NCIB 8710). Liquid suspension culture was prepared from this original one by aseptically breaking the glass ampoule using a pair of sterile pliers and then transferring it into an Erlenmeyer flask containing sterile growth medium. The composition of the medium used is as follows :

Sucrose	40 g/L	
Molasses	20 g/L	**Maintenance**
Na_2HPO_4	0.4 g/L	**Medium A**
Yeast extract	5 g/L	

The pH was adjusted to 7.5 with 4M NaOH. The medium was sterilized for 20 minutes at 115 °C. 100 mL of this sterile medium in a 250 mL culture flask were inoculated with one ampoule (containing $3.5 - 4.0 \times 10^8$

organisms per mL) of the freeze-dried culture of *L. mesenteroides* NRRL B-512F. Three identical flasks were stored at 4 °C in a refrigerator. Every week, approximately 5 mL of the culture from each flask were aseptically transferred to a flask of sterile medium respectively. In order to protect the culture from contamination, agar slopes or slants were also used for long term preservation. The composition of the agar medium is as follows :

Sucrose	20 g/L	
Yeast extract	5 g/L	**Maintenance**
Tryptone	2.5 g/L	**Medium B**
K_2HPO_4	20 g/L	**(Sucrose Agar)**
Agar	20 g/L	

All the constituents except sucrose were combined with 90% of the water; the pH was adjusted to about 7.4 with 4M NaOH, and the mixture was heated to dissolve the agar without scorching or burning. The sucrose, dissolved in the rest of the water was then added. MaCartney bottles containing about 10 mL of the sucrose agar medium were plugged with loose screw caps and sterilized for 15 minutes at 121 °C. The caps were screwed down tightly after sterilization was complete. After cooling, the medium was allowed to solidify in an inclined position. This gave a relative large growing area for the bacteria. The agar slopes inoculated with liquid culture were stored at 4 °C in the refrigerator for one month before being renewed.

The inoculum for the main fermentation vessel was prepared in advance of the time for inoculation from the stock culture by transferring 6 mL of the culture into a 500 mL Erlenmeyer flask containing 60 mL of sterile medium. The composition of the medium used was identical to the main fermentation medium and is described in the following section. The flask was incubated on a rotary shaker (Gallenkamp) for about 14 hours at

the temperature to be used in the experiment (23 °C). After 14 hours, the concentration of biomass in the flask was usually about 1 g/L. This resulted in an initial cell concentration of about 0.06 g/L in the fermenter of 1 litre working volume.

It was found that increasing inoculum size will reduce the lag phase of cell growth. Therefore, a different inoculum was used in some experiments. The inoculation proportion was about 17%, i.e. 200 mL of seed culture were used to inoculate 1 litre fermenter. The composition of the medium used was the same as maintenance medium A. The preparation procedure was similar to that described above. Since growth of cells in the inoculum culture was not under strict control, variations of inoculum cell concentration were expected.

4.1.2 Preparation of Fermentation Medium

It is known that *L. mesenteroides* has complex nutritional requirement. The cells need an external source of some amino acids and other growth factors. In the inoculum preparation stage, the growth factors were provided by molasses which were also a supplementary carbohydrate source. Corn-steep liquor had been used as nitrogen source and growth factors in the fermentation medium. But yeast extract was found to be more appropriate for this purpose because it contains high proportions of amino acids. The fermentation medium used throughout all experiments was chosen as follows :

Sucrose	variable	
Yeast extract (Difco)	40 g/L	
K_2HPO_4	20 g/L	**Medium F**
R salts	0.5 % (v/v)	
Antifoam (Polypropylene glycol)	0.2 % (v/v)	

The solid constituents were dissolved in a small amount of distilled water, then the liquid constituents were introduced with stirring, and finally the solution was diluted to the required volume. The pH of the medium was adjusted to 7.2 with 3M H_2SO_4. This medium was found to be able to provide all the necessary nutrient components for growth and enzyme synthesis. The carbon source sucrose was identified as the growth-limiting substrate.

4.1.3 Reagents for pH Regulation

The pH of the fermentation broth is controlled by adding sterile acid and base to the vessel. It was known that ammonium hydroxide exerts a deleterious effect on cell metabolism and enzyme synthesis. Phosphoric acid should also be avoided as it may have a detrimental effect on silicone rubber tubing. Hydrochloric acid can corrode stainless steel at all concentrations so it was not used here. Sodium hydroxide (4M) and sulphuric acid (3M) were chosen to be the control reagents for all the experiments. Care must be taken when preparing sulphuric acid solution as great quantities of heat can be evolved.

The method of preparing the acid and base reservoirs was similar. A 250 mL and a 500 mL borosilicate glass conical flasks were used for acid and base reservoirs respectively. A larger flask was used for base reservoir because the actual pH control action for *L. mesenteroides* fermentation requires alkali addition only. Both flasks were modified to include an outlet nipple at the base of the vessel, to which silicone rubber tubing was fixed. The tube arrangement consisted of a long piece of silicone rubber tubing, the free end of which was fitted with a "male" stericonnector to enable connection to the fermentation vessel. If the Delta pumps were used for addition of acid and base, then a segment of 108 mm long silicone rubber tubing with PTFE nipples fixed to both ends was inserted into the tubing line

to enable connection to the Delta pump with correct tension. All tubing connections were secured firmly with wire or preferably with Unex hose clips.

The stericonnector end of the tubing line was wrapped in aluminium foil or steam sterilizable plastic paper and secured with autoclave tape. The tubing was sealed close to the reservoir with a Hoffman pinch clamp. When the tubing was properly arranged, the well cleaned reservoir was charged with about half of its capacity of prepared acid or base. The top mouth of the flask was sealed with a steam sterilizable foam bung. An additional quantity of acid and base was prepared and placed in a conical flask sealed with a foam bung. This was used to replenish the reservoir if necessary. These reservoirs were sterilized for 15 minutes at 121 °C in a table autoclave (LIFE SCIENCE LABORATORY).

4.1.4 Medium Supplement

In some experiments fresh sterile nutrient medium such as sucrose solution was required to be aseptically fed into the fermentation vessel. The method of preparing a reservoir for this medium supplement was similar to the base reservoir. The reservoir in this case, however, was a 1 litre glass jar with a bottom outlet nipple. The outlet was fitted with a silicone rubber tubing sealed close to the reservoir with a Hoffman clamp. The free end of the tubing was fitted with a "male" stericonnector, and covered with aluminium foil or steam sterilizable plastic paper. All the necessary connections were secured with wire or hose clips. The top mouth was sealed with steam sterilizable foam bung. The reservoir was sterilized for 15 minutes at 121 °C.

4.2 Experimental Procedures

4.2.1 Vessel Preparation

A standard procedure was adopted for preparation of the fermentation vessel throughout all experiments. This is detailed as follows :

(a) All the removable parts of the vessel and top plate except the agitator bearing housing were disassembled, carefully washed in hot detergent and rinsed, twice in tap water and once in distilled water. The individual parts were then dried in a warm oven.

(b) The bladed baffle was compressed into the glass vessel and secured with a spring clip so it sat tightly against the vessel wall.

(c) The rubber 'O' rings used to seal the connecting parts were inspected for wear and replaced if necessary.

(d) The vessel was charged with the required fermentation medium. There must be at least 500 mL medium in the culture vessel so that all of the probes were covered with liquid.

(e) The top plate was replaced onto the glass vessel and sealed with a large silicone rubber 'O' ring (No.52). Three screw clamps were attached and gently tightened to secure the top plate onto the vessel.

(f) The platinum resistance thermometer was inserted into the top plate through the knurled nut collar and 'O' ring. The knurled collar was tightened "thumb-tight". The 2-pin electrical connector from the sensor was wrapped in aluminium foil or steam sterilizable plastic paper and sealed with autoclave tape.

(g) The electric heater was inserted into the top plate through the appropriate port sealed with rubber 'O' ring, ensuring that the heater was pushed down for maximum depth in the vessel. The knurled collar was tightened "thumb-tight". the detachable electric lead was disconnected from the heater and inspected for damage and put to one side for connection after sterilization. The lead terminal of the heater was wrapped in aluminium foil or steam sterilizable plastic paper and sealed with autoclave tape.

(h) The calibrated pH electrode was inspected for mechanical damage and replaced if necessary. The electrolyte level was checked and replenished if necessary. The glass electrode was carefully inserted into the vessel through the corresponding top plate port, ensuring that the baffle was not aligned to the port. The knurled nut collar was then tightened by hand, taking care not to crack the glass. The detachable electrode lead was disconnected, inspected for damage and put to one side for connection after sterilization. The terminal of the electrode was wrapped in foil or steam sterilizable plastic paper and sealed with autoclave tape.

(i) The membrane on the dissolved oxygen electrode was inspected and replaced if damaged. The electrolyte level in the electrode was also checked and replenished to the required level if necessary. The electrode was then inserted into the vessel through the appropriate port and silicone rubber 'O' ring. The knurled collar was then tightened "thumb-tight". The detachable lead for the electrode was disconnected, checked and put to one side for attachment after sterilization. The plastic shorting cap was fitted to the top of the electrode so that the electrode would be automatically conditioned during sterilization. The shorted lead terminal was wrapped in aluminium foil or steam sterilizable plastic paper and secured with autoclave tape.

(j) The stainless steel sampling probe and PTFE hood were assembled, the silicone rubber tubing joining the steel tube to the hood being checked carefully for signs of wear. The connections of the tubing to the hood and tube were secured with wire or Unex hose clips. A Hoffman clamp was fitted to the rubber tubing to prevent siphoning of culture medium from the vessel to the sample bottle during sterilization. A clean Bijou bottle was screwed into the sampling hood. The sampling assembly was then inserted into the vessel through the sampling port and 'O' ring and the collar tightened "thumb-tight". A 10 mL steam sterilizable plastic syringe was fitted to the side arm of the sampling hood with a short length of silicone rubber tubing (3 mm in diameter) and secured with wire or hose clips. The sampling bottle was loosened by 1/4 turn and held to the sample hood with autoclave tape. The piston of the syringe was also held to its barrel with autoclave tape.

(k) Short pieces of silicone rubber tubing were fitted to the addition and inoculation ports and secured with wire or hose clips. The "female" half of a stainless steel stericonnector was fitted to the free end of each piece of tubing and secured with wire or hose clips. A silicone rubber 'O' ring was placed in each stericonnector and the opening was wrapped in aluminium foil or steam sterilizable plastic paper, held in place with autoclave tape. The tubings were individually sealed with Hoffman clamps.

(l) A sterilizing miniature air filter was checked to ensure free flow of air and a piece of silicone rubber tubing fastened to each end. The tubing connected to the filter outlet was then fixed onto the gas inlet nipple located on the agitator bearing housing. The tubing was firmly sealed with a Hoffman clamp to prevent flooding of the filter with nutrient solution during sterilization. The other end of the air inlet line was left open.

(m) A short length of stainless steel tube was fitted to the shell-side of a small glass condenser with silicone rubber tubing and the steel tube fitted through the top plate with a knurled nut collar and rubber 'O' ring. The steel tube was adjusted to keep the end in the vessel well above the expected level of fermentation broth or foam and the collar was tightened. A short piece of silicone rubber tubing was used to join the outlet of the condenser cooling coils to the inlet of the cooling finger. The tubing was secured with wire or hose clips.

(n) Another sterilizing miniature air filter was checked for free flow and then fitted with a piece of silicone rubber tubing to each end. The tubing connected to the filter inlet was then fixed to the air outlet end of the glass condenser. This gas outlet was not clamped as it provided the necessary vent to the vessel during sterilization. All the tubing connections were secured with hose clips.

4.2.2 Sterilization and Connection of Apparatus

Sterilization was usually achieved by moist heat at higher pressure, i.e. autoclaving. Because the complete vessel was too large for the table autoclave, a pilot-plant autoclave (ASTELL) was used for this purpose. The vessel and its various fittings were put in the autoclave, ensuring all parts safely positioned and the two air filters held in vertical position. The fermenter vessel was autoclaved for 15 minutes at 121 °C. Care was taken to reduce the autoclave pressure slowly after the sterilization process completed to avoid damage to the vessel and probes, especially the glass electrodes.

The sterilized culture vessel was removed from the autoclave, and mounted onto the agitator assembly and secured. The two half ends of the stirrer shaft were coupled together and locked into position by a rotating sleeve. While the vessel was still hot, the sample bottle was tightly screwed into the sampling hood, the air inlet line was aseptically connected together and a small flow of air was introduced into the vessel, without stirring, in order to aid drying of the air filters.

The electrodes and probes were then connected accordingly. The cold water line to the condenser and cooling finger was connected. A small flow of cold tap water was run through the condenser and the cooling finger. The acid and base reservoirs were connected to their peristaltic pumps accordingly. The foil or plastic paper covering the stericonnectors was removed, the connectors flamed before quickly joining them. Care was taken not to overtighten the connectors or else the 'O' ring inside would be flattened and constrict the flow. The initiated inoculum vessel was connected to the inoculation port in the same way.

4.2.3 Inoculation and Monitoring of Culture

A fermentation experiment was started by loading and running the computer control program. For aerobic cultures, the vessel was stirred at defined speed and sparged with air at defined flow rate. When the fermentation medium was brought to the preset operating temperature and the dissolved oxygen meter indicated 100% air saturation, the two clamps on the inoculation line were released, and the air flow rate reduced to allow the inoculum culture entering the vessel via the sterile silicone tubing and the inoculation port. The time at which inoculation took place was noted for the purpose of regular sampling. The computer clock incorporated in the control program made the task easier. Immediately after inoculation was completed, the tubing line connecting to the inoculum flask was sealed tightly near the port by a Hoffman clamp. A positive pressure of about 2 psi was maintained in the fermenter, ensuring that leakage would be outward rather than inward. For aerobic cultures, the dissolved oxygen level was allowed to drop to 60% air saturation during fermentation. It can be controlled above this level by manually adjusting aeration rate or agitation speed. The pH of the fermentation broth was controlled at 6.7, and the temperature was controlled at 23 °C for all experiments.

4.2.3.1 Sampling

After inoculation of the fermenter, samples were withdrawn from the vessel at regular intervals, usually from 15 minutes to 30 minutes. The sample was used for determination of microbial growth, enzyme activity, and periodically for pH check and sterility test. As described before, samples were removed from the fermenter by means of a sampling device which consists of a stainless steel tube and a PTFE hood. A sterile plastic syringe was used to draw culture broth from the vessel into a sterile Bijou bottle which was screwed into the PTFE hood. Normally one sample was taken in

the form of two volumes. The first 10 mL was taken and discarded because it represented approximately the amount of culture trapped in the sampling tube that may be different from the bulk broth of well-mixed vessel. Another volume of 10 mL was taken and analyzed subsequently.

To avoid possible contamination during a sample-taking process, the following steps were followed :

(a) The sample bottle on the hood was tightened and the Hoffman gate clamp on the silicone tubing was released.

(b) The syringe piston was withdrawn until the required amount of culture broth entered the sample bottle. The piston was then depressed to empty the sampling line.

(c) The tubing line was sealed by the gate clamp. The sample bottle was removed from the hood.

(d) The PTFE hood was quickly flamed and an empty sterile sample bottle was attached and tightened.

4.2.3.2 Contamination Test

Metabolism of sucrose by *L. mesenteroides* produces acetic and lactic acids. The pH of the culture broth should therefore decrease as the fermentation proceeds. Clearly, any increase of pH value would give an indication of contamination of the culture. Two methods of culture examination were utilized here. Periodically during a fermentation the sample was diluted in sterile Ringer solution and used to prepare a glass slide smear. The Gram stain of this slide was examined under the oil immersion objective of a microscope. *L. mesenteroides* cells were revealed to be Gram positive

bacteria.

The alternative method of cell examination was to streak and incubate the culture on a selective agar plate. The medium of Tween agar was adjusted to pH 7.0 for this purpose. *L. mesenteroides* NRRL B-512F produces white colonies on the plate. Details of preparing Tween agar plates are described in Appendix A.

4.3 Analytical Methods

Due to practical difficulties and the complex nature of fermentation processes direct methods of on-line measurement of microbial cell mass and enzyme activity were not applicable here. These two important parameters can only be determined by sampling and subsequent analyses. The apparent deficiency of this method was the long time delay in acquiring meaningful values. However, this may be advantageous in certain circumstances because samples can be stored in deep-frozen form and analyzed later.

4.3.1 Biomass Determination

For the purpose of quantification of microbial growth, it is essential to obtain a reliable estimation of biomass concentration using the most appropriate method available. The choice of the method of measuring biomass depends mainly on the properties of the organism, the properties of the culture medium and the accuracy required.

Bacteria generally reproduce by the process of binary fission. Increases in biomass concentration are accompanied by increases in the number of cells. Therefore, bacterial growth can be followed by counting the number of cells in a sample. It is known that cells of *Leuconostoc mesenteroides* are very small and often occur in pairs or chains. Direct microscopic counting

method is thus prone to large errors because it often fails to distinguish between single cells and groups or chains of cells. Furthermore, the size of *L. mesenteroides* cells is not reported to change greatly under varying environmental conditions. It is thus clear that the serial-dilution cell counting approach is inappropriate in this case.

Direct estimation of dry cell weight (DCW) is widely used for the purpose of quantifying the amount of cell mass in many fermentations. It involves separating the organism from the medium, washing the organism and drying it. Although the dry cell weight differs substantially from the mass of living cells which contains approximately 80% water, it is a very useful parameter for normalizing fermentation data. The disadvantages are that the method requires a rather large sample and separation of bacteria from the culture broth by centrifugation is time-consuming and tedious.

The optical density (turbidity or absorbance) is defined as the negative logarithm to base ten of the ratio of the transmittance of a sample to that of a reference or standard material. According to Beer-Lambert law, the optical density (OD) of a suspension of microorganisms varies with the concentration of biomass, thus providing a basis for measurement of cell mass. The optical density can be determined at a carefully selected wavelength on any commercially available spectrophotometer. The optical density values may then be converted into biomass concentration by reference to a standard curve relating optical density to dry cell weight. This method is convenient and capable of instantaneous, automatic on-line measurement. However, there are limits in using this method. The optical density of a culture broth is only proportional to biomass concentration over a limited range of lower values. It does not distinguish dead cells from viable cells. In addition, the colour of the growth medium can considerably affect the optical density value. The use of certain antifoaming agents can also cause erroneous measurements. Nonetheless, the optical density

measurements at 590nm have been found successful in estimation of cell concentration of *L. mesenteroides*. This technique was used in all the experiments.

The optical density of a sample was determined by a UV spectrophotometer (PYE-UNICAM, SP6-400) at 590nm using 10mm light-path cuvettes (KARTELL). Original samples were usually diluted with 0.5% gluteraldehyde solution to keep the optical density in the lower linear range. All optical density readings were made on diluted samples. The use of gluteraldehyde as the diluent ensured no cell growth in the sample. The gluteraldehyde also had the effect of preventing lysis of cells. It was noted that at the beginning of a culture, the broth colour had an effect on the optical density because the blank reference used was the colourless gluteraldehyde solution. A correction was thus made later for the optical density of the sterile medium. At the exponential growth phase, a large dilution rate was needed so the broth colour did not have an important effect on the optical density.

Preliminary experiments were carried out to examine the relationship between the optical density at 590nm and biomass concentration of *L. mesenteroides* grown on sucrose as the source of carbohydrate. In some fermentation runs, dry cell weights of samples were also analyzed. A calibration curve was obtained showing a linear relationship between the two variables for optical density measurements of lower than 0.7. Further discussion is given in the next chapter.

4.3.2 Enzyme Assay

As described before, the concentration of an enzyme is usually expressed in terms of its activity under a prescribed set of standard conditions for that particular enzyme. The dextransucrase unit (DSU) is defined as the amount of enzyme which will convert 1 mg of sucrose to dextran in 1 hour, thus liberating 0.5263 mg of fructose, at pH 5.2 and 25 °C. The dextransucrase activity can be determined in the presence of sucrose by measuring the production of reducing sugar during the zero order enzymatic reaction under the defined conditions. The determination of fructose is based on the oxidation of fructose by metal compounds in alkaline solutions. The dinitrosalicylic colorimetric method (Hostettler *et al.*, 1951) was used for this purpose. This method is selective and capable of detecting very small amounts of fructose.

The preparation of alkaline 3,5-dinitrosalicylic acid reagent (Sumner reagent) and acetate buffer are given in Appendix B. The analytical procedure is detailed as follows:

(a) The enzyme solution was properly diluted by 0.1M pH 5.2 acetate buffer when necessary, ensuring that the diluted enzyme concentration was less than 50 DSU/mL. The dilution factor *d* was noted.

(b) Two millilitres of the diluted enzyme solution were added to 8.0 mL of a 6.25% sucrose solution in 0.1M acetate buffer at pH 5.2. Immediately after mixing, the solution was divided equally into 3 test tubes, which were incubated at 25 °C for time intervals of 0, 10, and 20 minutes, respectively.

(c) At the end of the designated incubation period an aliquot of 1.0 mL of the incubated solution was added to 2.0 mL of freshly prepared Sumner

reagent in a pyrex test tube and placed immediately in a boiling-water bath for five minutes. At the end of the five minutes reaction the test tube was cooled in ice. This procedure was carried out for each incubation period.

(d) After cooling, the solutions were diluted to 25.0 mL with distilled water in volumetric flasks. This was used to keep the optical density within the linear range.

(e) A blank reference and a standard solution were prepared respectively. The blank consists of 1.0 mL of distilled water mixed with 2.0 mL Sumner reagent then boiled, cooled, and diluted as outlined in step (c) and (d). The standard consists of 1.0 mL of 2.0 g/L fructose solution (0.2 g fructose dissolved in 100 mL of distilled water) mixed with 2.0 mL of Sumner reagent then boiled, cooled and diluted similarly.

(f) The optical density of the above solutions (including the standard) was determined at 530nm on the spectrophotometer against the blank.

It was observed that inaccurately measured volumes and inadequate mixing of solutions led to large discrepancies in the calculated enzyme activities. Therefore, care was taken to ensure that all solutions were well mixed. Special pipettes (GILSON) equipped with a digital volumeter were used to deliver solutions whenever necessary. The pipette has excellent accuracy and reproducibility.

The optical density determined above was plotted against the incubation time. The slope of the linear plot and the correlation coefficient were calculated by least-square method. The enzyme activity was determined as follows:

$$EA = \frac{\alpha \times d \times 2 \times 60}{OD_s \times 0.5263 \times 0.2} \qquad [4.1]$$

or

$$EA = \frac{\alpha \times d \times 1140}{OD_s} \qquad [4.2]$$

where

EA : enzyme activity (DSU/mL)
α : slope of the plot of OD_{530nm} vs incubation time
d : dilution factor of the enzyme sample
OD_s : optical density of fructose standard at 530nm

The correlation coefficient γ provides information as to how good the line of the OD points. The closer γ is to 1 the better the correlation. It is obvious that more accurate results will be obtained and the experimental error will be reduced if more points are available. However, the number of incubation times was not increased over three because of practical difficulties. Nonetheless, the reducing sugar method was found suitable for enzyme activity measurement.

Conversion of different units used for dextransucrase activity in the literature is given in Appendix C for reference.

Chapter 5 Kinetics of Aerobic Cell Growth

The growth of a microbial cell is the result of a large number of enzymatically catalyzed reactions, many of which occur simultaneously and are carefully regulated by a complex set of internal cell mechanisms. The kinetics of the growth process is therefore the kinetics of the integrated enzymatic activity. Various parameters and interactions influence the kinetic behaviour of cell populations. During the course of the cellular reactions, cells consume nutrients and convert substrates from the environment into metabolic end products. The cells generate heat and, in turn, the environment temperature sets the temperature of the cells. Due to accumulation of cells and of cellular metabolic products, the environmental parameters such as broth pH, temperature, and rheological properties are often not spatially uniform and may change with time, and thus influence cell kinetics significantly. Furthermore, in a growing cell population, cells of different ages may exhibit different types of metabolic functions and activities.

Clearly, it is hardly practical or possible to construct a kinetic model which describes all the reactions occurring within the cell. In most instances simplified mathematical descriptions of the kinetics are often sufficient for process development and optimization. Concerning the cultural environment, it is common practice that the growth medium is designed so that all the necessary components but one are present in sufficiently large quantities that changes in their concentrations do not significantly affect overall reaction rates. Thus, a single component becomes the rate-limiting nutrient, and only the concentration of this one component needs to be considered when analyzing the effects of medium composition on cell growth kinetics. Other environmental parameters such as pH, temperature and dissolved oxygen concentration are often controlled and maintained

constant by external means. Therefore, it is reasonable to assume that changes in these parameters do not significantly affect microbial kinetics over the time scale or within the range of variation encountered in a typical experiment or typical process situation.

5.1 Possible Modelling Approaches

The range of mathematical representations for the cellular phase of microbial systems can be classified according to the number of components used in the cellular representation and whether or not the cells are viewed as a heterogeneous collection of discrete entities. One such perspective, which was first presented by Ramkrishna and is very useful for describing the various modelling approaches available, is summarized in Figure 5.1. The main classification is made on the basis of the integrity of the individual cell. An unsegregated (lumped, or distributed) perspective considers average cellular properties; cells are viewed conceptually as an integral, indistinguishable component of the biophase, i.e. the external conditions are assumed to reflect conditions within the cell. A segregated model, on the other hand, recognizes the variability of individual cells, and the distribution of cells within the abiotic environment; distinction is made between individual cells on the basis of some recognizable traits. The degree of detail with which a cell or cellular components are divided is reflected in the cell structure and forms another basis for classification of population kinetics. A structured model is a multicomponent cellular representation which includes detail of the chemicals and organelles of the cell – for example nuclear matter and protein, while an unstructured model ignores the variation in metabolic activities from cell to cell and describes the cell by a single state variable. Finally, all of the models can be either deterministic or stochastic in nature. Deterministic models give a precise description of the cell population behaviour, whereas stochastic models only predict a probability for the behaviour of the cellular system.

The actual population of microbial cells is always segregated and structured, and its growth and reproduction should be treated stochastically. However, the segregated nature of microbial organisms can reasonably be simplified by an unsegregated model if cell-to-cell heterogeneity does not substantially influence kinetic processes of interest. In a balanced growth state, all cellular synthesis activities are coordinated in such a way that the average cellular composition is not affected by proliferation of the population. In this situation, models which ignore the multicomponent nature of the cells may be adequate. Although stochastic population models can be constructed to describe the randomness of reactions and mass transfer processes within individual cells, these models have not shown significant advantages relative to simpler deterministic ones when dealing with populations with an enormous number of cells.

Therefore, it is useful to assume the most idealized situation, namely an unsegregated (lumped), unstructured deterministic model, when analyzing and describing growth of cellular population. The mathematical simplicity of such a model permits a deeper analysis of its implications. Various modifications such as cell maintenance, multiple substrates and inhibitory effects can then be added. Such models are still unstructured, partly because of the experimental inability to measure intracellular conditions. In certain circumstances, however, it is expected that more detailed models have advantages in describing the system. For example, by employing a structured model, known features of the biochemical reaction network in the cell can be utilized directly in the kinetic representation, enabling more detailed aspects of cellular metabolism to be examined, including the lag and stationary phases. Similarly, known features of the cell cycle may be readily incorporated and used to enhance the validity and range of application of a kinetic model for a cell population by use of a segregated approach.

It can thus be seen that kinetic models can range from very simple to

extremely sophisticated. Simple kinetic models are easy to manipulate but may not provide enough information to describe the cell population. Sophisticated models sometimes give a better view of the metabolic process, but may yield insuperable difficulties in acquiring the right values for the many parameters present and in the handling of the model. An ideal model will, therefore, be the right balance between simplicity and reliability whilst serving its goal. The best modelling procedure is to start as simple as possible, taking into account the most important mechanisms, variables and parameters which influence the processes of primary interest. Additional complexity is gradually included if necessary.

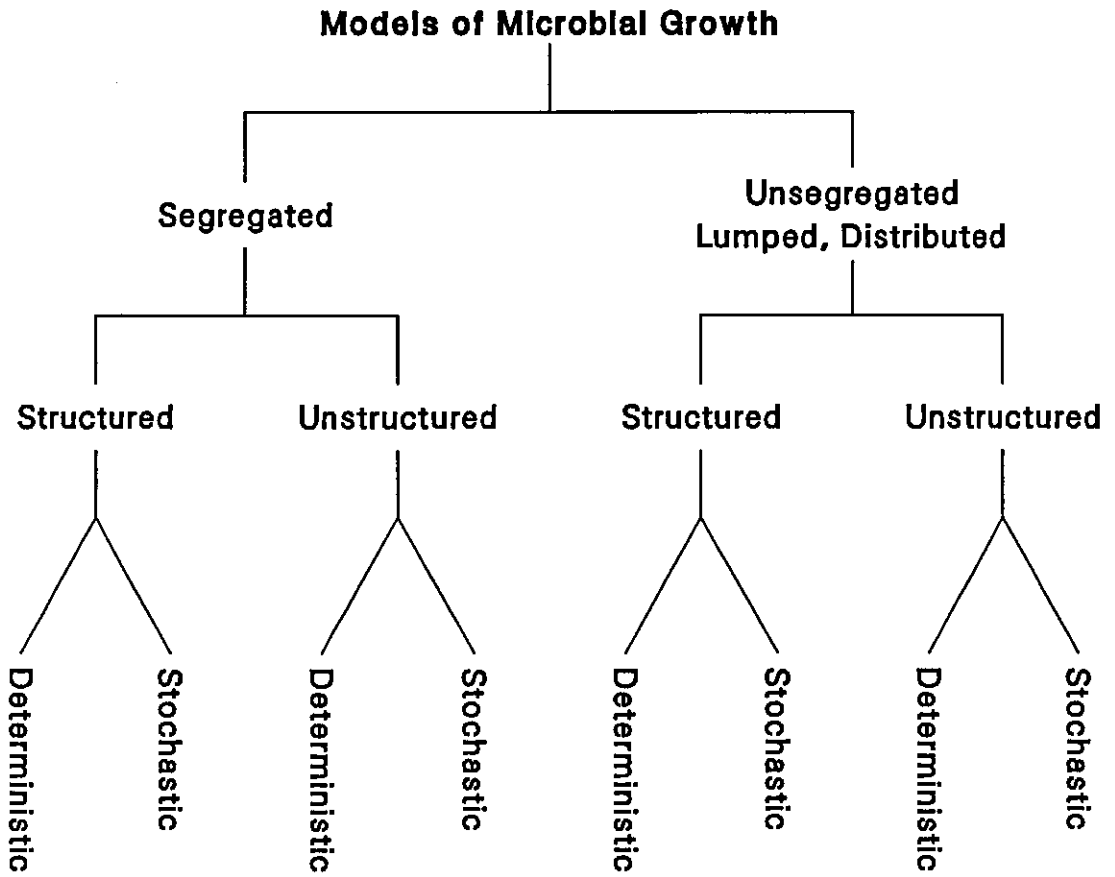

Fig. 5.1 Classification of Cell Growth Kinetics (adapted from RamKrishna)

5.2 The Monod Growth Kinetics

As previously indicated, it is common practice to limit the total cell growth by limiting the amount of one nutrient when formulating cultural medium. The reason for this is that excessive amount of a nutrient can inhibit or even poison cell growth. Moreover, if the cells grow too extensively, their accumulated metabolic end products will often disrupt the normal biochemical processes of the cells. As a result, one of the basic premises in the construction of cell growth models has been that one nutrient can be identified from the medium as the growth-limiting substrate which governs the kinetic behaviour of the cell population. One of the most widely used models relating the growth of cells on a single limiting substrate is the Monod model. It can be defined as an unsegregated, unstructured deterministic model. The conceptual assumptions on which the model is based are described by Barford and Hall (1978) as follows:

(a) Growth is balanced; that is to say, the ratio of all cell components and the metabolic activity of the organism remain constant throughout the growth cycle. Hence biomass in the culture may be represented by a single variable.

(b) The single variable describing the amount of cell material is the mass of viable cells.

(c) Each cell is growing on a medium containing the identified limiting substrate; that is, a known essential medium constituent will run out completely and hence stop growth before the concentration of any other substrate has been reduced to a level which will affect the kinetics.

(d) Growth may be described as a single reaction step with all the restrictions this places on the stoichiometry of growth and the overall

culture dynamics; that is, all yields are constant and there is no possibility of dynamic lags.

(e) The biomass is not considered to form a separate phase.

With these assumptions, the specific growth rate μ typically changes with the concentration of the limiting substrate s according to a hyperbolic function proposed by Monod in 1942. The Monod equation states that :

$$\mu = \frac{1}{x}\frac{dx}{dt} = \frac{\mu_{max} s}{K_s + s} \qquad [5.1]$$

or

$$r_x = \mu x \quad = \mu_{max} \frac{s}{K_S + s} x \qquad [5.2]$$

In these equations, μ_{max} represents the maximum specific organism growth rate achievable when $s \gg K_s$ and the concentrations of all other essential nutrients in the growth medium are unchanged, and r_x is the volumetric rate of cell growth (assumed to be first order in biomass concentration). K_s is termed the saturation constant which is the value of the limiting substrate concentration where the specific growth rate is half its maximum value. The saturation constant is inversely related to the affinity of the organism for the substrate.

The Monod equation has its basis on the underlying enzymatic reactions for growth. The form of the Monod equation can be derived by analogy with the pseudo-steady-state saturation kinetic model of an enzyme-catalyzed reaction with a single substrate (Michaelis-Menton equation) even though it is hard to rigorously verify such a mechanistic approach in real cultures. Due to the fact that the true kinetics of the

individual enzymes in the multi-enzyme system of the growing cell cannot be elaborated, the Monod equation describes only the overall growth of a developing cell population. As in other areas of engineering, however, the relatively simple Monod model can be applied reasonably to describe the complex process of microbial growth.

5.3 Estimation of Kinetic Parameters in the Monod Equation

A mathematical model for a system can only be of practical utility if the physical or biological parameters in the model are able to be evaluated. For a microbial system, the evaluation of the kinetic parameters usually requires reference to be made to the system in the form of experimental investigations. Various methods have been developed for estimating these parameters.

5.3.1 Graphical Evaluation by Simple Transformations

The Monod equation [5.1], when plotted with the specific growth rate μ against the limiting substrate concentration s, represents a rectangular hyperbola passing through the origin with the line $\mu = \mu_{max}$ as a horizontal asymptote. The parameters which characterize the equation are the maximum specific growth rate μ_{max}, which is theoretically attained when the biomass has been "saturated" by an infinite concentration of the growth-limiting substrate, and K_s, the saturation constant which is numerically equal to the concentration of the limiting substrate when $\mu = \mu_{max}/2$. Since the equation in its original form is nonlinear with respect to the substrate concentration, it is quite difficult to estimate the two parameters accurately from a plot of the specific growth rate versus time. To facilitate the evaluation of these parameters, by rearranging equation [5.1] the following three transformations are derived for data plotting and graphical analysis :

$$\frac{1}{\mu} = \frac{1}{\mu_{max}} + \frac{K_s}{\mu_{max}} \frac{1}{s} \qquad [5.3]$$

$$\frac{s}{\mu} = \frac{K_s}{\mu_{max}} + \frac{1}{\mu_{max}} s \qquad [5.4]$$

$$\mu = \mu_{max} - K_s \frac{\mu}{s} \qquad [5.5]$$

Each of the three equations suggests an appropriate linear plot. Of these transformations, equation [5.3] is known as the *Lineweaver-Burk* or *double reciprocal plot.* In this method, the reciprocal of the specific growth rate is plotted against the reciprocal of the limiting substrate concentration; a straight line is fitted to the data points, and μ_{max} is calculated as the reciprocal of the intercept of the line on the ordinate. The saturation constant K_s is obtained either by multiplying the slope of the line K_s/μ_{max} by μ_{max} or by extrapolating the straight line to the abscissa where the intercept will be $-1/K_s$. In a Lineweaver-Burk plot, the dependent and independent variables are separated on both sides of the equation. The growth rate values near μ_{max}, which are most accurately measured by experiments, will tend to be clustered near the origin, while those smallest growth rate values which are likely to have the largest errors will be away from the origin. Obviously, these points will tend most strongly to determine the slope of the straight line. Thus, a linear least squares fitting without proper weighting is not adequate with such a plot.

The second transformation, equation [5.4], corresponds to the *Eadie plot.* By plotting s/μ against the concentration of the limiting substrate s, this method tends to spread out data points for the relatively accurate higher values of the specific growth rate so that the slope of the straight line, $1/\mu_{max}$, can be determined accurately. It is noticed that the straight line often

intercepts the ordinate axis at a point quite close to the origin, so that accurate calculation of K_s by this method is subject to large errors. The third transformation, equation [5.5], is often referred to as the *Hofstee plot.* In this method, the specific growth rate μ is graphed against μ/s. The appearance of the measured variable μ, which is subject to the largest experimental errors, on both coordinates indicates that the plot will show some degree of inevitable correlation, and the ordinary method of fitting a line to the data points by the method of least squares is theoretically no longer applicable.

Dowd and Riggs (1965) carried out a detailed comparison of the above three transformations for analysis of enzyme kinetic data by computer simulations. The reliability of the estimates of the kinetic parameters was assessed. The conclusions drawn are applicable to the Monod kinetics for cell growth. Parameter estimates obtained by the Lineweaver-Burk plot were shown to be the least reliable, irrespective of the error assumed for the specific growth rate. The estimates obtained by the Eadie plot was slightly superior to the estimates obtained by the Hofstee plot when the error of the specific growth rate was small, but the reverse was true when the error was large. The Hofstee plot often had the further advantage of providing a warning of unreliable data or an inappropriate model, since the deviations from the proposed model were often exaggerated. In contrast, the Lineweaver-Burk plot tended to give a deceptive "good" fit, even with unreliable data points. As a result, the Lineweaver-Burk plot was recommended to be abandoned as a method for estimating parameters of hyperbolic kinetics.

Since microbial growth data tends to be even more subject to experimental deviation than enzyme kinetic data, the above linear forms of hyperbolic kinetics should be used with careful considerations when estimating the kinetic parameters in the Monod equation. A better strategy for evaluating μ_{max} and K_s would be such that μ_{max} is to be first determined

from the Eadie plot by calculating the slope accurately, and the saturation constant K_s is then estimated from a graph of μ vs s following that K_s is equal in magnitude and dimension to the substrate concentration where μ is equal to $\mu_{max}/2$.

Although such graphical evaluation methods are simple and rapid and can sometimes provide adequate answers, they do not provide any estimate of the reliability of the fitted parameters. Hence, the linear graphical analysis is only used for preliminary parameter evaluation.

5.3.2 Statistical Analysis by Direct Search

In order to obtain estimates of the kinetic parameters as well as their reliability, statistical methods should be used to fit kinetic data to the assumed rate equation. As in the graphical evaluation methods, the actual specific growth rates at various concentrations of limiting substrate are needed and, for this, initial growth rates at different initial substrate concentrations in a series of batch growth experiments are usually used. Typically, the value of the substrate concentration is known with some precision and the experimental error appears in the value of the corresponding specific growth rate. Therefore, for practical purposes, the substrate concentrations are considered to be accurately measured and the experimental errors are limited to the growth rate.

If the experimental errors in the measurement of specific growth rate are random and normally distributed, and the variance of error within each group of measurements is approximately the same, it can be shown theoretically that the least squares estimates of the kinetic parameters are unbiased and have minimum variance compared with all other unbiased estimates. The problem can be stated mathematically in the form of minimizing the following error function :

$$ERR = \sum_{1}^{N} [\mu_i - \mu(s_i; \mu_{max}, K_s)]^2 \qquad [5.6]$$

This method of least squares is simple to apply if μ is linear in the parameters to be determined. However, since $\mu(s_i; \mu_{max}, K_s)$ is generally nonlinear with respect to the parameters μ_{max}, K_s, as in the Monod equation [5.1], a direct search has to be made on the parameters to minimize the error function. This can readily be performed by a computer program as various search routines are available. A FORTRAN program employing NAG (Numerical Algorithms Group) library routines was written and implemented on the Honeywell Multics computer for this task.

It is essential in nonlinear direct search methods that appropriate preliminary estimates of the nonlinear parameters are employed as an initial starting point. The magnitudes of these kinetic parameters should be known from available kinetic models. In many cases, the preliminary estimates can be obtained by proper methods of graphical analysis as previously described. With a good starting point, the search program runs very fast.

Of equal importance as evaluating parameters which give the best fit of data to an assumed kinetic model is obtaining some index of the precision of these estimates, so that one can tell whether the values are significant, and so that the significance of differences between values can be determined. The most commonly used precision index is the standard deviation, which is the square root of the variance. Estimates of the variances of the parameters can easily be calculated from the Hessian of the error function [5.6] at the solution if nonlinear direct search methods are used to make the least squares fitting. Approximation of the variances is included in the search program which also computes a confidence interval for the fitted parameters.

The variance of the error distribution is estimated as the mean square of deviations about the fitted model, MSD, and is an index of the inherent

variability of the experimental data. As for the Monod kinetics, since the two parameters, namely, μ_{max} and K_s, are derived from the experimental data by the method of direct least squares search, the degree of freedom of deviations about the fitted equation, DFD, and the variance estimate (MSD) are calculated as follows :

$$DFD = N - 2 \qquad [5.7]$$

$$SSD = \Sigma [\mu_i - \mu(s_i; \mu_{max}, K_s)]^2, \ i = 1, N \qquad [5.8]$$

$$MSD = SSD/DFD \qquad [5.9]$$

where N is the number of data points, and SSD denotes the sum of squares of deviations about the fitted equation calculated at the solution (μ_{max}, K_s).

The standard deviations of the fitted parameters are used to evaluate the results. When the standard deviations are 10% or less of the values themselves, the assumed model is a good fit to the experimental data, and considerable confidence can be had in the results. When the standard deviations are larger (up to 20% of the values), more uncertainty exists, and if the standard deviations exceed 25% of the values, the assumed model is hardly a significant one, and the experiment should be repeated with greater precision.

The direct least squares search can thus be seen as an important general method for evaluating kinetic parameters. The method is easy to use and can provide estimates of the reliability of the results. A further advantage is that it is possible to fit complex rate equations which cannot be converted into a form without nonlinear parameters. Models which are difficult to handle graphically can readily be fitted by the direct search method.

5.3.3 Data Transformation Technique

A general method for analysis of experimental data in terms of a nonlinear model by means of data transformations (Box & Cox, 1964) has been successfully applied to microbial growth kinetics (Wilson, 1985). The basic strategy of this technique is to carry out a whole batch culture experiment and estimate the transformed parameters in the model.

The underlying theory of the data transformation technique is based on sample statistics. It assumes that there exists a particular family of transformations which can convert the proposed nonlinear model into a linear one. The transformed data points are presumed to be drawn from a population which is independent and normally distributed with constant variance σ^2. Thus, the probability of occurrence of a particular transformed data point can be calculated from the likelihood function for a set of N transformed data points. In order to provide a common base for comparison of various values of the transformation parameters, the probability is calculated on the base of the original data space by multiplying the Jacobian of the transformed data vector with respect to the original data vector. The maximum-likelihood estimate is then obtained by maximizing the likelihood function based on the original data space, or, equivalently, the logarithm of the function. If the population variance can be approximated by the sample variance, this problem becomes a linear least squares direct search on the transformation parameters, with the objective function to be minimized being the variance σ^2, calculated from the transformed data, with the square of the Nth root of the Jacobian as a scaling factor. The linear least squares estimate from this set of minimizing transformation parameters will then yield the values of the original parameters.

Strictly speaking, the Monod model is only applicable to situations where balanced growth is assumed. In batch cultures, the cellular

environment is continually varying so that batch growth can never be exactly balanced. However, the relative change in environmental state during the early stages of batch growth may be slight indeed, so that the cell population may adapt to the environment and growth is essentially balanced, provided that no rate-limiting factor takes effect before such adaptation is complete. For practical purposes, balanced growth can be assumed for full batch growth process, so that the Monod equation can be used to represent the growth kinetics. The data transformation procedure for the Monod kinetics is described as follows :

In a batch culture, the rate of consumption of the limiting substrate is given by :

$$\frac{ds}{dt} = - q_s x \qquad [5.10]$$

where q_s is the specific metabolic rate or metabolic quotient which is proportional to the specific growth rate. q_s is related to μ by the following function :

$$q_s = \mu / Y_s \qquad [5.11]$$

where Y_s is the biomass yield coefficient which is defined as :

$$Y_s = - dx/ds \qquad [5.12]$$

Thus, combining equations [5.10] and [5.11] gives

$$\frac{ds}{dt} = -\mu x / Y_s \qquad [5.13]$$

Referring to the assumption that Y_s is constant, equation [5.12] can be

integrated from the start of the culture to give :

$$x - x_0 = Y_s(s_0 - s) \qquad [5.14]$$

Evaluation of equation [5.14] at stationary phase conditions, where the substrate is assumed to be exhausted and biomass concentration reaches its maximum, x_{max}, and the subtraction of the general form of equation [5.14] yields :

$$s = (x_{max} - x)/Y_s \qquad [5.15]$$

Substitution of equation [5.15] into [5.1] and subsequent rearrangement leads to :

$$\frac{dz}{dt} = \mu_{max} \quad \frac{z(1-z)}{K^* + (1-z)} \qquad [5.16]$$

where z is the fractional biomass concentration and K^* is a dimensionless saturation constant, defined as :

$$z = x/x_{max} \qquad [5.17]$$

$$K^* = K_s Y_s/x_{max} = K_s Y_s/(s_0 Y_s + x_0) \qquad [5.18]$$

If the inoculum is grown on the same medium as the main culture, and both the inoculum cells and medium are transferred to the main culture, equation [5.18] can be approximated as :

$$K^* = K_s/s_0 \qquad [5.19]$$

Integration of equation [5.16] between the initial time and an arbitrary time t gives the following batch growth equation :

$$\ln \frac{z}{(1-z)^{\epsilon}} - \ln \frac{z_0}{(1-z_0)^{\epsilon}} = \mu^* t \qquad [5.20]$$

where

$$\epsilon = K^*/(1 + K^*) \qquad [5.21]$$

and

$$\mu^* = \mu_{max}/(1 + K^*) \qquad [5.22]$$

Equation [5.20] can also be written in a different form as :

$$\left[(1+K^*)\ln(z) - K^*\ln(1-z)\right]\Big|_{z0}^{z} = \mu_{max} t \qquad [5.23]$$

Inspection of this batch growth equation suggests that a suitable linearizing transformation would be :

$$w = (1+K^*)\ln(z) - K^*\ln(1-z) \qquad [5.24]$$

giving the model as :

$$w = w_0 + \mu_{max} t \qquad [5.25]$$

with transformation parameter being the dimensionless saturation constant K^*.

Assuming that there are N pairs of data and they are independent, the Jacobian for transformation [5.25] is given by :

$$J = \prod_{i=1}^{N} \left[(1+K^*)/z_i + K^*/(1-z_i)\right] \qquad [5.26]$$

Thus the transformation used for the Monod equation is redefined as:

$$w' = w/(J^{1/N}) = [(1+K^*)\ln(z) - K^*\ln(1-z)]/(J^{1/N}) \quad [5.27]$$

This leads to the transformed model :

$$w' = w'_0 + \mu_{max}t/(J^{1/N}) \quad [5.28]$$

The transformation parameter K^* can be evaluated by minimizing the following function :

$$E = \sigma^2/(J^{2/N}) \quad [5.29]$$

here σ^2 is calculated from the transformed data.

The obvious advantage of this data transformation technique over the previously described methods is that only one experiment is enough to obtain an estimate of the kinetic parameters in the model. Although the technique also requires a direct search to be carried out on the transformation parameters, the dimension of the search is reduced and an initial estimate of the parameters is not needed. The inherent disadvantage associated with this technique is that an accurately measured final biomass concentration at stationary phase is required. This poses practical difficulties if the cultural time is long. Furthermore, the estimated parameters only represent the growth kinetics at the particular substrate concentration. It is known that many microbial systems exhibit a lag phase at the start of the growth. This lag phase is not dealt with by the Monod kinetics. The data transformation technique may give rise to poor fit to the experimental data if the lag phase is included. With consideration of these aspects, the data transformation method is only used for preliminary data examination.

5.4 Preliminary Growth Experiments

For practical convenience, preliminary experiments were carried out under aerobic conditions to investigate biomass measurement technique and cell growth yield on carbon sources. Some of the experiments were performed separately. The results of these experiments are presented below for later reference.

5.4.1 Measurement of Biomass Concentration

As described in the previous chapter, the optical density measurement at 590nm was chosen to serve as an indicator of the growth of *L. mesenteroides*. This approach has been shown to be rapid and reliable for the organism under investigation. To provide a common base for comparison of various experimental data, it is necessary to convert the optical density measurements into dry cell concentrations which are widely used in bioengineering field. For this purpose, a calibration curve was prepared from preliminary experimental results. The calibration data, presented graphically in Figure 5.2, shows a linear relationship between optical density and dry cell concentration for optical density measurements of less than 0.7. The relationship can be expressed by the following equation :

$$x = 0.26\ OD_{590nm} \qquad [5.30]$$

for $OD_{590nm} < 0.7$.

This is obtained by fitting a straight line to the data in the linear range by means of least squares method. A correlation coefficient of over 0.99 indicates a good linearity between the two variables. Similar to the statistical analysis method outlined for estimation of kinetic parameters in the previous section, the standard deviation of the estimated slope of the fitted line is

calculated. The ratio of the standard deviation to the estimated slope is less than 2%, indicating that the obtained proportionality between biomass concentration and optical density is a good estimate.

The calibration curve was initially obtained in one experiment which was performed in collaboration with two students (Howarth & Reynolds) who were doing a project in the same laboratory. The operating conditions of the experiment were the same as all other experiments. The original data was later supplemented by points gathered from several different experiments in which the dry cell weight of a sample was analyzed as a random check. These two sets of data are illustrated in different symbols in Figure 5.2, the square representing the original data, while the ring denoting the supplementing point. The basic strategy of calibration is to determine the optical densities of serial dilutions of a large sample, the dry cell concentration of which is to be measured. Details of the calibration procedure and results are given in Appendix D.

To make best use of optical density measurements, equation [5.30] suggests that culture samples should be appropriately diluted to bring the optical density readings within the lower linear range. It should also be noted that determination of optical density immediately after sampling is necessary to minimize experimental error. It is known that when measuring optical density of living cultures, the increasing motility of the cells, motivated by the presence of the light beam, causes the spectrophotometer reading to fluctuate. It is thus necessary to add a germicidal compound to the cell suspension before measuring the optical density. The use of 0.5% gluteraldehyde solution as the diluting liquid serves this purpose. This treatment has been found useful for stabilizing the optical density.

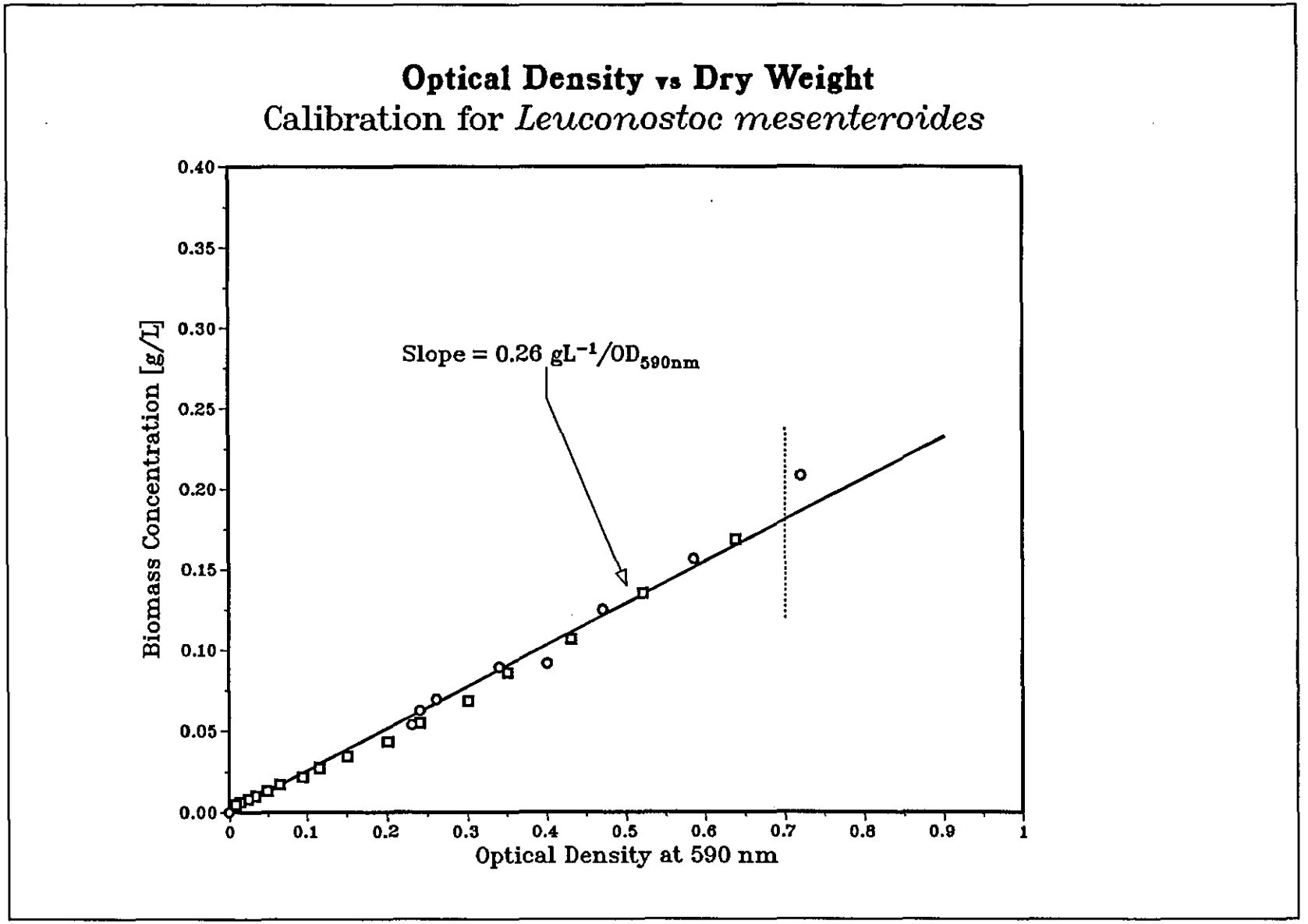
Optical Density vs Dry Weight
Calibration for Leuconostoc mesenteroides
Slope = 0.26 gL⁻¹/OD590nm
Biomass Concentration [g/L]
Optical Density at 590 nm
0.00
0.05
0.10
0.15
0.20
0.25
0.30
0.35
0.40
0
0.1
0.2
0.3
0.4
0.5
0.6
0.7
0.8
0.9
1

Figure 5.2

5.4.2 Aerobic Growth Yield on Sucrose

When the growth rate of a cell population is related to limiting substrate by a relationship such as the well-established Monod equation [5.1], definite connections emerge among reactor operating conditions and microbial kinetic and stoichiometric parameters. It has been observed frequently that the amount of biomass formed by cell growth is in proportion to the amount of substrate consumed. This relationship is usually expressed in terms of the growth yield coefficient, which is defined as :

$$Y_{x/s} = (\Delta x)/(\Delta s) \qquad [5.31]$$

where Δx is the increase in biomass concentration consequent on utilization of the amount of substrate Δs. For concision and clarity, $Y_{x/s}$ is usually designated as Y_s. A more rigorous definition of the growth yield, introduced in equation [5.12], is given by :

$$Y_s = -\, dx/ds \qquad [5.32]$$

The growth yield coefficient is important as a means of expressing the quantitative nutrient requirement of an organism. It plays a critical role in formulating bioreactor material balances and making most effective and systematic use of reaction kinetics. The growth yield is especially useful if it is approximately constant for the cultivation system concerned. A constant yield coefficient means that knowledge of either the biomass concentration or the substrate concentration change suffices to determine the other quantity, thus eliminating one variable in reactor design calculations. The stoichiometric relationship which a constant yield factor provides is also potentially useful for bioreactor monitoring since measurement of substrate concentration implies a corresponding estimate of the cell concentration or vice versa if initial values of both quantities are known.

Strictly speaking, not all of the substrate taken up from the medium by an organism is incorporated into the cell mass. The substrate, especially carbon source, also provides the energy necessary for cell synthesis and cell maintenance (or endogeneous metabolism) which is not directly related to or coupled with the synthesis of more cells. Recognized maintenance functions include active transport of ions and other substances across cell membranes to maintain concentration gradients between the cell and its environment, replacement synthesis of decayed cell constituents, and cell motility. For chemoheterotrophs like *L. mesenteroides* growing in a minimal medium which provides only the essential nutrients, a single substrate often serves as both carbon and energy source, so that the total substrate utilization Δs in equation [5.31] may contain three parts: Δs_a for assimilation, Δs_g for growth energy, and Δs_m for maintenance energy. That is to say:

$$\Delta s = \Delta s_a + \Delta s_g + \Delta s_m = \Delta s_a + \Delta s_e \qquad [5.33]$$

Thus, the growth yield defined by equation [5.31] only represents the overall growth yield coefficient. It does not distinguish assimilation and dissimilation of substrate. While the precise proportion of the part of the carbon source which is assimilated into cellular material to that part which is dissimilated to provide energy is often unknown in a minimal medium, the carbon source in a complex medium is almost completely dissimilated for energy production. Therefore, the growth yield coefficient is often expressed in terms of the energy source consumed. Evidence has shown that growth yield is directly proportional to the amount of energy produced in the form of ATP (adenosine triphosphate), the known intermediate energy carrier of the cell.

A large number of factors influence the growth yield of a given cultivation system. These include the composition of the medium, the pH and temperature, as well as the specific growth rate and cell maintenance

which is characterized by the maintenance coefficient. The impact of growth rate on the yield coefficient is minimal when the maintenance coefficient is small. However, organisms with large maintenance coefficients will exhibit a rapid decline in the yield coefficient as the specific growth rate decreases. Further factors include the dissolved oxygen concentration, ionic strength, trace element deficiency, and the presence of inhibitors. Above all, the metabolic pathway of the substrate utilization determines the growth yield.

Theoretically, the biomass yield coefficient on the limiting substrate is assumed to be constant if the growth of the cells follows the Monod kinetics. In a batch culture operated under constant environmental conditions, the following relationship can be derived :

$$x - x_0 = Y_s(s_0 - s) \qquad [5.34]$$

where x_0 and s_0 are the initial biomass and substrate concentrations respectively and x and s are the corresponding concentrations during the growth of the culture. When the culture reaches its maximum biomass concentration, x_{max}, the growth-limiting substrate is assumed to be depleted, i.e. s = 0. Thus, we have :

$$x_{max} = x_0 + Y_s s_0 \qquad [5.35]$$

Considering the fact that inoculum is always prepared so that the growth is at the exponential phase rather than at the stationary phase when transferring to the main culture, it is possible that considerable amount of limiting substrate in the inoculum remains. To simplify the case, let s_0 be the total limiting substrate present in the inoculum and the main culture medium, thus equation [5.35] reduces to:

$$x_{max} = Y_s s_0 \qquad [5.36]$$

Equation [5.36] constitutes the basis for experimental yield determination. For the growth-limiting substrate, a plot of x_{max} against s_0 should be a straight line passing through the origin with slope Y_s. It should be emphasized here that s_0 is the total limiting substrate concentration.

The implications of equation [5.36] are worth considering. An increase in the initial substrate concentration should result in a proportional increase in the maximum final biomass concentration attainable. If the experimental data shows a linear relationship between x_{max} and s_0, the first conclusion will be that the energy source is limiting the growth indeed, at least for the range of substrate concentrations concerned. Thus, the growth-limiting substrate can be experimentally identified by yield analysis. If the x_{max} *vs* s_0 plot yields a curve that intersects the ordinate at a positive value, a small amount of unknown energy source may be present in the medium. However, if the plot shows a curve with an inflection point, it may be that the cell metabolism is different at lower and higher concentrations of the substrate.

A series of batch culture experiments were carried out under aerobic conditions using fermentation medium F (see section 4.1.2) at low sucrose concentrations which are suitable for enzyme production (sucrose concentration < 3%). Cell growth was monitored by determining the optical density of culture samples. The final biomass concentration was calculated as an average of two samples taken from the culture when growth had reached completion, typically after 24 hours from inoculation. Taking into account all the sucrose-equivalent sugars in the inoculum used, the experimental results in the form of an x_{max} *vs* s_0 plot are presented in Figure 5.3. Details of yield determination are given in Appendix E.

The growth medium used in these experiments is formulated according to a rough stoichiometric analysis of the bacterial composition, so that neither nitrogen nor phosphate should be limiting cell growth. Sucrose is

believed to be the growth-limiting substrate at low concentrations. It can be seen from Figure 5.3 that this assumption is consistent with the experimental findings since a linear relationship exists between the maximum biomass concentration and the total initial substrate concentration. A straight line is thus fitted to the data for substrate concentrations below 30 g/L by the method of least squares. The correlation coefficient of the fitted line is over 0.99, indicating an excellent linear fit. However, the straight line does not pass through the origin, as implied by equation [5.36]. Rather, at zero substrate concentration, it intersects the origin at a positive value for biomass concentration, as shown in Figure 5.3. This reveals the possible presence of a small but significant amount of unknown energy source upon which the organism can grow in the absence of the limiting substrate in the medium.

By analyzing the medium composition, it is believed that the high concentration of yeast extract used in the medium is the cause of this "blank" growth. Yeast extract in the medium is used mainly as a nitrogen source. It also serves as a comprehensive source of growth factors because it contains a wide range of amino acids, vitamins and inorganic salts. Although the exact chemical makeup of the yeast extract is unknown, over 10 per cent of carbohydrates are usually present, including glycogen, trehalose and pentoses, among which trehalose and some pentoses are known carbon sources for *L. mesenteroides*. Thus it is clear that about 4 grams per litre potential carbon sources are available to the metabolism of cells in the medium. The amount of carbohydrate contributed to cell growth in the yeast extract can be estimated from the yield plot by dividing the intercept on the ordinate by the slope of the line; a value of about 1.9 g/L is obtained. This estimate suffers the greatest error because the magnitude of growth at extremely low substrate concentrations is too small to measure accurately.

It was expected that the linear relationship between the final biomass

concentration and the initial substrate concentration in batch cultures cannot hold for high sucrose concentrations because other components in the medium may be exhausted and cause the growth of the cell mass to stop before the high sucrose concentration falls to the limiting level. This was reflected in the experiments which were performed at high sucrose concentrations. The growth yield decreased as the initial sucrose concentration was high.

Therefore, for the range of substrate concentrations suitable for dextransucrase synthesis, the biomass yield coefficient under aerobic conditions is estimated to be about 0.15 g biomass/g sucrose, i.e.

$$Y_s = 0.15 \text{ g biomass/g sucrose} \qquad [5.37]$$

which is the slope of the fitted line in Figure 5.3. The standard error of the yield coefficient, calculated as a measurement of the goodness of the data regression, is about 4% of the obtained yield value. Thus, the yield coefficient can be used with confidence.

Estimation of Yield Coefficient

Aerobic Growth of *Leuconostoc mesenteroides* on Sucrose

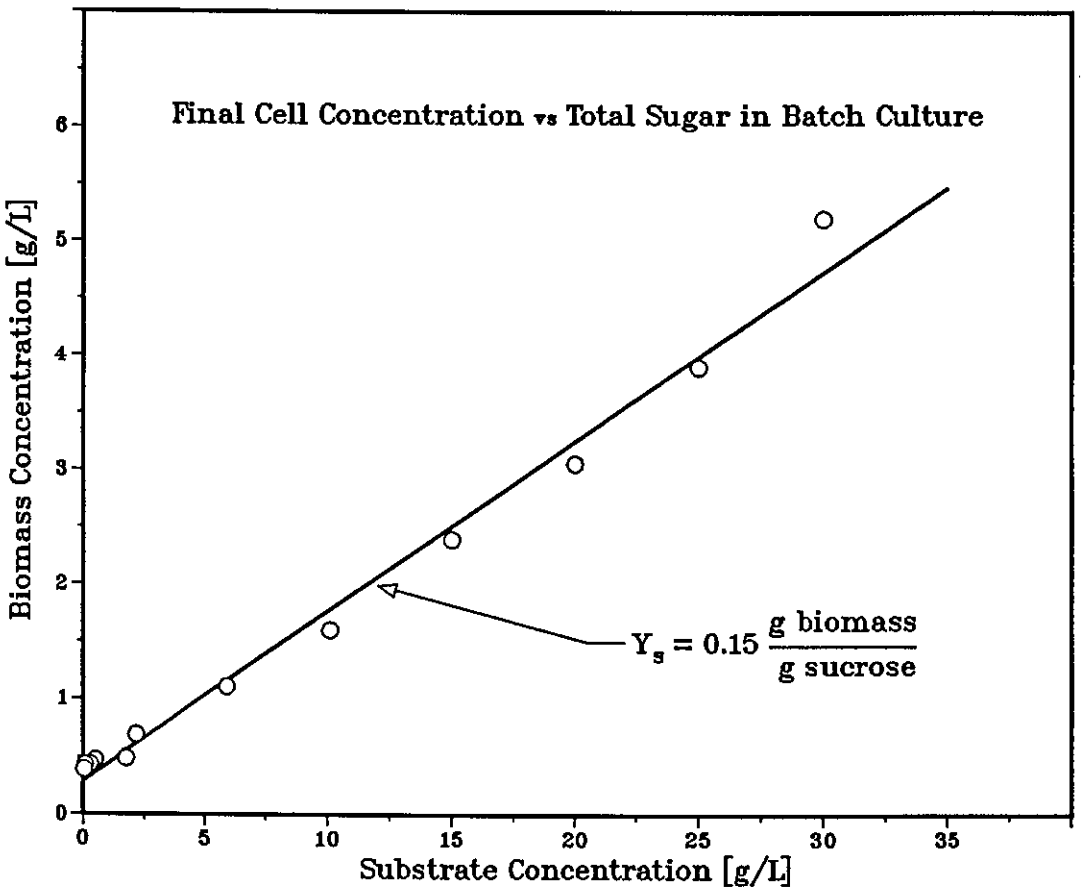

Figure 5.3

5.5 Determination of Specific Growth Rates

In order to model a process and determine the model parameters with statistical significance, it is very important that the experiments are properly designed. For studies of microbial growth kinetics, the specific growth rates must be obtained accurately. For this purpose, the continuous culture seems to be the choice. In an ideal continuous-flow stirred-tank reactor (CSTR), known as chemostat when used for cultivation of cells, a self-regulating steady state can be established. In the steady state, the specific growth rate of the biomass is determined by the medium flow rate, or rather, equal to the dilution rate when the medium feed stream consists only of sterile nutrient. Therefore it is possible to fix the specific growth rate of the cell at any value from zero to the maximum in chemostat cultures, thus enabling straightforward kinetics determinations. Another important feature in a chemostat is that the cell population can adjust to a steady environment and achieve or closely approximate a state of balanced growth, which is more difficult to achieve routinely in batch cultures as described before. However, as compared with batch cultivations, the equipment required for chemostat experiments is more expensive and more complicated. For instance, keeping a constant medium flow rate and maintaining a constant working culture volume would be a formidable control task. Furthermore, achieving steady-state conditions in a chemostat may take hours or even days, magnifying the possibility of contamination which ruins the experiment. Another problem concerns the difficulty of accounting properly for the considerable wall growth in chemostat cultures. Finally, a kinetic model based on steady-state chemostat data may not be appropriate when the model is intended mainly for batch processes.

In view of these arguments, and for practical considerations, continuous culture was not used for obtaining kinetic data. Most experiments were carried out in batch method. A special substrate-feed technique based on

batch culture was also investigated for determining the specific growth rates.

5.5.1 Aerobic Batch Culture

As commonly adopted in kinetic studies, the fermenter is presumed to be well stirred and sufficiently aerated so that cultural conditions are effectively homogeneous throughout the vessel, and dissolved oxygen in the fermenter is always maintained above the limiting level. This approximation can be met satisfactorily in laboratory-scale fermenters.

In a simple homogeneous batch culture, the concentrations of nutrients, cells and metabolic products vary with time as growth proceeds. To reflect the different changes in the cell and its environment, growth is commonly divided into several phases. After a lag period, where no increase in biomass is evident, and a brief accelerating phase, growth usually occurs at the maximum rate and finally decelerates and ceases due to either nutrient exhaustion, or accumulation of an inhibitory product or some change in the physical environment. After the cell population reaches its maximum size, there may be a stationary phase where the amount of biomass remains constant. The biomass concentration may eventually decline as a result of maintenance metabolism or autolysis.

Since the Monod model and other single-substrate kinetic models deal with only the exponential and decelerating growth phases, the exponential growth of a cell population is the major concern in kinetic experiments. To a reasonable approximation, growth is balanced during this stage of batch cultivation. A material balance on the biomass in a batch culture gives :

$$\frac{d}{dt}(Vx) = Vr_x \qquad [5.38]$$

where V is the culture volume (litre), r_x is the volumetric growth rate expressed as the amount of biomass formed by cell growth per unit volume per unit time ($gL^{-1}hr^{-1}$). If no liquid is added to or removed from the fermenter and if gas stripping of culture liquid is negligible, then the culture volume V is constant, and equation [5.38] reduces to :

$$\frac{dx}{dt} = r_x = \mu x \qquad [5.39]$$

The specific growth rate μ changes with the environment, particularly with the concentration of the limiting substrate as suggested by the Monod kinetics. However, the initial specific growth rate μ_0 which corresponds to the initial substrate concentration s_0 at the beginning of the culture after the lag phase can be considered as being constant for a small time interval. Thus, on integration of equation [5.39] with a constant μ_0, we have :

$$\ln(x) = \ln(x_0) + \mu_0 t \qquad [5.40]$$

where x_0 is the biomass concentration when exponential growth starts. Equation [5.40] suggests that the plot of ln(x) against time will be a straight line with slope μ_0. This exponential relationship is only valid in the exponential growth phase. The duration of the exponential growth phase depends on the initial substrate concentration as well as the kinetic behaviour of the cell population. If the experiment shows a long exponential growth phase, the first conclusion would be that substrate limitation may not significantly affect the growth kinetics. This should give a rough idea of the cell kinetic behaviour.

A series of batch experiments were carried out in the bench-top fermenter, normally with 1.5 litre working volume. Medium F defined in section 4.1.2 was used as the main fermentation medium with varying initial

sucrose concentrations. The experimental method was as discussed in section 4.2. The culture was controlled at pH 6.7 and temperature 23 °C.

After inoculation, aeration was applied to keep a high dissolved oxygen concentration in the medium. The growth was followed by optical density measurements of samples taken at least once an hour. The growth usually approached the stationary phase about 10 hours after inoculation when sufficient inoculum was used. The experimental results, converted to biomass concentrations, are presented in Appendix F.

From the results obtained for each initial sucrose concentration, which was corrected for the hidden carbohydrates in yeast extract, a natural logarithmic relationship between biomass concentration and culture time was plotted. The time intervals, for which the plot had a nearly linear shape, were approximated to a straight line by least squares fit. From its slope the initial specific growth rate μ was determined for each initial substrate concentration. It was noted that the length of the lag phase, which was usually short, if properly identified, did not affect the specific growth rate by least squares linear regression on the semilogarithmic growth curve in the exponential phase. Details of the calculation can also be found in Appendix F.

5.5.2 Constant-Substrate Fed-Batch Culture

If the growth of a microorganism follows a population-independent form of kinetics such as the Monod equation, a controlled addition of fresh nutrient medium to a batch culture could be used to establish a constant substrate concentration in the vessel and presumably therefore a constant metabolic rate of metabolism by the culture. The constant rate could be maintained at the optimum by maintaining the substrate at the proper level for a relatively long time, thus enabling accurate determination of the growth rate. Theoretically, it can be shown that the rate of substrate addition must be an exponential function of time if the specific growth rate is the controlled metabolic characteristic.

Suppose that a batch culture is continuously fed with sterile nutrient medium at a volumetric flow rate of F which is regulated so that the concentration of the limiting substrate in the fermenter remains constant throughout the cultivation process. Assuming also that no culture broth is withdrawn until after the fermentation is completed, then the material balances on the cell mass and the limiting substrate may be written in the following forms, respectively.

$$\frac{d}{dt}(xV) = \mu xV \qquad [5.41]$$

$$\frac{d}{dt}(sV) = Fs_{in} - \frac{\mu xV}{Y_s} \qquad [5.42]$$

where μ is the specific growth rate, and is, in general, a function of the substrate concentration, s_{in} is the concentration of the limiting substrate in the entering feed stream, and V is the culture volume which is continuously changing due to substrate addition. Assuming that the densities of the entering liquid stream and of the culture broth are approximately the same,

and that the density does not change significantly with time during fermentation, then a total mass balance on the fermentation contents leads to :

$$\frac{dV}{dt} = F \qquad [5.43]$$

The assumption of substrate concentration being constant gives the following pseudo-steady state equation :

$$\frac{ds}{dt} = 0 \qquad [5.44]$$

which indicates that the specific growth rate is constant. Thus equation [5.41] can be integrated between the initial time and an arbitrary culture time t, giving

$$xV = x_0 V_0 e^{\mu t} \qquad [5.45]$$

where x_0 and V_0 represent the initial biomass concentration and culture volume, respectively.

Carrying out the differentiation indicated on the left-hand side of equation [5.41], substituting for dV/dt using equation [5.43], ds/dt using equation [5.44], and xV using equation [5.45], and rearranging the results yields :

$$F = \frac{\mu x_0 V_0 e^{\mu t}}{Y_s(s_{in} - s)} \qquad [5.46]$$

Equation [5.46] shows that the nutrient feeding flow rate should increase exponentially in proportion to the growth of cells. Substituting F into equation [5.43] and integration gives :

$$V/V_0 = \{1 - \frac{x_0}{Y_s(s_{in}-s)}\} + \frac{x_0 e^{\mu t}}{Y_s(s_{in}-s)} \qquad [5.47]$$

It can be seen from this equation that the culture volume also increases in an exponential fashion. From equation [5.45], we obtain :

$$x/x_0 = \{(1 - \frac{x_0}{Y_s(s_{in}-s)}) + \frac{x_0 e^{\mu t}}{Y_s(s_{in}-s)}\}^{-1} e^{\mu t} \qquad [5.48]$$

Analysis of equation [5.48] shows that the biomass concentration approaches $Y_s(s_{in}-s)$ when the culture time approaches infinity, i.e.

$$\lim_{t\to\infty} x = Y_s(s_{in} - s) \qquad [5.49]$$

By defining

$$x_{fm} = Y_s(s_{in} - s) \qquad [5.50]$$

and

$$z = x/x_{fm} \qquad [5.51]$$

equation [5.48] becomes

$$z = \{1 + [(1-z_0)/z_0]e^{-\mu t}\}^{-1} \qquad [5.52]$$

or

$$\ln\{z/(1-z)\} = \ln\{z_0/(1-z_0)\} + \mu t \qquad [5.53]$$

Equation [5.52] shows that the biomass concentration in the fermenter increases with time in a sigmoidal curve of the logistics type. Equation [5.53] suggests that a linear plot of ln[z/(1-z)] against culture time t should give the specific growth rate μ, which is dependent on the substrate concentration s, by its slope.

Although the process employing such an exponential substrate-feed

scheme is inherently transient because of the accumulation of cells and medium in the fermenter, the pseudo-steady state conditions of constant environment and constant metabolism can be maintained over many generations. Hence, the linear relationship, shown in equation [5.53] between the transformed variable ln[z/(1–z)] and culture time t, may be valid for a large time interval, thus providing an accurate way for growth rate determination. This technique would be a significant improvement on batch cultures if properly implemented, especially in the case of large saturation constants which have important effect on cell kinetics.

In theory, the substrate feed stream has been shown to follow an exponentially increase flow pattern if the substrate concentration in the fermenter is to be maintained constant. However, it is difficult to obtain an exponential flow rate in practice. For the culture system being investigated, it has been observed from proprietary industrial fermentations that there exists an approximate linear relationship between the amount of substrate as sucrose consumed and the amount of sodium hydroxide added to the fermenter to maintain a fixed pH of 6.7 at temperature 23 °C. The fermentations revealed that one mole of sucrose consumed would require addition of 1.4 moles of sodium hydroxide to keep pH constant at 6.7. This relationship may thus provide an indirect means of controlling a constant sucrose concentration in the fermenter by regulating the pH while simultaneously supplying fresh sucrose medium to compensate consumption of the substrate in the fermenter.

A special fed-batch system was designed for this purpose. Basically, this substrate-feed system was a modification to the alkali pH control used in batch cultures. Sucrose was mixed with sodium hydroxide to a specific ratio determined from the above described relationship. A fixed pH of 6.7 was set for the fermentation as usual. As the fermentation broth became acidic due to consumption of sucrose by the cells, the alkali/sucrose mixture was added.

Therefore, pH and substrate concentration can be maintained at predetermined levels respectively.

Letting R denote the sucrose consumption to NaOH addition ratio and M denote the molarity of NaOH in the feeding mixture of substrate and base, the material balance on sucrose in the fermenter, generally described by equation [5.42], takes the following form :

$$\frac{d}{dt}(sV) = Fs_{in} - 40MFR \qquad [5.54]$$

where the sucrose consumption to base addition ratio R is given by :

$$\begin{aligned} R &= 1 \text{ mole sucrose}/1.4 \text{ mole NaOH} = 342/56 \\ &= 6.1125 \text{ g sucrose/g NaOH} \end{aligned} \qquad [5.55]$$

By substituting the total mass balance equation [5.43] and the pseudo-steady state equation [5.44] into equation [5.54], the following relationship between s_{in} and s can be obtained :

$$s_{in} = 40MR + s = 244.5M + s \text{ (g/L)} \qquad [5.56]$$

Thus, the maximum biomass concentration attainable in such a system would be :

$$x_{fm} = Y_s(s_{in} - s) = 244.5MY_s \qquad [5.57]$$

It was noted from equation [5.56] that the sucrose concentration in the entering stream was proportional to the molarity of NaOH. A high concentration of NaOH would correspond to a high sucrose concentration, thus making dissolution of substrate difficult. Furthermore, high concentrations of sucrose and NaOH would result in serious caramelization

when mixed together. In view of these problems, one molarity of sodium hydroxide solution was used in this culture method for pH control, i.e. M = 1. Therefore, for Y_s = 1.5 g biomass/g sucrose, we have :

$$s_{in} = 244.5 + s \quad (g/L) \qquad [5.58]$$

$$x_{fm} = 244.5 \times 0.15 = 36.675 \quad (g/L) \qquad [5.59]$$

A series of experiments for determination of specific growth rates were carried out by using the above described fed-batch technique. The initial culture volume was 1 – 1.2 litre so that additional medium can be accommodated in the fermenter. The preparation and monitoring procedures were basically the same as discussed in section 4.2. In order to prevent caramelization, the following procedure was adopted when preparing the feeding mixture of sucrose and NaOH according to the composition determined above.

The mixture was prepared as two separate solutions.

(a) 40 grams (1 mole) of NaOH were dissolved in distilled water to make up 200 mL solution.

(b) s_{in} was calculated according to equation [5.58], where s is the sucrose concentration to be used in the fermenter. The amount of sucrose required was dissolved in distilled water to make up 800 mL solution.

The above solutions were sterilized separately at 121 °C for 15 minutes. They were then allowed to cool before mixing together aseptically, usually before inoculation.

The temperature of the culture was set at 23 °C, and the pH was set at 6.7. As the fermentation proceeded, the pH of the culture broth declined as a

result of organic acid production by the metabolism of *L. mesenteroides*. The pH control action was accompanied by sucrose addition so that an approximate constant level of limiting substrate was maintained in the fermenter. For practical reasons, the substrate-feeding system was usually shut off after about 10 hours growth.

For each sucrose concentration employed in the experiments, a correction was made for the carbohydrates contained in yeast extract. The growth data was transformed and plotted using equations [5.51], [5.53] and [5.59]. The specific growth rate corresponding to the sucrose concentration in the fermenter was determined by the slope of the regression line in the range where the plot has a nearly linear shape. The experimental results showing the growth curve and calculation of growth rate are given in Appendix G.

5.6 Kinetic Analysis of Growth Data

The modelling process usually proceeds in a parallel manner. After an experiment has been carried out, preliminary analysis of the results is taken. If the experimental data deviates greatly from the desired model, more experiments are required. Properly distributed data points within the range of interest reduces the number of experiments needed. About ten points should be enough to allow accurate estimation of the model parameters.

For the fermentation system under investigation, kinetic analysis was usually carried out after a growth experiment to choose the substrate concentration to be used in the next experiment so that a proper spread of data points is obtained. Of the kinetic data obtained from the batch and fed-batch cultures, preliminary examination did not give a clear indication of what equation form the growth rate follows because the specific growth rates showed great scatter. For substrate concentrations of lower than 10 g/L, the experimental data actually exhibited a substrate inhibition pattern. Although reasonable fit was obtained for these points by using models describing substrate inhibition, further experiments at higher substrate concentrations rejected these models. Duplicate determinations of the specific growth rate also showed large discrepancy of the data. On the whole, the Monod model emerged to be appropriate for describing such a system.

The experimental results are presented in Table 5.1. The data is analyzed using the Monod kinetic equation [5.1] by employing the statistical method described in section 5.3.2. Table 5.1 summarizes the values of the estimated model parameters and the results of the statistical analysis. A plot of specific growth rate against substrate concentration is shown in Figure 5.4. The solid line in Figure 5.4 represents the Monod relationship [5.1] calculated after substitution of the estimated parameters, μ_{max} and K_s, determined by means of direct least squares search. It can be seen from the

plot that the agreement between the predicted and the observed values is not particularly good, underlining the complex nature of the biological system. The greatest discrepancy appears at low substrate concentrations. This seems to be due to the small range of variations in the cell concentration which can lead to errors. Another plausible explanation would be that the method of determining the specific growth rate by approximating the slope of a straight line may have introduced further errors.

However, the model is considered to accord fairly well with the experimental data if the peculiar high and low points are discarded. This is supported by the fact that the calculated standard deviations of the estimated parameters and the variance are very small. The standard deviation of μ_{max} is less than 2% of the estimated value, while the standard error of K_s is only 0.09% of the estimated saturation constant value. The estimated constants can be rounded to give a reasonable μ_{max} value of 0.5 hr^{-1} and a reasonable K_S value of 0.9 g/L. The Monod equation does correlate the experimental data, but deviations in industrial growth experiments are to be expected.

It was noted from the yield experiments that sucrose may not be the limiting substrate when its concentration in the fermenter is high. This was confirmed by batch cultures carried out at high sucrose concentrations (>40 g/L). In these experiments, the initial exponential growth phase did not last as long as supposed, and the maximum cell concentration did not reach the value as predicted from the biomass yield coefficient. However, the initial specific growth rates of cells at these high sucrose concentrations were almost constant, thus providing an estimate of the maximum specific growth rate in the Monod model.

The estimated saturation constant was found to be below the smallest substrate concentration used in the experiments. Parameter estimation using lower substrate concentrations poses difficulties in practice. By the

characteristic of the Monod equation, specific growth rates at lower substrate levels will contribute very little to the fitted curve because the curve is assumed to go through the origin, and the variances of these specific growth rates will be large enough to accommodate a wide range of initial values of the specific growth rate. Therefore, very low substrate experiments will be of little help in determining the kinetic parameters.

The data transformation technique discussed in section 5.3.3 was also used for estimating kinetic parameters in batch cultures. This method did not give consistent estimates of the parameters. In some cases, using this technique resulted in unreasonable, or even meaningless parameter values. The method was also extremely sensitive to the data points selected. Excluding an apparent lag phase led to significantly different parameter estimates, while the goodness of the fit, assessed by the variance, was not much improved. An example of this technique, which gives comparable results, is presented in Appendix H.

Table 5.1 Statistical Analysis of Growth Kinetic Data

Substrate concentration (g/L)	Specific growth rate (hr^{-1})
2.0000	0.2850
2.4000	0.3520
2.9000	0.4320
4.4000	0.5140
5.9000	0.4700
6.9000	0.5050
9.4000	0.4570
11.9000	0.4310
11.9000	0.4890
16.9000	0.4550
21.9000	0.5030
31.9000	0.4650
41.9000	0.5030
51.9000	0.5260
101.9000	0.5220

Estimation of Kinetic Parameters by Least Squares Search :-

Maximum specific growth rate	=	0.5171
Standard deviation of μ_{max}	=	0.0096
95% confidence interval	=	0.4964 , 0.5379
Saturation constant	=	0.9019
Standard deviation of K_s	=	0.0008
95% confidence interval	=	0.9001 , 0.9037
Sum of squares of deviation	=	0.0229
Variance	=	0.0018

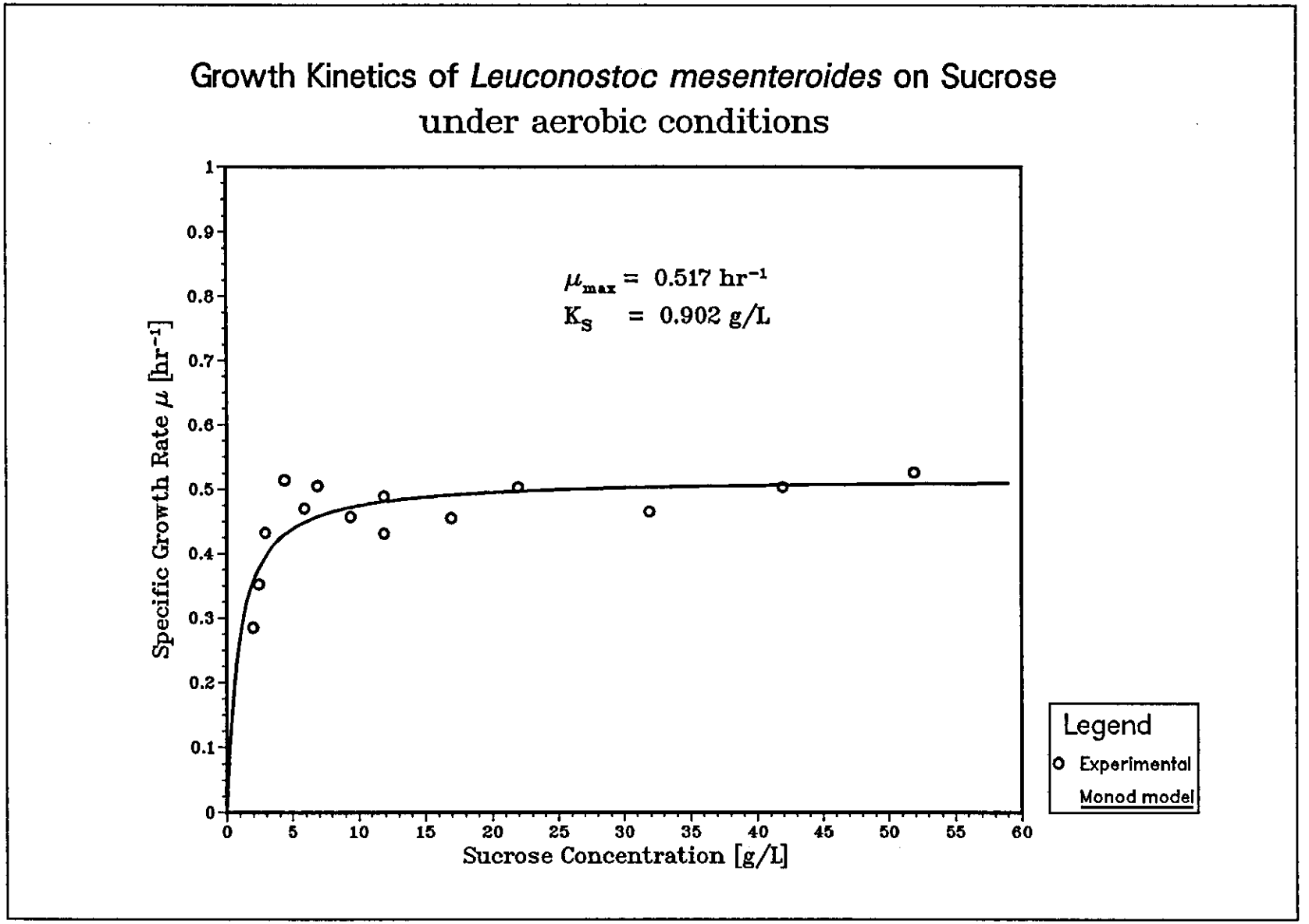
Growth Kinetics of Leuconostoc mesenteroides on Sucrose under aerobic conditions
μ_{max} = 0.517 hr^{-1}
K_S = 0.902 g/L
Specific Growth Rate μ [hr^{-1}]
Sucrose Concentration [g/L]
0
0.1
0.2
0.3
0.4
0.5
0.6
0.7
0.8
0.9
1
0
5
10
15
20
25
30
35
40
45
50
55
60
Legend
Experimental
Monod model

Figure 5.4

Chapter 6 Effect of Oxygen on Cell Growth

For aerobic bioprocesses such as the *L. mesenteroides* fermentation being investigated it is evident that in addition to other substrates, oxygen could also be growth limiting. In aerobic metabolism, oxygen acts as the ultimate electron or hydrogen acceptor. This process is mediated by an oxidase enzyme. In a batch fermentation the course of cell growth is significantly influenced by the oxygen transfer rate, quantified by the volumetric oxygen transfer coefficient K_La. The experimental examination of this effect is complicated by the fact that *L. mesenteroides* is a facultative anaerobe. In the oxygen-limited state the metabolism of *L. mesenteroides* can be a combination of aerobic and anaerobic metabolism. The anaerobic process causes accumulation of ethanol which inhibits cell growth. In addition, the time required for the transition from fully aerobic growth to fully anaerobic growth is not known. Therefore, it is difficult to examine the cell growth closely in a simple approach.

6.1 Modelling Approaches

6.1.1 Non-interactive Model

Kinetic modelling has been successfully aided by the concept of non-interaction. A non-interactive model is one in which the specific growth rate is only limited by one substrate at a time. The growth rate is equal to the lowest rate that would be predicted from the separate single-substrate model. If the Monod kinetics [5.1] is assumed for cell growth either on oxygen or on a carbon source, then only the substrate which predicts the lowest cell concentration will enter into the kinetic model. The following equations thus apply in a batch culture.

$$\frac{1}{x}\frac{dx}{dt} = \mu = \mu_{max,s}\ \frac{s}{s + K_s} \qquad [6.1]$$

for $$\frac{s}{K_s} < \frac{C_l}{K_o} \qquad [6.2]$$

or $$x = x_s\ ,\ \text{if } x_s < x_o \qquad [6.3]$$

$$\frac{1}{x}\frac{dx}{dt} = \mu = \mu_{max,o}\ \frac{C_l}{C_l + K_o} \qquad [6.4]$$

for $$\frac{C_l}{K_o} < \frac{s}{K_s} \qquad [6.5]$$

or $$x = x_o\ ,\ \text{if } x_o < x_s \qquad [6.6]$$

The advantage of non-interactive model lies in the relative simplicity of the process equations obtained following the assumption that only one substrate is limiting the growth at a time. However, the models are discontinuous functions at the transition point from one limiting substrate to another. Furthermore, the models will predict high values of specific growth rate in the region where s/K_s and C_l/K_o are small.

6.1.2 Double-Substrate Interactive Model

In general, it is possible that the concentrations of two or more substrates can affect the overall cell growth simultaneously. The following section will demonstrate the mechanisms of double-substrate growth model.

6.1.2.1 Mechanisms of Cell Growth on Two Limiting Substrates

By analogy with enzyme kinetics (Michaelis-Menton mechanism), the following reactions of the biomass, X, with the growth-limiting substrates, S (Sucrose), and, G (Oxygen) are suggested.

dissociation constant
⇓

$$X + S \Longleftrightarrow XS \qquad K_s \qquad [6.7]$$

$$X + G \Longleftrightarrow XG \qquad K_g \qquad [6.8]$$

A ternary complex may be formed with both substrates attached to the cell.

$$XS + G \Longleftrightarrow XSG \qquad K_{sg} \qquad [6.9]$$

$$XG + S \Longleftrightarrow XSG \qquad K_{gs} \qquad [6.10]$$

$$XSG \rightarrow X + P \qquad [6.11]$$

is the rate-limiting process.

Assuming equilibria in the first four reactions, we have

$$K_s = [X][S]/[XS] \qquad [6.12]$$

$$K_g = [X][G]/[XG] \qquad [6.13]$$

$$K_{sg} = [XS][G]/[XSG] \qquad [6.14]$$

$$K_{gs} = [XG][S]/[XSG] \qquad [6.15]$$

Here square brackets are used to denote concentration of the substance indicated inside the brackets.

Decomposition of the complex XSG to biomass and product is considered to be irreversible with rate constant k.

$$v = k[XSG] \qquad [6.16]$$

is the rate of substrate breakdown.

The specific rate of substrate utilization is given by

$$q = v/x \qquad [6.17]$$

where the total biomass concentration x is equal to the sum of the concentration of free biomass plus the concentrations of the three complexes XS, XG, and XSG, i.e.

$$x = [X] + [XS] + [XG] + [XSG] \qquad [6.18]$$

By straightforward arithmetic manipulation of equations [6.12] to [6.18] we obtain

$$q = \frac{q_m}{1 + K_{sg}/[G] + K_{gs}/[S] + (K_gK_{gs} + K_sK_{sg})/2[G][S]} \qquad [6.19]$$

where $q_m = k$ is the maximum rate of substrate utilization, which is obtained when the biomass is saturated with substrates due to excess S an G.

Note that the equilibria of reactions [6.7] - [6.10] require

$$K_sK_{sg} = K_gK_{gs} \qquad [6.20]$$

Rearrangement of equation [6.19] gives

$$q = \frac{q_m^*}{[S] + K_s^*} \qquad [6.21]$$

where

$$q_m^* = \frac{q_m[G]}{[G] + K_{sg}} \qquad [6.22]$$

$$K_s^* = \frac{K_{gs}[G] + K_s K_{sg}}{[G] + K_{sg}} \qquad [6.23]$$

Thus equation [6.21] can be written in the form

$$q = \frac{q_m[S]}{[S] + K_s^*} \quad \frac{[G]}{[G] + K_{sg}} \qquad [6.24]$$

If Y is the growth yield, then the specific cell growth rate is

$$\mu = q/Y \qquad [6.25]$$

By substituting for the specific rate of substrate utilization, q, in terms of μ, we derive

$$\mu = \frac{\mu_m[S]}{[S] + K_s^*} \quad \frac{[G]}{[G] + K_{sg}} \qquad [6.26]$$

It can be seen from the above equation that if [G], for example, oxygen concentration, is maintained constant, the cell growth will follow the Monod kinetics. However, equations [6.22] to [6.26] show that the apparent maximum specific growth rate and saturation coefficient are dependent on [G], i.e. oxygen concentration.

The mechanism suggested here is the general case. It can be simplified by assuming

$$K_{gs} = K_s \qquad [6.27]$$

$$K_{sg} = K_g \qquad [6.28]$$

That is to say, reactions [6.7] and [6.10] have the same dissociation constant, K_g; also reactions [6.8] and [6.9] have the same dissociation constant, K_s. Therefore, equation [6.23] becomes

$$K_s^* = K_s \qquad [6.29]$$

and equation [6.26] will be

$$\mu = \frac{\mu_m[S]}{[S] + K_s} \quad \frac{[G]}{[G] + K_g} \qquad [6.30]$$

This is a double substrate Monod/Monod model under both oxygen and carbon limiting conditions. The reaction [6.11] in which product is derived from the biomass, carbon and oxygen complex indicates the aerobical oxidative metabolism of organisms such as *Leuconostoc mesenteroides*. Therefore, theoretically, equation [6.30] might describe the behaviour of the organism under aerobic cultural conditions.

The quasi-steady state assumption upon which the model is derived may be only valid provided that the biomass yield is sufficiently small.

The three parameters in the model can be estimated separately. When the concentration of oxygen in the cell culture is far greater than the saturation coefficient for oxygen, the growth kinetics becomes a single-substrate Monod model for sucrose, the carbon source for growth of

L. mesenteroides. If [S] is large enough, the single-substrate Monod model can be used to describe the oxygen effect on cell growth.

The double-substrate growth model (called a Megee-type in literature) is used in the study of oxygen effect on growth of *Leuconostoc mesenteroides*.

6.2 Kinetic Formulation of Batch Process

Assuming the fermenter is well mixed. If endogeneous metabolism and cell death are neglected, material balances in a batch culture may be written as follows

Biomass balance

$$\frac{dx}{dt} = r_x \qquad [6.31]$$

Carbon substrate balance

$$\frac{ds}{dt} = -\frac{r_x}{Y_s} \qquad [6.32]$$

Dissolved oxygen balance

$$\frac{dC_l}{dt} = K_L a(C_g - C_l) - r_x/Y_o \qquad [6.33]$$

Here the growth rate r_x depends on the specific growth rate μ of cells and its functional form is determined by the particular kinetic model adopted. In this case

$$r_x = \mu x = \mu_{max} x \frac{s}{s + K_s} \frac{C_l}{C_l + K_o} \quad [6.34]$$

$$\mu = \mu_{max} \frac{s}{s + K_s} \frac{C_l}{C_l + K_o} \quad [6.35]$$

In these equations, x, s, C_l are the cell, substrate, and dissolved oxygen concentrations, respectively. K_La is the volumetric oxygen transfer coefficient and C_g is the concentration of oxygen in the liquid phase which would be in equilibrium with the sparged air. Y_s and Y_o are the biomass yields based on substrate and oxygen consumptions, respectively.

The maximum specific growth rate μ_{max} and saturation coefficient for substrate K_s are attained from the aerobic growth model which is a single-substrate Monod-type.

μ_{max} = 0.5 hr^{-1}
K_S = 0.9 gL^{-1} sucrose

and

Y_S = 0.15 (g biomass)/(g sucrose)

under operating conditions, i.e. at a temperature of 23 °C and pH of 6.7. C_g is assumed to be the oxygen solubility in pure water at the same temperature and 1 atm although this value is generally greater than the true concentration.

$$C_g = 8.8 \times 10^{-3} \ gL^{-1}$$

The dissolved oxygen is measured electronically by the oxygen probe. It is convenient to express C_l in terms of electrode readings or dissolved oxygen tension. Thus C_g is the initial calibrated point.

C_g = 100 % air saturation

Normalizing the equations by introducing a dimensionless variable

$$C_{lf} = C_l/C_g \qquad [6.36]$$

We have the following equations

$$\frac{dx}{dt} = r_x \qquad [6.37]$$

$$\frac{ds}{dt} = -r_x/Y_s \qquad [6.38]$$

$$\frac{dC_{lf}}{dt} = K_La(1 - C_{lf}) - r_x/Y_o^* \qquad [6.39]$$

and

$$\mu = \mu_{max} \frac{s}{s + K_s} \frac{C_{lf}}{C_{lf} + K_o^*} \qquad [6.40]$$

$$r_x = \mu x \qquad [6.41]$$

where

$$Y_o^* = C_g Y_o \qquad [6.42]$$

$$K_o^* = K_o/C_g \qquad [6.43]$$

Generally cell growth exhibits a lag phase after inoculation. If an inoculum is not taken from a culture in the exponential growth phase but in the stationary phase or from a culture with a qualitatively different medium or under different conditions, the synthetic enzymes must be induced. A lag phase with slowly increasing specific growth rate is the result of this

adaptation process. The duration of the lag phase is hard to predict. Mathematically, it depends on the inoculum size but not on the initial substrate concentration.

By incorporating a lag time t_L into the rate equation, a more general case is obtained.

$$r_x = 0 \text{ , where } x = x_0 \text{ , for } 0 \leq t < t_L \qquad [6.44]$$

$$r_x = \mu x \text{ , for } t \geq t_L \qquad [6.45]$$

6.3 Estimation of Volumetric Oxygen Transfer Coefficient

The fermenter is operated at an agitation speed of 400 rpm and an aeration flow rate of about 4 VVM (volume gas per volume liquid per minute). The volumetric oxygen transfer coefficient K_La is estimated both with and without cell growth under such conditions.

6.3.1 Measurement of K_La Value in Absence of Cells

The volumetric oxygen transfer coefficient K_La with air-sparged water or fermentation medium without cell growth is determined by direct measurement of the rate of increase in dissolved oxygen tension after it has been lowered to zero by passing an oxygen-free gas such as nitrogen through the aeration system for a certain time. The dissolved oxygen tension is followed for a period after the start of the re-aeration. This is called the static gassing-out method.

The overall volumetric oxygen transfer rate is

$$\frac{dC_l}{dt} = R = K_La(C_g - C_l) \qquad [6.46]$$

which on integration gives

$$\ln(1 - C_l/C_g) = - K_La\, t \qquad [6.47]$$

Here, C_g = 100 % air saturation.

This equation describes the time course of dissolved oxygen from the start of re-aeration. Figure 6.1 illustrates the graphical procedure for determining K_La value from the slope of the $\ln(1 - C_l/C_g)$ against time graph.

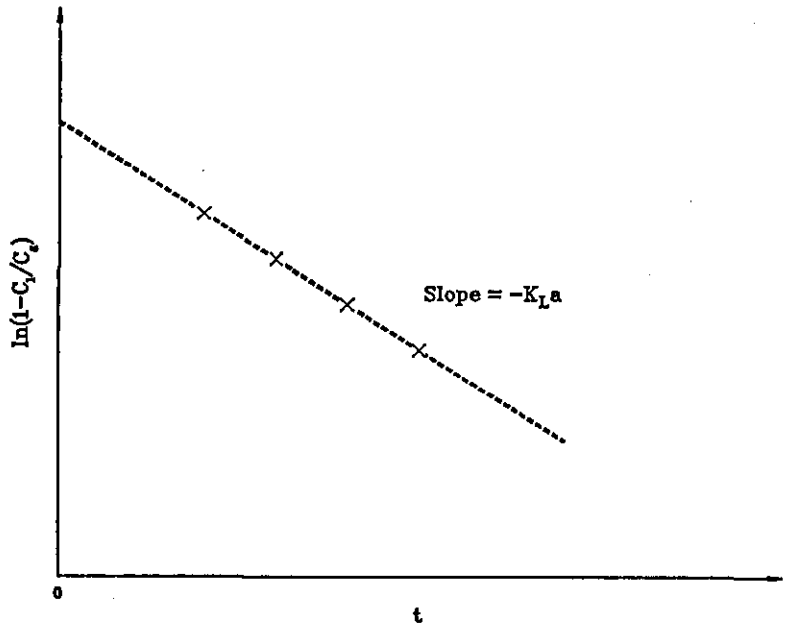

Fig. 6.1 Graphical Representation of Static Gassing–out Data

Experiments were carried out to determine the volumetric oxygen transfer coefficient using distilled water. An average K_La value of 40 hr^{-1} was obtained. An example can be found in Appendix I.

6.3.2 Dynamic Measurement of K_La Value During Culture

The dynamic gassing-out method for measurement of K_La value is based on following the dissolved oxygen during a brief interruption of the aeration of the fermentation system. During cell growth, the aeration is stopped and the agitation reduced to minimize surface aeration whilst retaining the homogeneity of the culture. The time course of the consequent decrease in dissolved oxygen due to respiration is monitored to obtain the rate of oxygen uptake by the total microbial population. Then before the critical oxygen concentration (usually 6 % air saturation) is reached, aeration is re-commenced and the increasing dissolved oxygen concentration is

recorded as a function of time.

The time course of the dissolved oxygen concentration is described as follows :

When aeration is stopped

$$\frac{dC_l}{dt} = -q_{O_2}x \qquad [6.48]$$

where x is the biomass concentration at time t, $q_{O_2}x$ is constant over the short period of interruption.

Upon resumption of aeration

$$\frac{dC_l}{dt} = K_La(C_g - C_l) - q_{O_2}x \qquad [6.49]$$

Figure 6.2 shows typical time course of dissolved oxygen and determination of $q_{O_2}x$ for the dynamic gassing-out method.

By rearrangement of Equation [6.49] we have

$$C_l = -(K_La)^{-1}(dC_l/dt + q_{O_2}x) + C_g \qquad [6.50]$$

From this relation, with constant K_La, it can be determined as the reciprocal of the straight line slope from a plot of C_l versus $(dC_l/dt + q_{O_2}x)$ on arithmetic scale.

Since under steady-state

$$q_{O_2}x = K_La(C_g - C_{l,init}) \qquad [6.51]$$

Equation [6.49] can also be integrated to give

$$\ln\left(\frac{C_{l,init} - C_l}{C_{l,init} - C_{l1}}\right) = -K_La(t - t_1) \qquad [6.52]$$

It follows from this equation that the K_La value can be determined from the slope of the plot of a function of C_l, i.e. $\ln[(C_{l,init}-C_l)/(C_{l,init}-C_{l1})]$ against time. This is demonstrated in Figure 6.3.

Since only a single measuring device, a dissolved oxygen electrode, is used, the results of this method will always be internally consistent.

A large number of factors influence the volumetric oxygen transfer coefficient K_La. These include the fermenter configuration such as baffles and location of air sparger, air flow rate and agitation speed. In addition, The actual K_La values within a fermenter may vary markedly as the fermentation proceeds.

During a culture, the viscosity of the fermentation broth increases with the biomass concentration, thus leading to a decrease in oxygen transfer coefficient. On the other hand, slight foam production might enhance the oxygen transfer rate. In a batch culture under the same operating conditions, an average value of slightly lower than 40 hr^{-1} was obtained for K_La by the dynamic method. One typical set of data is given in Appendix I.

Fig. 6.2 Time Course of Dissolved Oxygen
and Determination of $q_{O_2}x$ for the Dynamic Method

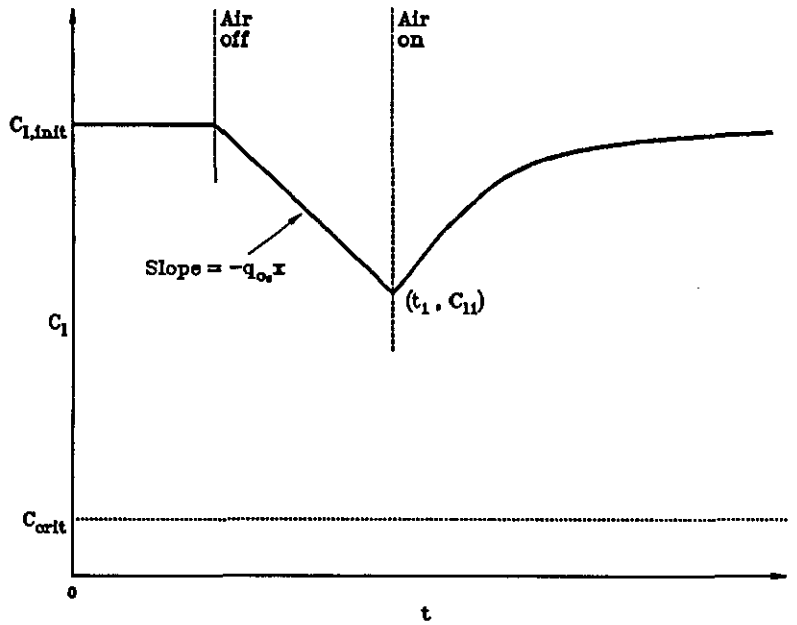

Fig. 6.3 Graphical Representation for the Determination of K_La
in the Dynamic Gassing-out Method

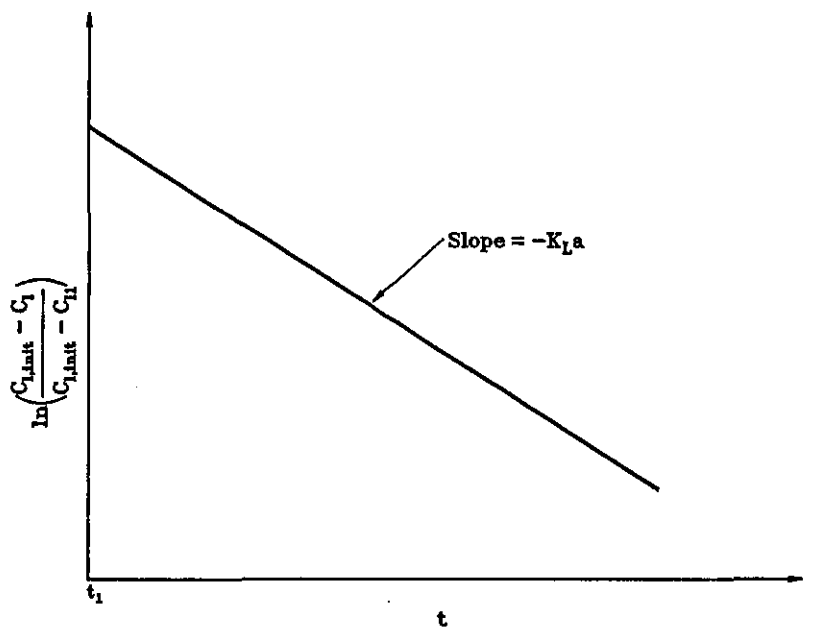

6.4 Initial Estimation of Cell Yield on Oxygen

The yield factor of cells for oxygen is not available. An approximate estimate, however, can be obtained from ATP generation and stoichiometric relationship in aerobic metabolism.

6.4.1 Y_{ATP} Approach

The growth yield of an organism is found to be proportional to the amount of ATP produced by its catabolic processes. Pirt (1975) estimated the theoretical maximum bacteria yield for oxygen based on ATP yield when glucose is the carbon source to be 3.39 g dry biomass/g oxygen.

Similarly, assuming that 2 ATP moles are produced per mole of atomic oxygen taken up when sucrose is the carbon source, that is P/O ratio = 2, and that 2 ATP moles are produced per mole of sucrose during glycolysis, then the total ATP produced per mole of sucrose oxidized will be 50 moles. Taking the ATP yield of biomass Y_{ATP} to be the maximum value achievable with bacterial cultures, i.e. 25 g dry biomass/mole ATP (Stouthamer & Bettenhausen, 1973), then the theoretical maximum growth yield for oxygen is.:

$$Y_{o,max} = 50 \times 25/(12 \times 32) = 3.26 \text{ g dry biomass/g oxygen}$$

6.4.2 Stoichiometric Analyses of Aerobic Metabolism of *Leuconostoc mesenteroides*

Material balances in terms of stoichiometrically balanced equations for simultaneous microbial growth and product formation from cell metabolism can be written and stoichiometric calculation of yields is possible if the composition of the organism cell is known. Generally the composition of cells expressed elementally or as compounds varies with growth conditions and substrates used. Little information pertaining to the elementary composition of *Leuconostoc mesenteroides* is available. Dussap and Gros proposed a C,H,O formula for anaerobic growth of *L. mesenteroides* on glucose as $CH_{1.75}O_{0.4}$.

The elemental composition of a typical bacterium given by Humphrey (1968) as follows is adopted in the estimation of biomass yields for *L. mesenteroides* under aerobic conditions.

C,	53 %	(by weight);
H,	7.3 %	(by weight);
O,	19 %	(by weight);
N,	12 %	(by weight);
Ash,	8 %	(by weight).

With these assumptions, an empirical formula for 100 g cells of this composition would be:

$$C_{4.41}H_{7.3}N_{0.86}O_{1.19}$$

6.4.2.1 Stoichiometric Relationship of Aerobic Cell Growth on Glucose

According to Bergey, *Leuconostoc mesenteroides* has an aerobic oxidative metabolism yielding equimolar quantities of lactate, acetate and carbon dioxide.

Assuming $Y_{x/g}$ = 0.15 g biomass/g glucose, then

$$C_6H_{12}O_6 \rightarrow 0.27\ C_{4.41}H_{7.3}O_{1.19}$$

Balancing with the appropriate factors for O_2 consumption, lactate, acetate, CO_2, and H_2O production gives the following stoichiometric equation :

$$\underset{\text{glucose}}{C_6H_{12}O_6} + 0.4695\ O_2 \rightarrow \quad 0.27 \quad \underset{\text{cell}}{C_{4.41}H_{7.3}O_{1.19}} +$$

$$+ 0.80155\ \underset{\text{lactic acid}}{C_3H_6O_3} + 0.80155\ \underset{\text{acetic acid}}{C_2H_4O_2} + 0.80155\ CO_2 + 1.00675\ H_2O \qquad [6.53]$$

The stoichiometric cell yield on oxygen will be

$$Y_{x/o} = 1.793 \text{ g biomass/g oxygen}$$

6.4.2.2 Aerobic Cell Growth on Sucrose

Considering the sucrose fermentation in the same way, equimolar quantities of lactate, acetate and CO_2, H_2O are also the main metabolites of aerobic oxidative cell metabolism of *Leuconostoc mesenteroides* on sucrose.

Assuming $Y_{x/s}$ = 0.15 g biomass/g sucrose, then

$$C_{12}H_{22}O_{11} \rightarrow 0.51345\ C_{4.41}H_{7.3}O_{1.19}$$

Filling in the balancing factors for O_2 consumption, lactic acid, acetic acid, CO_2 and H_2O formation gives :

$$\underset{\text{sucrose}}{C_{12}H_{22}O_{11}} + 0.991\ O_2 \rightarrow \quad 0.51345\ \underset{\text{cell}}{C_{4.41}H_{7.3}O_{1.19}} +$$

$$+ 1.6226\ \underset{\text{lactic acid}}{C_3H_6O_3} + 1.6226\ \underset{\text{acetic acid}}{C_2H_4O_2} + 1.6226\ CO_2 + 1.0128\ H_2O \qquad [6.54]$$

From this stoichiometric equation we have

$$Y_{x/o} = 1.62 \text{ g biomass/g oxygen}$$

In equations [6.53] and [6.54], nitrogen has been neglected in the material balance.

The foregoing analyses based on Y_{ATP} and stoichiometric equations show that the yield coefficient of *Leuconostoc mesenteroides* for oxygen will be in the region of 1.5 to 3 g biomass/g oxygen. An initial value of 2.5 g biomass/g oxygen will be used in the computer simulation.

6.5 Simulations and Analyses of Experimental Results

Three batch fermentations, designated **O1**, **O2**, and **O3**, were carried out to investigate the effect of oxygen on cell growth. The fermenter was aerated at a flow rate of about 4 VVM and the stirrer speed was kept constant at 400 rpm. The volumetric oxygen transfer coefficient was estimated to be about 40 hr^{-1} under the operating conditions for such a configuration. In these three experiments, cell growth was followed by measuring cell concentrations at a time interval of half an hour. Dissolved oxygen level was also recorded as per cent of air saturation. These results are presented graphically in Figures 6.4 to 6.9. Tabulated experimental results can be found in Appendix J.

In all three batch fermentations, the fermenter is regulated at a temperature of 23 °C and pH of 6.7. The initial conditions are presented as follows in Table 6.1. The initial oxygen level was calibrated at 100 per cent air saturation.

Table 6.1 Initial Conditions for Batch Cultures O1 - O3

	Initial Sucrose Concentration (g/L)	Initial Cell Concentration (g/L)
Batch Culture **O1**	60	0.224
Batch Culture **O2**	25	0.240
Batch Culture **O3**	25	0.114

Computer simulations are used extensively in the study to facilitate data analysis and model construction. Simulations are performed by a specialized simulation language ACSL (Advanced Continuous Simulation Language), which is implemented on a PRIMEC computer. The ACSL language is especially suitable for modelling systems which can be

described by time dependent, nonlinear differential equations such as the fermentation model discussed here.

6.5.1 Simulation of the Single-Substrate Model

The experimental results are compared with those performed with high oxygen tension in a fully aerated system. It was found that the exponential growth phase of these experiments seems to follow the same pattern as those high oxygen tension experiments. This indicates that the effect of oxygen on growth quantified by the saturation coefficient for oxygen K_o or K_o^* is very small. To see the effect clearly, first we simply let $K_o = 0$ or $K_o^* = 0$, that is to say, sucrose is the only growth-limiting substrate.

Simulations were performed for these experiments by using a single substrate growth rate equation and the process equations [6.37] to [6.39] described in section 6.2. With different values of Y_o^* or Y_o between the initial estimate $Y_{o,init}$ and $Y_{o,max}$, equations [6.37] to [6.40] are solved numerically by an ACSL simulation program. A Y_o value of 2.6 g biomass/g oxygen is found to fit the dissolved oxygen data above zero satisfactorily. This value is larger than the stoichiometric yield but certainly smaller than the theoretical maximum biomass yield for oxygen. The simulation results are demonstrated in Figures [6.4] to [6.9] with legend "Model A".

Notice that for the dissolved oxygen curve there is a sharp fall at the beginning, or more precisely at the beginning of the exponential growth phase. This is the inoculation characteristic of an ideal batch fermentation process described by equations [6.37] to [6.40]. A considerable amount of oxygen is utilized to accommodate the healthy cells introduced in the inoculum. It is obvious from equation [6.33] or [6.39] that the initial rate of oxygen concentration decreasing depends on the inoculum size.

$$\frac{dC_{lf}}{dt} = -r_x/Y_o^* = -\mu_0 x_0/Y_o^* \qquad [6.55]$$

Taking fermentation O1 for example,

$$x_0 = 0.224 \text{ g/L}$$
$$Y_o = 2.6 \text{ g/g} \quad \text{or} \quad Y_o^* = 0.023$$
$$\mu_0 = 0.493 \text{ hr}^{-1}$$

Then

$$\frac{dC_{lf}}{dt} = -4.8 \text{ hr}^{-1}$$

If linearizing $C_{lf} = C_{lf}(t)$ near time zero, we have :

$$C_{lf} = 1.0 - 4.8t \qquad [6.56]$$

Simple arithmetic calculation gives $t(C_{lf} = 0.8) = 2.5$ minutes. This means that the dissolved oxygen would drop to 80 per cent of the initial value in just 2.5 minutes if no aeration at the beginning of fermentation.

However, the actual biological system is much more complicated than the system described by the unstructured models [6.31] - [6.43]. Cells contained in the inoculum cannot simply utilize the nutrients available in a new environment such as a different fermentation medium. Some new enzymes have to be induced and the time required to synthesize the optimum amount of a new enzyme may be very long. The physiological state of the inoculum culture is also an important factor in the initial adaptation process of cells to the new culture environment. The model proposed does not include these effects.

For the single-substrate limited growth, an analytical solution to equations [6.37] - [6.41] can be obtained :

$$\frac{Y_s K_s}{Y_s K_s + x_{max}} \ln\left(\frac{x_{max} - x_0}{x_{max} - x}\right) + \ln\left(\frac{x}{x_0}\right) = \mu_{max} \frac{x_{max} t}{Y_s K_s + x_{max}} \quad [6.57]$$

where x_{max} denotes the maximum (final) biomass concentration achieved when the limiting substrate sucrose is exhausted by the cells.

By introducing a fractional cell concentration variable

$$z = x/x_{max} \quad [6.58]$$

the solution will be

$$\ln[z/(1-z)^{\varepsilon}] - \ln[z_0/(1-z_0)\varepsilon] = \mu^* t \quad [6.59]$$

here

$$K^* = \frac{K_s}{s_0 + x_0/Y_s} \quad [6.60]$$

$$\varepsilon = \frac{K^*}{1 + K^*} \quad [6.61]$$

$$\mu^* = \frac{\mu_{max}}{1 + K^*} \quad [6.62]$$

on integration of equation [6.39] we have

$$C_{lf} = 1 - \frac{x_0 \mu_{max}}{Y_o^*(K_L a + \mu_{max})} \{\exp(\mu_{max} t) - \exp(-K_L at)\} \quad [6.63]$$

For $K_s \ll s_0$, i.e. small saturation coefficient, the first item on the left hand side of equation [6.57] can be ignored, and $Y_s K_s \approx 0$, then

$$\ln(x) - \ln(x_0) \approx \mu_{max} t \qquad [6.64]$$

or

$$x \approx x_0 \exp(\mu_{max} t) \qquad [6.65]$$

which is the form of exponential growth.

Because of the small size of inoculum used in batch culture O3, there exists an obvious lag phase in cell growth illustrated in Figure 6.9. Nonetheless, the model still fits the experimental data reasonably well by incorporating an appropriate lag time t_L (here $t_L = 1.1$ hour) in the growth rate equation.

6.5.2 Maximum Possible Oxygen Transfer Rate

In a batch fermentation system under specified operating conditions the maximum possible oxygen transfer rate is $K_L a C_g$: all oxygen entering the bulk fermentation broth is assumed to be rapidly consumed by cells. The maximum possible oxygen utilization rate is seen to be $x\mu_{max}/Y_o$. Evidently, if $K_L a C_g$ is much larger than $x\mu_{max}/Y_o$, microbial metabolism is the main resistance to increased oxygen consumption and the process appears to be biochemically limited. Conversely, the reverse inequality apparently leads to C_l near zero, and the fermenter seems to be in the mass transfer limited mode.

For the batch system being investigated here the specific cell growth rate is almost constant during fermentation due to small saturation coefficient for substrate and comparatively large initial sucrose concentration employed. The maximum volumetric oxygen transfer rate is

$$K_L aC_g = 40 \times 0.0088 = 0.352\ gL^{-1}hr^{-1}$$

As the fermentation proceeds, the cell concentration increases, so does the oxygen utilization rate. This results in rapid drop in oxygen concentration in the fermenter. A pseudo steady-state appears when the oxygen level falls to zero (It can never be below zero) :

$$K_L aC_g = \frac{\mu x|_{Cl=0}}{Y_o} \qquad [6.66]$$

if $\mu = \mu_{max} = 0.5\ hr^{-1}$, then

$$x|_{Cl=0} = K_L a\ Y_o^*/\mu_{max} = 1.84\ g/L$$

This indicates that the dissolved oxygen level in the fermenter drops to zero when cell concentration reaches about 2 g/L (this could happen as long as the initial sucrose concentration is larger than $1.84/Y_s = 12$ g/L). Since the saturation constant in the Monod kinetic model is relatively much smaller than the initial concentrations of the limiting substrate, the organism in the batch cultures is seen to follow an exponential growth law with the specific growth rate being the maximum value of 0.5 hr^{-1} as shown in equation [6.65]. Thus the time at which the dissolved oxygen level falls to zero can be approximated as:

$$t|_{Cl=0} = \frac{1}{\mu_{max}} \ln \left\{\frac{x|_{Cl=0}}{x_0}\right\} \qquad [6.67]$$

The smaller the inoculum size x_0 the longer the time will be.

Taking $x_0 = 0.224$ g/L as in batch culture O1, then

$$t|_{Cl=0} = 4.2\ hr$$

This can be seen clearly in the experimental data shown in Figure 6.4 and Figure 6.6.

For batch culture O3, $x_0 = 0.114$ g/L

$$t|_{Cl=0} = 5.6 \text{ hr}$$

This is also in good agreement with the experimental result if an appropriate lag time is taken into account.

Although the single substrate growth model is found to fit the experimental data satisfactorily above zero oxygen level, the role oxygen played in cell metabolism is still not clear. The model will fail after oxygen concentration falls to zero. Since oxygen has been consumed by the cell or utilized in cell metabolism in some way, the model cannot be used to predict cell growth after oxygen concentration becomes zero. It can be seen from Figure 6.5 that there is a large difference between experimental data of cell growth and the predicted values after about 6 hours of fermentation.

6.5.3 Simulation of the Double-Substrate Model

It is seen from the previous section that oxygen has little effect on aerobic cell metabolism of *L. mesenteroides*. However, the question remains how much the effect can be in terms of the saturation coefficient for oxygen. It is possible to justify the effect of oxygen by simulation of the double substrate growth model for the three experiments.

Simulations were carried out for the double substrate model by using a modified ACSL program similar to that for the single substrate model. The results of simulation are presented in Figures 6.4 to 6.9 with legends "Model B" and "Model B1", respectively.

For Model B, $K_o^* = 0.001$ or $K_o = 0.1$ % air saturation
For Model B1, $K_o^* = 0.0001$ or $K_o = 0.01$ % air saturation

As discussed earlier, in a batch culture with constant K_La value, when growth is oxygen limited, or more accurately, oxygen-transfer limited, the growth rate dx/dt will become constant and the specific growth rate will decrease. This linear growth phenomenon is the result of insufficient oxygen supply due to the transport limitations described before. Constant activity of enzymes may be the cause.

The linear growth rate can be determined by assuming a pseudo steady-state for oxygen balance at an oxygen level of zero.

$$\frac{dx}{dt} = K_La Y_o^* = 40 \times 0.023 = 0.92 \text{ gL}^{-1}\text{hr}^{-1} \qquad [6.68]$$

Equation [6.68] shows that the linear growth rate is only dependent on the oxygen transfer capability and growth yield on oxygen. It implies that oxygen entering the system is quickly consumed by the cells. The linear growth will disappear by applying an adequate K_La value.

It is noted from the simulation results in Figures 6.4 to 6.7 that little difference is obtained for K_o values of 0.1% and 0.01% air saturation. This indicates that small values of K_o can be treated as being effectively zero.

It can be seen from Figure 6.7 and Figure 6.9 that there are no significant differences between the double-substrate model and the single-substrate model. However, the difference between the two models for batch culture O1 cannot be ignored. For batch cultures O2 and O3, the initial sucrose concentrations are much lower than that of batch culture O1. The carbon sources soon are exhausted after the dissolved oxygen tension drops to its lowest point. But there is still a considerable amount of sucrose left in

the medium in batch culture O1 after the dissolved oxygen level falls to near zero. It is noted that the actual cell growth lies between the two curves. We can propose, therefore, that *Leuconostoc mesenteroides* can utilize oxygen quite efficiently. Since in practice the fermentation broth cannot be perfectly mixed, some cells in the well-aerated area use whatever oxygen is available and grow using an aerobic pathway. Because the organism is a facultative anaerobe, some necessary enzymes are produced and cells in the less-aerated area grow anaerobically if there is still enough carbon source available. The actual cell metabolism is a combination of the two phenomena. Although little information concerning process models of anaerobic metabolism is available and this subject is out of the scope of the current study, it can be seen from the stoichiometric relationship discussed before and the difference between the experimental data and the pure aerobic model (Model A) that anaerobic growth rate is much lower than aerobic growth.

From the foregoing discussion it can be concluded that sucrose is the only growth-limiting substrate under aerobic conditions. For the enzyme-producing fermentations in which the inducer sucrose is employed under 20 g/L, the single-substrate model can be used to predict enzyme production. Because the biomass yield under aerobic conditions is higher than anaerobic yield, it could be an advantage to use aerobic culture in enzyme-producing fermentations rather than anaerobic culture.

Figure 6.4

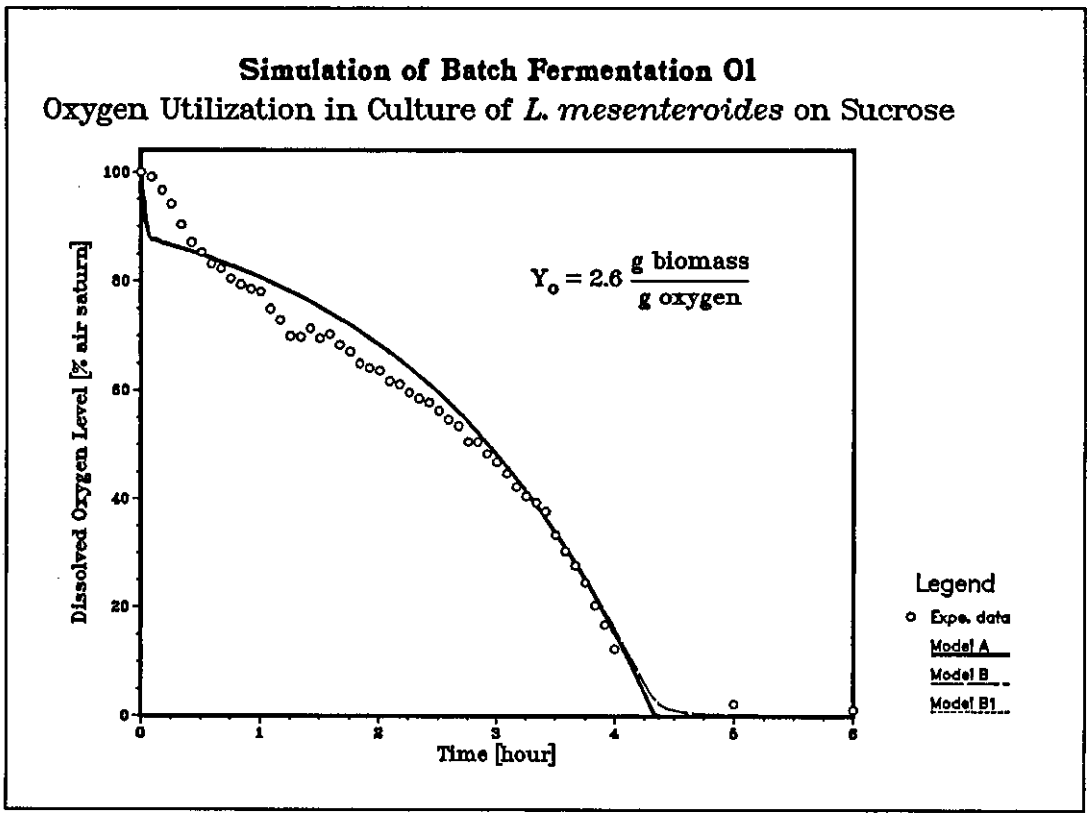

Figure 6.5

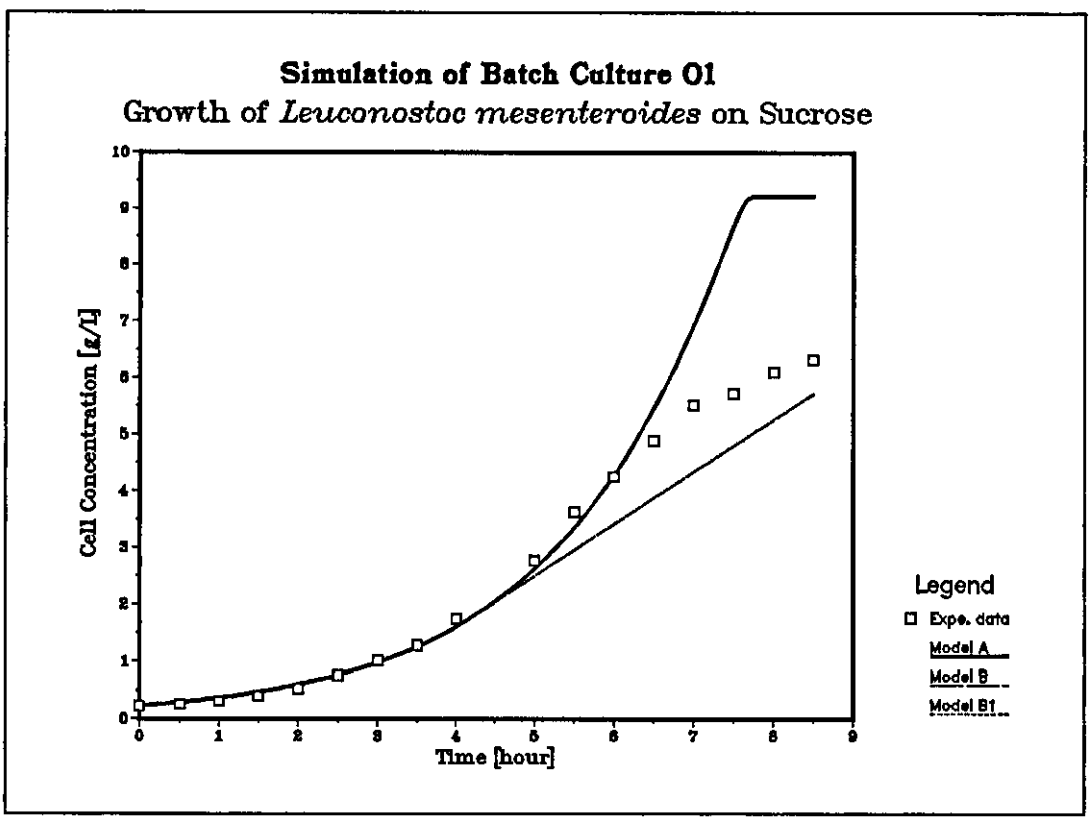

Figure 6.6

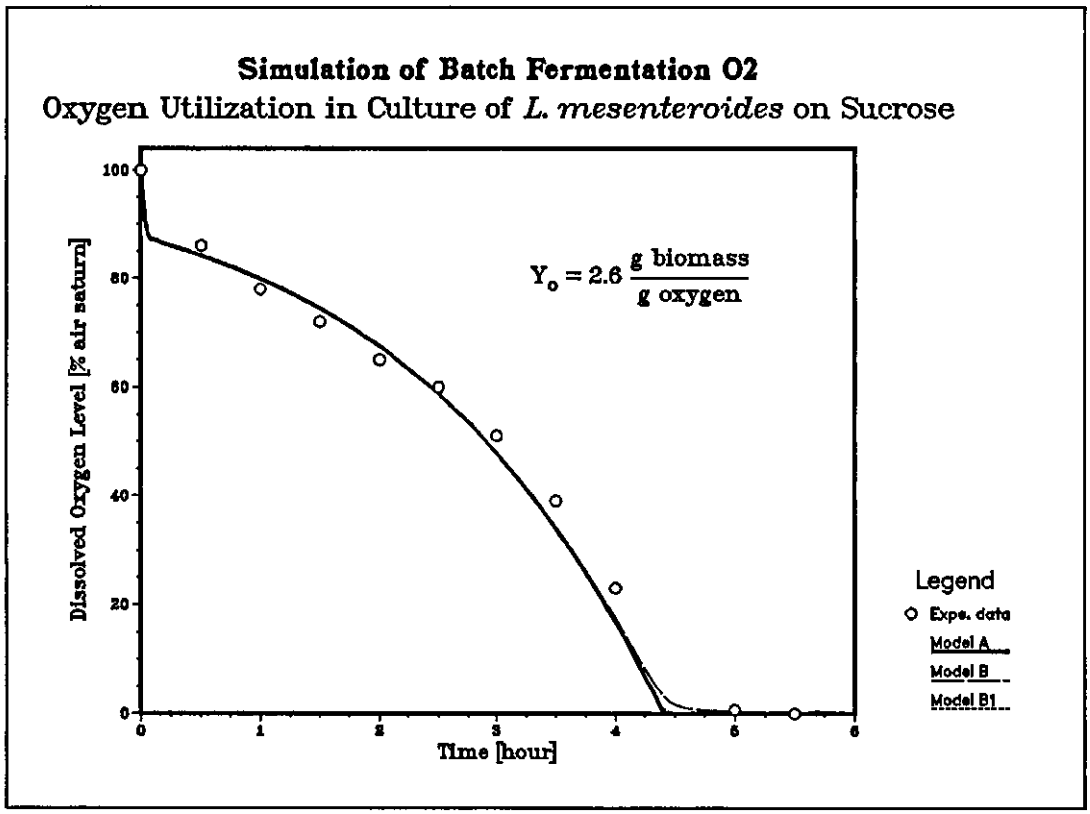

Figure 6.7

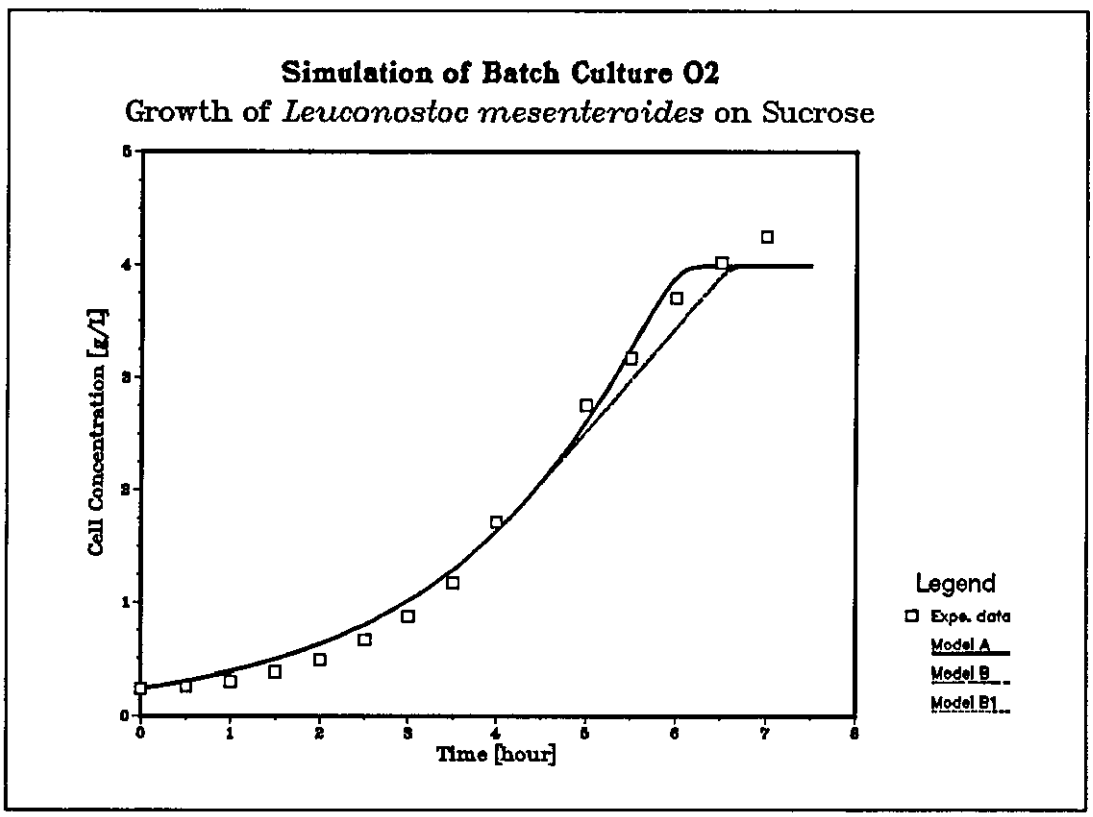

Figure 6.8

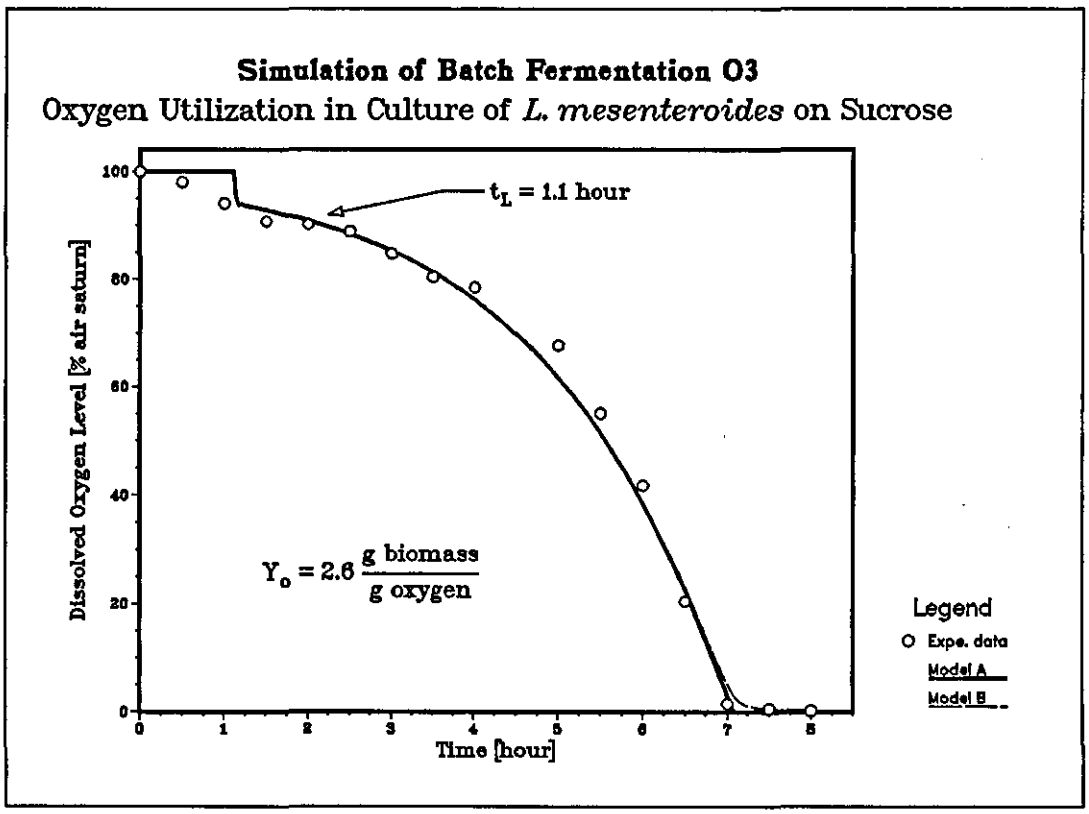

Figure 6.9

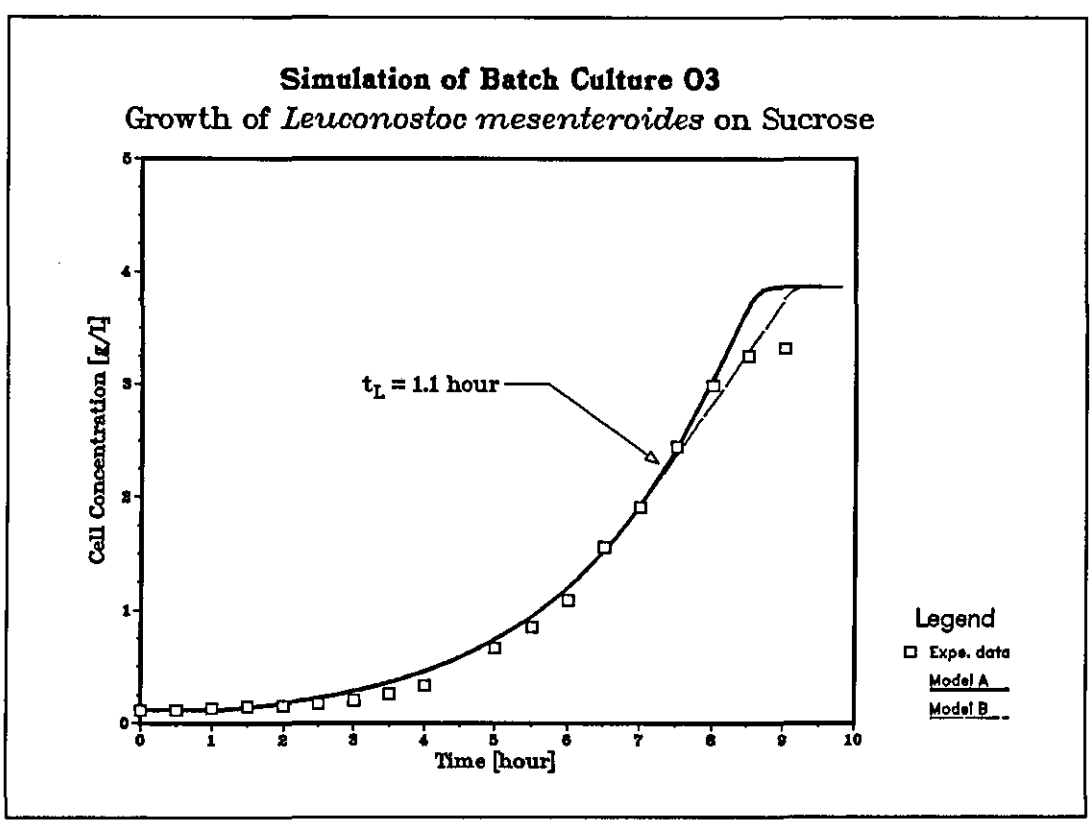

Figure 6.10

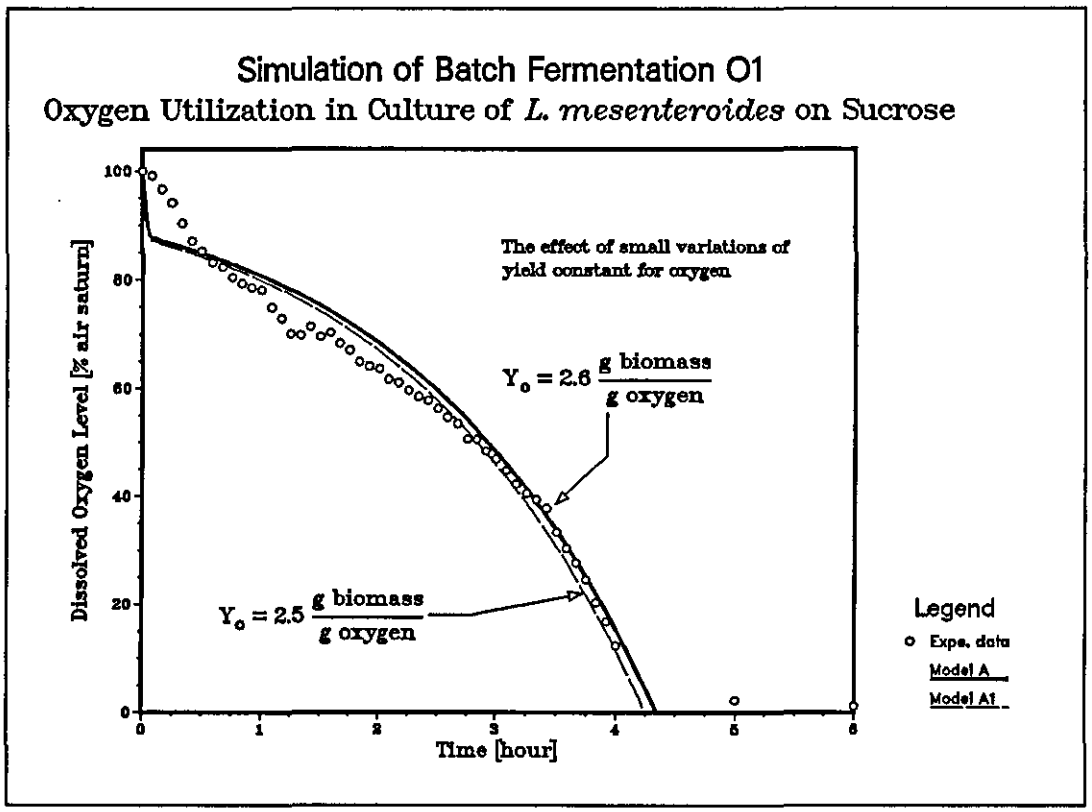

Figure 6.11

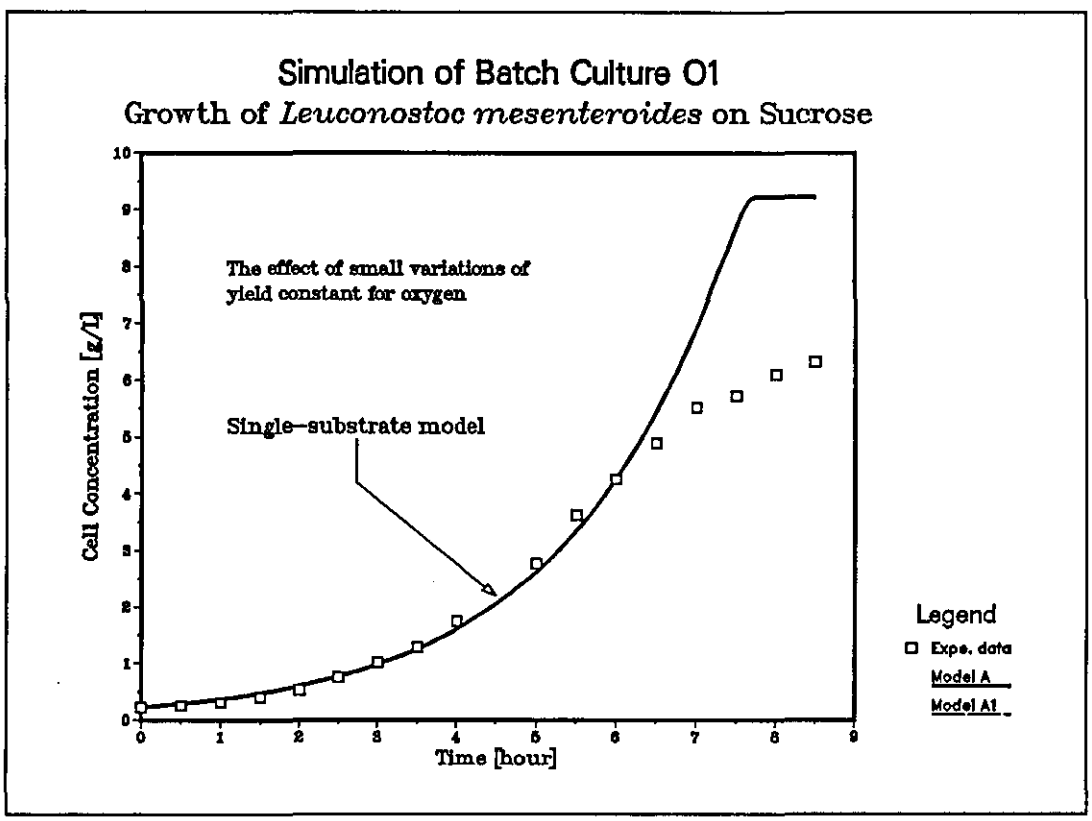

Chapter 7 Process Kinetics of Enzyme Biosynthesis

There are two equally complex processes associated with growth of microorganisms. In order to grow and reproduce, cells must ingest some raw materials from their environment. Consequently, metabolic end products are released from the cell into the surroundings. From the perspective of engineering, the latter process is of great importance since these metabolic end products are often valuable and have actual or potential industrial applications. The development of fermentation processes is frequently involved in improving the productivity of the desired metabolites by environmental and genetic manipulations.

A variety of metabolic end products is released into the environment by growing cells. In many cases, these products are the result of primary energy-yielding metabolism. Alcohols and organic acids are frequent examples of catabolic metabolism end products. However, there exist other important metabolic products which have complex molecules and serve special functions for the cell. Many such products, like antibiotics and extracellular enzymes, which are not required for growth in pure culture, are often referred to as secondary metabolites. Generally, microorganisms synthesize secondary metabolites when the cells and their environment are at appropriate conditions. The extracellular enzymes are synthesized within the cell and then secreted into the environment as extracellular proteins. It is known that the synthesis frequently occurs under genetic control. The mechanism of enzyme secretion, however, is obscure and varies widely from one organism to another. Bacteria usually secrete small protein enzymes which are free of carbohydrate and lack sulphur bridges. In most instances, the secreted enzyme is synthesized by membrane-bound polysomes and transferred by a vectorial process into the plasma membrane and ultimately into the external cell wall which releases the enzyme.

Microorganisms are known to possess intricate control systems which ensure efficient use of material and energy resources for survival. The biosynthesis of the extracellular enzymes is influenced by numerous factors of metabolic control mechanisms. The synthesis of certain enzymes is normally repressed in the absence of the substrates of the enzymes. These enzymes can be induced only when their substrates or substrate analogues are present in the growth medium. Dextransucrase is one example of the inducible enzymes. As described before, this enzyme catalyzes the polymerization of sucrose to the polysaccharide dextran. Its substrate, sucrose, is the only known requisite inducer of enzyme production by growing cells of *Leuconostoc mesenteroides.*

In principle, the amount of a particular enzyme produced by a particular microorganism can vary tremendously since enzyme formation can be either stimulated or inhibited by cell control mechanisms, which in turn are influenced by environmental conditions. The biosynthesis of extracellular enzymes is, therefore, dictated by kinetic regulation and activity of the cells. Among the important factors for enzyme production are temperature, pH, medium composition, aeration, and stage of the cell growth. These conditions are usually determined empirically for each enzyme and each strain. The kinetics of the formation of extracellular enzymes is in general poorly understood.

With the development of modern optimization methods which can be used to determine the optimum control profiles for biological processes, knowledge on product formation kinetics is potentially valuable and is becoming increasingly important for the improvement of process performance. Although extremely complex reaction processes abound in the living cells and always render difficult the construction of models which can describe all aspects of cell metabolism, the guiding principle here in kinetic study of enzyme formation is again careful definition of the intended

application and scope of use of the kinetics. For practical usefulness, models are preferred to be both realistic and simple, with no unnecessary complexities.

7.1 General Approaches to Product Formation Kinetics

It is obvious that the three phenomena which characterize the fermentation processes, i.e. substrate utilization, cell growth and product formation, are intimately bound together. The kinetics of product synthesis is virtually the relationship between the rate of product formation and the rate of cell growth, which is determined by the net rate of biosynthesis. The types of kinetic representations that may be employed for product formation by microorganisms parallel those used to depict cell population growth. Structured and unstructured, segregated and unsegregated approaches exist.

7.1.1 Simple Unstructured Models

The simplest types of product formation kinetics are the unstructured models which describe the macroscopic behaviour of the fermentation system. Product formation cannot occur without the presence of cells. Thus it is expected that product formation will be coupled to cell growth or cell mass depending upon the metabolic regulatory controls.

In general, the product formation rate r_p is given by

$$r_p = \frac{dp}{dt} = q_p x \qquad [7.1]$$

where x is the biomass concentration, p is the product concentration and q_p represents the specific rate of product formation. When there is a simple stoichiometric connection between product formation and cell growth, the

fermentation exhibits growth associated product kinetics where product formation rate is directly proportional to the cell growth rate, i.e.

$$r_p = Y_{p/x} r_x \qquad [7.2]$$

or

$$\frac{dp}{dt} = Y_{p/x} \frac{dx}{dt} \qquad [7.3]$$

where $Y_{p/x}$ is the product yield factor referred to biomass formed. It is usually abbreviated to Y_p for concision. It follows that

$$dp = Y_p dx \qquad [7.4]$$

and the specific product formation rate is given by

$$q_p = Y_p \mu \qquad [7.5]$$

Generally, growth associated kinetics arises when the metabolic products are essential to the function of the cells. In most case, these result from primary energy metabolism.

In many fermentations, especially those involving secondary metabolism, product formation usually occurs after the cellular processes associated with growth have declined in importance. It has been commonly observed that significant secondary metabolite appears relatively late in batch cultivations. Occasionally, a simple nongrowth associated model suffices for product formation kinetics in such cases where the production rate is related to the concentration of cells rather than the growth rate.

$$r_p = \beta x \qquad [7.6]$$

Many fermentations have been shown to exhibit a combined kinetic behaviour. In these cases, product formation is partly associated with growth and partly independent of growth rate. This behaviour is best described by the Leudeking-Piret equation.

$$r_p = \alpha r_x + \beta x \qquad [7.7]$$

This is a general kinetic form when the product is the result of energy-yielding metabolism. It should be noted, however, in the exponential growth phase of a batch cultivation, where $r_x = \mu x$, equation [7.7] becomes :

$$r_p = (\alpha\mu + \beta)x = (\alpha + \beta/\mu)r_x \qquad [7.8]$$

This relationship indicates that during the exponential growth phase it is not possible to distinguish between growth-associated, nongrowth-associated and mixed types of kinetics.

It should also be noted that product formation by growing cells may occur simultaneously with chemical reactions of the product in the medium, such as spontaneous decomposition or degradation of extracellular enzymes. the product accumulation rate will be influenced by the additional product reaction rate.

For the complex secondary metabolites and products of intermediary metabolism, the unstructured kinetic models represent extreme simplifications of the actual cellular processes involved, due to lack of detailed metabolic pathways and knowledge of individual reaction kinetics. However, these models are useful in process development.

7.1.2 Complicated Kinetics of Enzyme Production

It is possible to construct kinetic models at the level of molecular events and interactions, especially in the case of protein enzyme synthesis. Such models should prove valuable for environmental and genetic optimization. The basic assumption is that the rate of enzyme synthesis is limited by the amount of specific mRNA (messenger ribonucleic acid) available. By correlating the enzyme synthesis rate with the concentration of mRNA coding for the production of the enzyme and the efficiency of utilization of this mRNA at the ribosomes, it often results in equations expressing the intracellular product concentration directly in terms of parameters which characterize gene expression and mRNA and product stability in the cell. The degradation of active enzyme can be readily incorporated in such an approach.

Consideration of molecular interactions in formulating kinetic models has obvious benefits. The parameters in the model always have precise physical interpretations and can often be measured in separate, in vitro experiments. Also, models at this level have potential capability for quantitative optimization of the genetic controls of the organism. However, a large quantity of experimental data is usually required to establish such genetically structured models. The utility of these models is therefore restricted in practice.

Kinetic models relating product formation to the segregated nature of cell populations can also be formulated. The benefit of this approach is the opportunity of connecting cell cycle features and other single-cell properties with overall characteristics of the populations. Product formation kinetics describing the rate of secondary metabolite synthesis based on the age distribution has been found successful in some cases. However, the mathematical complexity of segregated kinetic models also restrains their

general application.

7.2 Empirical Kinetics of Dextransucrase Production

Dextransucrase production from *Leuconostoc mesenteroides* growing on sucrose is a very complex process. Information pertaining to the mechanism of enzyme synthesis is not available. Since dextransucrase is induced by sucrose, a considerable amount of dextran will be formed concomitantly during the enzyme production if the inducer concentration is high in the medium. Moreover, the enzyme is relatively unstable under the conditions employed for production. Kinetic description of such complications is difficult and requires a great deal of experimental effort.

It has been frequently observed that the production course of dextransucrase in fermentations of *L. mesenteroides* parallels the growth of the cells, and significant enzyme activity occurs a certain time behind the growth. This phenomenon indicates growth-associated kinetic behaviour of enzyme synthesis. Also, the observation reveals the possibility of dextransucrase being the end product of secondary metabolism. To reflect the lag phase in dextransucrase production, one simple approach is to assume that enzyme is produced only after the concentration of cells in the fermenter has reached a certain level. In a batch cultivation, if decomposition of enzyme is negligible, the mass balance on the enzyme shows that the rate of accumulation of enzyme must be equal to the net rate of enzyme formation in the fermenter. Thus,

$$\frac{d}{dt}(pV) = Vr_p \qquad [7.9]$$

Here the culture volume V is considered to be constant, r_p is the volumetric enzyme synthesis rate in terms of enzyme activity units produced by cell per

unit volume per unit time ($DSUmL^{-1}hr^{-1}$). For growth associated product formation kinetics, equation [7.9] becomes

$$\frac{dp}{dt} = Y_p \frac{dx}{dt} \qquad [7.10]$$

with the following condition :

$$p = 0 \quad , \quad \text{for } x < x_d \qquad [7.11]$$

where x_d denotes the threshold biomass concentration above which enzyme is produced by the cells.

Suppose that enzyme production has a constant yield factor on biomass. Integration of equation [7.10] subject to condition [7.11] can be achieved analytically, with the result

$$p = Y_p x - p_d \qquad [7.12]$$

where

$$p_d = Y_p x_d \qquad [7.13]$$

Equation [7.12] shows that enzyme activity in a batch cultivation is linearly related to the biomass concentration. The plot of enzyme activity against cell concentration will yield a straight line with slope Y_p. The threshold concentration of biomass can also be estimated from such a plot as the intercept of the straight line on the abscissa.

The advantage of such a simple approach lies in the simplicity of the relationship [7.12] between the enzyme produced and the concentration of

cells. In a certain sense, it also accounts for the lag feature of enzyme production. Less experimental data are required to estimate the parameters in the model, which can be employed in complicated situations.

It was proposed by Brown and Vass (1973) that a particular product may only be synthesized by those cells which are considered to be matured in a maturation time t_m. Product formation rate is therefore associated with the rate of formation of mature cells. It follows that the rate at which product forming cells appear in the culture system at an arbitrary time t would be the same as the rate at which new cells were being generated at time $(t-t_m)$. Hence, by applying this concept to dextransucrase production in a batch cultivation system, the material balance on enzyme in the fermenter leads to

$$\frac{dp}{dt} = Y_p\left(\frac{dx}{dt}\right)_{t-t_m} \qquad [7.14]$$

$$p = 0 \quad , \quad \text{for } t < t_m \qquad [7.15]$$

This form of process equation is the same as [7.10] but with a shifted time base to allow for cell maturation. Integration of equation [7.14] gives

$$p = Y_p x_{t-tm} \quad , \quad \text{for } t \geq t_m \qquad [7.16]$$

If growth is exponential we may write $x = x_0\exp(\mu t)$, where x_0 is the initial biomass concentration. Thus we find that

$$p = Y_p x_0 \exp[\mu(t-t_m)] \quad , \quad \text{for } t \geq t_m \qquad [7.17]$$

Considering $\exp(-\mu t_m) \approx 1 - \mu t_m$ when $\mu t_m \ll 1$, rearrangement of equation [7.17] yields

$$p = Y_p x(1 - \mu t_m) \qquad [7.18]$$

Compared to the suggested threshold biomass description, the maturation time model introduces a primitive concept of cell age distribution and seems to be more rational in dealing with the product formation lag. However, the model is not easy to handle despite its simple form. The parameters in the model, i.e. product yield factor Y_p and the maturation time t_m can be estimated by a graphical trial-and-error procedure. A series of graphs are constructed by plotting enzyme activity at time t against biomass concentration at time $(t - \theta)$ over a range of values of θ. Then the maturation time t_m is given by the value of θ at which the plot shows a straight line passing through the origin. The parameter Y_p can be estimated as the slope of this line according to equation [7.16]. Due to practical difficulty in obtaining enzyme production data, this method is usually not reliable and only gives approximate parameter estimates.

7.3 Kinetic Analysis of Batch Enzyme Production Data

A series of specially designed batch experiments were carried out to study the kinetics of enzyme production. The experimental method was basically the same as discussed in section 4.2. The fermenter was operated at pH 6.7 and temperature 23 °C. Aeration was sufficient to maintain near-saturation level of dissolved oxygen. As usual, the growth of cells was determined by optical density measurements. Enzyme production was followed by measuring the activity of enzyme as discussed in section 4.3.2. The experimental results are presented in Appendix K.

It was noted in the experiments that no significant enzyme was detected until the cell concentration reached a critical level. Due to the relatively large errors in measurements of enzyme activity, the small values obtained for the enzyme activity corresponding to cell concentrations below the critical value can be ignored. Since only a few data points were available for each experimental run, a model describing the average behaviour of the system would be desirable. The kinetic data from the five experiments **E1, E2, E3, E4** and **E5** is analyzed using the growth associated model [7.12]. The modelling procedure is illustrated in Figure 7.1 and the detailed regression analysis is given in Appendix K.

In a batch culture, the enzyme synthesis kinetics can be described by the following equations :

$$p = 20.28x - 13.63 \quad , \quad \text{for } x > x_d \qquad [7.19]$$

$$Y_p = 20.28 \ \text{(DSU/mL)/(g/L)} \qquad [7.20]$$

where x is the cell concentration (g/L), p is the enzyme concentration in terms of its activity (DSU/mL). The threshold cell concentration is given by

$$x_d = 0.672 \text{ g/L} \quad [7.21]$$

It can be seen from Figure 7.1 that the experimental data is scattered and a linear relationship between enzyme activity and cell concentration is an approximation. However, the experimental data does show growth associated kinetic behaviour, and the proposed empirical model is reasonable in terms of parameter estimation error. The estimated standard deviation of Y_p is less than 6 per cent of the parameter value, while the largest error occurs in the estimate of the threshold cell concentration.

The maturation time model [7.16] is also used to fit the enzyme production data obtained in the batch cultures. A trial-and-error procedure yields the following results :

$$Y_p = 20.98 \text{ (DSU/mL)/(g/L)} \quad [7.22]$$

$$t_m = 1 \text{ hour} \quad [7.23]$$

and the enzyme synthesis model

$$p_t = 20.98x_{(t-1)} \quad [7.24]$$

The results are also shown in Figure 7.2, in which the enzyme activity at time t hour is plotted against cell concentration at time (t–1) hour. It can be seen from this graph that the model accords reasonably well with the experimental data. This is substantiated by the fact that estimated standard deviation of the enzyme production yield coefficient is below 5%. The estimated enzyme production yield factor is also in good agreement with the value of $Y_p = 20.28$ obtained by the growth associated model.

Equation [7.24] indicates that significant production of dextransucrase from *Leuconostoc mesenteroides* occurs 1 hour after cell growth. Although

this time lag is only approximate, it reveals the significance of cell age in microbial product formation.

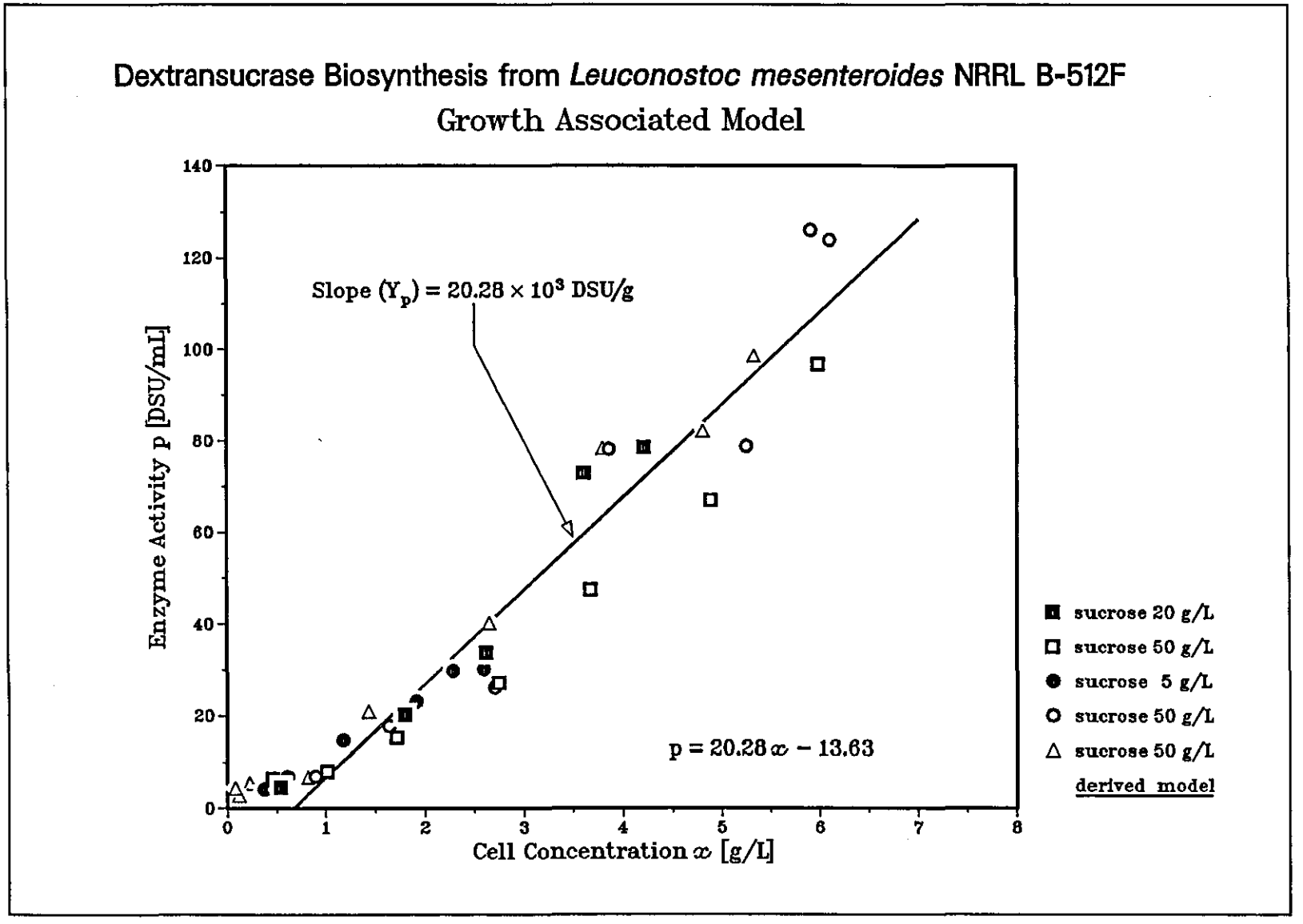
Dextransucrase Biosynthesis from *Leuconostoc mesenteroides* NRRL B-512F
Growth Associated Model
Slope (Y_p) = 20.28 × 10^3 DSU/g
p = 20.28 x − 13.63
Enzyme Activity p [DSU/mL]
Cell Concentration x [g/L]
0
20
40
60
80
100
120
140
0
1
2
3
4
5
6
7
8
sucrose 20 g/L
sucrose 50 g/L
sucrose 5 g/L
sucrose 50 g/L
sucrose 50 g/L
derived model

Figure 7.1

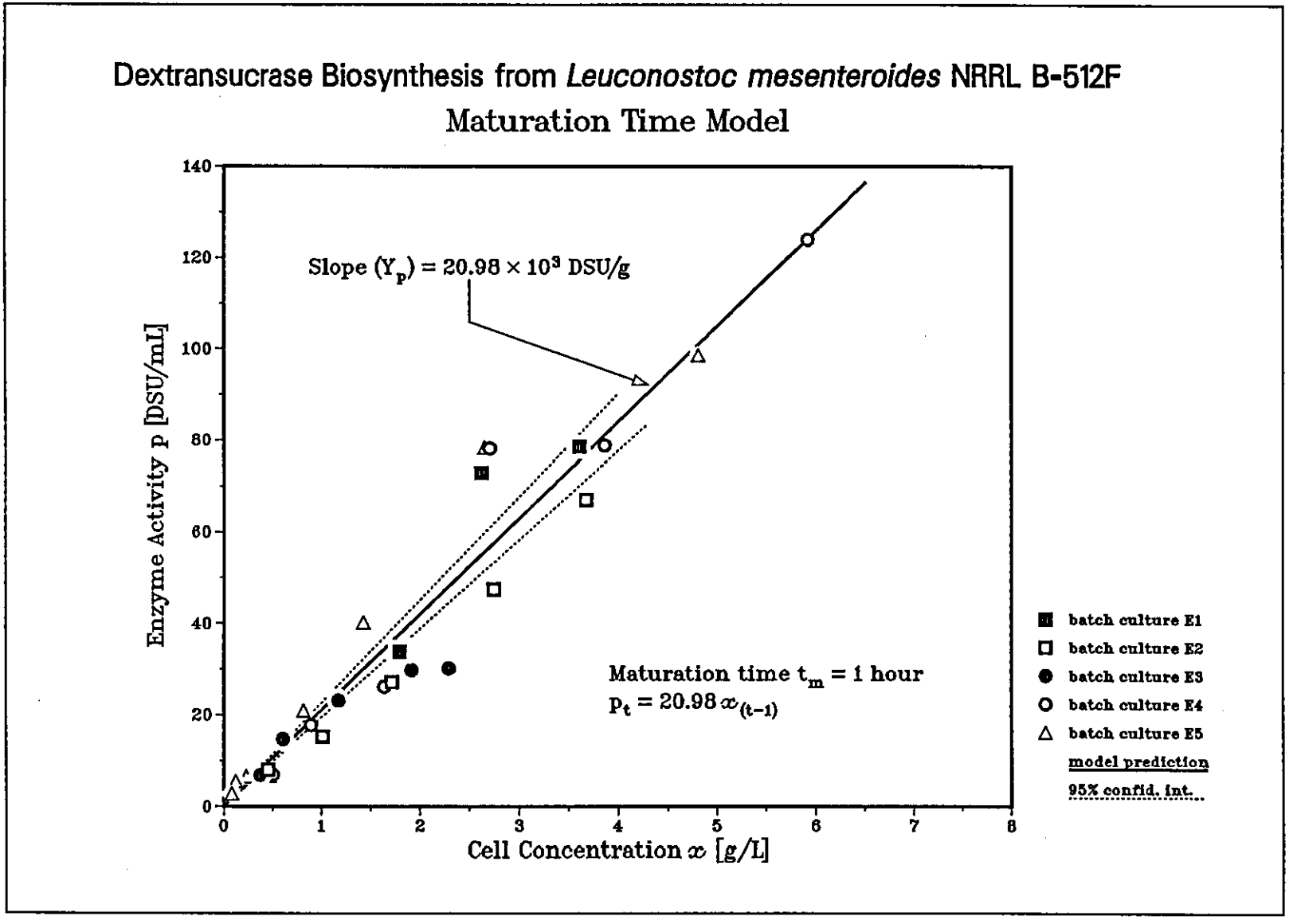
Dextransucrase Biosynthesis from *Leuconostoc mesenteroides* NRRL B-512F
Maturation Time Model
Slope (Y_p) = 20.98 × 10^3 DSU/g
Maturation time t_m = 1 hour
$p_t = 20.98\, x_{(t-1)}$
Enzyme Activity p [DSU/mL]
Cell Concentration x [g/L]
0
20
40
60
80
100
120
140
0
1
2
3
4
5
6
7
8
batch culture E1
batch culture E2
batch culture E3
batch culture E4
batch culture E5
model prediction
95% confid. int.

Figure 7.2

7.4 Analysis of Published Enzyme Production Data

To test the validity of the suggested enzyme production model, an independent source of data is best used for analysis. There are few sources of enzyme data in the literature, which are acquired in compatible cultural conditions. Difficulty also arises here due to the different units employed to express cell concentration and enzyme activity.

One useful source is presented by McAvoy (1981). Cells of *Leuconostoc mesenteroides* NRRL B-512F were grown in a sucrose medium similar to the main culture medium employed in this study. Four runs of fermentation were carried out in a 4 litre stirred-vessel at pH 6.7 and temperature 23 °C. The vessel was aerated so that the dissolved oxygen concentration was always above 50 % air saturation. In the experiments, a sterile sucrose-base mixture feeding system was linked to the pH control of the fermentation so that sucrose concentration in the fermenter was maintained approximately constant while the pH was kept at 6.7. The initial background sucrose concentrations used were between 4.75 *g/L* and 10 *g/L*. To facilitate kinetic analysis and provide a common base for comparison, the reported growth data in optical density is converted to biomass concentration in terms of dry cell weight by reference to a calibration curve. Correction is also made for the enzyme activity so that the unit is consistent with the unit used in this study. The results are presented in Figure 7.3.

Although the culture was operated in fed-batch mode, it was noted from the original data that the culture volume did not change substantially relative to its base value during the fermentation. For enzyme production purposes, the fermentation can be treated as batch cultivation. The growth associated enzyme synthesis model [7.12] for batch cultures is applied to the collected data and the kinetic parameters, Y_p and x_d are estimated by simple linear regression. The following specific values are found to represent the

kinetic behaviour of the system. Details of the analysis are given in Appendix K.

$$p = 23.91x - 13.46 \quad , \text{ for } x > x_d \qquad [7.25]$$

$$Y_p = 23.91 \text{ (DSU/mL)/(g/L)} \qquad [7.26]$$

$$p_d = 13.46 \text{ (DSU/mL)} \qquad [7.27]$$

$$x_d = 0.563 \text{ (g/L)} \qquad [7.28]$$

Although the data shows great scattering, as seen from Figure 7.3, the model parameters obtained are in agreement with the previous findings and support the proposed growth associated model. The discrepancy is likely attributable to the approximation of the fed-batch culture.

Similarly, the maturation time model is also applied to fit the data. The results from this analysis are presented in Figure 7.4. The following model parameters are obtained by trial-and-error method

$$Y_p = 25.23 \text{ (DSU/mL)/(g/L)} \qquad [7.29]$$

$$t_m = 1 \text{ hour} \qquad [7.30]$$

and the enzyme production model is given by

$$p_t = 25.23x_{(t-1)} \qquad [7.31]$$

In Figure 7.4, the enzyme activity in DSU/mL at an arbitrary time t is plotted against cell concentration in dry weight g/L at time 1 hour earlier. Compared with Figure 7.3, it was found that a maturation time below 1 hour would improve the fit, thus yielding a lower enzyme yield factor. As previously described, lack of enzyme data prevents reliable estimation of kinetic parameters by means of trial-and-error procedures.

The kinetics of the extracellular enzymes under fermentation conditions are in general difficult to model. In the case of dextransucrase production from *Leuconostoc mesenteroides*, the substrate sucrose plays a key part in the process of enzyme induction. A more rational model is, therefore, expected to include the effect of the inducer substrate. Furthermore, other metabolic products accumulated during cell growth may exert an influence on the enzyme synthesis. The permeation processes of the extracellular enzyme may also play a significant role in the kinetics of the overall process. Although these factors are not dealt with in the present situation due to experimental difficulty, the proposed simple growth-associated model and maturation time model are of potential utility in engineering applications.

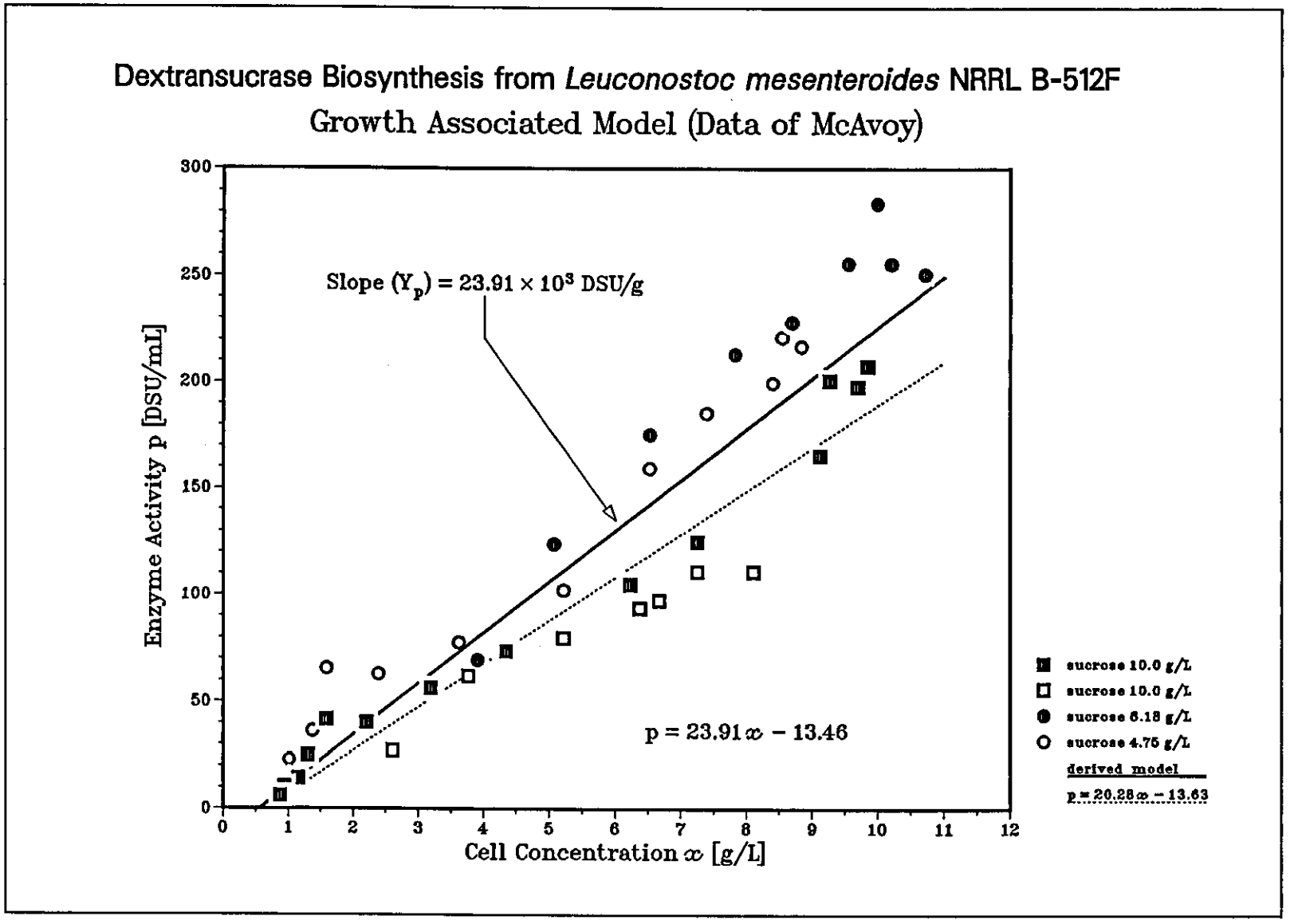
Dextransucrase Biosynthesis from *Leuconostoc mesenteroides* NRRL B-512F
Growth Associated Model (Data of McAvoy)
Slope (Y_p) = 23.91 × 10^3 DSU/g
p = 23.91x − 13.46
Enzyme Activity p [DSU/mL]
Cell Concentration x [g/L]
0
50
100
150
200
250
300
0
1
2
3
4
5
6
7
8
9
10
11
12
sucrose 10.0 g/L
sucrose 10.0 g/L
sucrose 6.18 g/L
sucrose 4.75 g/L
derived model
p = 20.28x − 13.63

Figure 7.3

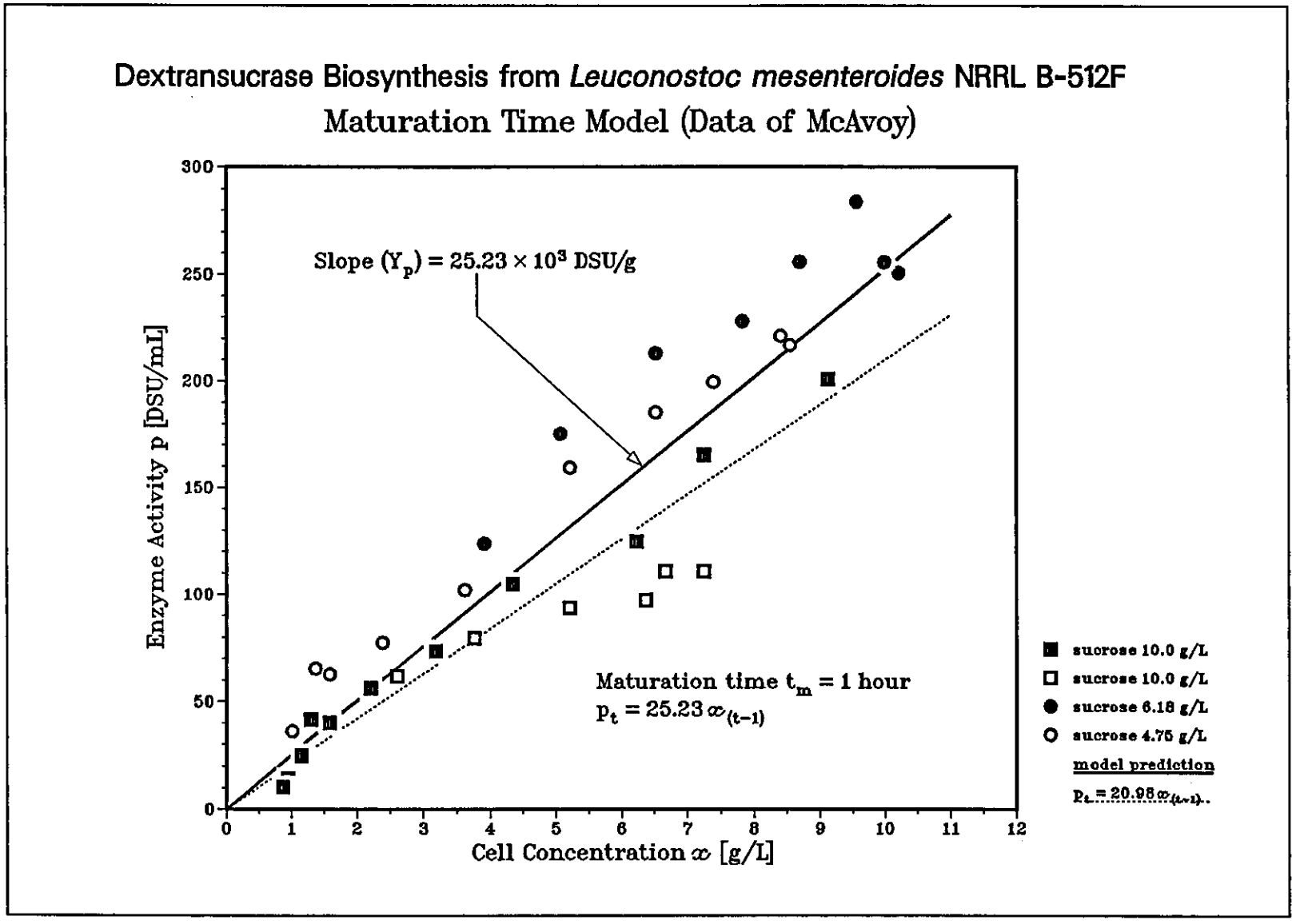
Dextransucrase Biosynthesis from Leuconostoc mesenteroides NRRL B-512F
Maturation Time Model (Data of McAvoy)
Slope (Y_p) = 25.23 × 10^3 DSU/g
Maturation time t_m = 1 hour
$p_t = 25.23\,x_{(t-1)}$
Enzyme Activity p [DSU/mL]
Cell Concentration x [g/L]
0
50
100
150
200
250
300
0
1
2
3
4
5
6
7
8
9
10
11
12
sucrose 10.0 g/L
sucrose 10.0 g/L
sucrose 6.18 g/L
sucrose 4.75 g/L
model prediction
$p_t = 20.98\,x_{(t-1)}$

Figure 7.4

Chapter 8 Simulation of Fed-Batch Fermentation

In a batch fermentation process, all the required nutrients are added to the fermentation vessel before inoculation. During the process, no material, except for molecular oxygen transfer in an aerobic process and NaOH or other chemical reagents for pH regulation, enters or leaves the fermentation vessel. In a chemostat continuous cultivation, fresh fermentation medium is continuously introduced to the cultural vessel at a constant rate and fractions of fermentation broth are removed from the vessel at the same flow rate so that the volume remains constant. Fed-batch culture interposes between these two kind of operations. It differs from batch and continuous cultures in that one or more nutrients are fed into the fermenter during cultivation and apart from sampling, the final products are only harvested at the end of fermentation. The culture volume in fed-batch operation is, therefore, continuously changing. One type of widely used fed-batch culture is semi-batch culture in which only the limiting carbon source is utilized in the feeding stream. The basic characteristic of fed-batch fermentation is that the concentrations of nutrients can be controlled by changing the flow rate of feeding nutrients.

In general, fed-batch fermentation has the advantage of achieving high cell concentrations over conventional batch culture, as it reduces substrate inhibition by maintaining low concentrations of substrate which may inhibit cell growth at high concentrations in the fermenter. Besides, continuous feeding of substrate in fed-batch culture can reduce agitation power consumption and enhance oxygen transfer efficiency by maintaining a low-viscosity fermentation broth in biopolymer production. Fed-batch culture technique can also be used in aerobic processes to restore lost water due to evaporation in aerobic processes which require a long reaction period. Furthermore, a fed-batch process is much easier to operate than a chemostat

culture in kinetic studies because it does not require an outflow and volume control.

The aerobic growth and enzyme production models developed in previous chapters are applied to simulate a fed-batch fermentation similar to an industrial procedure for enzyme production (Schneider, 1980; Alsop, 1983).

8.1 Mathematical Models of Fed-Batch Process

As before, the fermenter vessel is assumed to be well mixed so that each phase of the vessel content is of uniform composition. The growth of *Leuconostoc mesenteroides* cell is only limited by the concentration of the limiting substrate sucrose. As shown in chapter 6, the effect of oxygen on cell growth can be ignored. A sterilized solution of the growth-limiting substrate with concentration s_{in} is aseptically fed into the fermenter vessel according to a predetermined pattern F(t). Figure 8.1 shows the schematic representation of such a system.

8.1.1 Fed-Batch Operation Without Sampling

First considering the case in which the amount of samples taken from the fermenter for analyses of cell growth and enzyme synthesis is negligible. The pH of the fermentation broth is regulated at 6.7 by addition of 4M NaOH solution. The amount of NaOH added to the fermentation system is negligible.

With these assumptions, the dynamic process of fed-batch fermentation can be formulated as follows :

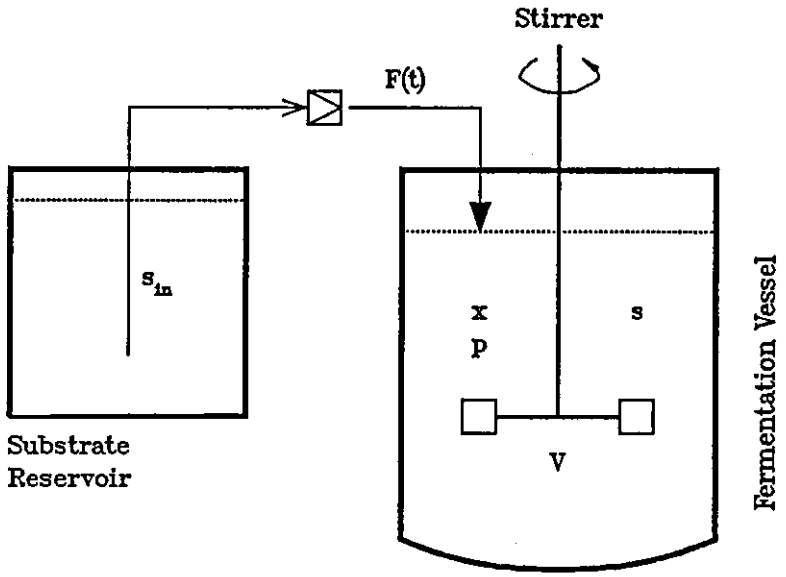

Fig. 8.1 Schematic Diagram of Fed–Batch Fermentation

Balance of biomass in the liquid phase

$$\frac{d}{dt}(xV) = r_x V \qquad [8.1]$$

Balance of limiting substrate in the liquid phase

$$\frac{d}{dt}(sV) = F(t)s_{in} - r_x V/Y_s \qquad [8.2]$$

Balance of enzyme accumulated in the fermentation broth

$$\frac{d}{dt}(pV) = Vr_p \qquad [8.3]$$

where

$$r_x = \mu x \qquad [8.4]$$

with μ according to the Monod kinetics as shown in chapter 5.

$$\mu = \frac{\mu_{max} S}{K_s + s} \qquad [8.5]$$

The estimated growth kinetic constants are

μ_{max} = 0.5 hr^{-1}
K_s = 0.9 g/L sucrose
Y_s = 0.15 g biomass/g sucrose

The production of dextransucrase by *L. mesenteroides* is associated with cell growth according to a maturation time model as described in chapter 7.

$$r_p(t) = Y_p r_x(t - t_m) \text{ , for } t \geq t_m \qquad [8.6]$$
$$r_p(t) = 0 \text{ , for } t < t_m \qquad [8.7]$$

where the estimated kinetic constants are

Y_p = 20.98 (DSU/mL)/(g/L)
t_m = 1 hour

Assuming that the densities of the substrate feeding stream and of the culture broth are the same, and that the density does not change substantially with time as fermentation proceeds, then the following equation applies :

$$\frac{dV}{dt} = F(t) \qquad [8.8]$$

Combining equation [8.1] and [8.8] yields :

$$\frac{dx}{dt} = \mu x - xF(t)/V \qquad [8.9]$$

Equation [8.2] reduces for this system to :

$$\frac{ds}{dt} = \frac{F(t)}{V}(s_{in} - s) - \mu x/Y_s \qquad [8.10]$$

Similarly, equation [8.3] becomes :

$$\frac{dp}{dt} = Y_p r_x (t - t_m) - pF(t)/V \ , \ \text{for } t \geq t_m \qquad [8.11]$$

$$\frac{dp}{dt} = 0 \ , \ \text{for } t < t_m \qquad [8.12]$$

By introducing the dilution rate D as :

$$D(t) = F(t)/V \qquad [8.13]$$

Then equations [8.9] to [8.11] become

$$\frac{dx}{dt} = \mu x - D(t)x \qquad [8.14]$$

$$\frac{ds}{dt} = D(t)(s_{in} - s) - \mu x/Y_s \qquad [8.15]$$

$$\frac{dp}{dt} = Y_p r_x (t - t_m) - D(t)p \ , \ \text{for } t \geq t_m \qquad [8.16]$$

In these equations,

x	=	biomass concentration, g/L
s	=	substrate concentration in the fermenter, g/L
p	=	product (enzyme) concentration, DSU/mL
V	=	culture volume, L
s_{in}	=	growth-limiting substrate concentration in the feeding stream, g/L.

Equations [8.5] to [8.16] provide the mathematical model for the fed-batch fermentation process when samples removed from the fermentation vessel are not accounted for. These nonlinear equations can be solved numerically with given initial conditions and given substrate-feeding function F(t).

8.1.2 Fed-Batch Operation With Sampling

In experiments carried out on a laboratory-scale bench-top fermenter, the amount of samples withdrawn for off-line analyses for cell concentration and enzyme activity cannot be neglected because of small volume of culture in the fermenter. The simulation technique can be used to examine the effect of sampling during fermentation. Assuming samples are taken at a rate of f(t) (L/hr) illustrated in Figure 8.2, the following mass balances apply

for growing cells

$$\frac{d}{dt}(xV) = r_x V - f(t)x \qquad [8.17]$$

for the limiting substrate

$$\frac{d}{dt}(sV) = F(t)s_{in} - r_x V/Y_s - f(t)s \qquad [8.18]$$

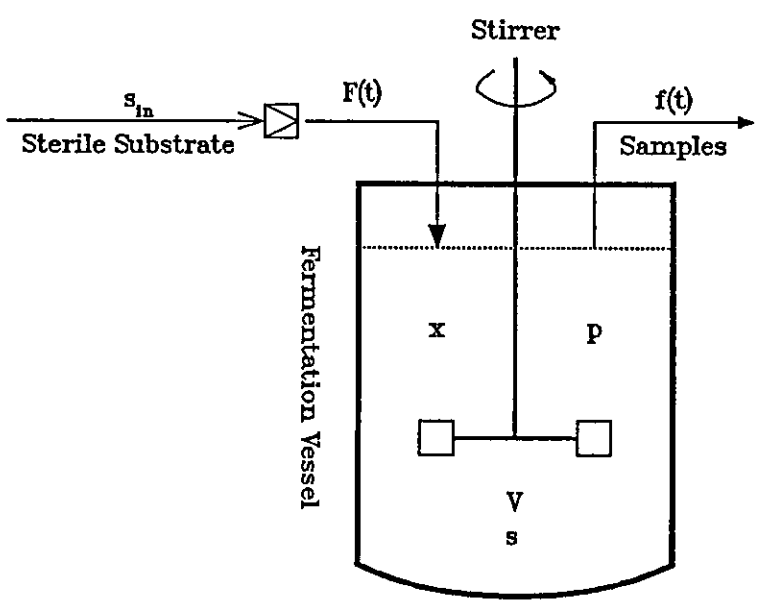

Fig. 8.2 Schematic Diagram of Fed–Batch Operation with Sampling

for the enzyme produced

$$\frac{d}{dt}(pV) = r_p V - f(t)p \qquad [8.19]$$

Similarly, the following relationship applies because the medium density does not change significantly with time during fermentation.

$$\frac{dV}{dt} = F(t) - f(t) \qquad [8.20]$$

Rearrangement of equations [8.17] to [8.20] and equations [8.4] and [8.6] gives :

$$\frac{dx}{dt} = \mu x - xF(t)/V \qquad [8.21]$$

$$\frac{ds}{dt} = (s_{in} - s)F(t)/V - \mu x/Y_s \qquad [8.22]$$

$$\frac{dp}{dt} = Y_p r_x(t-t_m) - pF(t)/V \text{ , for } t \geq t_m \qquad [8.23]$$

$$\frac{dV}{dt} = F(t) - f(t) \qquad [8.24]$$

Equations [8.21], [8.22] and [8.23] are formally identical with the corresponding balance equations [8.9] to [8.11] in a fed-batch fermenter without consideration of sampling process.

The process of sampling can be approximately represented by a train of pulse. An ACSL function of PULSE is defined as :

$$y = \text{PULSE(TZ, TP, TW)} \qquad [8.25]$$

y is a unit pulse train starting at the first calculation interval that equals or exceeds TZ. The period of this pulse train is TP and the width is TW. The function is illustrated graphically in Figure 8.3.

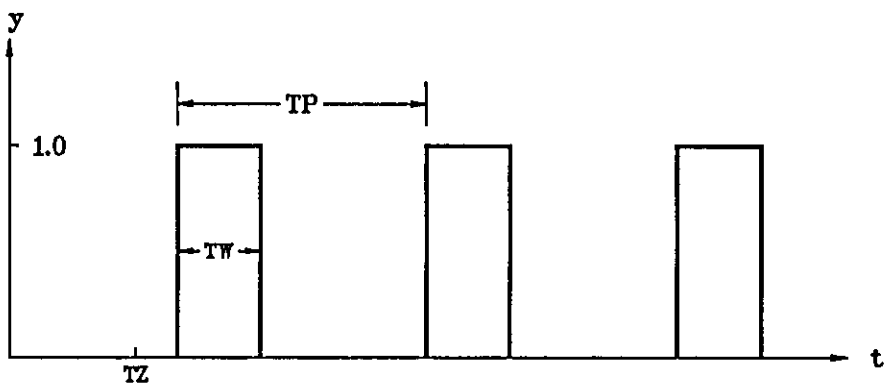

Fig. 8.3 ACSL Function y = PULSE(TZ , TP , TW)

Assuming that samples are taken at a time interval of T_{int} (hr), the size of a sample is A (L) and the time required to withdraw this amount of sample is T_{smp} (hr), then f(t) can be approximated by the following equation

$$f(t) = (A/T_{smp})PULSE(0, T_{int}, T_{smp}) \qquad [8.26]$$

This method of expressing f(t) is designated as "**Sampling model 1**".

Another way of modelling sampling process is to use the impulse function, that is to say, samples are taken instantaneously from the fermentation vessel.

$$f(t) = \sum_{n=0}^{\infty} A\delta(t-nT_{int}) , \quad L/hr \qquad [8.27]$$

Here $\delta(t-t_0)$ is the unit impulse function defined as :

$$\delta(t-t_0) = 0, \qquad \text{for } t \neq t_0 \qquad [8.28]$$

$$\delta(t-t_0) = \infty, \qquad \text{for } t = t_0 \qquad [8.29]$$

$$\int_{-\infty}^{\infty} \delta(t-t_0)dt = 1 \qquad [8.30]$$

On integration of Equation [8.24], we have

$$V(t) = V_0 + \int_0^t F(t)dt - \int_0^t \Sigma\, A\delta(t-nT_{int})dt \qquad [8.31]$$

Here V_0 is the initial volume of culture medium. The third term on the right hand side of this equation is given by mA,

where

$$m = INT(t/T_{int} + 1.0) \qquad [8.32]$$

INT is an ACSL function of integerization, i.e. m is the largest integer which is smaller or equal to $(t/T_{int} + 1.0)$.

Thus equation [8.31] can be written as :

$$V(t) = V_0 + \int_0^t F(t)dt - mA \qquad [8.33]$$

This algorithm for culture volume change can be easily implemented in an ACSL program. This method is designated as "**Sampling model 2**".

8.2 Description of the Fed-Batch Procedure for Enzyme Production

An attempt was made to emulate an industrial fed-batch procedure for dextransucrase production. *L. mesenteroides* was grown in a well-stirred batch fermenter which was continuously fed with fresh sterile nutrient medium containing the enzyme-inducer sucrose. The rate of sucrose addition was regulated in a step fashion. In order to carry out the experiment in the standard laboratory-scale bench-top fermenter, the initial volume of culture medium was reduced to 1.2 litre and the flow rates of feeding substrate were therefore scaled down accordingly on the volume basis.

The concentration of sucrose used in the feeding stream was 600 g/L. 800 mL of this nutrient supplement were prepared according to the method generally described in section 4.1.4. The solution was sterilized for 15 minutes at 121 °C.

The main fermentation medium was prepared by using medium F as described in section 4.1.2. An initial sucrose concentration of 10 g/L was employed in this case.

Sucrose	10 g/L
Yeast extract (Difco)	40 g/L
K_2HPO_4	20 g/L
R salts	0.5 % (v/v)
Antifoam (polypropylene glycol)	0.1 % (v/v)

After sterilization, cooling and regulation at 23 °C, the initial pH of the medium was set at 7.1. The fermenter was aerated and agitated so that the culture was under fully aerobic conditions during operation.

The pH of the culture broth was regulated at 6.7 during fermentation by

the addition of 4M NaOH. At 5 hours after inoculation, the peristaltic pump controlling medium addition was switched on and the sterile sucrose solution was added to the fermenter. The initial flow rate was 0.006 L/hr. After one hour this flow rate was doubled to 0.012 L/hr. After 7 hours of fermentation the sucrose flow rate was increased to 0.02 L/hr, after 8 hours to 0.028 L/hr and after 9 hours to 0.036 L/hr. The rate of sucrose addition was kept at this value for another hour. The peristaltic pump was then switched off, and the agitation speed and aeration flow rate were reduced to prevent overflow of culture medium.

The culture was monitored by taking samples at a time interval of half an hour. The cell concentration was determined by optical density measurements and the enzyme activity was determined by the analytical methods described in section 4.3.2.

8.3 Results of Simulation and Discussion

The experimental results of this fed-batch fermentation are presented in Appendix L. The initial conditions are summarized as follows :

$x_0 = 0.07$ g/L
$s_0 = 10$ g/L
$V_0 = 1.2$ L
$p_0 = 0$ DSU/mL

and

$s_{in} = 600$ g/L

The substrate feeding strategy employed here can be represented by a step function which is illustrated in Figure 8.4.

$$F(t) = F_0 STEP(T_0) + (F_1 - F_0)STEP(T_1) + (F_2 - F_1)STEP(T_2) + (F_3 - F_2)STEP(T_3) + (F_4 - F_3)STEP(T_4) - F_4 STEP(T_5) \quad [8.34]$$

where STEP is an ACSL function which generates a step change from zero to one in the output at a specified time. STEP is defined as :

$$y = STEP(TZ) \quad [8.35]$$

$$y = 0.0, \quad \text{for } t < TZ \quad [8.36]$$

$$y = 1.0, \quad \text{for } t \geq TZ \quad [8.37]$$

The flow rates of sucrose addition are listed below :

$F_0 = 0.006$ L/hr, $T_0 = 5$ hr
$F_1 = 0.012$ L/hr, $T_1 = 6$ hr
$F_2 = 0.020$ L/hr, $T_2 = 7$ hr
$F_3 = 0.028$ L/hr, $T_3 = 8$ hr
$F_4 = 0.036$ L/hr, $T_4 = 9$ hr
$T_5 = 10$ hour

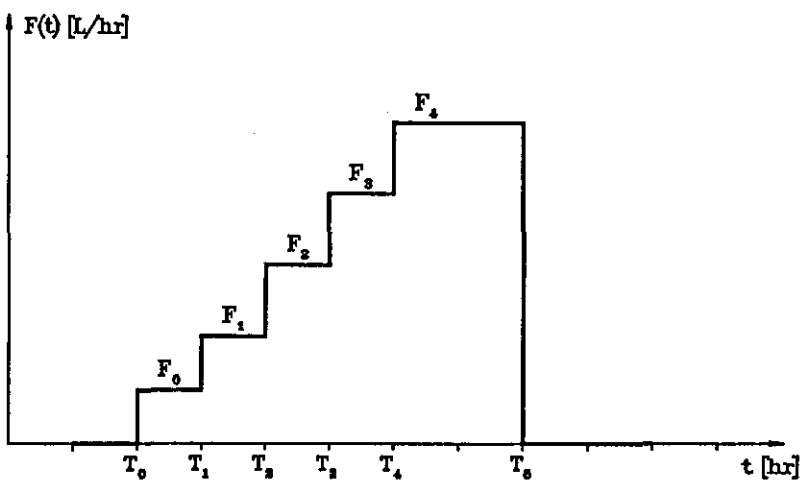

Fig. 8.4 Graphical Representation of Substrate Feeding Strategy

For samples of 20 mL, taken every half an hour, we have

$$A = 0.02 \quad L$$
$$T_{int} = 0.5 \quad hr$$

and the time needed to withdraw such a sample at a constant rate is about 30 seconds, i.e.

$$T_{smp} = 30 \text{ sec} = 1/120 \text{ hr}$$

For this set of parameters, the sampling process can be represented by a mathematical function according to equation [8.26] for model 1 :

$$f(t) = 2.4 \text{ PULSE}(0, 0.5, 1/120) \qquad [8.38]$$

With these conditions, the three models are used to simulate the fed-batch process. Sample computer output can be found in Appendix L. Results of simulation are presented in Figure 8.5 and Figure 8.6 in comparison with the experimental data. It can be seen from the simulation results that there are no significant differences between the three models during active cell growth and enzyme biosynthesis, indicating that the sampling process has little effect on the fermentation process provided the sample size is small relative to the culture volume. The two models depicting the process of sampling are seen to be effectively the same.

Figure 8.5 shows that predictions of the process model are in fairly good agreement with the experimental data of cell growth during active aerobic fermentation. Since the growth course was not followed after the dissolved oxygen level in the fermenter started to fall significantly (after 10 hours of fermentation), the growth stage approaching to the stationary phase is not clear. The model predicts that the growth of cells will effectively reach

the stationary phase after 11 hours of fermentation with the maximum biomass concentration being about 8.5 g/L in the case of negligible samples.

The substrate concentration in the fermenter was not measured due to practical difficulties. The simulation reveals that the concentration of the growth-limiting substrate in the vessel increases with the addition of fresh nutrient. This is partly due to the higher substrate concentration in the feeding stream. The simulation also shows that the limiting substrate is rapidly exhausted and the cell growth approaches the stationary phase after the substrate feed stops.

It can be seen from Figure 8.6 that the process model does not accord well with the experimental data of enzyme production in this particular case. The largest discrepancy occurs in the exponential growth phase. Considering the fact that the enzyme production model is derived from scattered data, the predictions of the model on the whole are reasonably satisfactory. Since enzyme production lags behind cell growth, enzyme synthesis after cell stops growth would be expected.

The enzyme yield factor determines the productivity of the fermentation. Figure 8.7 shows the effect of the product yield coefficient on enzyme biosynthesis. Simulation results are obtained with the lower bound and the upper bound of the estimated 95% confidence interval of the enzyme yield factor, and the value determined in fed-batch cultures (see section 7.4). It can be seen that the experimental data lies in the band of the model predictions. Figure 8.7 also indicates the possibility of a higher enzyme yield factor in fed-batch cultures.

The simulations of the proposed fed-batch process model employing cell growth and enzyme synthesis kinetics developed in previous chapters show that the simple kinetic model can be useful in predicting the behaviour

of a complex process such as a fed-batch fermentation. The simulation results also show that the process of enzyme production is much more complicated than the proposed model. The enzyme synthesis kinetics needs to be improved to describe the production limit and the lag phase more accurately.

Figure 8.5

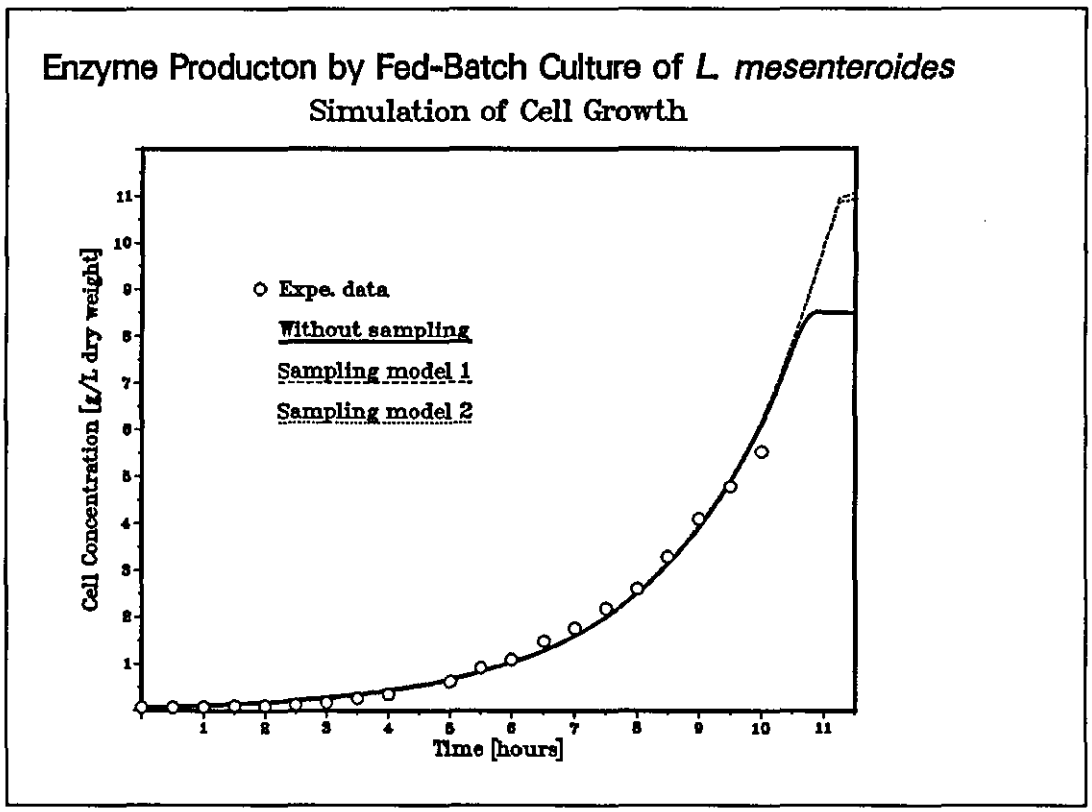

Figure 8.6

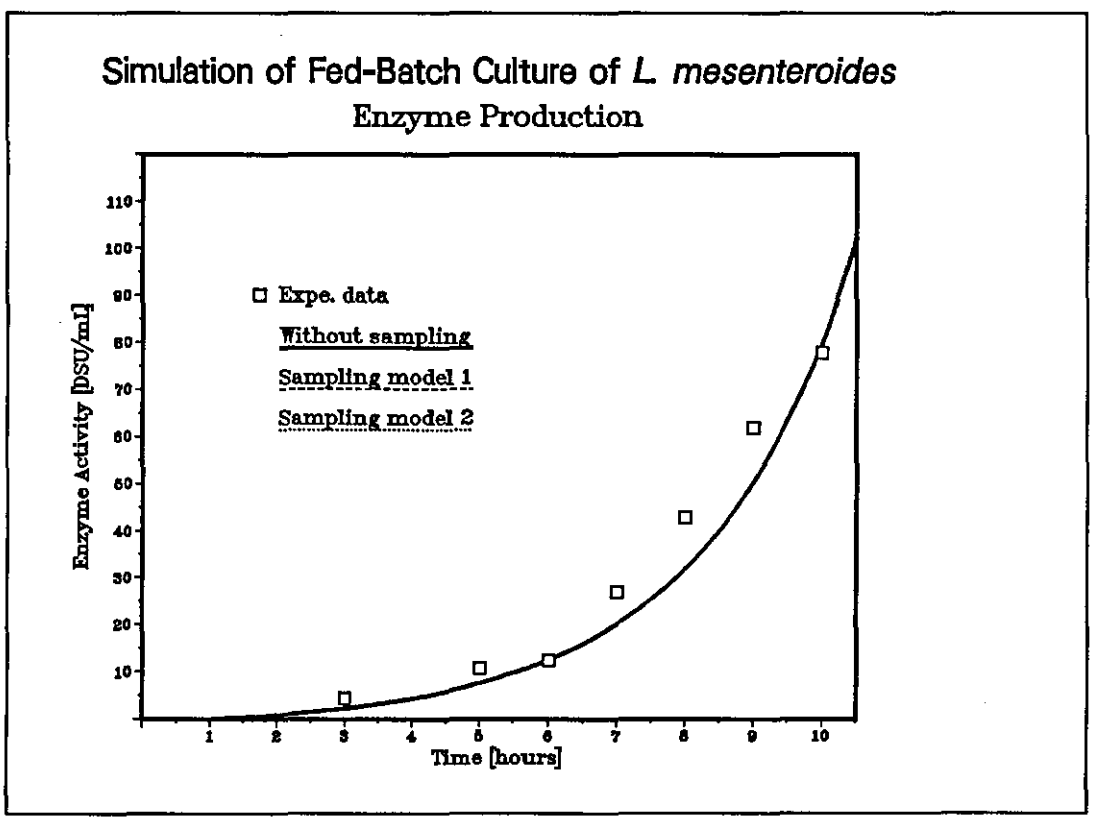

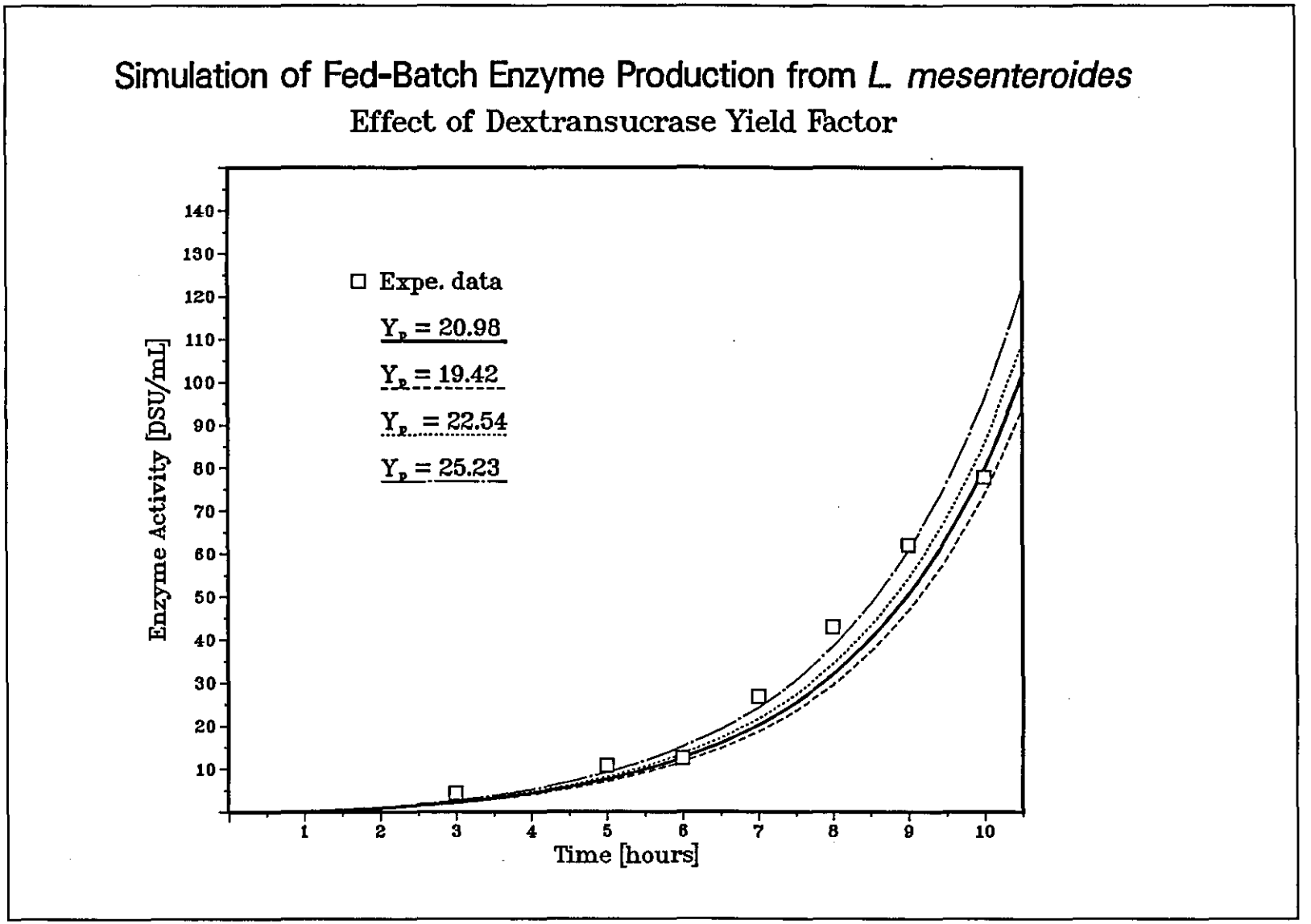
Simulation of Fed-Batch Enzyme Production from L. mesenteroides
Effect of Dextransucrase Yield Factor
Expe. data
Yp = 20.98
Yp = 19.42
Yp = 22.54
Yp = 25.23
Enzyme Activity [DSU/mL]
Time [hours]
10
20
30
40
50
60
70
80
90
100
110
120
130
140
1
2
3
4
5
6
7
8
9
10

Figure 8.7

Chapter 9 Summary and Conclusions

Mathematical modelling is an important investigative tool in engineering research and applications for it provides helpful insight into the process concerned. An appropriate engineering model is essential to mathematical analysis, design, development and experimentation of a complex system. Indeed, the heart of modern control and optimization techniques is the precise mathematical description of the system being considered. The increasing involvement of fermentation systems in industrial processes has added considerable impetus to the development of mathematical models for biological systems. Although significant advances have taken place in biological science research and in computing technology, successful mathematical modelling of microbiological processes is still hampered by the exceedingly complex activities occurring in the living cells. The purpose of modelling is to construct a mathematical formulation which can be used to predict the behaviour of the system. Due to the complex nature of the microbial systems, useful models for biological processes are often simplified mathematical descriptions of the macroscopic behaviour of the system under study. The commonly employed Monod model is an example of such approaches.

In this study, an endeavour was made to investigate the kinetics of an industry-based enzyme-producing fermentation process using the well-founded simple models. The aim was to acquire a better understanding of the process in a mathematically descriptive fashion so that improvements may be made on the existing production procedure to achieve higher yields of the enzyme by optimization methods.

A microcomputer-controlled laboratory scale fermentation system was set up to carry out the necessary experiments for data acquisition and model

verification. The bacterium *Leuconostoc mesenteroides* NRRL B-512F was grown in batch cultures under aerobic conditions. The fermentation was controlled so that the cultural conditions were favourable to the production of the extracellular enzyme dextransucrase, which is used to catalyze the polymerization of dextran.

9.1 Cell Growth

The kinetics of cell growth under the controlled environmental cultural conditions was studied closely by batch and special fed-batch techniques. Measurement of biomass concentration was realized by determination of optical density of culture samples at a selected wavelength of 590nm. From the experimental data obtained, the general features of aerobic metabolism of *L. mesenteroides* was discerned. Biomass yield experiments confirmed that sucrose is the growth-limiting nutrient component in the carefully formulated growth medium within the range of interest. The initial specific growth rates were determined for various substrate concentrations used. The Monod model was found to represent the growth kinetics satisfactorily. The kinetic parameters in the model were evaluated by a statistical curve fitting method and a data transformation technique. A saturation constant of 0.9 g/L for the substrate was obtained, indicating weak influence of the substrate on growth rate. The initial specific growth rates at high substrate concentrations were approximately constant within the experimental errors, giving a value of 0.5 hr^{-1} for the maximum specific growth rate. The model was found to accord well with the experimental data with statistical significance.

However, it was noticed that the kinetic data of cell growth in the lower range of substrate concentrations was scattered and the mean values of the kinetic parameters estimated over the whole range of the experimental data did not give the best fit to this part of the data. The saturation constant in the Monod model is seen to be strongly determined by the initial specific growth

rates obtained at low substrate concentrations. Thus, a large range of the saturation constant is expected from the experimental data. The lower limit of the saturation constant, which yields weak substrate limitation, can be estimated by fit the Monod model to the data points with high specific growth rates, while the upper limit of the saturation constant, which leads to strong substrate limitation, can be estimated by fit the model to those data points with low specific growth rates. Figure 9.1 shows the kinetic parameters estimated by such an approach. Calculations from these parameter estimates indicate that the specific growth rates are within 5% of the maximum value when the substrate concentration exceeds 6 g/L (weak growth-limitation) to 34 g/L (strong growth-limitation). The model with mean parameter estimates predicts virtually constant specific growth rates at substrate concentrations over 17 g/L.

The possibility of dissolved oxygen being simultaneously limiting the growth of cells was investigated. A galvanic electrode was used to measure the concentration of dissolved oxygen in terms of oxygen tension. Stoichiometric analyses and computer simulations were employed in the investigation. It was found that the dissolved oxygen was not limiting the growth process when the oxygen tension was maintained above a critical value of about 0.1 per cent air saturation.

In an industrial fermentation, the metabolism of *L. mesenteroides* on sucrose may be a combination of aerobiosis and anaerobiosis because the reactor vessel is often not perfectly mixed. Although no kinetic models describing the anaerobic enzyme-producing fermentations are available, it is known that a considerable amount of ethanol is produced in anaerobic cultures employed for whole-cell dextran production. The inhibitory effect of ethanol on cell growth was suggested to take the following kinetic form (Dussap & Gros, 1985) :

$$\mu = \mu_{max} \frac{s}{K_s + s} \frac{K_e}{K_e + C_e} \qquad [9.1]$$

where C_e is the concentration of ethanol produced (g/L). K_e is the inhibition constant, a value of 1.5 g/L was given at 25 °C, pH 6.7. An ideal batch culture under anaerobic conditions can thus be described by the following process equations :

$$\frac{dx}{dt} = \mu x \qquad [9.2]$$

$$\frac{ds}{dt} = -\mu x / Y_{s,ana} \qquad [9.3]$$

$$\frac{dC_e}{dt} = \mu x Y_{e/x} \qquad [9.4]$$

The anaerobic biomass yield coefficient $Y_{s,ana}$ was shown to be much lower than the yield coefficient under fully aerobic cultural conditions (Wilson, 1985). Simple stoichiometric analysis and ATP generation analysis similar to that presented in section 6.4 gave an approximate value of 0.07 g biomass/g sucrose, i.e. $Y_{s,ana} = 0.07$. This was confirmed by the data of Wilson (1985). The approximate stoichiometric yield coefficient of ethanol based on biomass, $Y_{e/x}$, was shown to be 1.23 g ethanol/g biomass (Dussap & Gros, 1985).

With these parameter estimates, equations [9.1] to [9.4] can be used to simulate an anaerobic batch culture. Figure 9.2 illustrates the simulation of a typical aerobic batch process excluding the growth lag phase. Simulations of aerobic kinetic model with different saturation constants are compared with the simulated anaerobic batch process under the same initial culture conditions. It can be seen that the proposed aerobic kinetic model can reasonably predict the growth process, while anaerobic cell growth is much inferior to the aerobic growth in terms of growth rate and biomass yield.

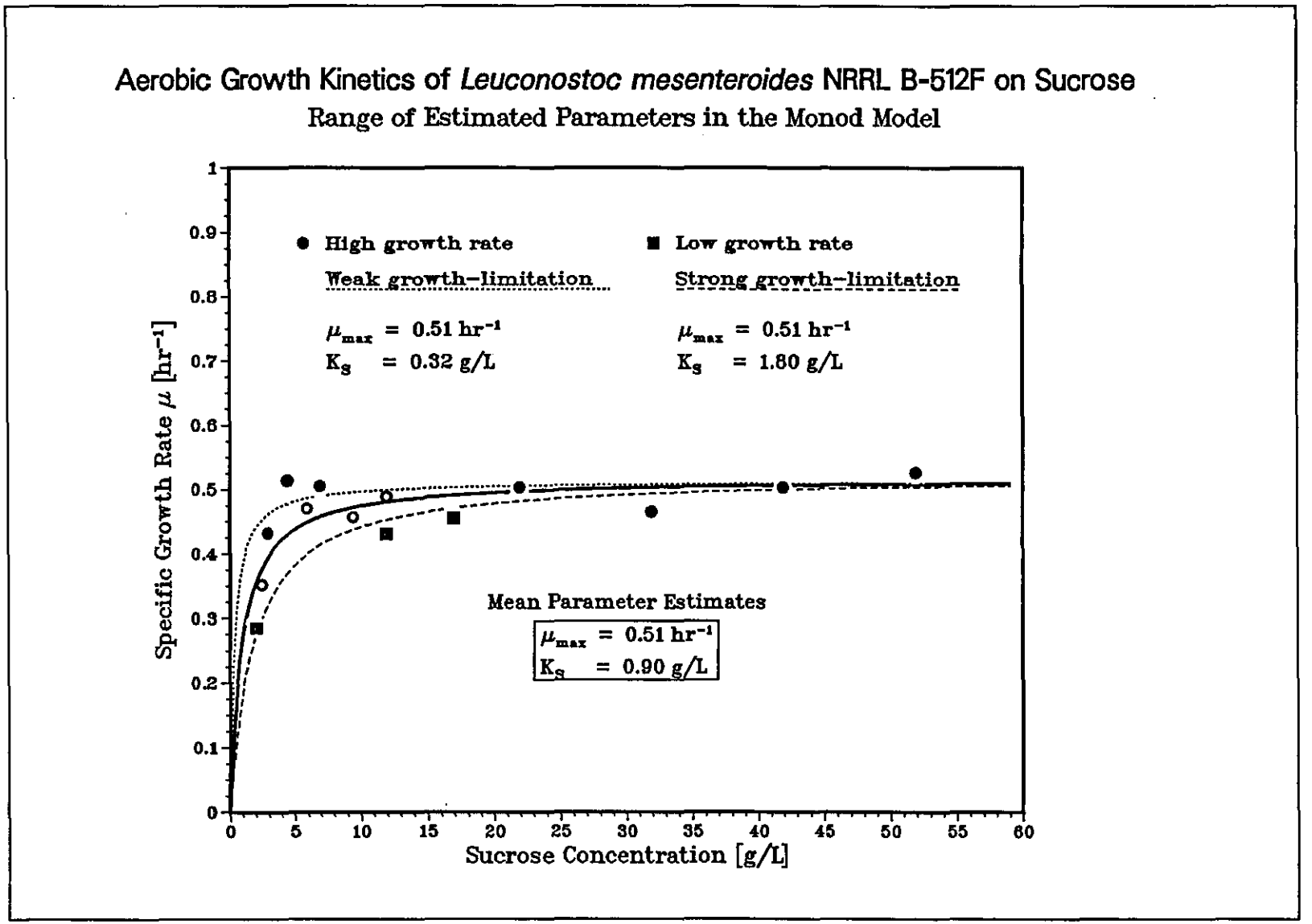
Aerobic Growth Kinetics of *Leuconostoc mesenteroides* NRRL B-512F on Sucrose
Range of Estimated Parameters in the Monod Model
High growth rate
Weak growth-limitation
μ_{max} = 0.51 hr^{-1}
K_S = 0.32 g/L
Low growth rate
Strong growth-limitation
μ_{max} = 0.51 hr^{-1}
K_S = 1.80 g/L
Mean Parameter Estimates
μ_{max} = 0.51 hr^{-1}
K_S = 0.90 g/L
Specific Growth Rate μ [hr^{-1}]
Sucrose Concentration [g/L]
0
0.1
0.2
0.3
0.4
0.5
0.6
0.7
0.8
0.9
1
0
5
10
15
20
25
30
35
40
45
50
55
60

Figure 9.1

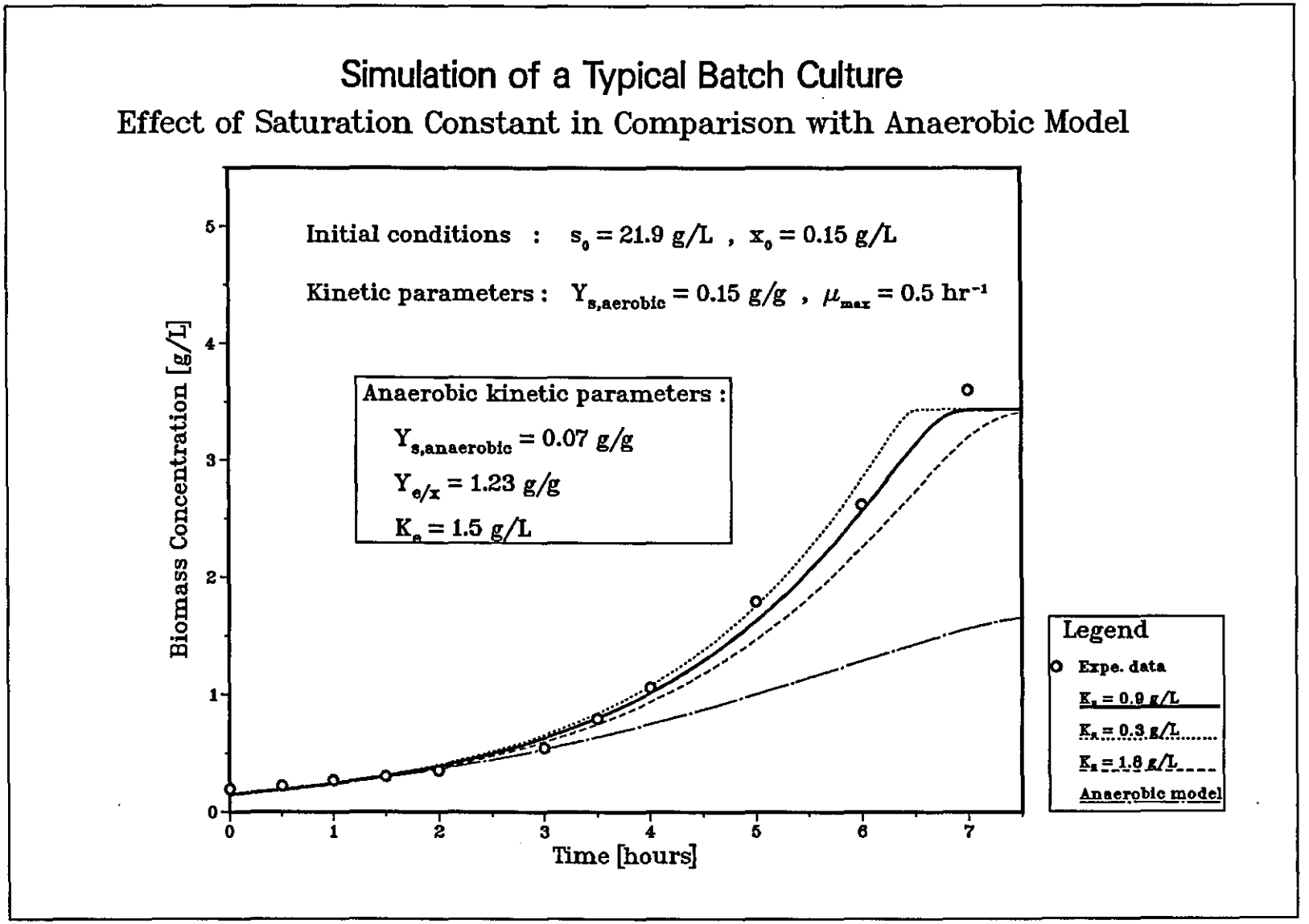
Simulation of a Typical Batch Culture
Effect of Saturation Constant in Comparison with Anaerobic Model
Initial conditions : $s_0 = 21.9$ g/L , $x_0 = 0.15$ g/L
Kinetic parameters : $Y_{s,aerobic} = 0.15$ g/g , $\mu_{max} = 0.5$ hr^{-1}
Anaerobic kinetic parameters :
$Y_{s,anaerobic} = 0.07$ g/g
$Y_{e/x} = 1.23$ g/g
$K_e = 1.5$ g/L
Biomass Concentration [g/L]
Time [hours]
0
1
2
3
4
5
6
7
Legend
Expe. data
$K_s = 0.9$ g/L
$K_s = 0.3$ g/L
$K_s = 1.8$ g/L
Anaerobic model

Figure 9.2

9.2 Enzyme Production

Dextransucrase production from growing cells of *L. mesenteroides* was elaborated by simple modelling approaches. The enzyme activity was determined by an analytical procedure. It was found that the synthesis of enzyme paralleled the growth of cells, but with a lag phase. The growth associated product formation kinetics was applied to the experimental data. The characteristic lag of enzyme production behind the growth process was considered in terms of an empirical threshold cell concentration, and more rationally in terms of cell maturation process and the degree of maturity characterized by a maturation time parameter. Analysis of published data corroborated the suggested model.

The characteristic lag of enzyme production observed in experiments may also be explained by the process of enzyme secretion from the cell across the cell membrane to the environment, which can be represented by a simple mass transfer process. Assuming that at an arbitrary time t during exponential cell growth in a batch culture, the total cell volume is V_c, and the total extracellular liquid volume is V which is essentially constant. Assuming also that the enzyme produced within the cell has a concentration of p_c, which is observed in the environment as p, then the following mass balances apply

$$\frac{d}{dt}(xV) = \mu xV \qquad [9.5]$$

$$\frac{d}{dt}(V_c p_c) = Y_p \mu x V - K V_c (p_c - p) \qquad [9.6]$$

$$\frac{d}{dt}(Vp) = K V_c (p_c - p) \qquad [9.7]$$

In these equations, x is the biomass concentration, μ is the constant specific

growth rate, Y_p is the enzyme yield coefficient on the basis of biomass produced and K is the volumetric enzyme transfer coefficient. The total cell volume V_c is much smaller than the total external liquid volume V. For exponential cell growth, the amount of enzyme produced within the cell and the amount of enzyme transferred to the environment are seen to be bound by the following relationship by manipulations with equations [9.5] to [9.7]:

$$V_c p_c + Vp = Y_p x V \qquad [9.8]$$

Using equation [9.8] to express $V_c P_c$ in terms of V_p and substituting this into equation [9.7] with $dV/dt = 0$, and $V_c/V \approx 0$, and rearrangement gives :

$$\frac{dp}{dt} + K_p = KY_p x \qquad [9.9]$$

This is a first order linear system equation, with the exponential biomass increase as the input and enzyme activity in the culture medium as the output. Integration of equation [9.9] with the initial enzyme activity being approximately zero leads to :

$$p = Y_{p,obs} x\{1 - \exp[-(K + \mu)t]\} \qquad [9.10]$$

where

$$Y_{p,obs} = KY_p/(K + \mu) \qquad [9.11]$$

The delay (lag) time of the system response can be represented by the equivalent dead time (Matsubara, 1965), which in this case is equal to the time constant of the exponential decay term in equation [9.10], i.e.

$$\tau = 1/(K + \mu) \qquad [9.12]$$

The asymptotic form of equation [9.10], which is effectively achieved when time t is three times of the lag time τ, that is to say

$$p = Y_{p,obs}x \qquad [9.13]$$

for $$t \geq 3/(K + \mu) \qquad [9.14]$$

Examination of equation [9.11] reveals that the virtual enzyme yield factor is larger than the observed value, which varies with the volumetric transfer coefficient K in a hyperbolic fashion according to equation [9.11]. Taking the lag time being about 1 hour obtained by cell maturation analysis in chapter 7, the volumetric enzyme transfer coefficient K is seen from equation [9.12] to be approximately equal to the specific growth rate in the exponential growth phase, which is essentially the maximum specific growth rate when the substrate concentration is over 17 g/L as previously described, i.e.

$$K = 0.5\ hr^{-1} \qquad [9.15]$$

Thus, the virtual enzyme yield factor Y_p is calculated from equation [9.11] to be approximately two times of the observed value, that is to say

$$Y_p = 42\ (DSU/mL)/(g/L) \qquad [9.16]$$

Statistical analysis of the available enzyme production data gave parameter values in agreement with the values obtained above. A thorough experimental examination of the time lag of enzyme production may be achieved by a series of carefully designed cascaded continuous cultures with small residence time.

The constructed kinetic models were applied to simulate a fed-batch fermentation. The results of simulations showed reasonably good agreement

between the model predictions and the experimental data. The simplified models have proved their effective practical utility.

9.3 Further Work

The investigations into the process kinetics of dextransucrase production have laid the foundation for further study. The process will not be restricted by the present empirical operating conditions. The model may be used in combination with optimization techniques to determine the optimum control profiles and establish optimum production conditions such as substrate feeding strategy so that maximum productivity of the enzyme can be achieved.

The effect of pH and temperature on enzyme production should also be examined in a mathematically descriptive way because these variables are relatively easy to control. Since industrial fermentations are likely to be operated under partly anaerobic conditions due to insufficient agitation and aeration, the transition process from aerobic metabolism to anaerobic metabolism is another topic worth pursuing. The anaerobic growth of cells in enzyme-producing fermentations is likely to be inhibited by ethanol production. Experiments are necessary to investigate the growth kinetics more closely. Enzyme production under anaerobic conditions should also be examined in detail so that a clear picture can be obtained for dextransucrase production.

NOMENCLATURE

a	specific area of mass transfer (bubble surface area per unit volume), m^{-1}
C_g	oxygen solubility, 100 % air saturation
C_l	dissolved oxygen concentration in the fermenter, g/L or % air saturation
C_{lf}	fractional oxygen concentration, C_l/C_g
D	dilution rate, hr^{-1}
EA	enzyme activity, DSU/mL
F, f	volumetric flow rate, L/hr
K	volumetric enzyme transfer coefficient, hr^{-1}
K_L	mass transfer coefficient at gas/liquid interface, m/hr
K_La	volumetric oxygen mass transfer coefficient, hr^{-1}
K_s	saturation constant for growth-limiting substrate, g/L
K^*	dimensionless saturation constant
K_o	saturation constant for oxygen, g/L or % air saturation
K_o^*	dimensionless saturation constant for oxygen, $= K_o/C_g$
OD	optical density
p	product concentration, g/L or DSU/mL

p_c	enzyme concentration in the cell, g/L or DSU/mL
q	specific rate of bioprocess (metabolic quotient), hr^{-1}
q_o	specific rate of oxygen utilization, hr^{-1}
q_p	specific rate of product formation, hr^{-1}
q_s	specific rate of biomass utilization, hr^{-1}
r	rate of reaction, g/L hr^{-1}
r_p	rate of product formation, g/L hr^{-1}
r_x	cell growth rate, g/L hr^{-1}
s	substrate concentration, g/L
S	total amount of substrate in culture, g
t	time, hr
t_L	lag period before exponential growth, hr
t_m	maturation period, hr
T	temperature, °C
V	volume of culture in fermenter, L
V_c	total volume of cells, L
w	data transformation
x	biomass concentration, g/L dry weight

x_d	threshold biomass concentration, g/L
x_{fm}	maximum biomass concentration in fed-batch culture, g/L
x_{max}	maximum biomass concentration in batch culture, g/L
X	total amount of biomass in culture, g
Y, $Y_{i/j}$	yield coefficient (component i/component j)
Y_s	biomass yield coefficient for substrate
Y_o	biomass yield coefficient for oxygen
Y_o^*	$= Y_oC_g$
Y_p	product yield coefficient on biomass
Y_{ATP}	overall ATP yield, g dry biomass/mol ATP
z	fractional biomass concentration
α, β	constants
μ	specific growth rate, hr^{-1}
μ_{max}	maximum specific growth rate, hr^{-1}
μ_0	initial specific growth rate, hr^{-1}
μ^*	specific growth rate, hr^{-1}
σ^2	variance
τ	time delay, hr

REFERENCES

General Texts

Aiba, S., Humphrey, A. E., & Mills, N. F. (1973)
Biochemical Engineering, 2nd ed., Academic Press, New York.

Atkinson, B., & Mavituna, F. (1983) *Biochemical Engineering and Biotechnology Handbook*, Macmillan Publishers Ltd., Surrey.

Bailey, J. E., & Ollis, D. F. (1986)
Biochemical Engineering Fundamentals, 2nd ed., McGraw Hill, New York.

Bergey, D. H. (Ed.) *Manual of Determinative Bacteriology*,
8th Edition 1974.

Dean, A. C. R., & Hinshelwood, C. (1966)
Growth, Function and Regulation in Bacterial Cells, Clarendon Press.

Doelle, H. W. (1975)
Bacterial Metabolism, 2nd ed., Academic Press, New York.

Humphries, J. (1874) *Bacteriology*.

Lehninger, A. L. (1975)
Biochemistry, 2nd ed., Worth Publishers, New York.

Monod, J. (1942) *Recherches sur la Croissance des Cultures Bacteriennes*,
Hermann and Cie, Paris.

Pirt, S. J. (1975) *Principles of Microbe and Cell Cultivation*,
Blackwell Scientific Publications.

Rehm, H. J., & Reed, G. (Eds.) *Biotechnology*, VCH Publishers, 1985.

Particular Topics

Alsop, R. M. (1983) "Industrial Production of Dextran"
Progress in Industrial Microbiology, **18**, 1 - 44.

Andrews, J. F. (1968) "A Mathematical Model for the Continuous Culture of Microorganisms Utilizing Inhibitory Substrates"
Biotech. Bioeng., **10**, 707 - 723.

Bailey, R. W., Barker, S. A., *et al.* (1957) "The Transglucosylase Action of Betacoccus Arabinosaceous Dextransucrase" *J. Chem. Soc.*, 3536 - 3541.

Bandyopadhyay, B., & Humphrey, A. E. (1967) "Dynamic Measurement of the Volumetric Oxygen Transfer Coefficient in Fermentation Systems"
Biotech. Bioeng., **9**, 533 - 544.

Barford, J. P., & Hall, R. J. (1978) "An evaluation of the Approaches to the Mathematical Modelling of Microbial Growth"
Process Biochemistry, **13**, 22 - 29.

Barker, J., Khan, M. A. M., & Sohomons, T. (1964)
"Mechanism of the Pasteur Effect" *Nature*, **201**, 1126 - 1127.

Bauchop, T., & Elsden, S. R. (1960) "The Growth of Microorganisms in Relation to Their Energy Supply" *J. Gen. Microbiol.*, **23**, 457 - 469.

Blanch, H. W. (1981) "Invited Review Microbial Growth Kinetics"
Chem. Eng. Commun., **8**, 181 - 211.

Box, G. E. P., & Cox, D. R. (1964) "An Analysis of Transformations"
J. Royal Stat. Soc, Series B **26**(2), 211 - 252.

Brown, D. E., & Vass, R. C. (1973) "Maturity and Product Formation in Cultures of Microorganisms" *Biotech. Bioeng.*, **15**, 321 -330.

Brunner, R. L. (1964) "Determination of Reducing Value : 3,5-Dinitrosalicylic Acid Method" *Methods in Carbohydrate Chemistry*, **4**, 67 - 71.

Chen, Y. E., & Kaboli, H. (1976) "Purification and Properties of Dextransucrase" *Proc. Annu. BioChem. Eng. Sym.*, 41 - 53.

Cleland, W. W. (1967), "The Statistical Analysis of Enzyme Kinetic Data" *Adv. Enzymol.*, **29**, 1 - 32.

Coleman, M. H. (1965) "Graphical Analysis of Enzyme Kinetic Data" *Nature*, **205**, 798 - 799.

DeMoss, R. D., Bard, R. C., & Gunsalus, I. C. (1951) "The Mechanism of the Heterolactic Fermentation : A New Route of Ethanol Fermentation" *J. Bacteriol.*, **62**, 499.

Doelle, H. W. (1981) "Basic Metabolic Processes" in Rehm, H. J., & Reed, G., (Ed.) *Biotechnology*, Vol. **1**, 113 - 210.

Dowd, J. E., & Riggs, D. S. (1965) "A Comparison of Estimates of Michaelis-Menton Kinetic Constants from Various Linear Transformations" *J. Biol. Chem.*, **240**(2), 863 - 869.

Dussap, C. G., & Gros, J. B. (1985) "Modelling of Dextran Production by *Leuconostoc mesenteroides*" *Bio-Sciences*, **4**(5), 119 - 125.

Ebert, K. H., & Schenk, G. (1968) "Mechanisms of Biopolymer Growth: The formation of Dextran and Levan" *Adv. Enzymol.*, **30**, 179 - 219.

Edwards, V. H. (1970) "The Influence of High Substrate Concentrations on Microbial Kinetics" *Biotech. Bioeng.*, **12**, 679 - 712.

Figures, W. R., & Edwards, J. R. (1976) *Carbohydrate Research*, **48**, 245 - 253.

Foster, F. H. (1968) "Dextran - Manufacture and Use"
Process Biochemistry, **3**, 15 - 19 and 55 - 62.

Fredrickson, A. G., Megee, R. D., & Tsuchiya, H. M. (1970)
"Mathematical Models for Fermentation Processes"
Advances in Applied Microbiology, **13**, 419 - 464.

Genghof, D. S., & Hehre, E. J. (1972)
Proc. Soc. Expt. Biol. Med., **140**, 1298.

Greulich, K. O., & Ludwig, H. (1977) "High Pressure Enzyme Kinetics of Dextransucrase" *Biophysical Chemistry*, **6**, 87 - 94.

Greulich, K. O., & Ludwig, H. (1979) "The Use of an Oscillating-Tube Densiometer as a Tool in Enzyme Kinetics. Determination of the Influence of Sodium Ascorbate on Invertase, Dextransucrase and Dextranase"
J. Biochem. Biophys. Methods, **1**, 327 - 334.

Heath, F. C., Hurwitz, J., & Horeckers, B. L. (1956) "Acetyl-phosphate Formation in the Phosphorolytic Cleavage of Pentose Phosphate"
J. American Chemical Society, **78**, 5449.

Hehre, E. J. (1941) "Production from Sucrose of a Serologically Reactive Polysaccharide by a Sterile Bacterial Extract" *Science*, **93**, 237 - 238.

Hehre, E. J. (1951) "Enzymic Synthesis of Polysaccharides: A Biological Type of Polymerization" *Advances in Enzymology and Related Subjects of Biochemistry*, **11**, 297 - 337.

Hehre, E. J. (1955) "Polysaccharide Synthesis from Disaccharides"
Methods in Enzymology, **1**, 178 - 192.

Hehre, E. J., & Suzuki, H. (1966) "New Reactions of Dextransucrase : α-D-Glucosyl Transfer to and from the Anomeric Sites of Lactulose and Fructose" *Arch. Biochem. Biophys.*, **113**, 675 - 683.

Hernandez, E., & Johnson, M. J. (1967) "Energy Supply and Cell Yield in Aerobically Growth Microorganisms" *J. Bacteriol.*, **94**(4), 996 - 1001.

Hestrin, S., Avineri-Shapiro, S., & Aschner, M. (1943) "The Enzymic Production of Levan" *Biochem. J.*, **37**, 450 - 456.

Hestrin, S. (1944) "Alleged Role of Fructofuranose in the Synthesis of Levan" *Nature*, **154**, 581.

Hollo, J., & Laszlo, E. (1941) "The Synthesis of Dextran : Importance of Sucrose Concentration in the Course of Dextran Fermentation" *Periodica Polytechnica*, **15**(1,2), 35 - 42.

Hosteller, F., Borel, E., & Deul, H. (1951) "Über die Reduktion der 3,5-Dinitrosalicylsäure durch Zucker" *Helvetica Chimica Acta*, **34**, 2132 - 3139.

Humphrey, A. E. (1968) in Mateles, R. I., & Tannenbaum, S. R. (Eds) *Single Cell Protein*, 330.

Iyata, K., & Yamamoto, T. (1975) "Dextransucrase as an Enzyme Associating with Alkaline Earth Metal Ions" *Agric., Biol. Chem.*, **39**(6), 1187 - 1192.

Jacobson, L. (1951) "Maintenance of Iron Supply in Nutrient Solutions by a Single Addition of Ferric Potassium Ethylenediamine Tetra-acetate" *Plant Physiology*, **26**, 411 - 413.

Jeanes, A. (1965) "Dextrans" *Methods in Carbohydrate Chemistry*, **5**, 118 - 127.

Jeans, A. (1966) "Dextran" in Mark, H. (Ed.) *Encyclopaedia of Polymer Science and Technology*, John Wiley and Sons Inc., Vol. **4**, 805 - 824.

Jeanes, A. (1977) "Dextrans and Pullulans : Industrially Significant α-D-Glucans" *American Chem. Soc. Symp.*, **45**, 284 - 298.

Johnson, M. K., & McCleskey, C. S. (1957) "Studies on the Aerobic Carbohydrate Metabolism" *J. Bacteriology*, **74**, 22 - 25.

Kaboli, H., & Reilly, P. J. (1980) "Immobilization and Properties of *Leuconostoc mesenteroides* Dextransucrase" *Biotech. Bioeng.*, **22**, 1055 - 1069.

Kobayashi, M., & Matsuda, K. (1980) "Characterization of the Multiple Forms and Main Component of Dextransucrase from *Leuconostoc mesenteroides* NRRL B-512F" *Biochimica et Biophysica Acta*, **614**, 46 - 62.

Kobayashi, M., Yokoyama, I., & Matsuda, K. (1985) "Effectors Differently Modulating the Dextransucrase Activity of *L. mesenteroides*" *Agric. Biol. Chem.*, **49**(11), 3189 - 3195.

Koepsell, H. J., & Tsuchiya, H. M. (1952) "Enzymatic Synthesis of Dextran" *J. Bacteriol.*, **63**, 293 - 295.

Lampen, J. O. (1972) "Mechanism of Enzyme Secretion by Microorganisms" *Biotech. Bioeng. Symposium*, **3**, 37 - 41.

Lawford, G. R., Kligerman, A., & Williams, T. (1979) "Dextran Biosynthesis and Dextransucrase Production by Continuous Culture of *Leuconostoc mesenteroides*" *Biotech. Bioeng.*, **21**, 1121 - 1131.

Levenspiel, O. (1980) "The Monod Equation: A Revisit and a Generalization to Product Inhibition Situations" *Biotech. Bioeng.*, **22**, 1671 - 1687.

Lopez, A., & Monsan, P. (1980) "Dextran Synthesis by Immobilized Dextransucrase" *Biochimie*, **62**, 323 - 329.

Luedeking, R., & Piret, E. L. (1959) " A Kinetic Study of the Lactic Acid Fermentation: Batch Process at Controlled pH" *J. Biochem. Microbiol. Tech. Eng.*, **1**, 393 - 412.

Matsubara, M. (1965) "On the Equivalent Dead Time"
IEEE Transactions on Automatic Control, **10**, 464 - 466.

McAvoy, A. (1981) MSc Thesis, University of Manchester.

McCleskey, C. S., Faville, L. W., & Barnett, R. O. (1947) "Characteristics of *L. mesenteroides* from Cane Juice" *J. Bacteriol.*, **54**, 697 - 708.

Miller, A. W., Eklund, S. H., & Robyt, J. F. (1986)
"Milligram to Gram Purification and Characterization of Dextransucrase from *Leuconostoc mesenteroides* NRRL B-512F"
Carbohydrate Research, **147**, 119 - 133.

Miller, A. W., & Robyt, J. F. (1984) "Stabilization of Dextransucrase from *Leuconostoc mesenteroides* NRRL B-512F by Nonionic Detergents, Poly(ethylene Glycol) and High-Molecular-Weight Dextran"
Biochimica et Biophysica Acta, **785**, 89 - 96.

Miller, A. W., & Robyt, J. F. (1986) "Activation of Dextransucrase by Calcium" *Biochimica et Biophysica Acta*, **880**, 32 - 39.

Monsan, P., & Lopez, A. (1981) "On the Production of Dextran by the Free and Immobilized Dextransucrase" *Biotech. Bioeng.*, **23**, 2027 - 2037.

Murphy, P. T., & Whistler, R. L. (1973) "Dextrans" *Industrial Gums : Polysaccharides and Their Derivatives*, 2nd ed., 513 - 542.

Neely, W. B. (1960) "Dextran : Structure and Synthesis"
Advances in Carbohydrate Chemistry, **15**, 341 - 369.

Neely, W. B., & Nott, J. (1962) "Dextransucrase, an Induced Enzyme from *Leuconostoc mesenteroides*" *Biochemistry*, **1**(6), 1136 - 1140.

Novak, M., *et al.* (1981) "Alcoholic Fermentation : on the Inhibitory Effect of Ethanol" *Biotech. Bioeng.*, **23**, 201 - 211.

Pasteur, L. (1861) *Bull. Soc. Chim. Paris*, 30 - 31.

Paul, F., Auriol, D., Oriol, E., & Monsan, P. (1984) "Production and Purification of Dextransucrase from *L. mesenteroides* NRRL B-512F" *Annals of New York Academy of Sciences*, 267 - 270.

Paul, F., Oril, E., Auriol, D., & Monsan, P. (1986) "Acceptor Reaction of a Highly Purified Dextransucrase With Maltose and Oligosaccharides. Application to the Synthesis of Controlled-Molecular-Weight Dextrans" *Carbohydrate Research*, **149**, 433 - 441.

Ramkrishna, D. (1979) "Statistical Models of Cell Populations" *Advances in Biochemical Engineering*, **11**, 1 - 48.

Reese, E. T. *et al.* (1969) "Modified Substrates and Modified Products as Inducers of Carbohydrases" *J. Bacteriol.*, **100**(3), 1151 - 1154.

Ringfeil, M., & Selenia, M. (1964) *Continuous Culture of Microorganisms*, Vol. **1**, 145 - 150.

Robyt, J. F., & Eklund, S. H. (1982) "Steriochemistry Involved in the Mechanism of Action of Dextransucrase in Synthesis of Dextran and the Formation of Acceptor Products" *Bioorganic Chemistry*, **11**, 115 - 132.

Robyt, J. F., & Walseth, T. F. (1978) "The Mechanism of Acceptor Reactions of *Leuconostoc mesenteroides* Dextransucrase" *Carbohydrate Research*, **61**, 433 - 445.

Robyt, J. F., & Walseth, T. F. (1979) "Production, Purification and Properties of Dextransucrase from *Leuconostoc mesenteroides* NRRL B-512F" *Carbohydrate Research*, **68**, 95 - 111.

Rorem, E. S. (1955) "Uptake of Rubidium and Phosphate Ions by Polysaccharide-producing Bacteria" *J. Bacteriol.*, **70**, 691 - 701.

Ryder, D. N., & Sinclair, C. G. (1972) "Model for Growth of Aerobic Microorganisms Under Oxygen Limiting Conditions" *Biotech. Bioeng.*, **14**, 787 - 798.

Scheibler, C. (1874) *Ver. Rubenzucker-Ind.*, **24**, 309 - 335.

Schneider, M., *et al.* (1980) *British Patent Appl. 2079290.*

Shu, P. (1961) "Mathematical Models for the Product Accumulation in Microbial Processes" *J. Biochem. Microbiol. Tech. Eng.*, **3**, 95 – 109.

Sinclair, C. G., & Ryder, D. N. (1975) "Models for the Continuous Culture of Microorganisms Under Both Oxygen and Carbon Limiting Conditions" *Biotech. Bioeng.*, **17**, 375 - 398.

Stouthamer, A. H., & Bettenhausen, C. (1973) "Utilization of Energy for Growth and Maintenance in Continuous and Batch Cultures of Microorganisms : A Reevaluation of the Method for the Determination of ATP Production by Measuring Molar Growth Yields" *Biochim. Biophys. Acta*, **301**, 53 - 70.

Terui, G., Okazaki, M., & Kinoshita, S. (1967) "Kinetic Studies on Enzyme Production by Microbes" *J. Ferment. Technol.*, **45**, 497 - 503.

Tsuchiya, H. M., Fredrickson, A. G., & Aris, R. (1966) "Dynamics of Microbial Cell Populations" *Advances in Chemical Engineering*, **6**, 125 - 203.

Tsuchiya, H. M., Koepsell, H. J., *et al.* (1952) "The Effect of Certain Cultural Factors on Production of Dextransucrase by *Leuconostoc mesenteroides*" *J. Bacteriol.*, **64**, 521 - 527.

Tsumuraya, Y., Nakamura, N., & Kobayashi, T. (1976) "Dextransucrase, and the Role of Metallic Ions in the Formation of Branch Links in Dextran Synthesis" *Agric. Biol. Chem.*, **40**(8), 1471 - 1477.

Van Tieghem, P. (1878) *Ann. Sci. Nat. Bot. Biol. Veg.*, 7, 180 - 203.

Whiteside-Carlson, V., & Carlson, W. W. (1949)
"The Vitamin Requirements of *Leuconostoc* for Dextran Synthesis"
J. Bacteriol., **58**, 135 - 141.

Wilson, P. D. G. (1985) PhD Thesis,
Loughborough University of Technology.

Yamane, T., & Shimizu, S. (1984)
"Fed-Batch Techniques in Microbial Processes"
Advances in Biochemical Engineering/Biotechnology, **30**, 147 - 194.

Yokayama, I., Kobayashi, M., & Matsuda, K. (1985)
"Comparison of the Multiplicity of Dextransucrase from Six Strains of *Leuconostoc mesenteroides*" *Agric. Biol. Chem.*, **49**(2), 501 - 507.

APPENDICES

Appendix A Preparation of Tween Agar Plates

Tween agar is a general plating medium for *Lactobacilli.* It is suitable for *Leuconostoc mesenteroides* when adjusted to pH 7.0. The composition of the medium is as follows:

Lab Lemco	1 % (w/v)
Peptone	1 % (w/v)
Yeast Extract (Difco)	0.5 % (w/v)
Glucose	1 % (w/v)
Triammonium Citrate	0.2 % (w/v)
Agar	2 % (w/v)
Salts solution	0.5 % (v/v)
Tween 80	0.05 % (v/v)

The salts solution has the following composition:

$MgSO_4.7H_2O$	8 % (w/v)
$MnSO_4.4H_2O$	2 % (w/v)

The medium is adjusted to pH 7.0 using 4M NaOH. The dissolved solution is distributed into MaCartney bottles, and sterilized for 15 minutes at 121 °C. Sterile petri dishes are used to prepare the agar plates.

Appendix B Preparation of Reagents for Enzyme Assay

Sumner Reagent

Ten grams of 3,5-dinitrosalicylic acid (DNSA) are suspended in approximately 200 mL of distilled water. A solution of 16 g of sodium hydroxide pellets in 150 mL of water is then added dropwise under efficient stirring, and if necessary, gently heated until a clear solution is obtained. 300 g of Rochelle salt (potassium sodium tartrate tetrahydrate) are then added in small portions. After dissolution, distilled water is added to a final volume of 1 litre.

The solution is filtered through glass wool and stored in an amber bottle to minimize the cumulative effects of exposure to air and evaporation. The reagent retains its effectiveness for at least a month if kept tightly stoppered.

Acetate Buffer

One litre of 0.1M acetate buffer of pH 5.2 requires 6.074 g of sodium acetate and 1.559 g of acetic acid. The pre-weighed sodium acetate is dissolved in about 500 mL of distilled water. 26 mL of 6% acetic acid are then added. The solution is finally adjusted to 1 litre with distilled water.

Appendix C Conversions of Enzyme Activity Units

It is usually difficult to determine the amount of enzyme in absolute terms of milligrams or moles. The quantity of enzyme is most conveniently expressed as some arbitrary unit that is measured by the production of a certain amount of product or by the disappearance of a certain amount of substrate in the reaction that the enzyme catalyzes under a set of defined conditions.

Three units are used in the literature to express dextransucrase activity. The most common one is DSU which is defined by Hehre (1946) as the amount of dextransucrase which will convert 1 mg of sucrose to dextran in 1 hour, thus producing 0.5263 mg of fructose as reducing sugar at pH 5.2, temperature 30 °C. The unit is also used by other workers at a different temperature (25 °C). This scheme is adopted in the current study.

Lawford, *et al.* (1979) expressed the dextransucrase activity as μg reducing sugar/min/mL at pH 5.5, temperature 30 °C. Assuming that the pH difference is negligible, then

$$1\ U_{Lawford} = \frac{1 \times 60}{1000 \times 0.5263} = 0.114\ DSU/mL \qquad [C.1]$$

A standard unit (U) of any enzyme is defined by the International Committee on Enzymes (EC) as the amount of enzyme which will catalyze the transformation of one micromole of the substrate per minute under a prescribed set of standard conditions for that particular enzyme. A temperature of 25 °C is suggested. The pH should be optimal for the enzyme, and the substrate concentration should be high enough to saturate the enzyme so that the kinetics of the assay will approach zero order with respect to substrate. Robyt and Walseth (1979) used this unit to express

dextransucrase activity at pH 5.0.

$$
\begin{aligned}
1\ \text{U} &= 1\ \mu\text{mol sucrose/min} \\
&= 0.342\ \text{mg sucrose/min} \\
&= 0.342 \times 60\ \text{mg sucrose/hour} \\
&= 20.52\ \text{DSU}
\end{aligned}
\qquad \text{[C.2]}
$$

Kaboli and Reilly (1980) also defined an equivalent unit at a different temperature and pH. The optimum condition for dextransucrase activity (pH 5.2, temperature 30 °C) was used. It can be seen that the units are not strictly convertible because of the different incubation temperature and pH used. This makes comparison of the results difficult.

Appendix D Preliminary Growth Experiment : Calibration of Optical Density Measurement for *Leuconostoc mesenteroides* NRRL B-512F

A batch culture of *L. mesenteroides* NRRL B-512F employing a medium containing 50 g/L sucrose was prepared by the normal experimental procedure. The experiment was carried out under the standard operating conditions, i.e. pH 6.7 and temperature 23 °C. The fermenter was aerated and agitated to maintain a high concentration of dissolved oxygen in the vessel. After inoculation, samples were withdrawn periodically from the fermenter to monitor cell growth by optical density measurements at a wavelength of 590nm on a spectrophotometer (PYE-UNICAM, SP6-400). After about 8 hours growth, a large sample was removed from the fermenter and diluted to a range of concentrations by 0.5% gluteraldehyde solution. The optical density of each of these diluted cultures was determined against a blank of the diluting liquid. The dry cell weight of the broth sample was determined by the following procedure :

(a) The broth sample was transferred to four pre-weighed centrifuging tubes. Each tube was filled with 30 mL of the culture broth. The weight of the tubes was noted in grams.

(b) About 0.05 mL of 50% (w/v) gluteraldehyde solution was added to each of the tubes to fix the cells and thus reduce the possibility of cell disruption. This was done immediately after the broth sample was taken from the fermenter.

(c) The tubes containing the treated broth sample were centrifuged at 2000 rpm for 5 minutes on a bench centrifuge (Baird & Tatlock) with four-way swing-out head. The tubes were arranged so that the total load

was symmetrical and diametrically balanced.

(d) The clear supernatant was removed and the cells resuspended in 30 mL distilled water in order to wash out residual medium.

(e) The tubes were centrifuged at 2000 rpm for 5 minutes.

(f) The procedure was repeated from (d) twice.

(g) The clear supernatant was removed and the cells resuspended in 2 mL distilled water.

(h) The four tubes of the resulting cell suspension were dried to a constant weight at 75 °C for 20 to 24 hours in vacuo.

(i) The four dried tubes were weighed and the net dry cell weight (DCW) in grams of the four tubes was noted as M_A, M_B, M_C, and M_D respectively.

(j) Assuming negligible loss of cells during centrifugation and washing, the dry cell concentration of the broth sample is calculated as follows :

$$x_b = \frac{M_A + M_B + M_C + M_D}{4 \times 30} \times 1000$$

$$= \frac{M_A + M_B + M_C + M_D}{0.12} \quad (g/L) \qquad [D.1]$$

(k) The dry cell concentration of a diluted sample is :

$$x_d = x_b/d \qquad [D.2]$$

where d is the dilution factor.

The same procedure was used occasionally for dry cell weight check in an experiment.

An example of dry cell weight determination is given below.

Tube	Weight of Tube (g)	Dried Weight (g)	Net DCW (g)
A	47.11	47.29	0.18
B	46.20	46.39	0.19
C	48.10	48.29	0.19
D	47.57	47.76	0.19

The dry cell concentration of the broth sample is :

$$x_b = (0.18 + 0.19 + 0.19 + 0.19)/0.12 = 6.25 \text{ g/L}$$

The optical density of the sample was measured by diluting the sample 40 or 50 times. Thus we have :

Dilution Factor	OD Reading	Dry Cell Concentration (g/L)
50	0.470	0.1250
40	0.585	0.1563

It should be emphasized here that the optical density reading is taken as if the dilution factor was one.

The results of the dry cell concentrations and the optical densities are given below in Table D.1.

Table D.1 Optical Density Calibration of *L. mesenteroides*

Case	Optical Density at 590nm	Biomass Concentration (g/L)
1	0.00000	0.00000
2	0.00875	0.00489
3	0.01427	0.00626
4	0.02445	0.00814
5	0.03414	0.01018
6	0.04923	0.01318
7	0.06468	0.01724
8	0.09480	0.02179
9	0.11489	0.02730
10	0.15005	0.03436
11	0.20021	0.04335
* 12	0.23000	0.05380
13	0.23991	0.05482
* 14	0.24000	0.06250
* 15	0.26000	0.06940
16	0.29984	0.06843
* 17	0.34000	0.08930
18	0.35046	0.08594
* 19	0.40000	0.09170
20	0.43007	0.10680
* 21	0.47000	0.12500
22	0.52026	0.13503
* 23	0.58500	0.15630
24	0.63849	0.16845
25	0.72000	0.20830

* dry weight check point

The dry cell concentration is plotted against optical density at 590nm. The calibration curve is presented in Figure 5.2. It can be seen that the optical density is linearly related to the biomass concentration for optical density readings less than 0.7.

A straight line through origin is fitted to the data for optical density measurements of lower that 0.7. The results of the regression analysis are given below.

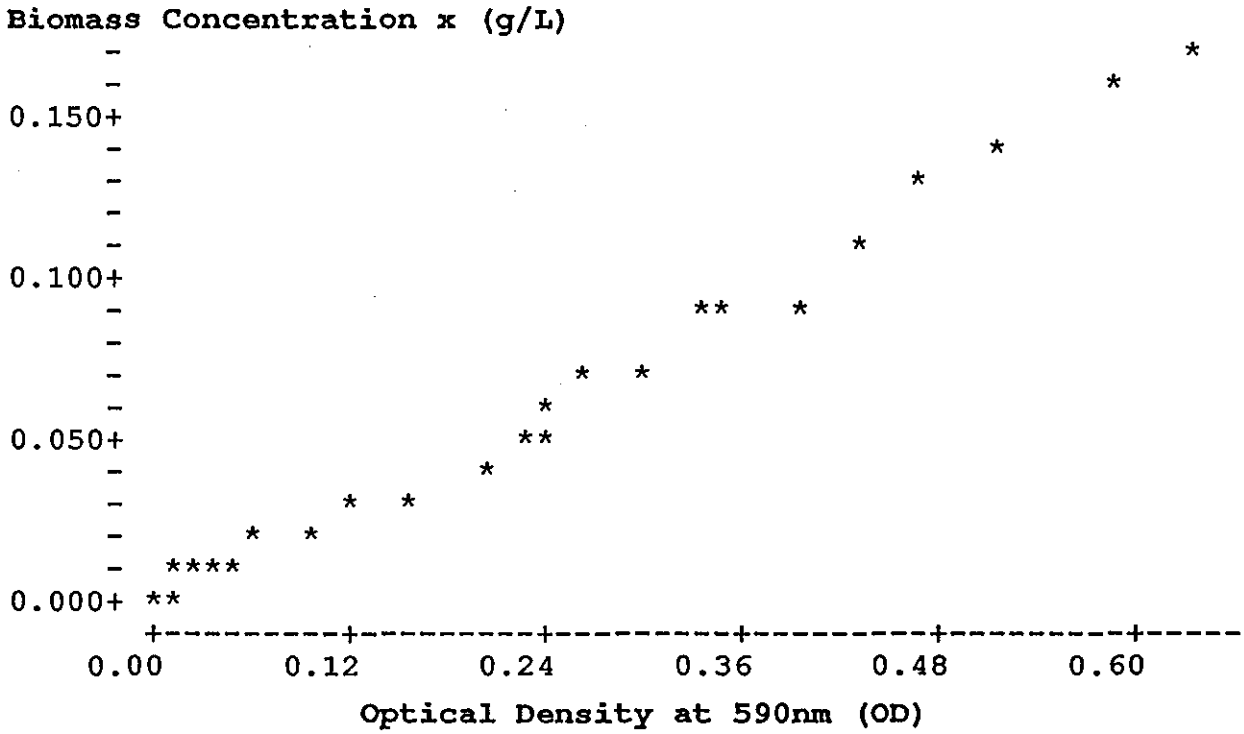

	N	MEAN	MEDIAN	TRMEAN	STDEV	SEMEAN
OD	24	0.2400	0.2350	0.2328	0.1936	0.0395
x	24	0.0606	0.0543	0.0584	0.0502	0.0103

	MIN	MAX	Q1	Q3
OD	0.0000	0.6385	0.0531	0.3876
x	0.0000	0.1684	0.0142	0.0911

Correlation of OD and x = 0.996

The regression equation is
x = 0.255 OD

Predictor	Coef	Stdev	t-ratio
Noconstant			
OD	0.254763	0.003088	82.51

s = 0.004625
Analysis of Variance

SOURCE	DF	SS	MS
Regression	1	0.14564	0.14564
Error	23	0.00049	0.00002
Total	24	0.14613	

Unusual Observations

Obs.	OD	x	Fit	Stdev.Fit	Residual	St.Resid
19	0.400	0.091700	0.101905	0.001235	-0.010205	-2.29R
23	0.585	0.156300	0.149037	0.001806	0.007263	1.71 X
24	0.638	0.168450	0.162664	0.001971	0.005786	1.38 X

R denotes an obs. with a large st. resid.
X denotes an obs. whose OD value gives it large influence.

Confidence interval of regression coefficient

Coef	Stdev	Lo_limit	Up_limit	95% C.I
0.254763	0.0030875	0.248376	0.261150	0.006387

A general linear regression yields the following results :

Mean of independent variable (OD)	=	0.2400
Mean of dependent variable (x)	=	0.0606
Standard deviation of independent variable	=	0.1936
Standard deviation of dependent variable	=	0.0502
Correlation coefficient	=	0.9959
Regression coefficient (slope)	=	0.2584
Standard error of slope	=	0.0050
t-value for slope	=	51.7244
Regression constant (intercept)	=	-0.0014
Standard error of constant	=	0.0015
t-value for constant	=	-0.9339

Analysis of Regression Table :-

Source	Sum of Squares	D.F.	Mean Square	F-value
Due to regression	0.0575	1	0.0575	2675.418
About regression	0.0005	22	0.0000	
Total	0.0580	23		

Appendix E Preliminary Growth Experiment : Estimation of Biomass Yield Coefficient on Sucrose

Batch cultures of *Leuconostoc mesenteroides* NRRL B-512F were grown on the following medium in which sucrose concentration varied.

Main culture medium :

Component	Concentration
Sucrose	variable
Yeast extract (Difco)	40 g/L
K_2HPO_4	20 g/L
R salts	0.5% (v/v)
Antifoam (polypropylene glycol)	0.2% (v/v)

All fermentations were carried out in the standard bench-top fermenter and controlled at pH 6.7 and temperature 23 °C. The fermenter was operated under aerobic conditions by proper aeration and agitation. The final cell concentration was determined by optical density measurement with reference to the standard calibration curve.

Different inoculum sizes were used in some of the experiments. To calculate the initial total sucrose-equivalent substrate present in the inoculum and the fermentation medium, molasses used in some inocula were considered to be sucrose. The results are listed below.

Table E.1 Estimation of Biomass Yield on Sucrose

Case	Initial Total Sucrose Concentration (g/L)	Final Maximum Biomass Concentration (g/L)
1	0.0567	0.390
2	0.1000	0.432
3	0.3000	0.437
4	0.5000	0.473
5	1.7670	0.489
6	2.1670	0.686
7	5.9000	1.105
8	10.1000	1.599
9	15.0000	2.110
10	20.0000	3.055
11	25.0000	3.900
12	30.0000	5.200

The final cell concentration is plotted against the initial total substrate concentration. The graph is given in Figure 5.3. It can be seen from the graph that the final biomass concentration increases linearly with the initial total sucrose concentration. A straight line is fitted to the data by means of least squares method. The slope of the regression line is the biomass yield coefficient on sucrose. The regression results are given below.

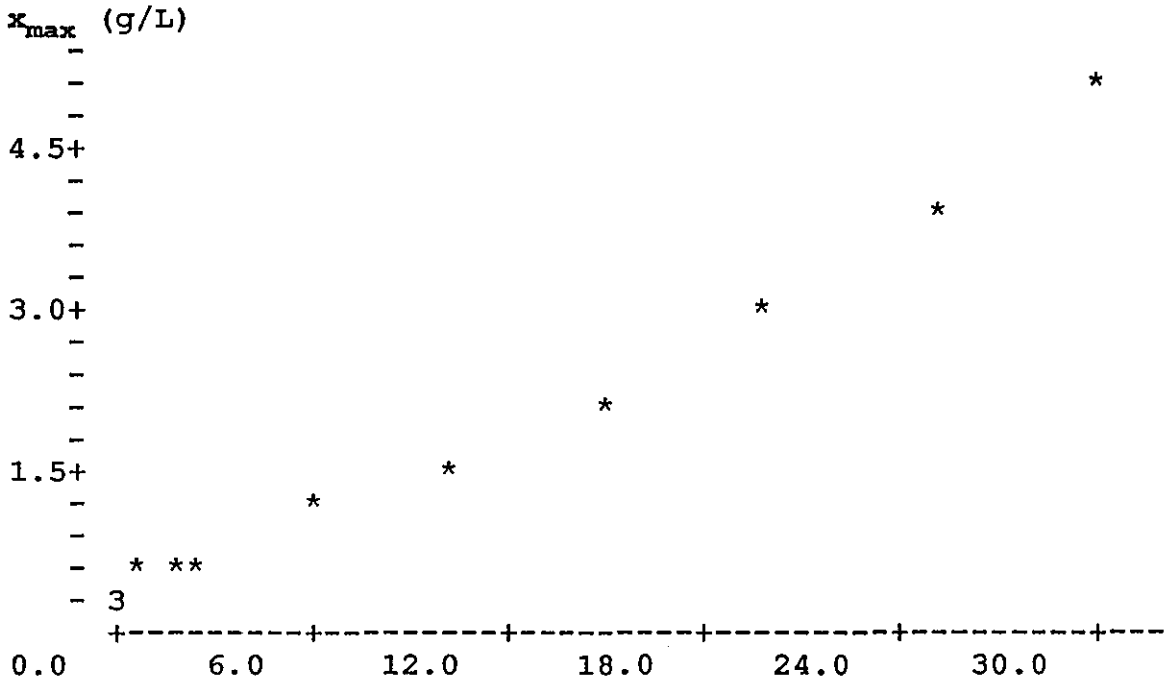

	N	MEAN	MEDIAN	TRMEAN	STDEV	SEMEAN
s_0	12	9.24	4.03	8.08	10.75	3.10
x_{max}	12	1.656	0.896	1.429	1.606	0.463

	MIN	MAX	Q1	Q3
s_0	0.06	30.00	0.35	18.75
x_{max}	0.390	5.200	0.446	2.819

Correlation of s_0 and x_{max} = 0.991

The regression equation is

$x_{max} = 0.288 + 0.148\ s_0$

Predictor	Coef	Stdev	t-ratio
Constant	0.28845	0.08861	3.26
s_0	0.148025	0.006407	23.10

s = 0.2284 R-sq = 98.2% R-sq(adj) = 98.0%

Analysis of Variance

SOURCE	DF	SS	MS
Regression	1	27.833	27.833
Error	10	0.521	0.052
Total	11	28.355	

Unusual Observations

Obs.	s_0	x_{max}	Fit	Stdev.Fit	Residual	St.Resid
12	30.0	5.2000	4.7292	0.1484	0.4708	2.71R

R denotes an obs. with a large st. resid.

Confidence intervals of regression constants

Coef	Stdev	Lo_limit	Up_limit	95% C.I.
0.288448	0.0886068	0.091019	0.485876	0.197428
0.148025	0.0064072	0.133749	0.162301	0.014276

Appendix F Determination of Initial Specific Growth Rates from Batch Culture Data

Environmental conditions for batch growth of *Leuconostoc mesenteroides* are listed below.

Main culture medium

Sucrose	variable
Yeast extract (Difco)	40 g/L
K_2HPO_4	20 g/L
R salts	0.5 % (v/v)
Antifoam (polypropylene glycol)	0.2 % (v/v)

Temperature	:	23 °C
pH	:	6.7
pO_2	:	> 60% air saturation

The experimental results from each run are presented in two separate plots. The first one is the cell concentration against culture time. The second one is a semilogarithmic plot which enables determination of the initial specific growth rate by means of least squares linear regression. Calculation is performed in natural logarithmic base, while for convenience the plot is constructed in logarithmic scale to base of ten.

Table F.1

Batch Growth of *Leuconostoc mesenteroides* NRRL B-512F
Initial substrate concentration = 2.00 g/L

Time (hour)	Cell Concentration (*g/L* dry weight)
0.00	0.0676
0.50	0.0832
1.00	0.1092
1.50	0.1274
2.00	0.1508
2.50	0.1716
3.00	0.1976
3.50	0.2288
4.00	0.2600
5.00	0.3328
5.50	0.4108
6.00	0.4316
6.50	0.4160
7.00	0.4108
7.50	0.4160
8.00	0.4004

Final cell concentration = 0.432 g/L

Initial specific growth rate = 0.285 hr^{-1}
on time interval of 1 – 5.5 hour

Figure F.1

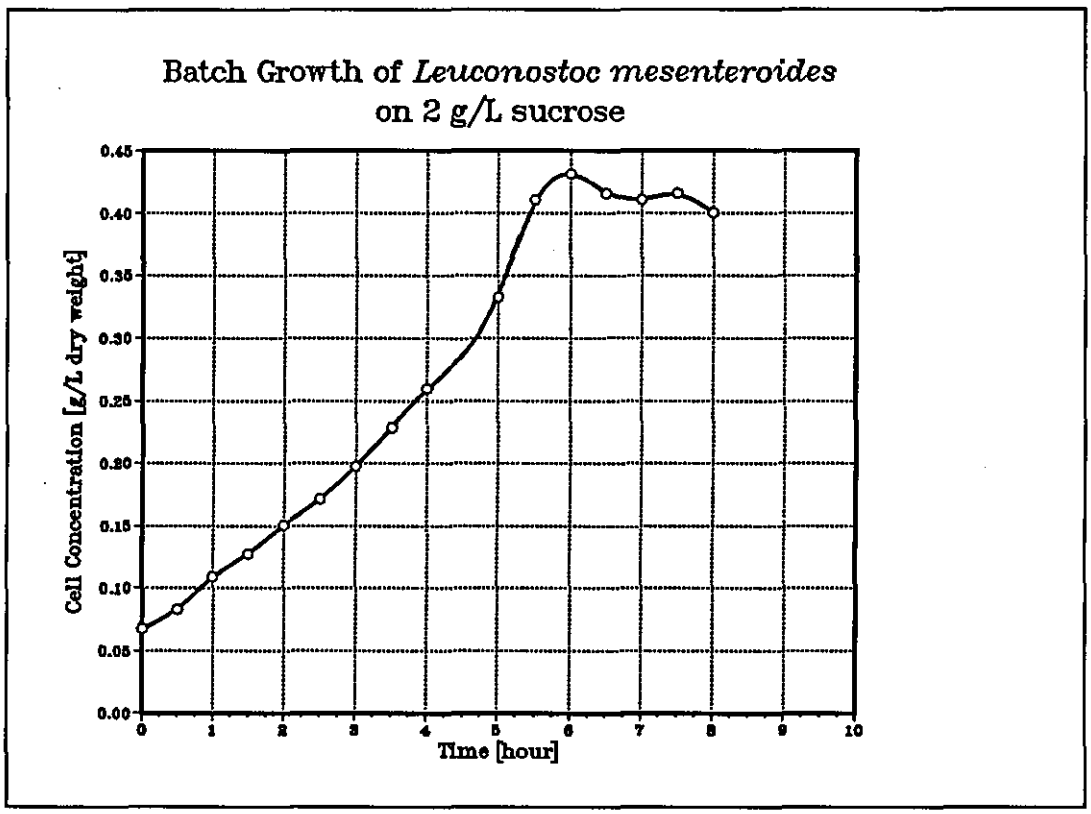

Figure F.2

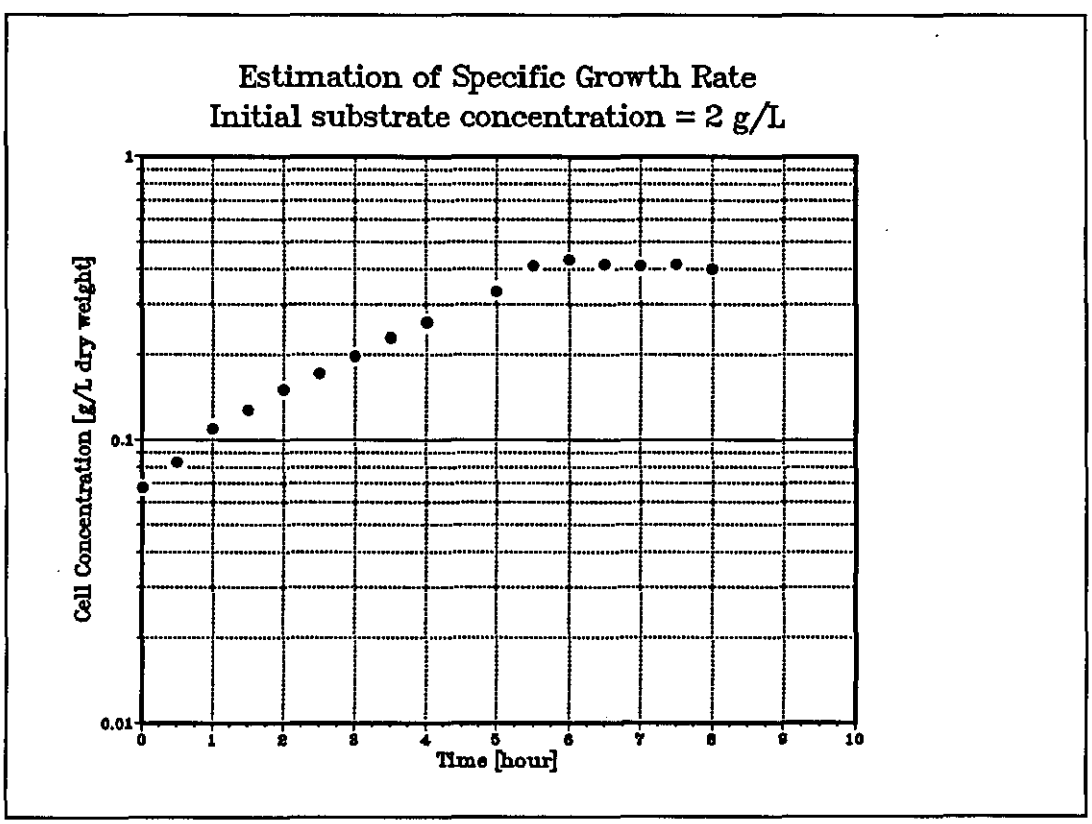

Table F.2

Batch Growth of *Leuconostoc mesenteroides* NRRL B-512F
Initial substrate concentration = 2.40 g/L

Time (hour)	Cell Concentration (*g/L* dry weight)
0.00	0.0494
0.50	0.0494
1.00	0.0598
1.50	0.0676
2.00	0.0962
2.50	0.1170
3.00	0.1300
3.50	0.1586
4.00	0.1794
5.00	0.2470
5.50	0.2860
6.00	0.3588
6.50	0.4264
7.00	0.4420
7.50	0.4524
8.00	0.4628
8.50	0.4732

Final cell concentration = 0.4732 g/L

Initial specific growth rate = 0.352 hr^{-1}
on time interval of 0.5 – 6.5 hour

Figure F.3

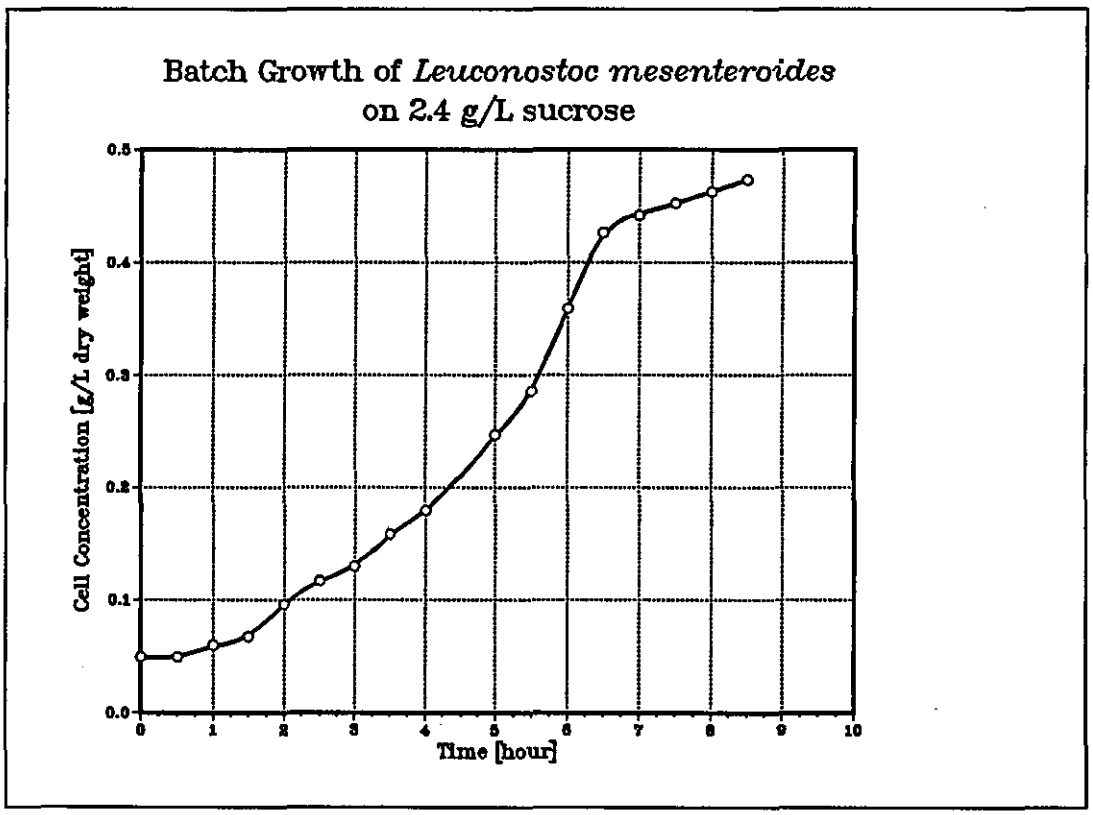

Figure F.4

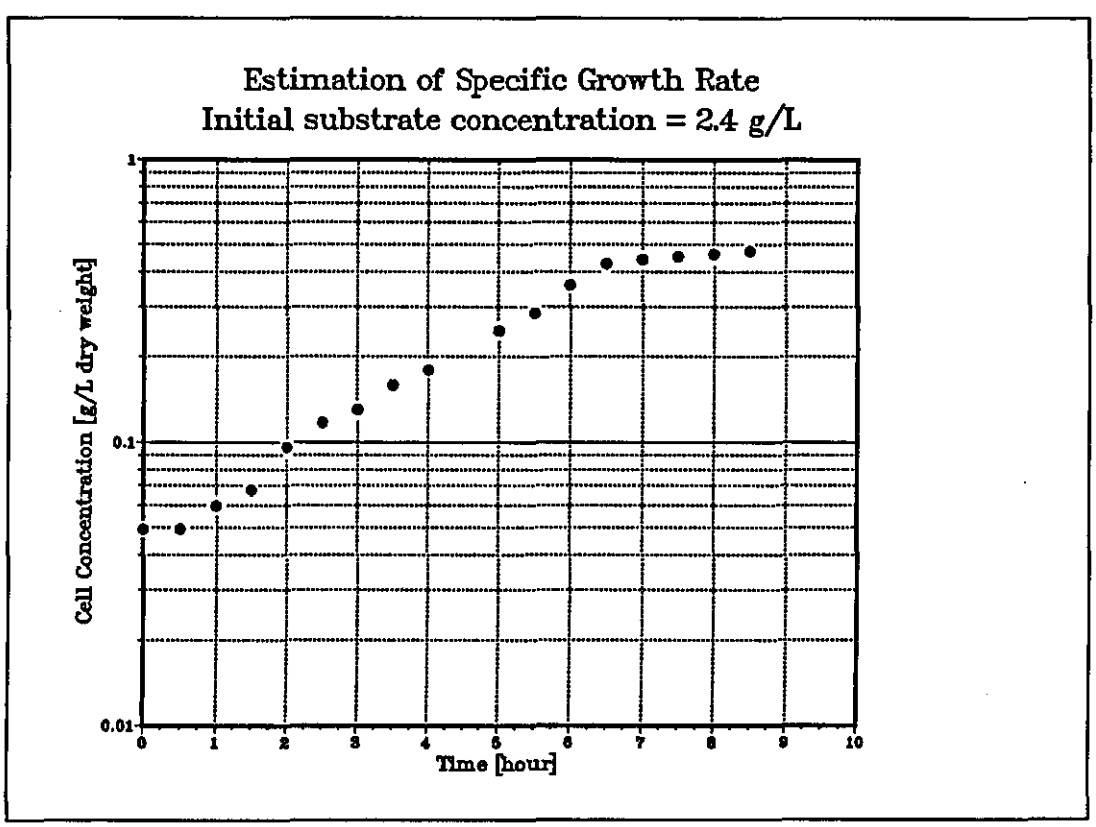

Table F.3

Batch Growth of *Leuconostoc mesenteroides* NRRL B-512F
Initial substrate concentration = 6.90 g/L

Time (hour)	Cell Concentration (*g/L* dry weight)
0.00	0.0884
0.50	0.0780
1.00	0.0728
1.50	0.0988
2.00	0.1144
3.00	0.1612
4.00	0.2366
5.00	0.3744
6.00	0.6084
7.00	1.1752
8.00	1.9110
9.00	2.2880
10.0	2.6000

Total carbohydrate concentration = 16.9 g/L
Final cell concentration = 2.6 g/L

Initial specific growth rate = 0.505 hr^{-1}
on time interval of 3 – 8 hour

Figure F.5

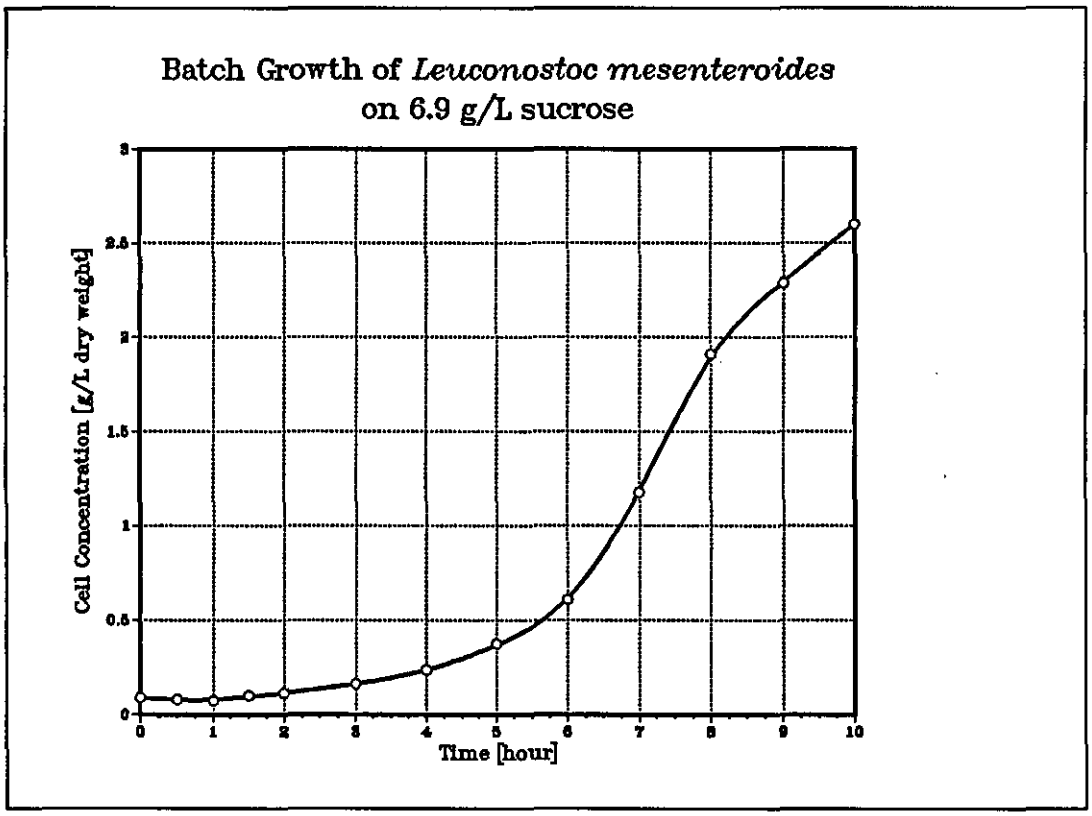

Figure F.6

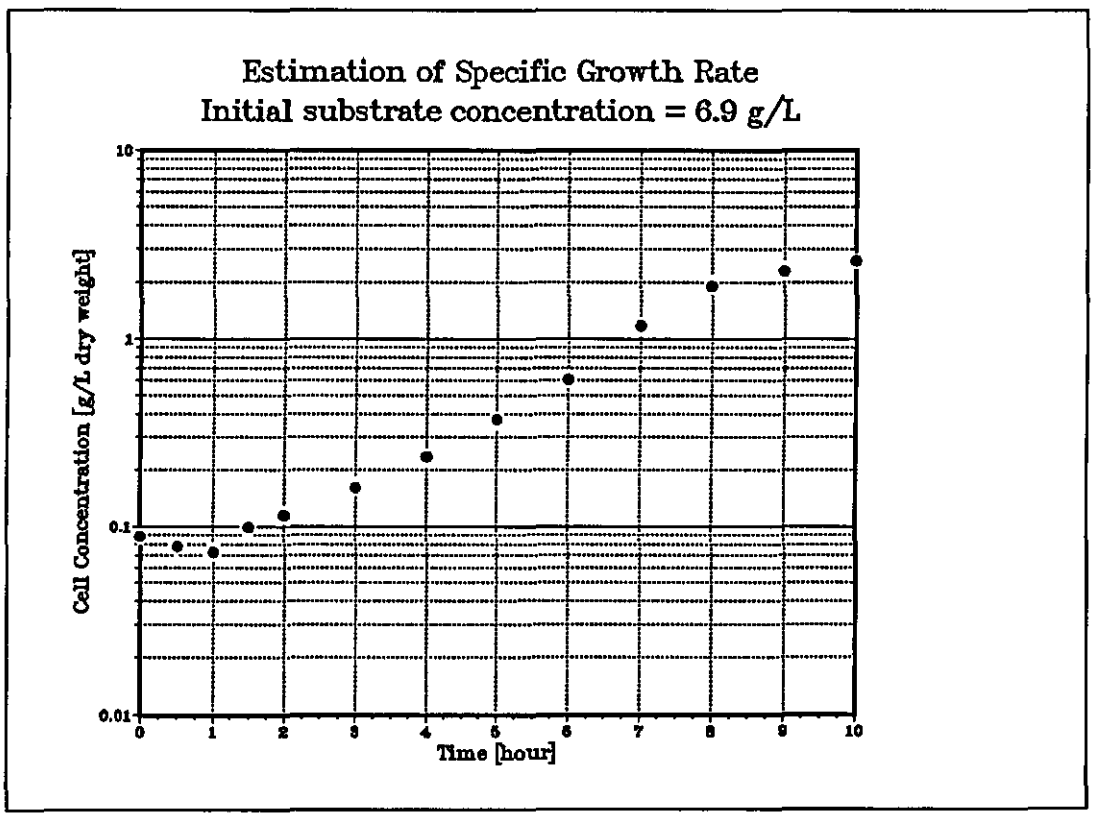

Table F.4

Batch Growth of *Leuconostoc mesenteroides* NRRL B-512F
Initial substrate concentration = 11.90 g/L

Time (hour)	Cell Concentration (*g/L* dry weight)
0.00	0.0832
1.00	0.0832
2.00	0.1040
4.00	0.3016
5.00	0.5408
6.00	0.8736
7.00	1.5210
8.00	2.0865

Total carbohydrate concentration = 21.9 g/L
Final cell concentration = 3.055 g/L

Initial specific growth rate = 0.489 hr^{-1}
on time interval of 1 – 8 hour

Figure F.7

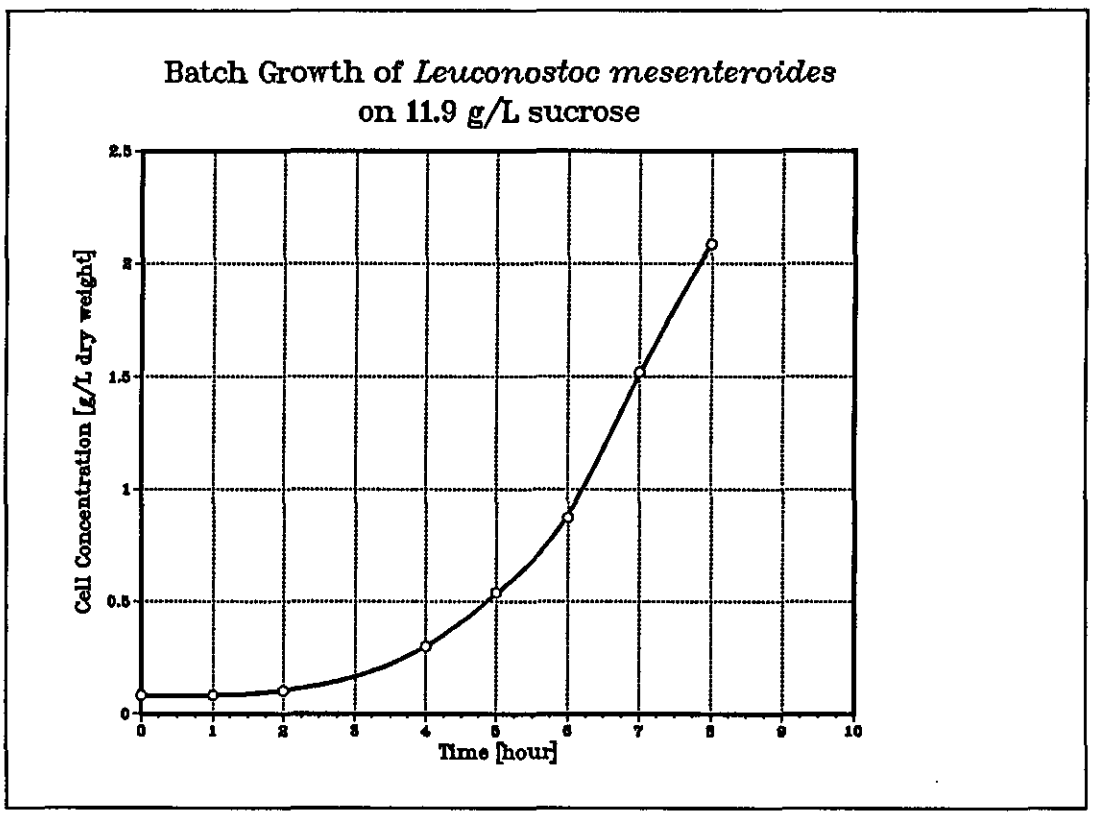

Figure F.8

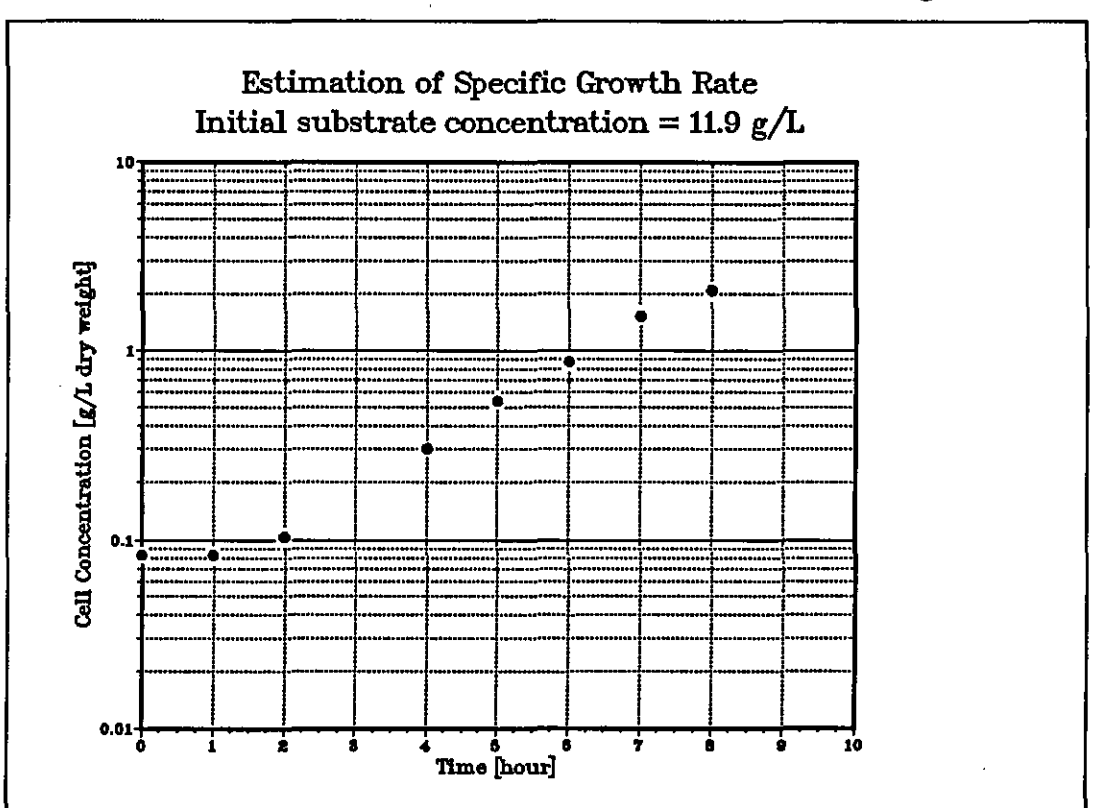

Table F.5

Batch Growth of *Leuconostoc mesenteroides* NRRL B-512F
Initial substrate concentration = 21.90 g/L

Time (hour)	Cell Concentration (*g/L* dry weight)
0.00	0.1508
0.50	0.1508
1.00	0.1716
2.00	0.1950
2.50	0.2223
3.00	0.2691
3.50	0.3042
4.00	0.3549
5.00	0.5421
5.50	0.7956
6.00	1.0608
7.00	1.7940
8.00	2.6208
9.00	3.6036
10.0	4.2120

Total carbohydrate concentration = 31.9 g/L
Final cell concentration = 5.2 g/L

Initial specific growth rate = 0.503 hr^{-1}
on time interval of 3.5 – 8 hour

Figure F.9

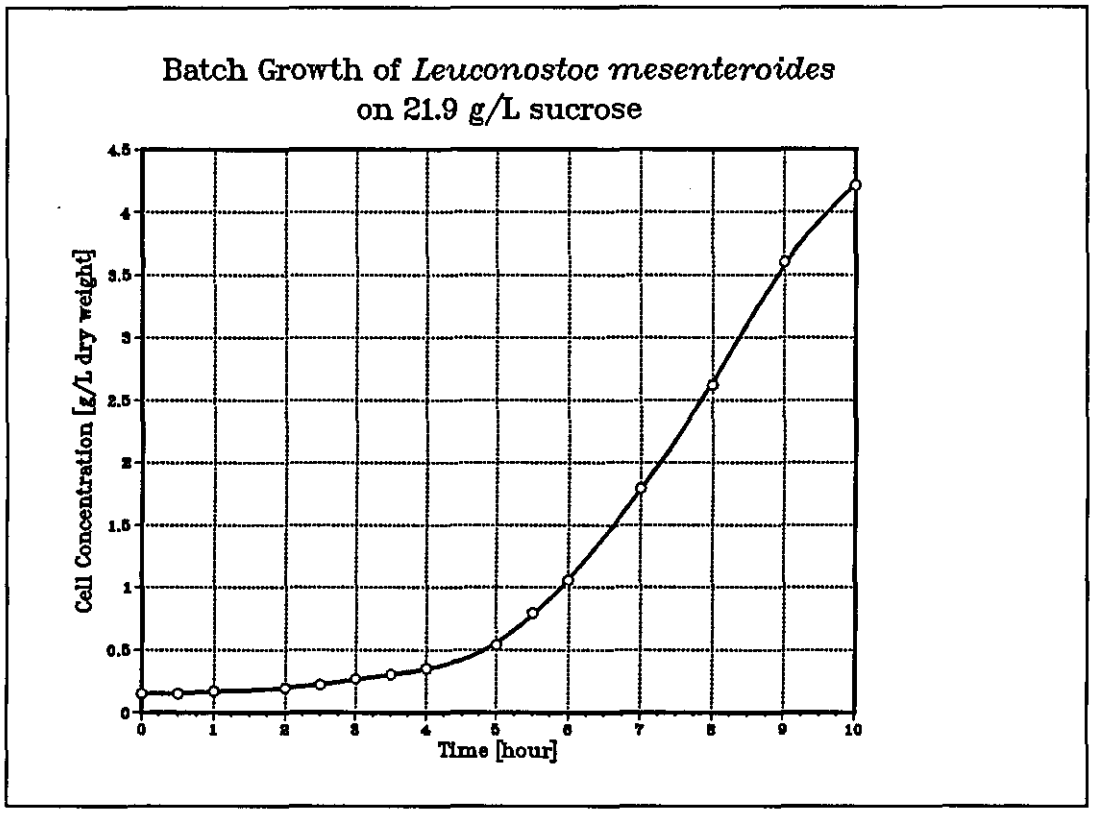

Figure F.10

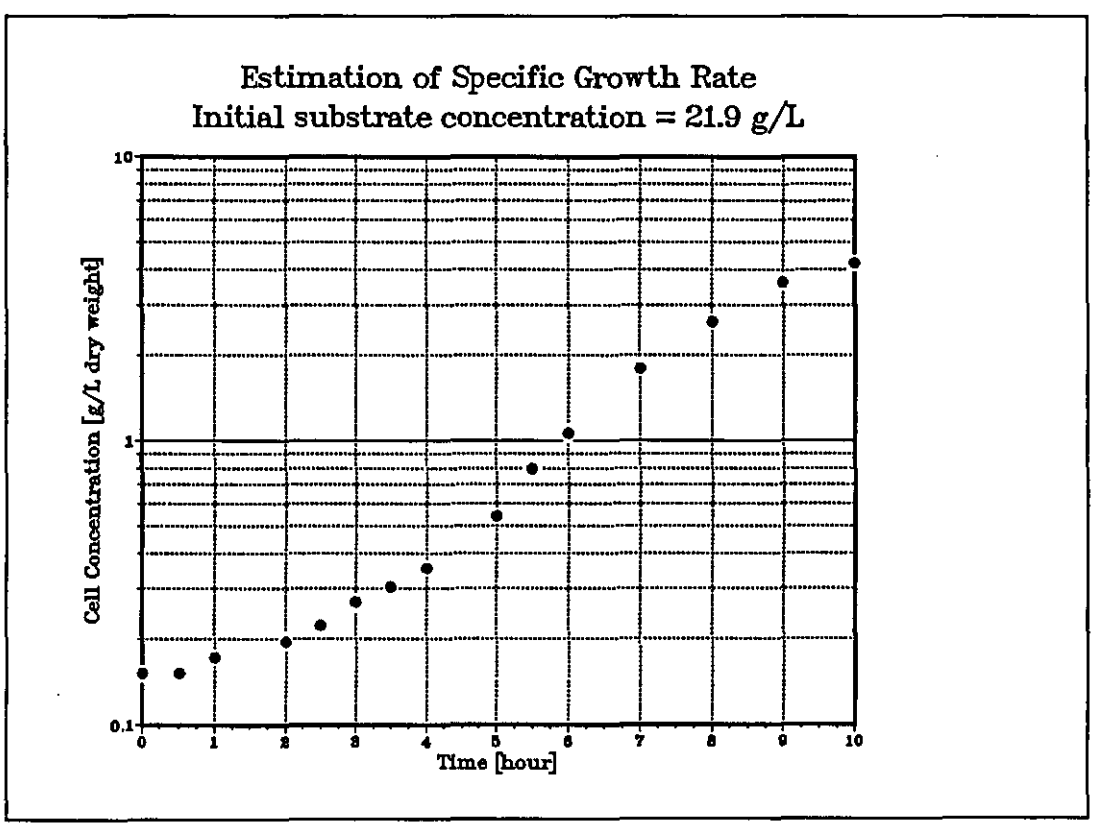

Table F.6

Batch Growth of *Leuconostoc mesenteroides* NRRL B-512F
Initial substrate concentration = 41.90 g/L

Time (hour)	Cell Concentration (*g/L* dry weight)
0.00	0.1482
0.25	0.1430
0.50	0.1508
1.00	0.1664
1.50	0.1820
2.00	0.2080
2.50	0.2340
2.75	0.2470
3.00	0.2600
4.00	0.3744
4.25	0.4251
4.50	0.4602
4.75	0.4992
5.00	0.5928
5.25	0.6656
5.50	0.7670
5.75	0.8970
6.00	1.0140
6.25	1.0920
6.50	1.2688
6.75	1.4742
7.00	1.7290
7.25	2.0124
7.50	2.1840
8.50	3.2240

Final cell concentration = 5.85 g/L
Initial specific growth rate = 0.503 hr^{-1}
on time interval of 4 – 8.5 hour

Figure F.11

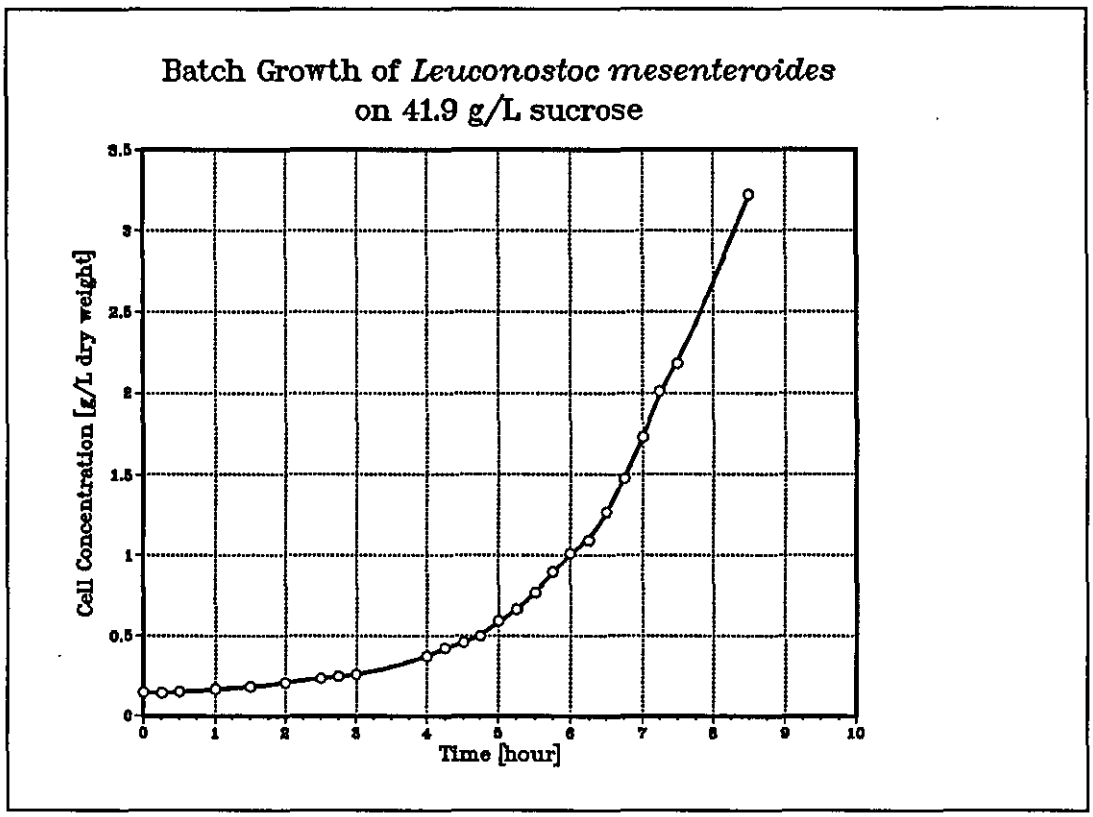

Figure F.12

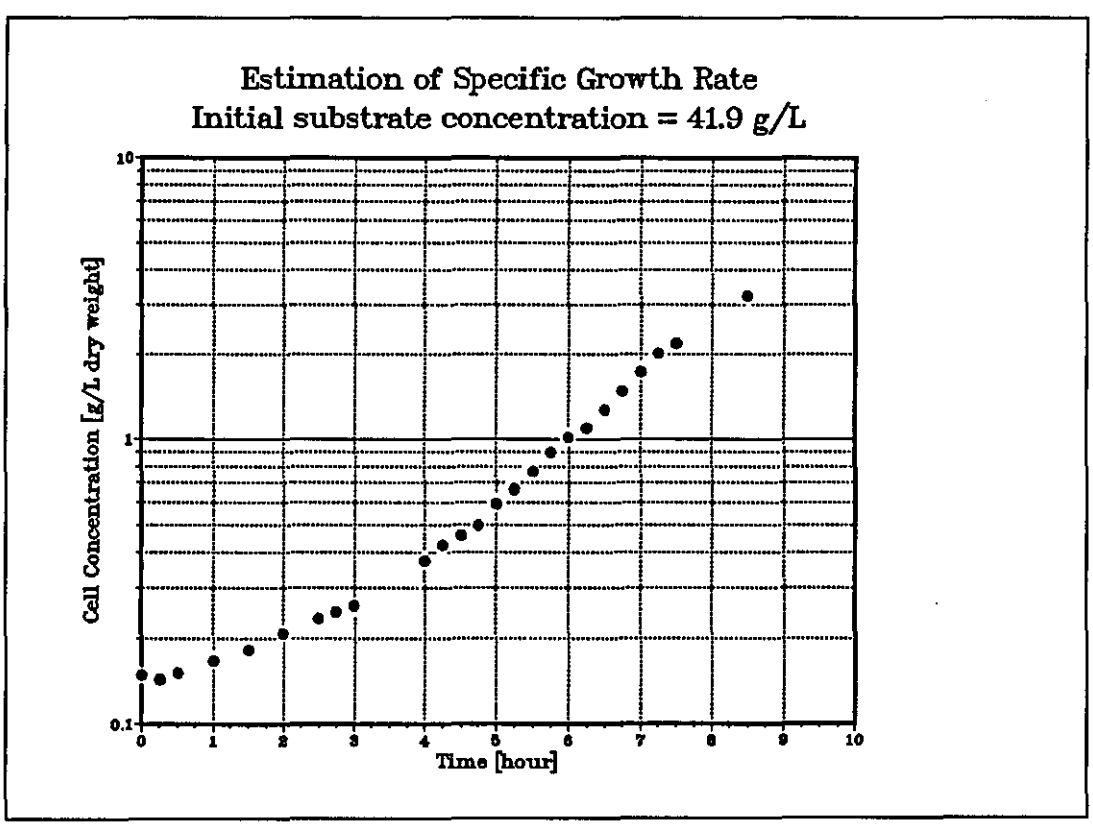

Table F.7

Batch Growth of *Leuconostoc mesenteroides* NRRL B-512F
Initial substrate concentration = 51.90 g/L

Time (hour)	Cell Concentration (*g/L* dry weight)
0.00	0.0936
0.50	0.0988
1.00	0.1092
1.50	0.1196
2.00	0.1300
3.00	0.1820
4.00	0.3042
5.00	0.4576
6.00	1.0140
7.00	1.7160
8.00	2.7456
9.00	3.6725
10.0	4.8880

Final cell concentration = 6.24 g/L

Initial specific growth rate = 0.526 hr^{-1}
on time interval of 3 – 9 hour

Figure F.13

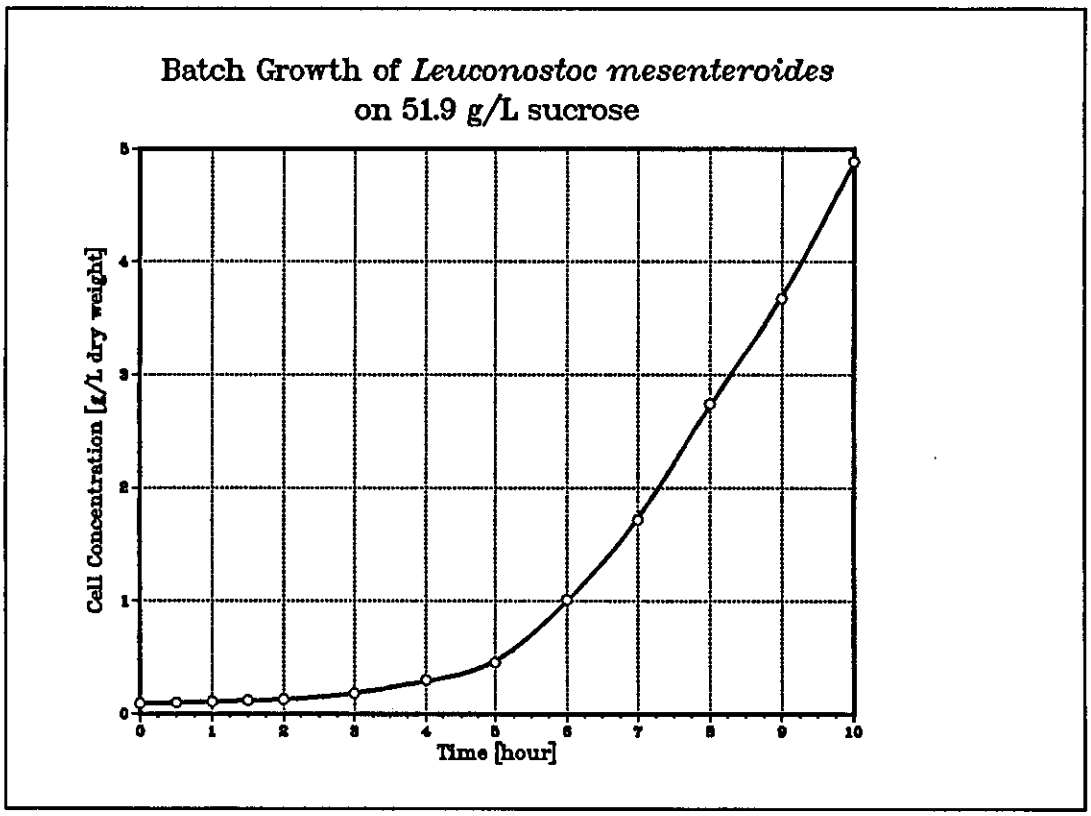

Figure F.14

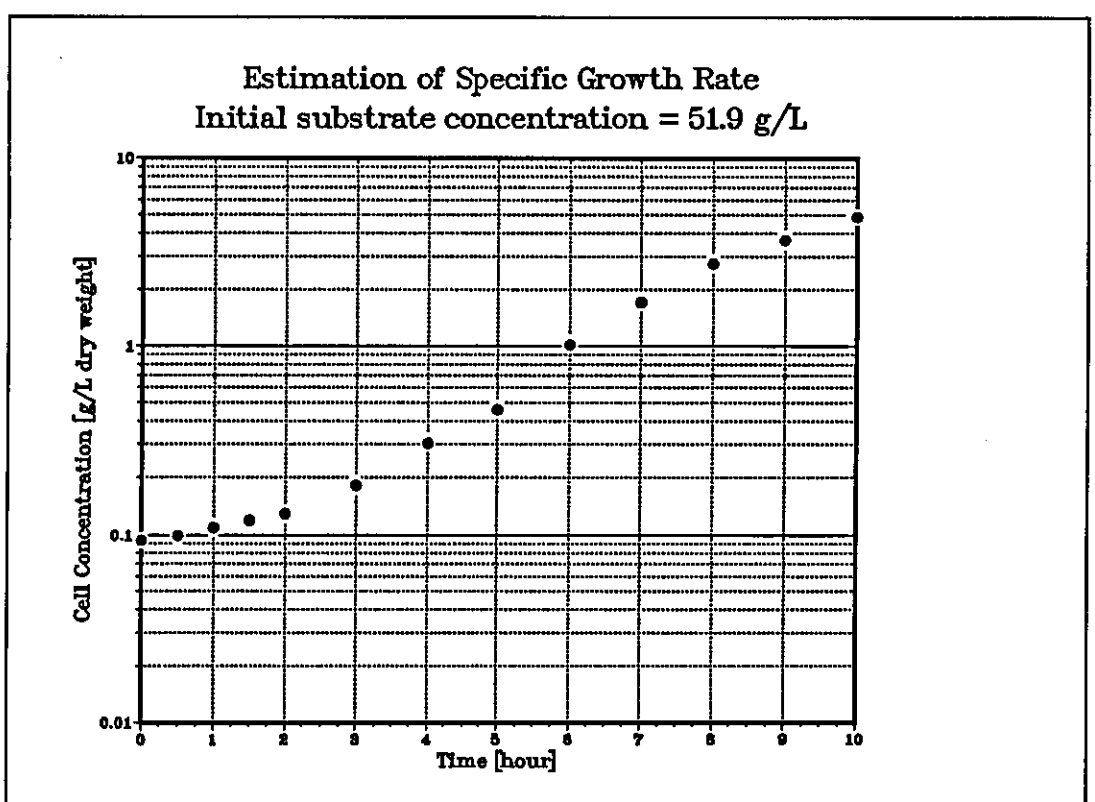

Table F.8

Batch Growth of *Leuconostoc mesenteroides* NRRL B-512F
Initial substrate concentration = 101.90 g/L

Time (hour)	Cell Concentration (*g/L* dry weight)
0.00	0.2288
0.50	0.2808
1.00	0.3016
1.50	0.3588
2.00	0.4524
2.50	0.5616
3.00	0.7696
3.50	0.9776
4.00	1.2688
5.00	2.4180
5.50	2.9120
6.00	3.3800
6.50	4.1340
7.00	4.7190
7.50	5.4600
8.00	6.1880
8.50	7.0200
9.00	7.1760

Final cell concentration = 9.0 g/L

Initial specific growth rate = 0.522 hr^{-1}
on time interval of 1 – 5.5 hour

Figure F.15

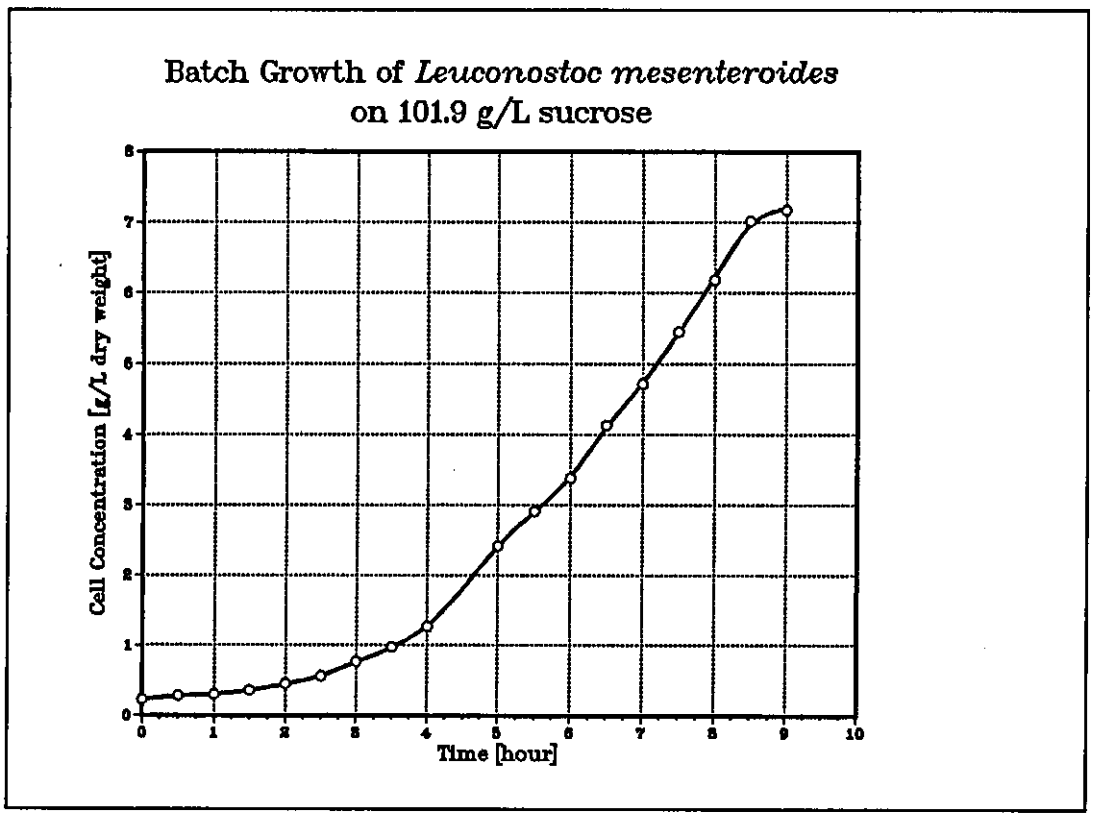

Figure F.16

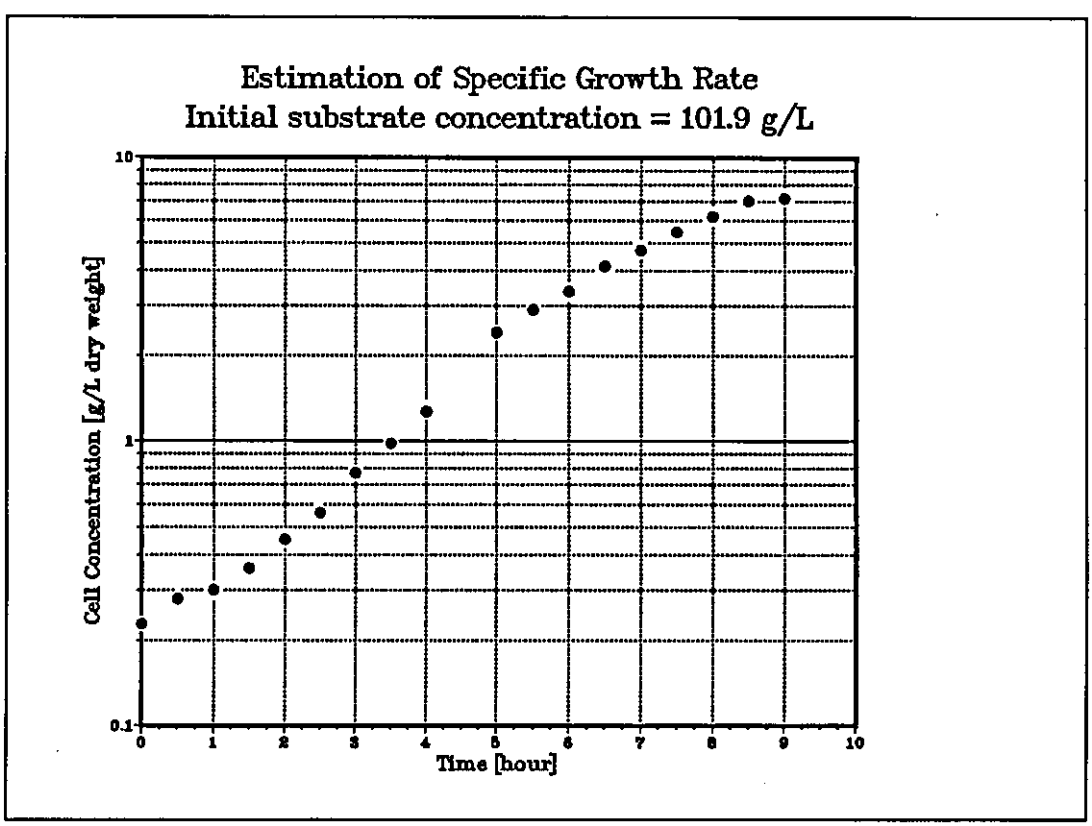

Appendix G Determination of Specific Growth Rates from Fed-Batch Culture Data

Environmental conditions for fed-batch growth of *Leuconostoc mesenteroides* are given as follows.

Main culture medium

Sucrose	variable
Yeast extract (Difco)	40 g/L
K_2HPO_4	20 g/L
R salts	0.5 % (v/v)
Antifoam (polypropylene glycol)	0.2 % (v/v)

pH control	:	1M NaOH
Temperature	:	23 °C
pH	:	6.7
pO_2	:	> 60 % air saturation

The fermentation was carried out as outlined in section 5.5.2. A sterile medium mixture of sucrose and sodium hydroxide was fed into the fermenter to regulate pH level and substrate concentration in the vessel.

The experimental results from each fed-batch culture are presented in two separate graphs. The first one is the growth curve featuring cell concentration against culture time. The second graph is constructed by plotting z/(1–z) versus culture time. The specific growth rate is determined by means of least squares linear regression in natural logarithmic base.

Table G.1

Fed-Batch Growth of *Leuconostoc mesenteroides* NRRL B-512F

Initial substrate concentration = 2.90 g/L
Substrate concentration in the feeding mixture = 247.4 g/L

Time (hour)	Cell concentration (g/L dry weight)	z/(1 – z)
0.00	0.1716	0.0047
0.25	0.1716	0.0047
0.50	0.1716	0.0047
0.75	0.1794	0.0049
1.00	0.1872	0.0051
1.25	0.1794	0.0049
1.50	0.2028	0.0055
1.75	0.1950	0.0053
2.00	0.2145	0.0058
2.25	0.2496	0.0068
2.50	0.2496	0.0068
2.75	0.2652	0.0072
3.00	0.2964	0.0081
4.00	0.3978	0.0108
4.25	0.4407	0.0120
4.50	0.4576	0.0125
4.75	0.5096	0.0139
5.00	0.5876	0.0160
5.25	0.6448	0.0176
5.50	0.7410	0.0202
5.75	0.8268	0.0225
6.00	0.9048	0.0247
6.25	0.9984	0.0272
6.50	1.1232	0.0306
6.75	1.2584	0.0343
7.00	1.3806	0.0376
7.25	1.5210	0.0415
7.50	1.6640	0.0454
7.75	1.8590	0.0507
8.00	1.9188	0.0523
8.25	2.1060	0.0574
8.50	2.3296	0.0635
8.75	2.4960	0.0681
9.00	2.4960	0.0681

Estimated specific growth rate = 0.432 hr^{-1}
on time interval of 4 – 7.75 hour

Figure G.1

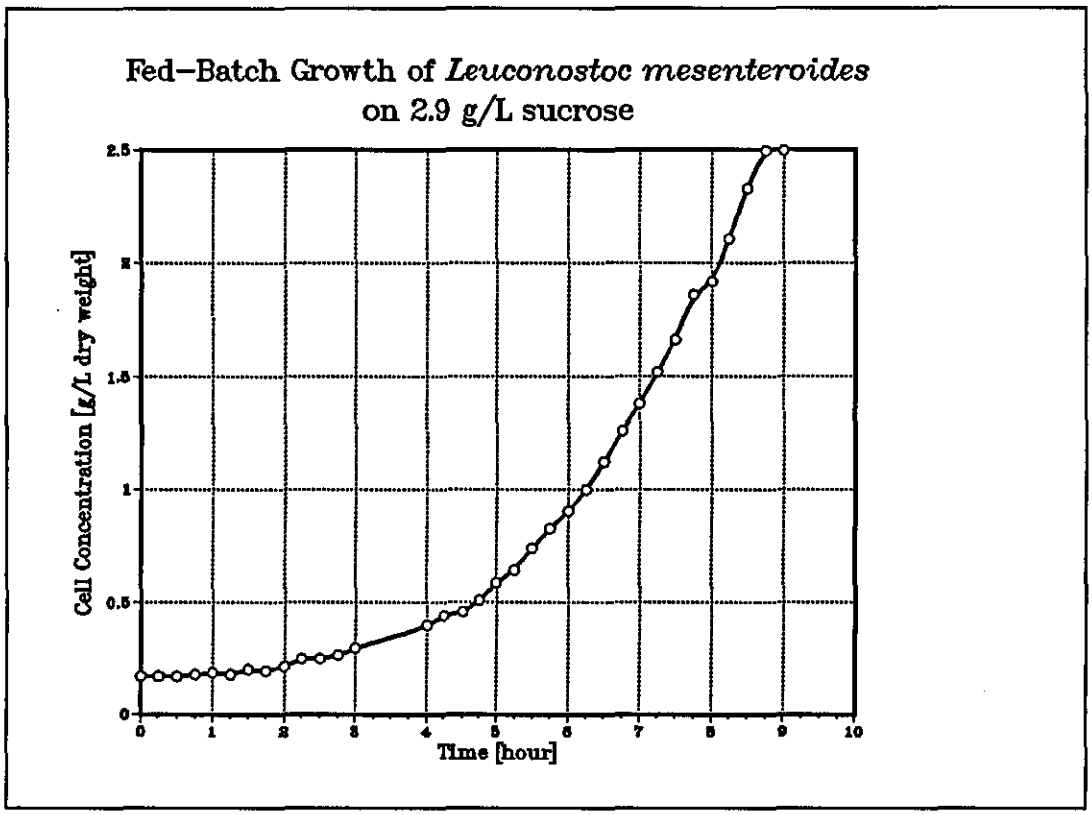

Figure G.2

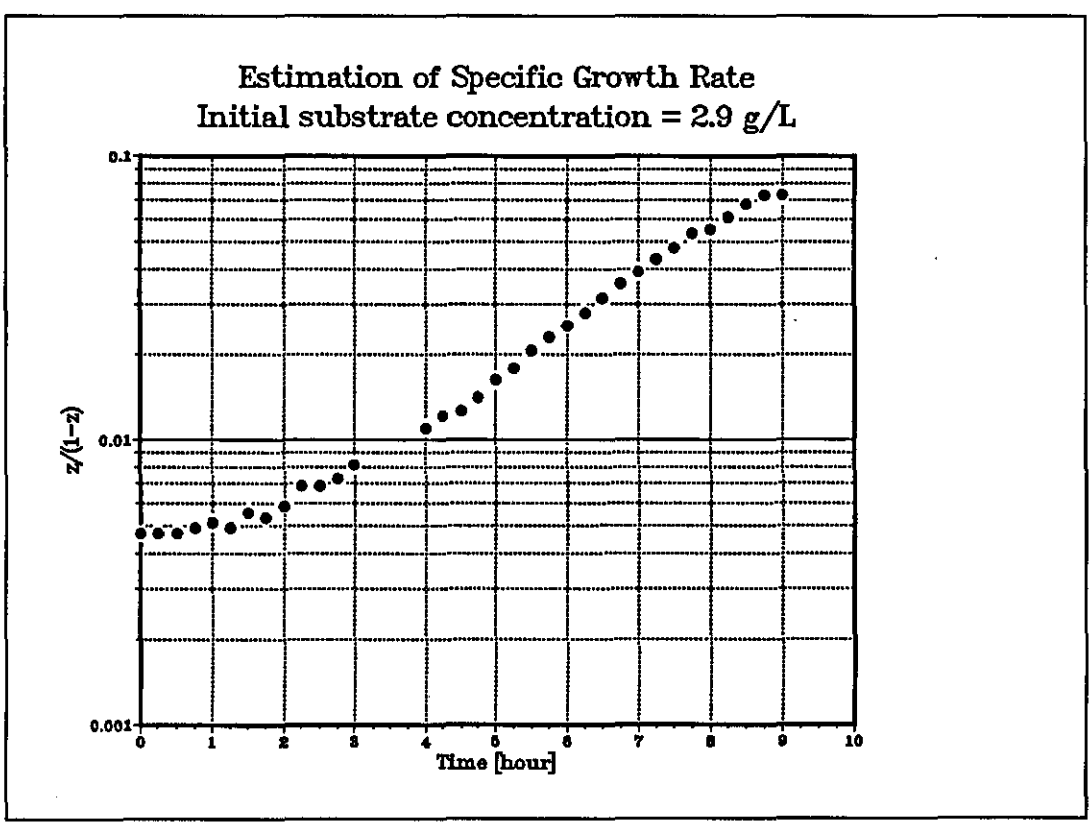

Table G.2

Fed-Batch Growth of *Leuconostoc mesenteroides* NRRL B-512F

Initial substrate concentration = 4.40 g/L
Substrate concentration in the feeding mixture = 248.9 g/L

Time (hour)	Cell concentration (g/L dry weight)	z/(1 – z)
0.00	0.1664	0.0045
0.25	0.1768	0.0048
0.50	0.1898	0.0052
0.75	0.1820	0.0050
1.00	0.1976	0.0054
1.25	0.2080	0.0057
1.50	0.2314	0.0063
1.75	0.2444	0.0067
2.00	0.2444	0.0067
2.25	0.2756	0.0075
2.50	0.2886	0.0079
3.00	0.3276	0.0089
3.50	0.3822	0.0104
3.75	0.4602	0.0125
4.00	0.4992	0.0136
4.25	0.5824	0.0159
4.50	0.6552	0.0179
4.75	0.7670	0.0209
5.00	0.8320	0.0227
5.25	0.9672	0.0264
5.50	1.0764	0.0293
5.75	1.2402	0.0338
6.00	1.4560	0.0397
6.25	1.6536	0.0451
6.50	1.9500	0.0532
6.75	2.0800	0.0567
7.00	2.3400	0.0638
7.25	2.5480	0.0695
7.50	2.6780	0.0730
7.75	2.7560	0.0751
8.00	3.0160	0.0822
8.25	3.0550	0.0833
8.50	3.5100	0.0957

Estimated specific growth rate = 0.514 hr^{-1}
on time interval of 3 – 7.5 hour

Figure G.3

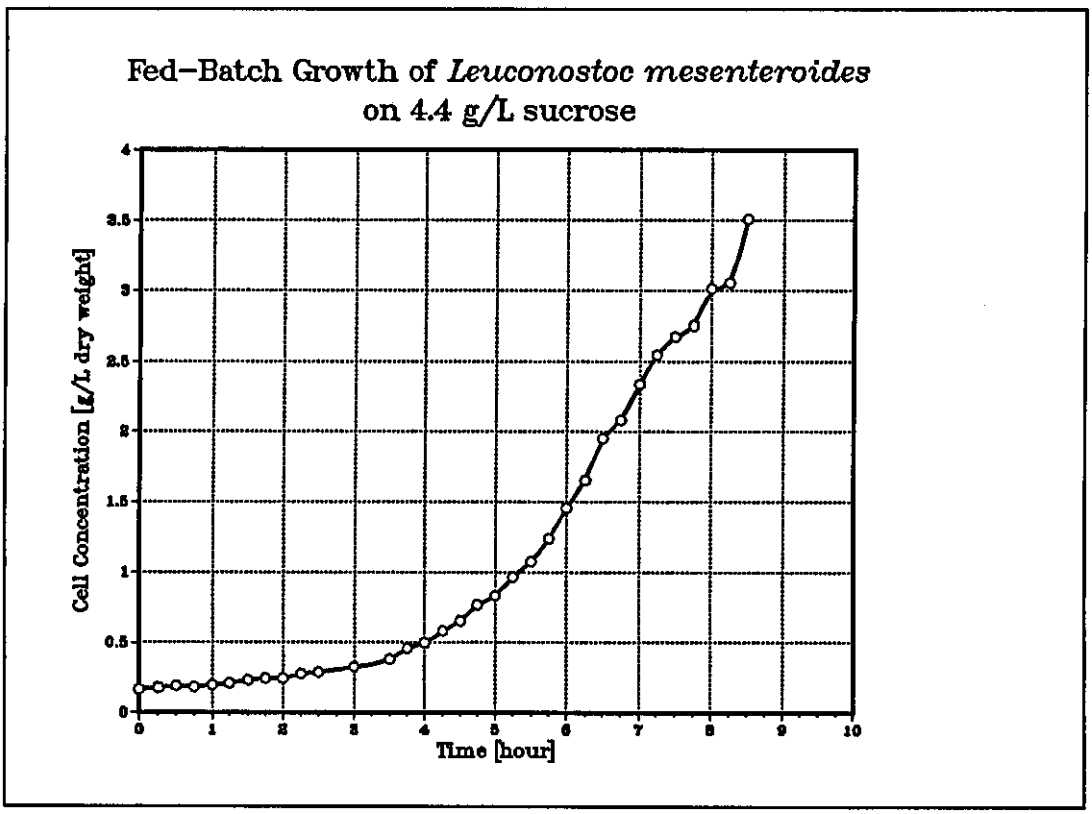

Figure G.4

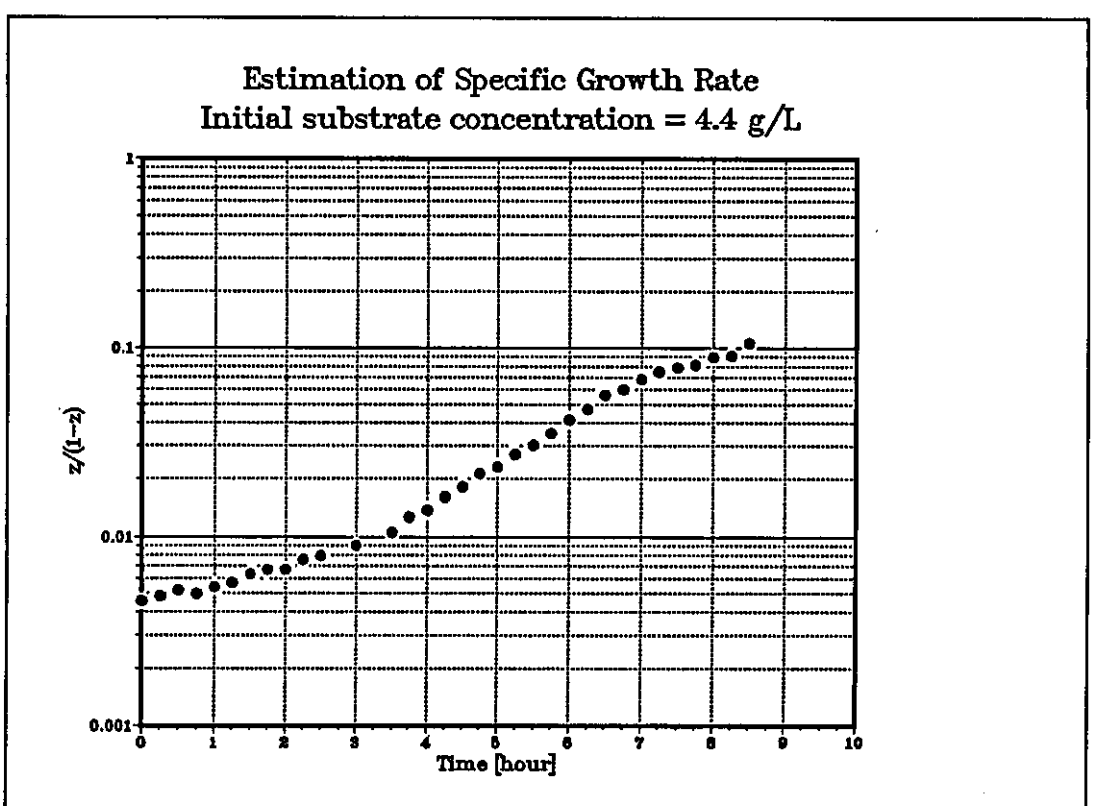

Table G.3

Fed-Batch Growth of *Leuconostoc mesenteroides* NRRL B-512F

Initial substrate concentration = 5.90 g/L
Substrate concentration in the feeding mixture = 250.4 g/L

Time (hour)	Cell concentration (g/L dry weight)	z/(1 – z)
0.00	0.2860	0.0078
0.25	0.1716	0.0047
0.50	0.1768	0.0048
0.75	0.1716	0.0047
1.00	0.1742	0.0047
1.25	0.1716	0.0047
1.50	0.1924	0.0052
1.75	0.1872	0.0051
2.00	0.1872	0.0051
2.25	0.2054	0.0056
2.50	0.2132	0.0058
2.75	0.2236	0.0061
3.00	0.2548	0.0069
4.00	0.3276	0.0089
4.25	0.3744	0.0102
4.50	0.4134	0.0113
4.75	0.4602	0.0125
5.00	0.5304	0.0145
5.25	0.5824	0.0159
5.50	0.6500	0.0177
5.75	0.7670	0.0209
6.00	0.8385	0.0229
6.25	0.9516	0.0259
6.50	1.0647	0.0290
6.75	1.1856	0.0323
7.00	1.2870	0.0351
7.25	1.4560	0.0397
7.50	1.6302	0.0444
7.75	1.7160	0.0468
8.00	1.8252	0.0498
8.25	2.0020	0.0546
8.50	2.1450	0.0585
9.00	2.2880	0.0624

Estimated specific growth rate = 0.470 hr^{-1}
on time interval of 4 – 7.5 hour

Figure G.5

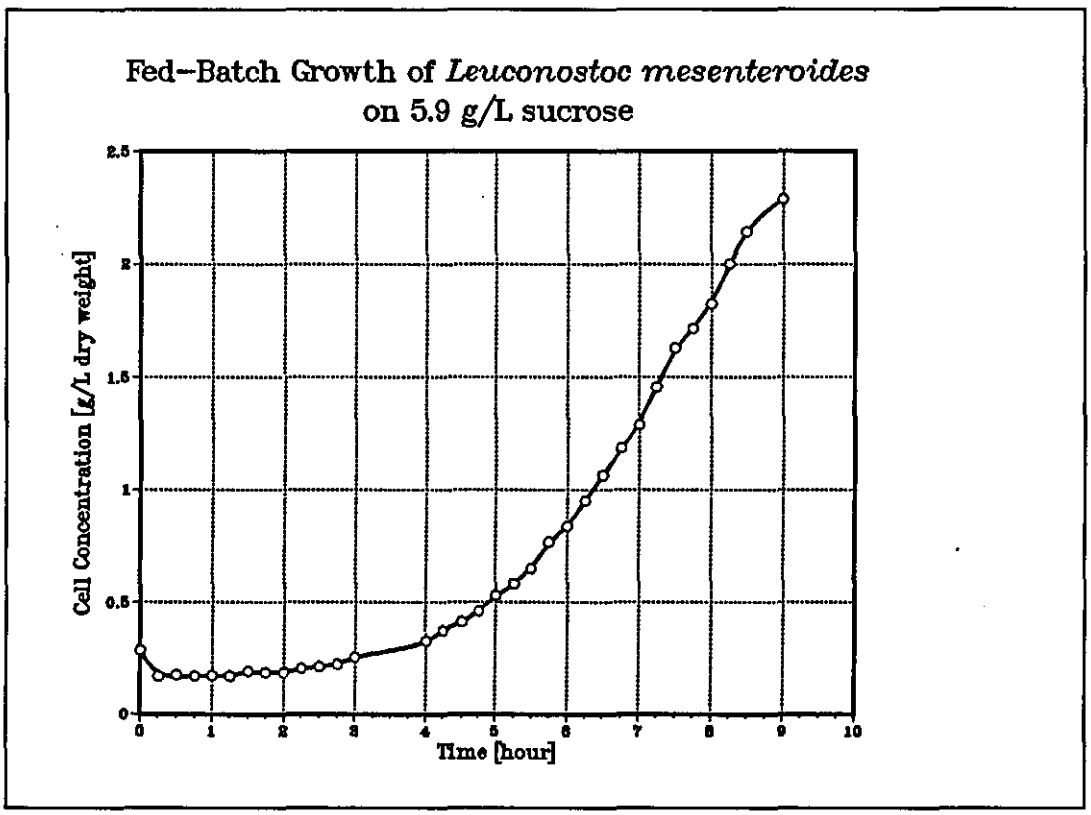

Figure G.6

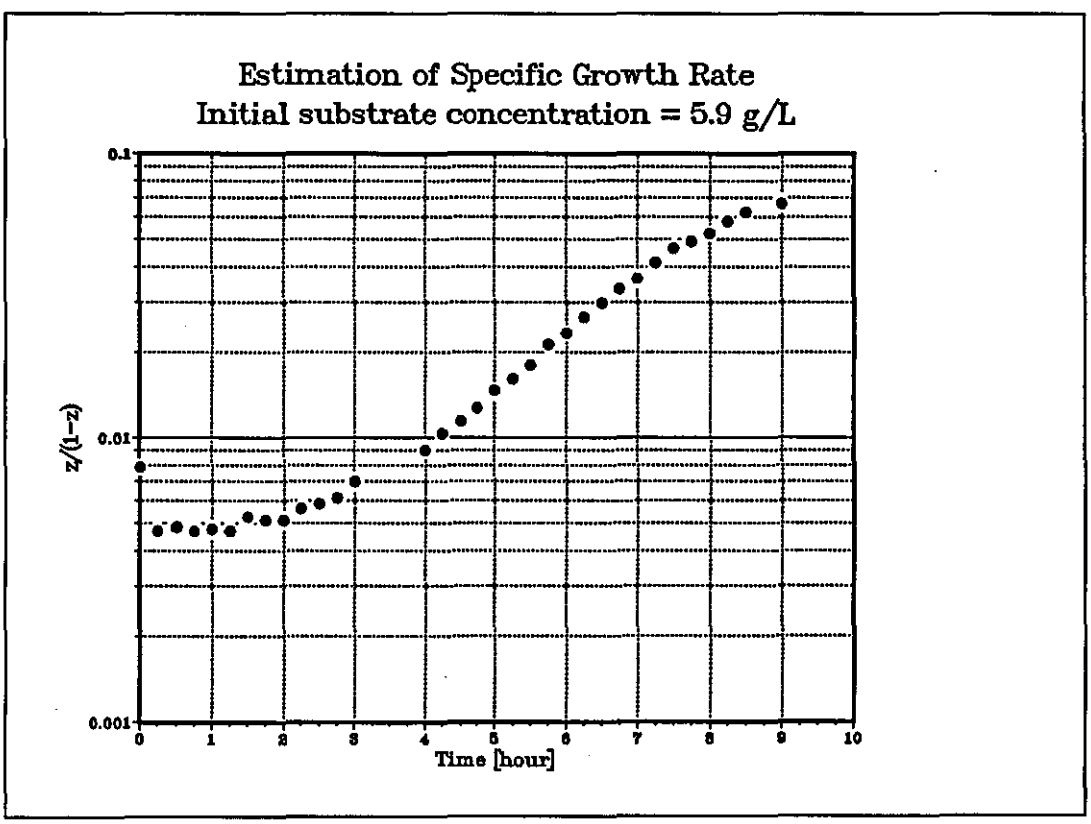

Table G.4

Fed-Batch Growth of *Leuconostoc mesenteroides* NRRL B-512F

Initial substrate concentration = 9.40 g/L
Substrate concentration in the feeding mixture = 253.9 g/L

Time (hour)	Cell concentration (g/L dry weight)	z/(1 – z)
0.00	0.2288	0.0062
0.25	0.1508	0.0041
0.50	0.1508	0.0041
0.75	0.1508	0.0041
1.00	0.1612	0.0044
1.25	0.1820	0.0050
1.50	0.1820	0.0050
1.75	0.1976	0.0054
2.00	0.2080	0.0057
2.25	0.2184	0.0060
2.50	0.2262	0.0062
2.75	0.2444	0.0067
3.00	0.2652	0.0072
4.00	0.3692	0.0101
4.25	0.4056	0.0111
4.50	0.4368	0.0119
5.00	0.5668	0.0155
5.25	0.6240	0.0170
5.50	0.7020	0.0191
5.75	0.7930	0.0216
6.00	0.8814	0.0240
6.25	0.9750	0.0266
6.50	1.1284	0.0308
6.75	1.2896	0.0352
7.00	1.3806	0.0376
7.25	1.5860	0.0432
7.50	1.7160	0.0468
7.75	1.9032	0.0519
8.00	2.0618	0.0562
8.25	2.2204	0.0605
8.50	2.3985	0.0654
8.75	2.5376	0.0692
9.00	2.7404	0.0747

Estimated specific growth rate = 0.457 hr^{-1}
on time interval of 4 – 8 hour

Figure G.7

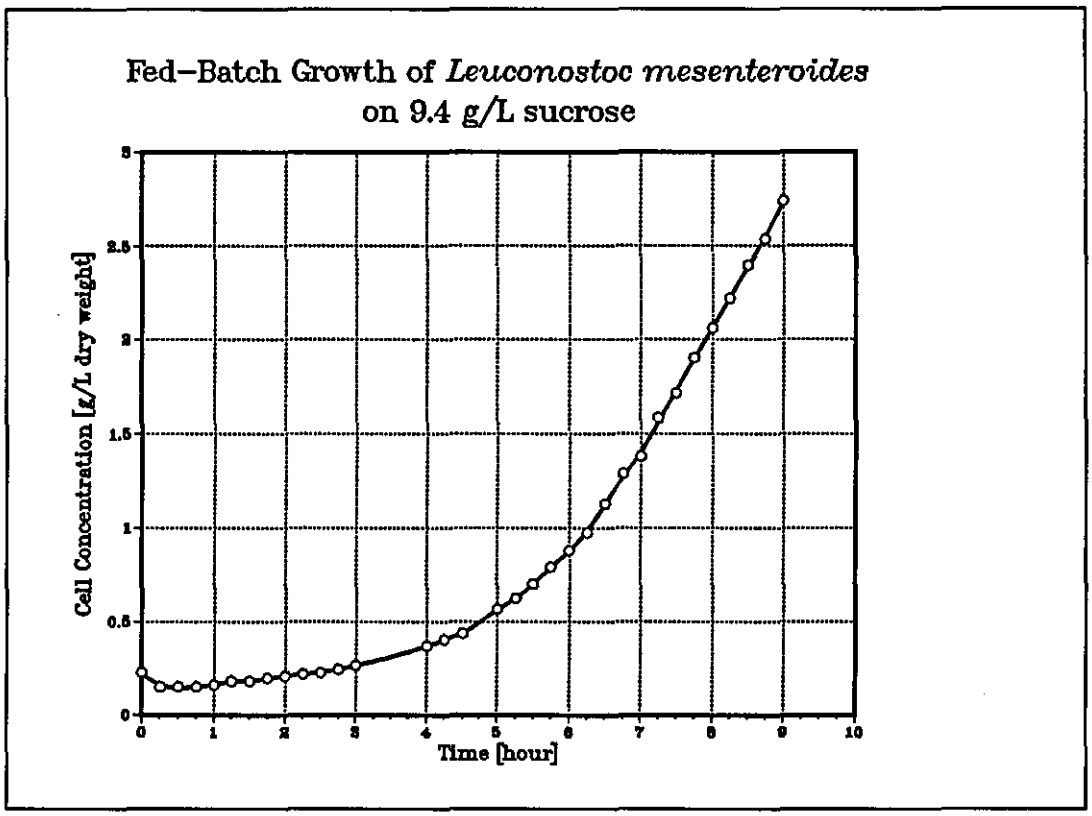

Figure G.8

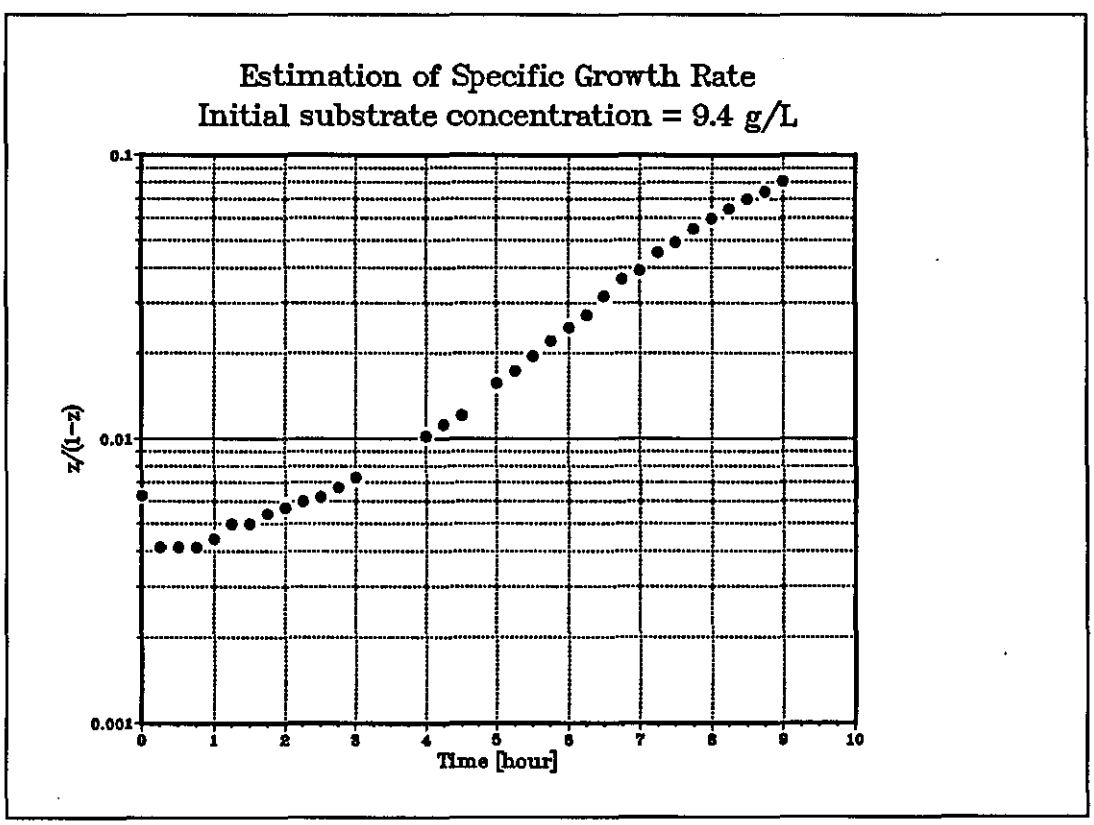

Table G.5

Fed-Batch Growth of *Leuconostoc mesenteroides* NRRL B-512F

Initial substrate concentration = 11.90 g/L
Substrate concentration in the feeding mixture = 256.4 g/L

Time (hour)	Cell concentration (g/L dry weight)	z/(1 – z)
0.00	0.2808	0.0077
0.25	0.1352	0.0037
0.50	0.1352	0.0037
0.75	0.1378	0.0038
1.00	0.1456	0.0040
1.25	0.1404	0.0038
1.50	0.1508	0.0041
1.75	0.1560	0.0043
2.00	0.1664	0.0045
2.25	0.1716	0.0047
2.50	0.1820	0.0050
2.75	0.1924	0.0052
3.00	0.2054	0.0056
4.00	0.2548	0.0069
4.25	0.2834	0.0077
4.50	0.3016	0.0082
4.75	0.3432	0.0094
5.00	0.3744	0.0102
5.25	0.4290	0.0117
5.50	0.4732	0.0129
5.75	0.5148	0.0140
6.00	0.5512	0.0150
6.25	0.6240	0.0170
6.50	0.7345	0.0200
6.75	0.8060	0.0220
7.00	0.8970	0.0245
7.25	1.0010	0.0273
7.50	1.1011	0.0300
7.75	1.2272	0.0335
8.00	1.4040	0.0383
8.25	1.5340	0.0418
8.50	1.6588	0.0452
8.75	1.8252	0.0498
9.00	1.9604	0.0535

Estimated specific growth rate = 0.431 hr^{-1}
on time interval of 4 – 9 hour

Figure G.9

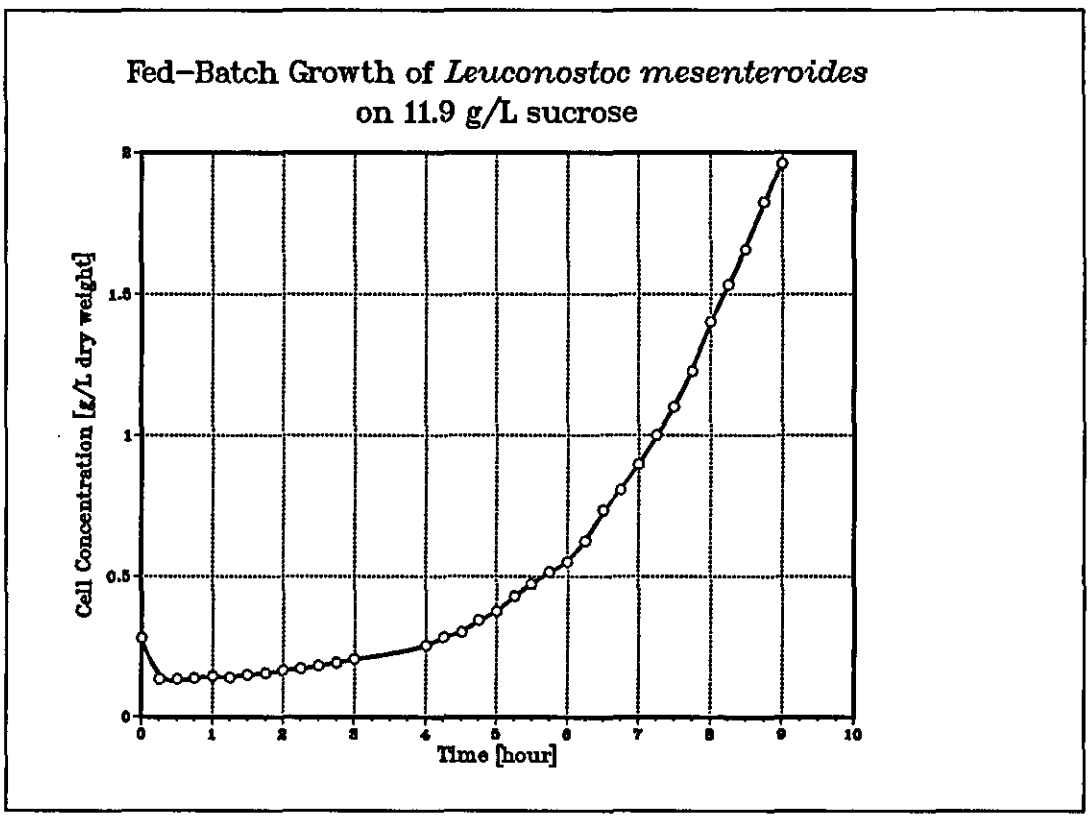

Figure G.10

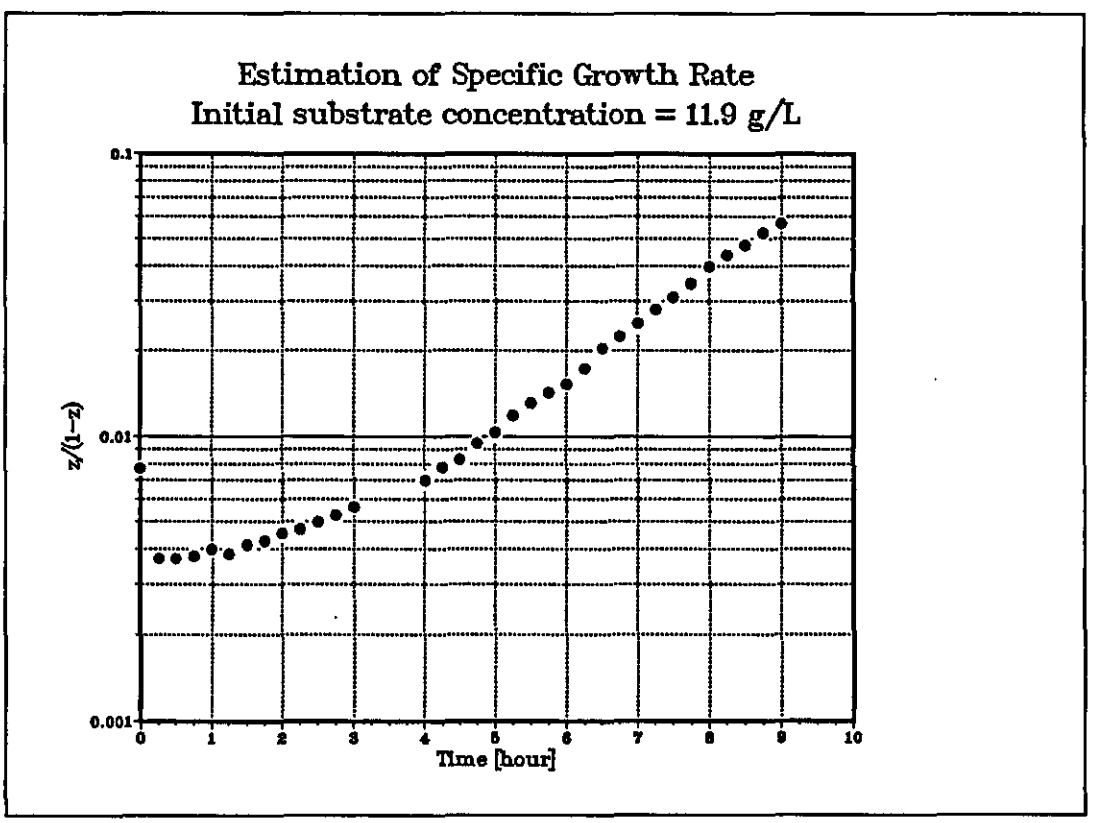

Table G.6

Fed-Batch Growth of *Leuconostoc mesenteroides* NRRL B-512F

Initial substrate concentration = 16.90 g/L
Substrate concentration in the feeding mixture = 261.4 g/L

Time (hour)	Cell concentration (g/L dry weight)	z/(1 – z)
0.00	0.4056	0.0111
0.25	0.2184	0.0060
0.50	0.2236	0.0061
0.75	0.2340	0.0064
1.00	0.2132	0.0058
1.25	0.2262	0.0062
1.50	0.2444	0.0067
1.75	0.2652	0.0072
2.00	0.2678	0.0073
2.25	0.2808	0.0077
2.50	0.2912	0.0079
2.75	0.3198	0.0087
3.00	0.3354	0.0091
4.00	0.4836	0.0132
4.25	0.5304	0.0145
4.50	0.5928	0.0162
4.75	0.6448	0.0176
5.00	0.6968	0.0190
5.25	0.8060	0.0220
5.50	0.8970	0.0245
5.75	1.0296	0.0281
6.00	1.1830	0.0323
6.25	1.3806	0.0376
6.50	1.5600	0.0425
6.75	1.7160	0.0468
7.00	1.8720	0.0510
7.25	2.0384	0.0556
7.50	2.1658	0.0591
7.75	2.3400	0.0638
8.00	2.5480	0.0695
9.00	3.1850	0.0868

Estimated specific growth rate = 0.455 hr^{-1}
on time interval of 4 – 8 hour

Figure G.11

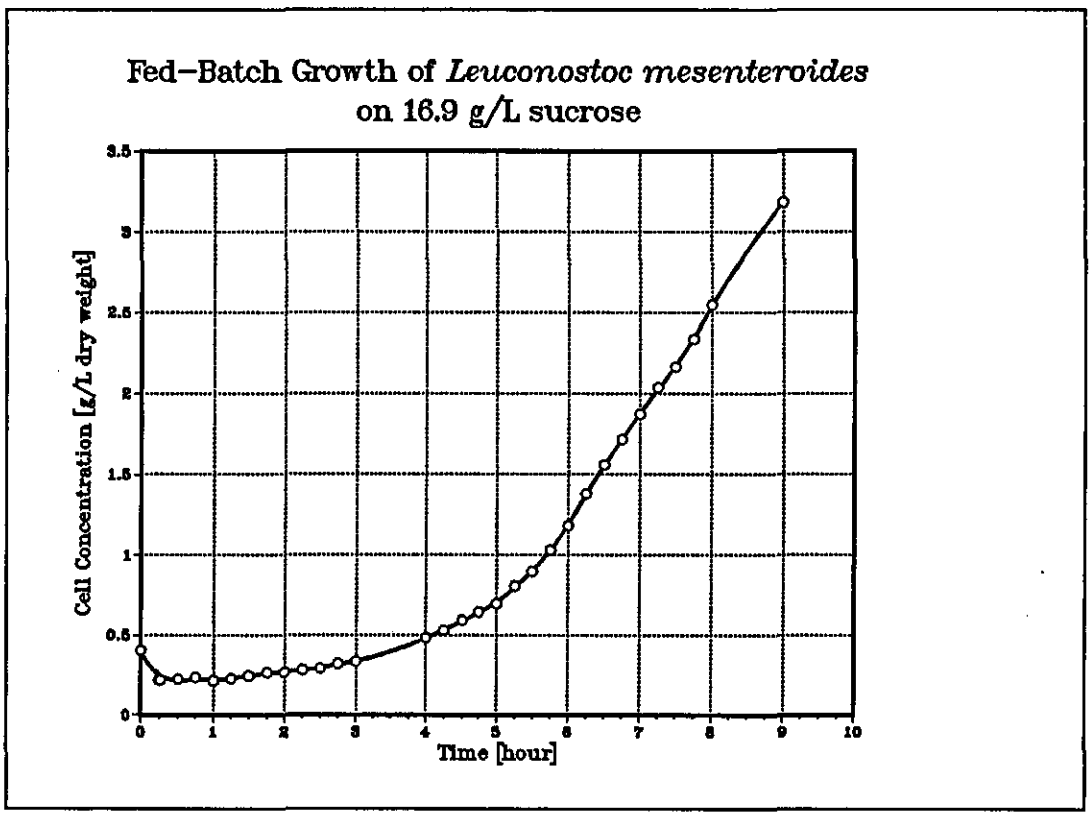

Figure G.12

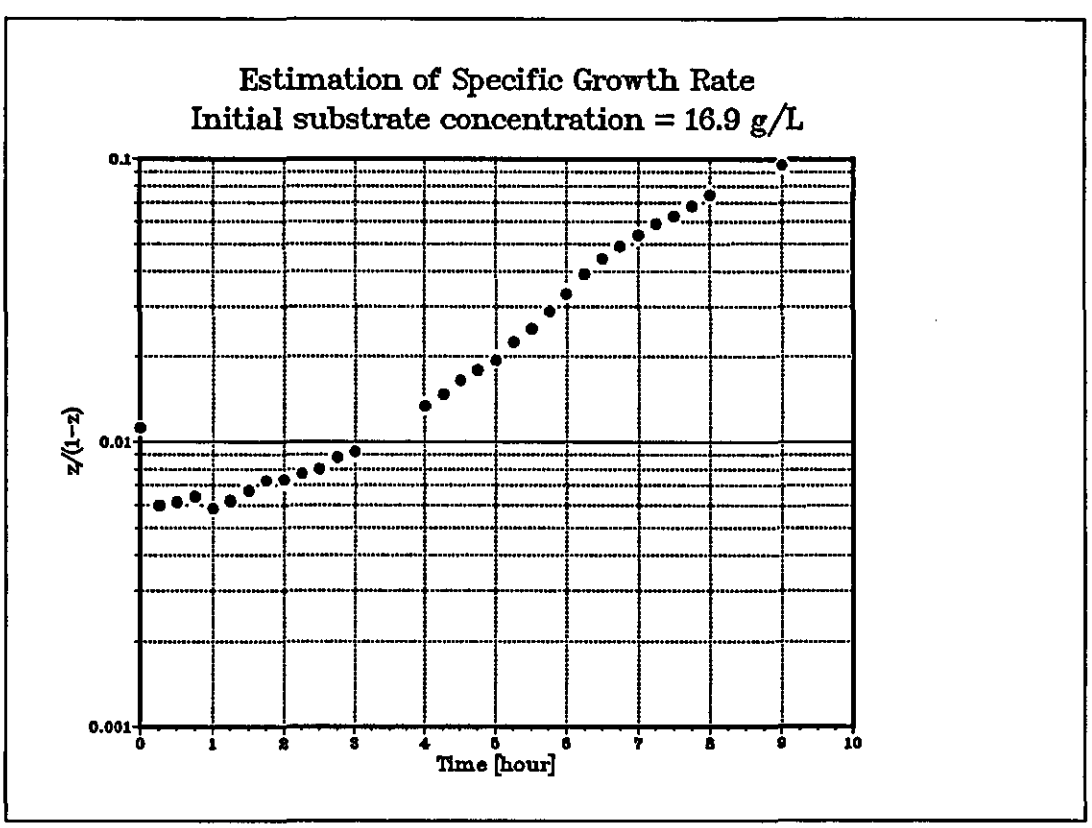

Table G.7

Fed-Batch Growth of *Leuconostoc mesenteroides* NRRL B-512F

Initial substrate concentration = 31.90 g/L
Substrate concentration in the feeding mixture = 276.4 g/L

Time (hour)	Cell concentration (g/L dry weight)	z/(1 – z)
0.00	0.2288	0.0062
0.25	0.1976	0.0054
0.50	0.1976	0.0054
0.75	0.1976	0.0054
1.00	0.2236	0.0061
1.25	0.2184	0.0060
1.50	0.2184	0.0060
1.75	0.2288	0.0062
2.00	0.2392	0.0065
2.25	0.2496	0.0068
2.50	0.2704	0.0074
2.75	0.2860	0.0078
3.00	0.3224	0.0088
4.00	0.4446	0.0121
4.25	0.4992	0.0136
4.50	0.5226	0.0142
4.75	0.5928	0.0162
5.00	0.6708	0.0183
5.25	0.7488	0.0204
5.50	0.8450	0.0230
5.75	0.9672	0.0264
6.00	1.0738	0.0293
6.25	1.2688	0.0346
6.50	1.4300	0.0390
6.75	1.5288	0.0417
7.00	1.7836	0.0486
7.25	1.8915	0.0516
7.50	2.0384	0.0556
7.75	2.3400	0.0638
8.00	2.4960	0.0681

Estimated specific growth rate = 0.465 hr^{-1}
on time interval of 4 – 8 hour

Figure G.13

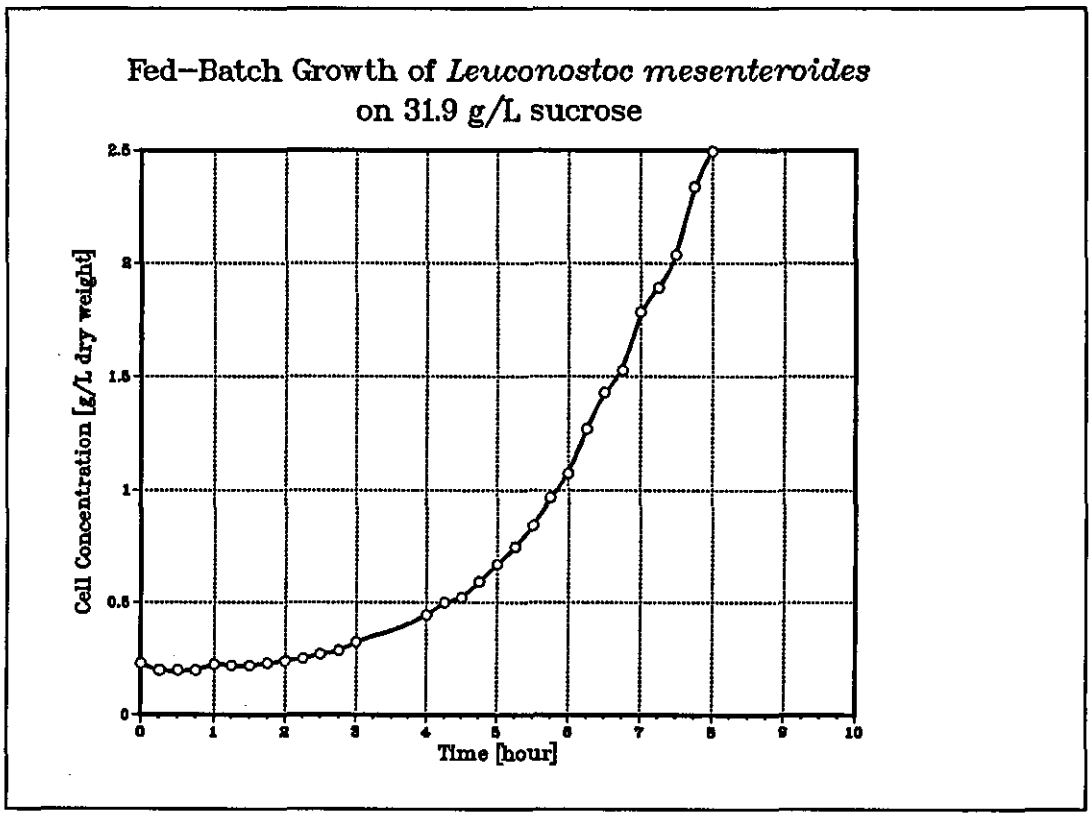

Figure G.14

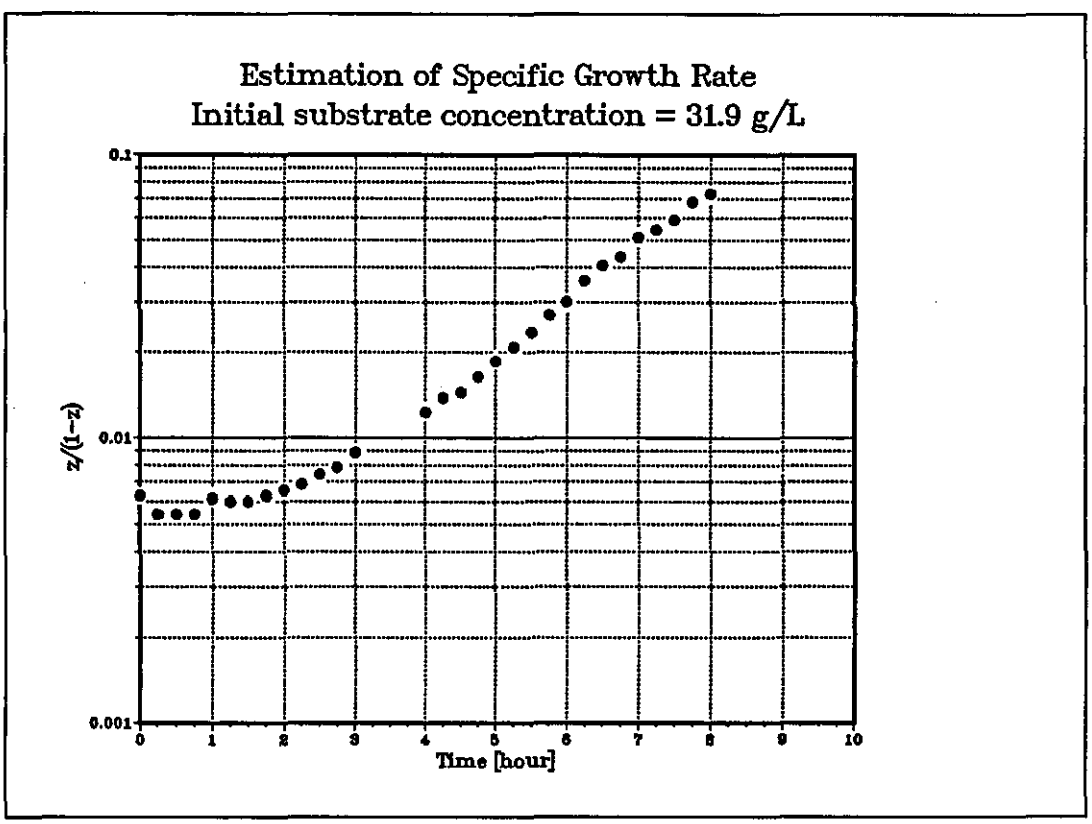

Appendix H Data Transformation Analysis of Batch Culture Data

Batch culture data of *Leuconostoc mesenteroides* NRRL B-512F growing on 11.9 g/L sucrose was analyzed using data transformation technique for the Monod kinetics described in section 5.3.3. The procedure was applied to the original data, giving comparable parameter values with estimates obtained by the initial specific growth rate method. The procedure was also applied to a set of data in which an apparent lag phase was discarded. The results are given below in Table H.1.

Table H.1

Analysis of Batch Growth of L. mesenteroides on 11.9 g/L Sucrose by Data Transformation Technique

Initial sucrose concentration = 11.9 g/L
Transformation parameter = K*

Case	Data Points	x_0 (g/L)	μ_{max} (hr^{-1})	K*	K_s (g/L sucrose)	r.m.s error
1	8	0.0595	0.499	0.088	1.047	0.018
2	7	0.0444	0.610	0.195	2.321	0.016

Modelling aerobic batch growth (initial substrate = 11.9 g/L)

Estimation performed at 15:26:40 on 01/21/89

Monod Kinetics :
Transformation parameter = K^*

Data used for parameter estimates :

Time	Concentration	Fractional Concentration
0.0000	8.32000E-02	0.02723
1.0000	8.32000E-02	0.02723
2.0000	1.04000E-01	0.03404
4.0000	3.01600E-01	0.09872
5.0000	5.40800E-01	0.17702
6.0000	8.73600E-01	0.28596
7.0000	1.52100E+00	0.49787
8.0000	2.08650E+00	0.68298

Maximum value of concentration = 3.05500E+00

8 data points supplied

Modelling aerobic batch growth (initial substrate = 11.9 g/L)

Monod Kinetics :
Transformation parameter = K^*

Direct Search on Transformation Parameter

Transformation Parameter		Variance
0.00000		3.92912E-03
0.40000		4.05947E-03
0.80000		4.35978E-03
1.20000		4.60527E-03
1.60000		4.79506E-03
2.00000		4.94321E-03
2.40000		5.06116E-03
2.80000		5.15693E-03
3.20000		5.23609E-03
3.60000		5.30253E-03
4.00000		5.35906E-03
4.40000		5.40770E-03
4.80000		5.44999E-03
5.20000		5.48709E-03
5.60000		5.51989E-03
6.00000		5.54910E-03
6.40000		5.57527E-03
6.80000		5.59885E-03
7.20000		5.62020E-03
7.60000		5.63963E-03
8.00000		5.65739E-03
8.40000		5.67367E-03
8.80000		5.68866E-03
9.20000		5.70251E-03
9.60000		5.71533E-03
10.00000		5.72725E-03

Modelling aerobic batch growth (initial substrate = 11.9 g/L)

Monod Kinetics :
Transformation parameter = K^*

Direct Search on Transformation Parameter

```
Transformation
     Parameter********************************************  Variance
      0.08957 **          .                                ** 3.89314E-03
      0.08958 **         .                                 ** 3.89314E-03
      0.08958 **       .                                   ** 3.89314E-03
      0.08958 **     .                                     ** 3.89314E-03
      0.08958 **    .                                      ** 3.89314E-03
      0.08958 **  .                                        ** 3.89314E-03
      0.08958 ** .                                         ** 3.89314E-03
      0.08958 **.                                          ** 3.89314E-03
      0.08958 **.                                          ** 3.89314E-03
      0.08958 **.                                          ** 3.89314E-03
      0.08958 **.                                          ** 3.89314E-03
      0.08959 ** .                                         ** 3.89314E-03
      0.08959 **  .                                        ** 3.89314E-03
      0.08959 **    .                                      ** 3.89314E-03
      0.08959 **     .                                     ** 3.89314E-03
      0.08959 **       .                                   ** 3.89314E-03
      0.08959 **         .                                 ** 3.89314E-03
      0.08959 **            .                              ** 3.89314E-03
      0.08959 **              .                            ** 3.89314E-03
      0.08959 **                 .                         ** 3.89314E-03
      0.08959 **                   .                       ** 3.89314E-03
      0.08960 **                      .                    ** 3.89314E-03
      0.08960 **                        .                  ** 3.89314E-03
      0.08960 **                          .                ** 3.89314E-03
      0.08960 **                            .              ** 3.89314E-03
      0.08960 **                           .               ** 3.89314E-03
              **********************************************
```

Modelling aerobic batch growth (initial substrate = 11.9 g/L)

Monod Kinetics :
Transformation parameter = K^*

Data Transformation Parameter Estimates

K^*	=	0.08959
Mu-max	=	0.49640
zinit	=	0.01878
xinit	=	0.05737

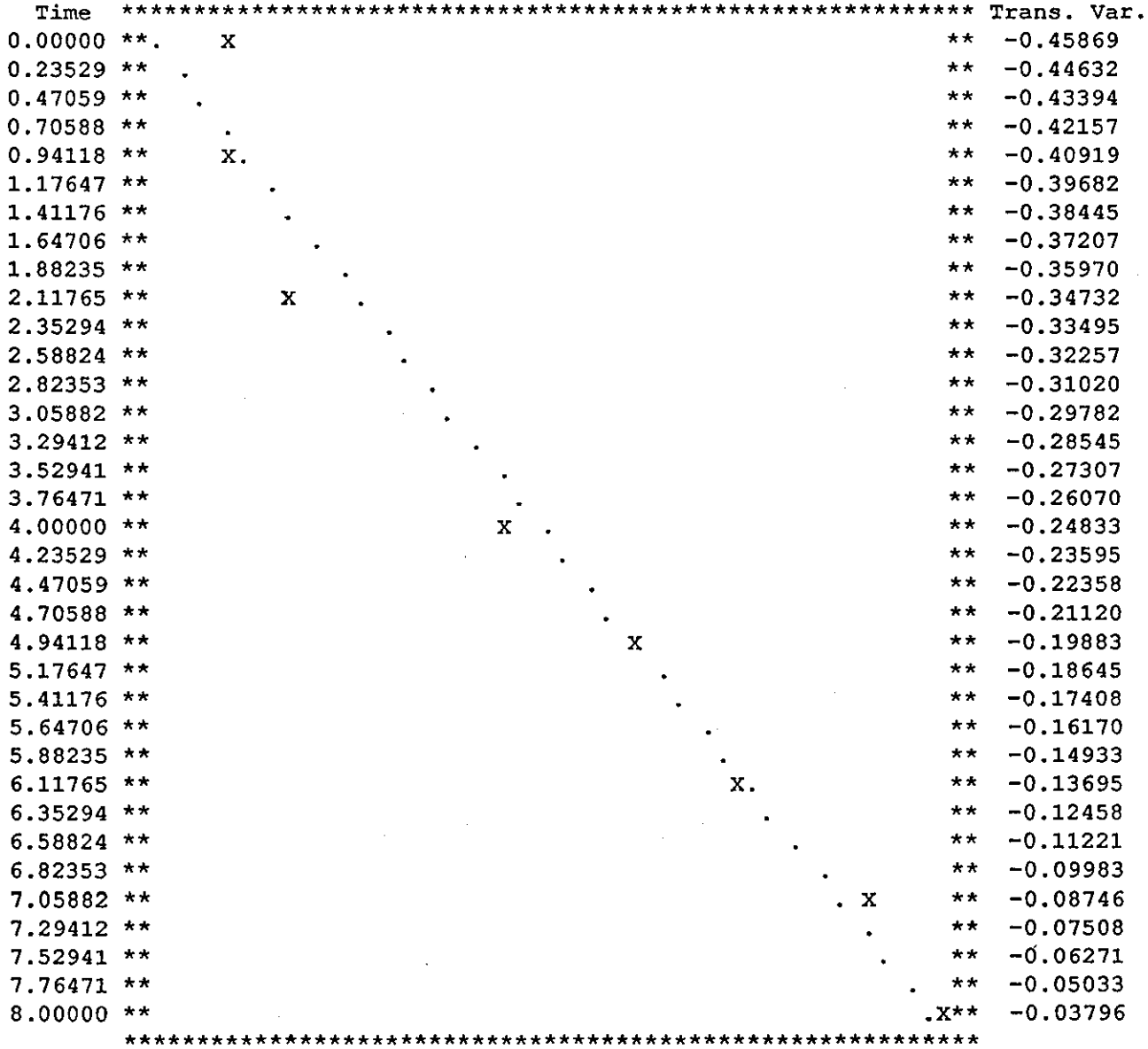

Legend : . = model X = data

Modelling aerobic batch growth (initial substrate = 11.9 g/L)

Monod Kinetics :
Transformation parameter = K^*

Data Transformation Estimates

K^*	=	0.08959
Mu-max	=	0.49640
zinit	=	0.01878
xinit	=	0.05737

Time		Frc. conc.
0.00000	X	0.01878
0.23529	.	0.02090
0.47059	.	0.02326
0.70588	.	0.02589
0.94118	X.	0.02881
1.17647	.	0.03206
1.41176	.	0.03568
1.64706	.	0.03970
1.88235	.	0.04418
2.11765	X.	0.04915
2.35294	.	0.05469
2.58824	.	0.06084
2.82353	.	0.06769
3.05882	.	0.07530
3.29412	.	0.08375
3.52941	.	0.09315
3.76471	.	0.10359
4.00000	X.	0.11519
4.23529	.	0.12807
4.47059	.	0.14237
4.70588	.	0.15824
4.94118	.X	0.17583
5.17647	.	0.19535
5.41176	.	0.21696
5.64706	.	0.24090
5.88235	.	0.26737
6.11765	X.	0.29663
6.35294	.	0.32892
6.58824	.	0.36450
6.82353	.	0.40363
7.05882	. X	0.44656
7.29412	.	0.49348
7.52941	.	0.54454
7.76471	.	0.59975
8.00000	.X	0.65889

Legend : . = model X = data

Modelling aerobic batch growth (initial substrate = 11.9 g/L)

Monod Kinetics :
Transformation parameter = K^*

Data Transformation Parameter Estimates

K^*	=	0.08959
Mu-max	=	0.49640
zinit	=	0.01878
xinit	=	0.05737

Time	Experimental Fractional Concentration	Model Fractional Concentration	Experimental Concentration	Model Concentration	Residual Fractional Concentration
0.000	0.02723	0.01878	8.32000E-02	5.73736E-02	8.45380E-03
1.000	0.02723	0.02959	8.32000E-02	9.03978E-02	-2.35607E-03
2.000	0.03404	0.04660	1.04000E-01	1.42360E-01	-1.25563E-02
4.000	0.09872	0.11519	3.01600E-01	3.51911E-01	-1.64683E-02
5.000	0.17702	0.18053	5.40800E-01	5.51507E-01	-3.50467E-03
6.000	0.28596	0.28164	8.73600E-01	8.60410E-01	4.31743E-03
7.000	0.49787	0.43546	1.52100E+00	1.33032E+00	6.24145E-02
8.000	0.68298	0.65889	2.08650E+00	2.01291E+00	2.40897E-02

Modelling aerobic batch growth (initial substrate = 11.9 g/L)

Monod Kinetics :
Transformation parameter = K^*

Direct Search on Model Parameters

Starting point :

K^*	=	0.08959
Mu-max	=	0.49640
zinit	=	0.01878
xinit	=	0.05737

Root-mean-square error : 0.02503

Finishing Point

K^*	=	0.08810
Mu-max	=	0.49882
zinit	=	0.01947
xinit	=	0.05948

Root-mean-square error : 0.01820

Search Report

IFAIL = 0

Search successful

Modelling aerobic batch growth (initial substrate = 11.9 g/L)

Monod Kinetics :
Transformation parameter = K^*

Direct Search Estimates

K^*	=	0.08810
Mu-max	=	0.49882
zinit	=	0.01947
xinit	=	0.05948

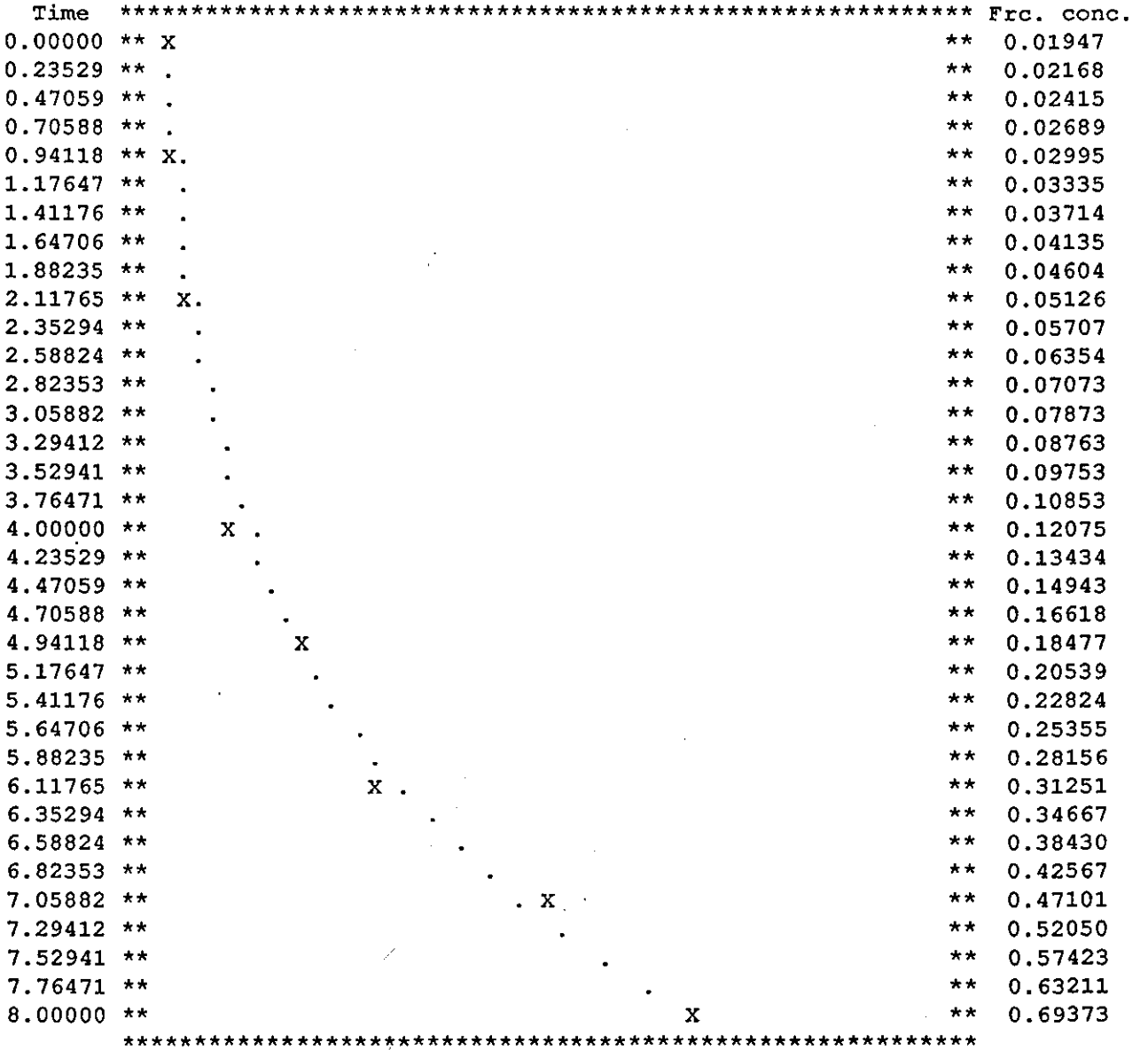

Legend : . = model X = data

Modelling aerobic batch growth (initial substrate = 11.9 g/L)

Monod Kinetics :
Transformation parameter = K^*

Direct Search Parameter Estimates

K^*	=	0.08810
Mu-max	=	0.49882
zinit	=	0.01947
xinit	=	0.05948

Time	Experimental Fractional Concentration	Model Fractional Concentration	Experimental Concentration	Model Concentration	Residual Fractional Concentration
0.000	0.02723	0.01947	8.32000E-02	5.94801E-02	7.76430E-03
1.000	0.02723	0.03077	8.32000E-02	9.39872E-02	-3.53100E-03
2.000	0.03404	0.04858	1.04000E-01	1.48422E-01	-1.45409E-02
4.000	0.09872	0.12075	3.01600E-01	3.68905E-01	-2.20311E-02
5.000	0.17702	0.18973	5.40800E-01	5.79610E-01	-1.27038E-02
6.000	0.28596	0.29665	8.73600E-01	9.06260E-01	-1.06905E-02
7.000	0.49787	0.45929	1.52100E+00	1.40313E+00	3.85813E-02
8.000	0.68298	0.69373	2.08650E+00	2.11936E+00	-1.07546E-02

Modelling aerobic batch growth (initial substrate = 11.9 g/L)

Estimation performed at 15:27:41 on 01/21/89

Monod Kinetics :
Transformation parameter = K^*

Data used for parameter estimates :

Time	Concentration	Fractional Concentration
1.0000	8.30000E-02	0.02717
2.0000	1.04000E-01	0.03404
4.0000	3.01600E-01	0.09872
5.0000	5.40800E-01	0.17702
6.0000	8.73600E-01	0.28596
7.0000	1.52100E+00	0.49787
8.0000	2.08650E+00	0.68298

Maximum value of concentration = 3.05500E+00

7 data points supplied

Modelling aerobic batch growth (initial substrate = 11.9 g/L)

Monod Kinetics :
Transformation parameter = K^*

Data Transformation Parameter Estimates

K^*	=	0.19474
Mu-max	=	0.61140
zinit	=	0.01405
xinit	=	0.04293

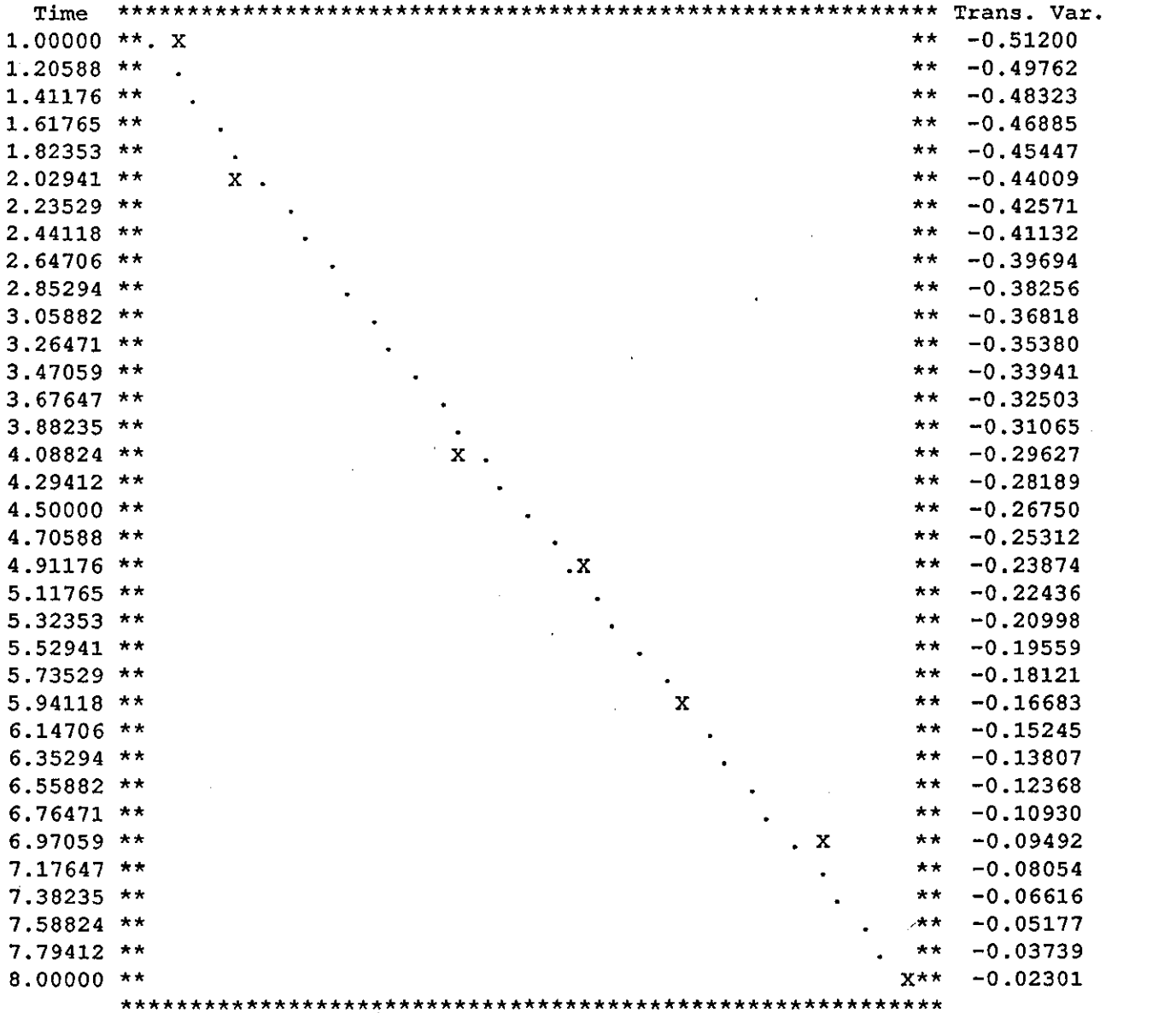

Legend : . = model X = data

Modelling aerobic batch growth (initial substrate = 11.9 g/L)

Monod Kinetics :
Transformation parameter = K^*

Data Transformation Estimates

K^*	=	0.19474
Mu-max	=	0.61140
zinit	=	0.01405
xinit	=	0.04293

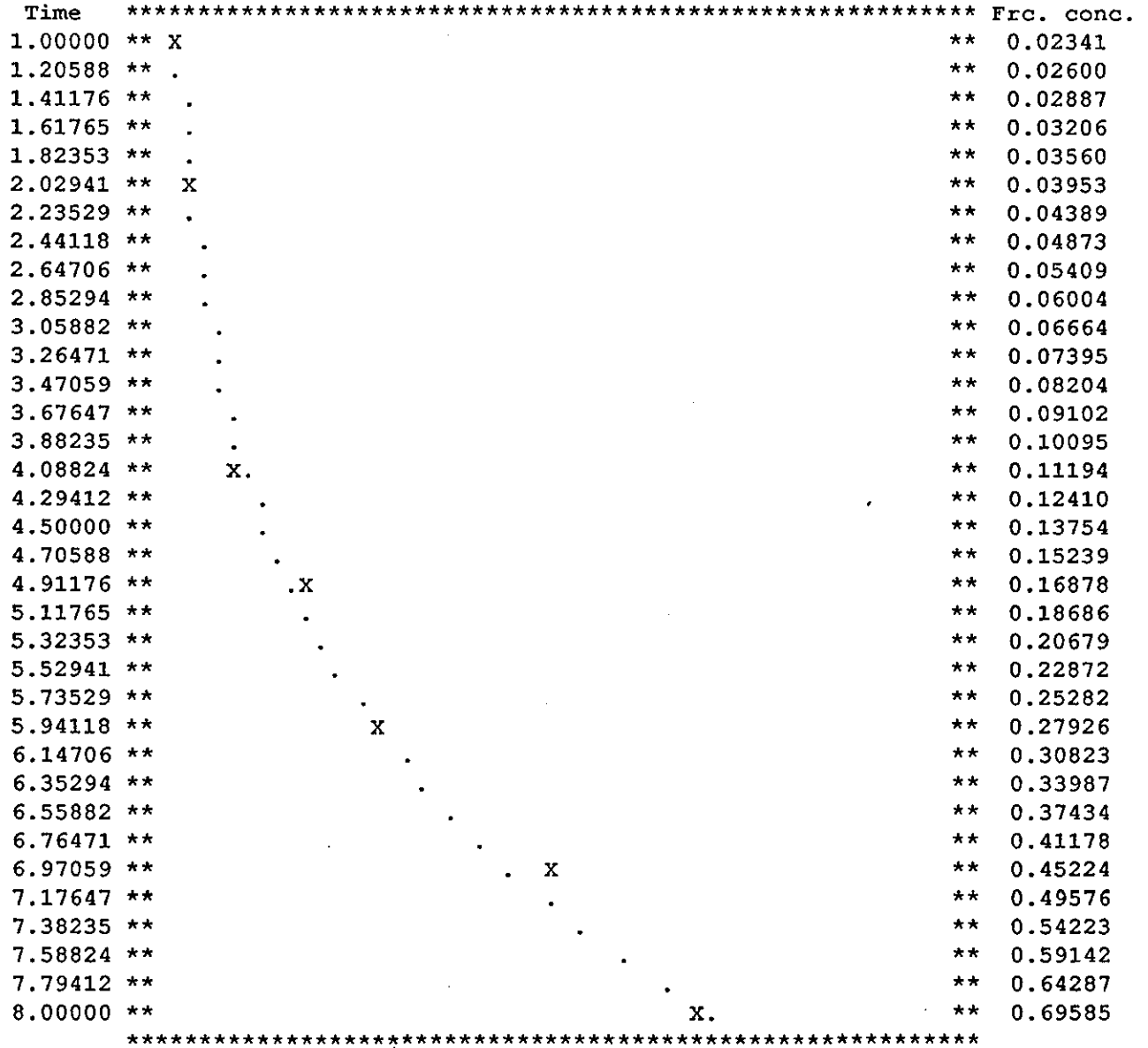

Legend : . = model X = data

Modelling aerobic batch growth (initial substrate = 11.9 g/L)

Monod Kinetics :
Transformation parameter = K^*

Data Transformation Parameter Estimates

K^*	=	0.19474
Mu-max	=	0.61140
zinit	=	0.01405
xinit	=	0.04293

Time	Experimental Fractional Concentration	Model Fractional Concentration	Experimental Concentration	Model Concentration	Residual Fractional Concentration
1.000	0.02717	0.02341	8.30000E-02	7.15098E-02	3.76112E-03
2.000	0.03404	0.03895	1.04000E-01	1.18982E-01	-4.90404E-03
4.000	0.09872	0.10709	3.01600E-01	3.27167E-01	-8.36881E-03
5.000	0.17702	0.17632	5.40800E-01	5.38647E-01	7.04845E-04
6.000	0.28596	0.28728	8.73600E-01	8.77626E-01	-1.31782E-03
7.000	0.49787	0.45828	1.52100E+00	1.40003E+00	3.95969E-02
8.000	0.68298	0.69585	2.08650E+00	2.12581E+00	-1.28679E-02

Modelling aerobic batch growth (initial substrate = 11.9 g/L)

Monod Kinetics :
Transformation parameter = K^*

Direct Search on Model Parameters

Starting point :

K^*	=	0.19474
Mu-max	=	0.61140
zinit	=	0.01405
xinit	=	0.04293

Root-mean-square error : 0.01623

Finishing Point

K^*	=	0.19537
Mu-max	=	0.60969
zinit	=	0.01452
xinit	=	0.04435

Root-mean-square error : 0.01563

Search Report

IFAIL = 0

Search successful

Modelling aerobic batch growth (initial substrate = 11.9 g/L)

Monod Kinetics :
Transformation parameter = K^*

Direct Search Estimates

K^*	=	0.19537
Mu-max	=	0.60969
zinit	=	0.01452
xinit	=	0.04435

Time		Frc. conc.
1.00000	** X	0.02414
1.20588	** .	0.02680
1.41176	** .	0.02975
1.61765	** .	0.03303
1.82353	** .	0.03666
2.02941	** X	0.04069
2.23529	** .	0.04516
2.44118	** .	0.05012
2.64706	** .	0.05562
2.85294	** .	0.06171
3.05882	** .	0.06846
3.26471	** .	0.07594
3.47059	** .	0.08423
3.67647	** .	0.09340
3.88235	** .	0.10355
4.08824	** X.	0.11477
4.29412	** .	0.12719
4.50000	** .	0.14091
4.70588	** .	0.15605
4.91176	** .X	0.17276
5.11765	** .	0.19119
5.32353	** .	0.21148
5.52941	** .	0.23379
5.73529	** .	0.25830
5.94118	** X	0.28517
6.14706	** .	0.31458
6.35294	** .	0.34668
6.55882	** .	0.38162
6.76471	** .	0.41952
6.97059	** . X	0.46043
7.17647	** .	0.50436
7.38235	** .	0.55119
7.58824	** .	0.60065
7.79412	** .	0.65224
8.00000	** X.	0.70517

Legend : . = model X = data

Modelling aerobic batch growth (initial substrate = 11.9 g/L)

Monod Kinetics :
Transformation parameter = K^*

Direct Search Parameter Estimates

K^*	=	0.19537
Mu-max	=	0.60969
zinit	=	0.01452
xinit	=	0.04435

Time	Experimental Fractional Concentration	Model Fractional Concentration	Experimental Concentration	Model Concentration	Residual Fractional Concentration
1.000	0.02717	0.02414	8.30000E-02	7.37415E-02	3.03060E-03
2.000	0.03404	0.04009	1.04000E-01	1.22475E-01	-6.04750E-03
4.000	0.09872	0.10982	3.01600E-01	3.35511E-01	-1.11001E-02
5.000	0.17702	0.18044	5.40800E-01	5.51250E-01	-3.42074E-03
6.000	0.28596	0.29331	8.73600E-01	8.96065E-01	-7.35361E-03
7.000	0.49787	0.46653	1.52100E+00	1.42524E+00	3.13448E-02
8.000	0.68298	0.70517	2.08650E+00	2.15429E+00	-2.21891E-02

Appendix I Estimation of Volumetric Oxygen Transfer Coefficient

Measurement of K_La in Air-Sparged Water

The fermenter vessel was charged with 1 – 1.5 litre of distilled water. The temperature was controlled at 23 °C. Agitation speed was set at 400 rpm and aeration flow rate was at about 4 VVM. The vessel was first deoxygenated by passing nitrogen through the aeration system. The dissolved oxygen concentration was recorded as per cent of air saturation for over 2 minutes after the start of re-aeration. The results were as follows :

Time (seconds)	Dissolved Oxygen Conc. C_l (% air saturation)	$(1-C_l/C_g)$
0.00	0.00	1.0000
10.00	8.10	0.9190
20.00	17.98	0.8202
30.00	30.09	0.6991
40.00	38.20	0.6180
50.00	44.16	0.5584
60.00	48.75	0.5125
70.00	53.54	0.4646
80.00	56.57	0.4343
90.00	58.52	0.4148
100.00	60.19	0.3981
110.00	61.75	0.3825
120.00	62.92	0.3708
130.00	63.80	0.3620
140.00	64.78	0.3522
150.00	65.56	0.3444

A graph was constructed by plotting $(1-C_l/C_g)$ in logarithmic scale versus time. The K_La value was determined by the slope of the initial linear portion of the curve.

$K_La = 0.0114\ sec^{-1} = 40.97\ hr^{-1}$

Measurement of K_La During Culture

During cell growth, aeration was stopped. The dissolved oxygen tension at this point was recorded as $C_{l,init}$. After one and half minutes, the dissolved oxygen tension dropped to C_{ll}. Aeration is then restored and the dissolved oxygen level was followed for another two minutes. The results were listed below.

Time (seconds)	Dissolved Oxygen Conc. C_l (% air saturation)	$\frac{(C_{l,init}-C_l)}{(C_{l,init}-C_{ll})}$
0.00	19.35	0.0000
90.00	12.41	1.0000
100.00	12.99	0.9164
110.00	13.58	0.8314
120.00	14.46	0.7046
130.00	15.05	0.6196
140.00	15.53	0.5504
150.00	16.02	0.4798
160.00	16.32	0.4366
170.00	16.61	0.3948
180.00	16.90	0.3530
190.00	17.10	0.3242
200.00	17.29	0.2968
210.00	17.39	0.2824

$C_{l,init}$ = 19.35 % air saturation
C_{ll} = 12.41 % air saturation

Following the principle described in section 6.3.2. $(C_{l,init}-C_l)/(C_{l,init}-C_{ll})$ was plotted in logarithmic scale against time. The K_La value was determined by the slope of the regression line.

$K_La = 0.0111\ sec^{-1} = 39.96\ hr^{-1}$

Figure I.1

Estimation of $K_L a$ Value in Air-Sparged Water

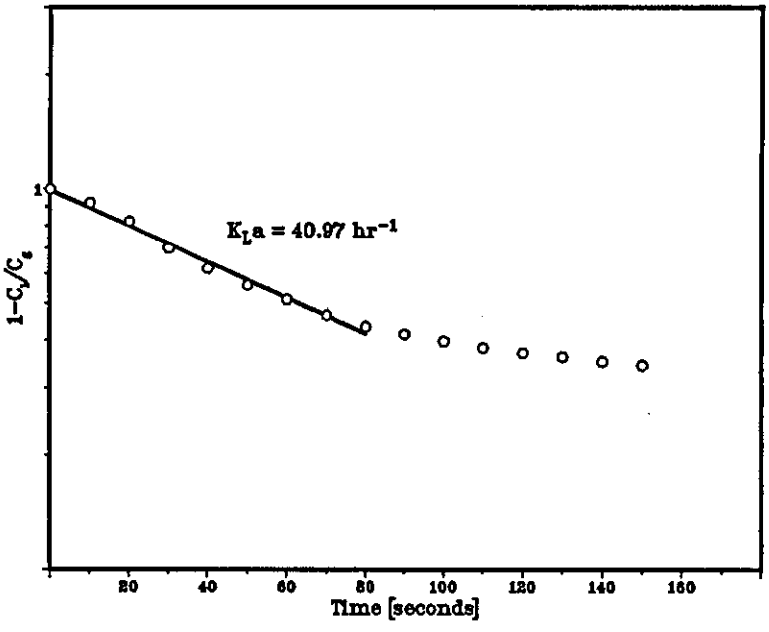

Figure I.2

Estimation of $K_L a$ Value During Batch Culture

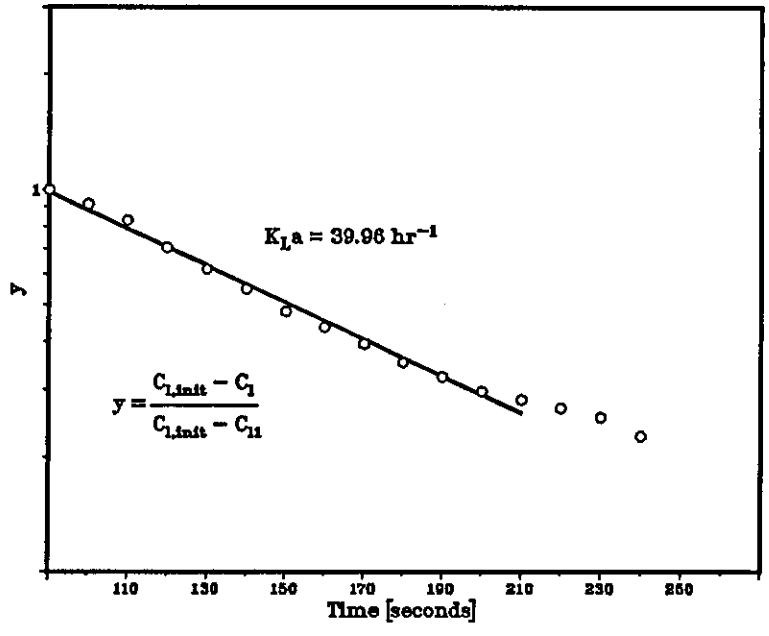

Appendix J Utilization of Dissolved Oxygen in Batch Cultures of *Leuconostoc mesenteroides*

Operating conditions for batch cultures of *L. mesenteroides*

Temperature	23 °C
pH	6.7
Agitation	400 rpm
Aeration	about 4 VVM

Table J.1

Experimental Data of Batch Culture O1

Time (hour)	Cell Concentration (g/L dry weight)
0.00	0.2236
0.50	0.2496
1.00	0.3068
1.50	0.3952
2.00	0.5252
2.50	0.7488
3.00	1.0088
3.50	1.2792
4.00	1.7472
5.00	2.7664
5.50	3.6270
6.00	4.2510
6.50	4.8880
7.00	5.5250
7.50	5.7200
8.00	6.1100
8.50	6.3180

Time (hour)	Dissolved Oxygen Concentration (% air saturation)
0.000	100.00
0.083	99.15
0.167	96.68
0.250	94.13
0.333	90.35
0.417	87.08
0.500	85.26
0.583	83.17
0.667	82.32
0.750	80.43
0.833	79.32
0.917	78.54
1.000	78.08
1.083	74.88
1.167	72.87
1.250	69.93
1.333	69.80
1.417	71.30
1.500	69.54
1.583	70.26
1.667	68.30
1.750	67.06
1.833	64.91
1.917	64.06
2.000	63.60
2.083	61.64
2.167	61.06
2.250	59.55
2.333	58.45
2.417	57.73
2.500	56.23
2.583	54.60
2.667	53.43
2.750	50.55
2.833	50.49
2.917	48.34
3.000	46.84
3.083	44.69
3.167	42.20
3.250	40.51
3.333	39.34
3.417	37.70
3.500	33.34
3.583	30.33
3.667	27.66
3.750	24.53
3.833	20.29
3.917	16.76
4.000	12.33
5.000	2.22
6.000	1.18
7.000	0.91
8.000	0.52

Table J.2

Experimental Data of Batch Culture O2

Time (hour)	Cell Concentration (g/L dry weight)	Dissolved Oxy. Conc. (% air saturation)
0.00	0.2392	100.00
0.50	0.2600	86.00
1.00	0.3016	78.00
1.50	0.3848	72.00
2.00	0.4888	65.00
2.50	0.6656	60.00
3.00	0.8736	51.00
3.50	1.1752	39.00
4.00	1.7160	23.00
5.00	2.7560	0.68
5.50	3.1720	0.00
6.00	3.7050	
6.50	4.0170	
7.00	4.2510	

Table J.3

Experimental Data of Batch Culture O3

Time (hour)	Cell Concentration (g/L dry weight)	Dissolved Oxy. Conc. (% air saturation)
0.00	0.1144	100.00
0.50	0.1144	98.04
1.00	0.1300	94.12
1.50	0.1430	90.78
2.00	0.1534	90.20
2.50	0.1716	88.82
3.00	0.2002	84.71
3.50	0.2600	80.39
4.00	0.3328	78.43
5.00	0.6656	67.65
5.50	0.8528	54.98
6.00	1.0920	41.76
6.50	1.5600	20.49
7.00	1.9110	1.53
7.50	2.4440	0.57
8.00	2.9900	0.20
8.50	3.2500	
9.00	3.3150	

Appendix K Kinetic Analyses of Enzyme Production from *Leuconostoc mesenteroides* NRRL B-512F

Environmental conditions for production of dextransucrase in batch cultures of *Leuconostoc mesenteroides* are given as follows.

Composition of culture medium

Sucrose	variable
Yeast extract (Difco)	40 g/L
K_2HPO_4	20 g/L
R salts	0.5% (v/v)
Antifoam (polypropylene glycol)	0.2% (v/v)

Temperature : 23 °C

pH : 6.7

Dissolved oxygen : > 60% air saturation

Five batch cultures, designated **E1**, **E2**, **E3**, **E4** and **E5**, were carried out in the bench-top fermenter. The experimental results are tabulated and two graphs are presented for each run. The first graph shows the time course of cell growth and enzyme synthesis. The second graph shows the relationship between enzyme activity and cell concentration and illustrates the trial-and-error procedure for estimating the maturation time.

Table K.1

Dextransucrase Production in Batch Culture E1

Initial sucrose concentration = 20.00 g/L

Time (hour)	Cell Concentration (g/L dry weight)
0.00	0.1508
0.50	0.1508
1.00	0.1716
2.00	0.1950
2.50	0.2223
3.00	0.2691
3.50	0.3042
4.00	0.3549
5.00	0.5421
5.50	0.7956
6.00	1.0608
7.00	1.7940
8.00	2.6208
9.00	3.6036
10.00	4.2120

Time (hour)	Enzyme Activity (DSU/mL)
5.00	4.6400
7.00	20.2150
8.00	33.8020
9.00	72.9070
10.00	78.5410
25.00	60.3140

Figure K.1

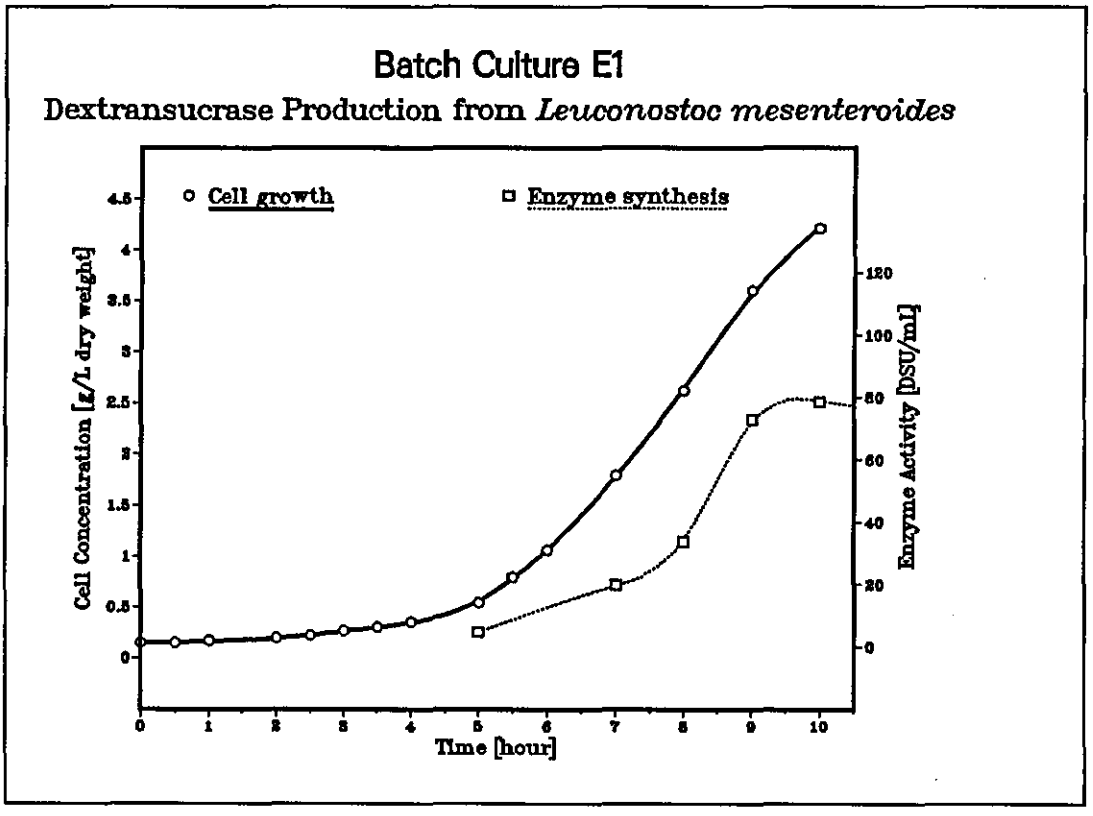

Figure K.2

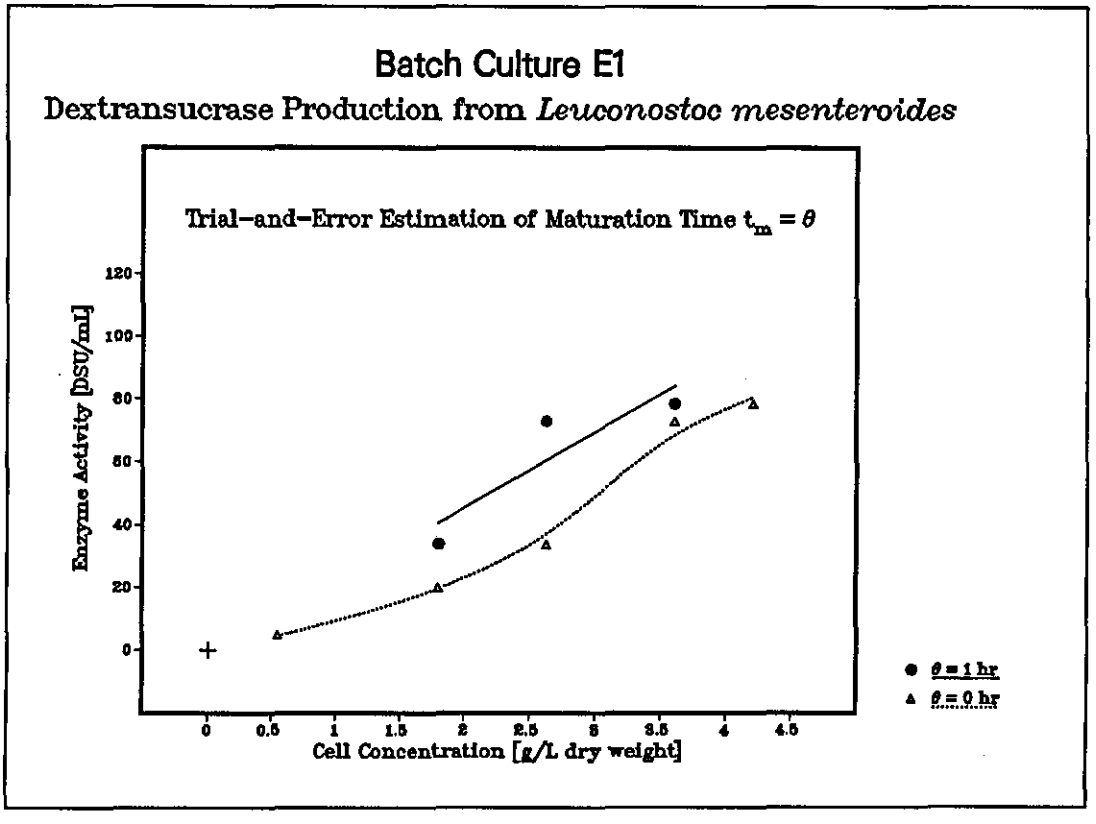

Table K.2

Dextransucrase Production in Batch Culture E2

Initial sucrose concentration = 50.00 g/L

Time (hour)	Cell Concentration (g/L dry weight)
0.00	0.0936
0.50	0.0988
1.00	0.1092
1.50	0.1196
2.00	0.1300
3.00	0.1820
4.00	0.3042
5.00	0.4576
6.00	1.0140
7.00	1.7160
8.00	2.7456
9.00	3.6725
10.00	4.8880

Time (hour)	Enzyme Activity (DSU/mL
5.00	6.4290
6.00	7.9530
7.00	15.2440
8.00	27.1740
9.00	47.3900
10.00	66.9420
24.00	96.7670
25.00	81.1260

Figure K.3

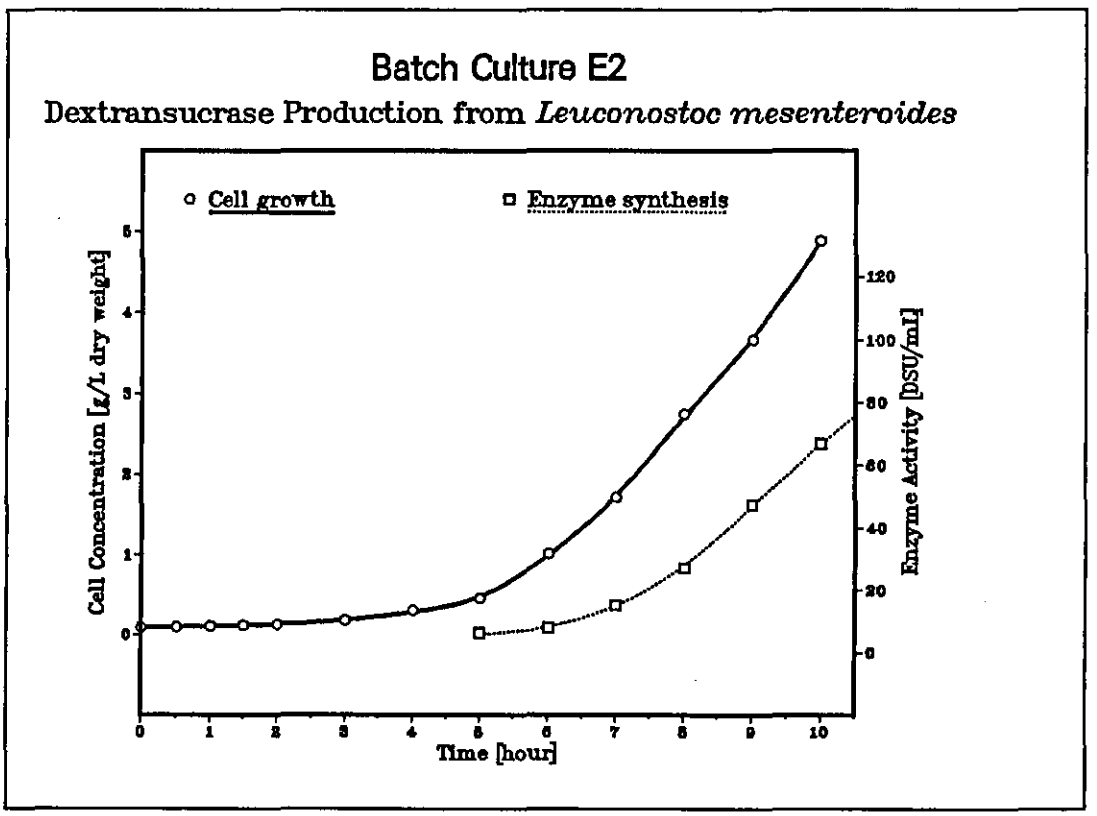

Figure K.4

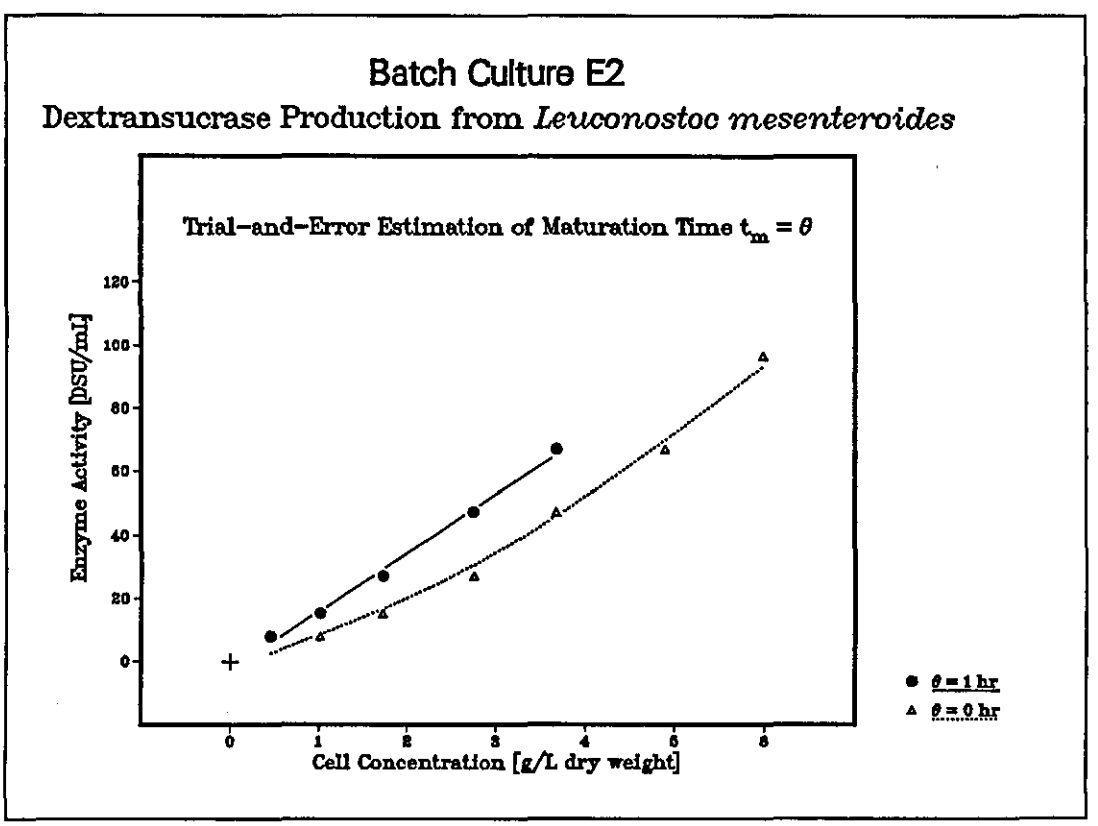

Table K.3

Dextransucrase Production in Batch Culture E3

Initial sucrose concentration = 5.00 g/L

Time (hour)	Cell Concentration (g/L dry weight)
0.00	0.0884
0.50	0.0780
1.00	0.0728
1.50	0.0988
2.00	0.1144
3.00	0.1612
4.00	0.2366
5.00	0.3744
6.00	0.6084
7.00	1.1752
8.00	1.9110
9.00	2.2880
10.00	2.6000

Time (hour)	Enzyme Activity (DSU/mL
5.00	4.1580
6.00	6.8400
7.00	14.6860
8.00	23.1350
9.00	29.7740
10.00	30.1760

Figure K.5

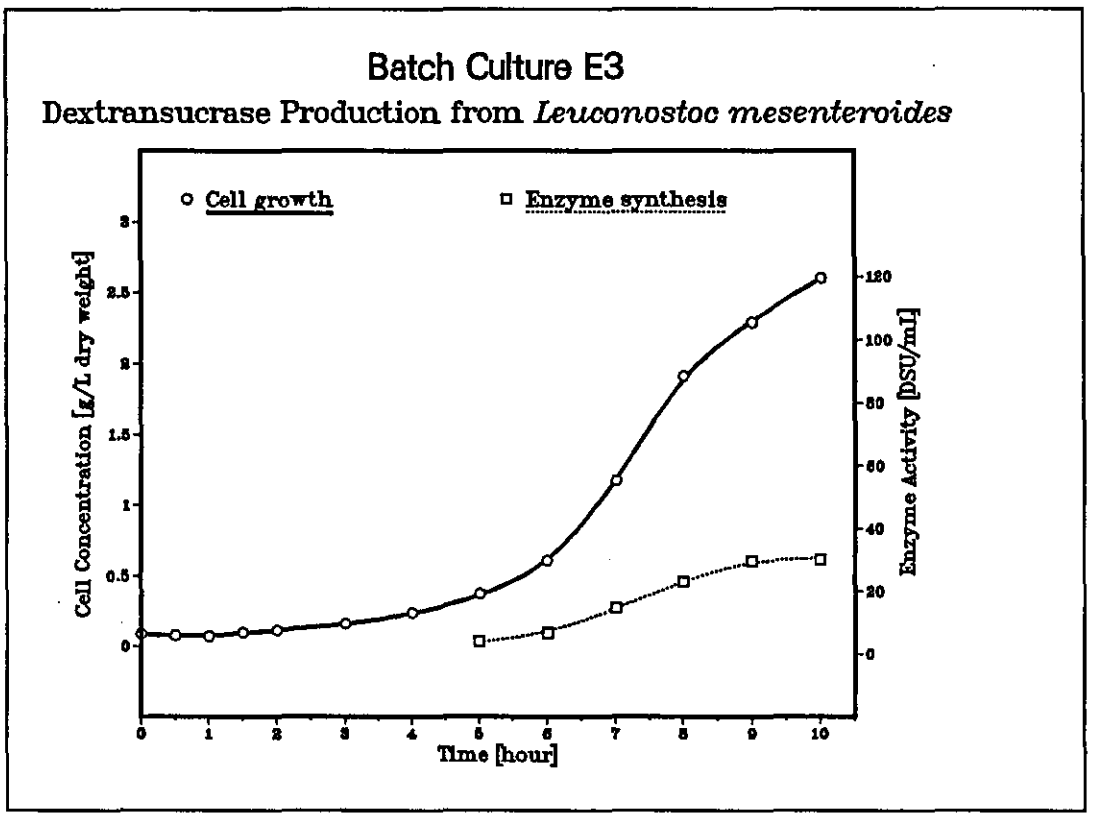

Figure K.6

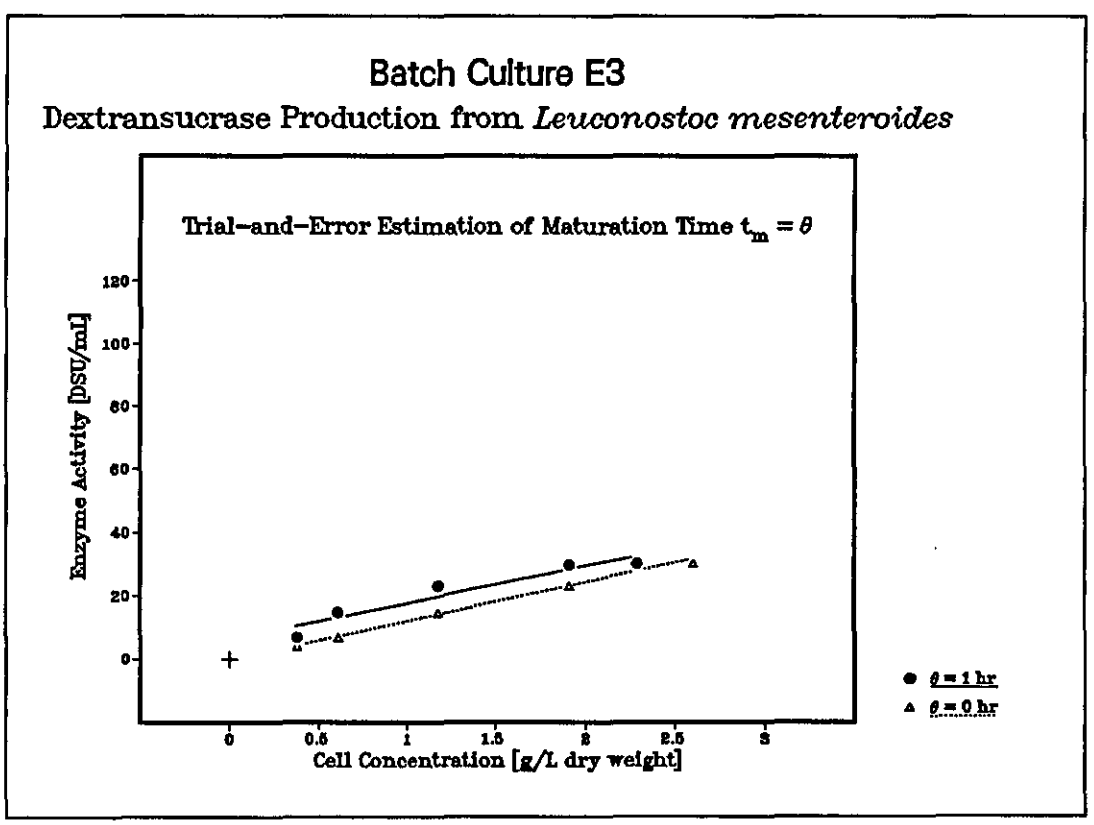

Table K.4

Dextransucrase Production in Batch Culture E4

Initial sucrose concentration = 50.00 g/L

Time (hour)	Cell Concentration (g/L dry weight)
0.00	0.0780
0.50	0.0520
1.00	0.0364
1.50	0.0676
2.00	0.0728
3.00	0.1404
4.00	0.2444
5.00	0.5070
6.00	0.8970
7.00	1.6380
8.00	2.7040
9.00	3.8610
10.00	5.2520

Time (hour)	Enzyme Activity (DSU/mL
5.00	6.0350
6.00	6.9070
7.00	17.7710
8.00	26.1530
9.00	78.1240
10.00	78.7940
24.00	126.0710
25.00	123.9250

Figure K.7

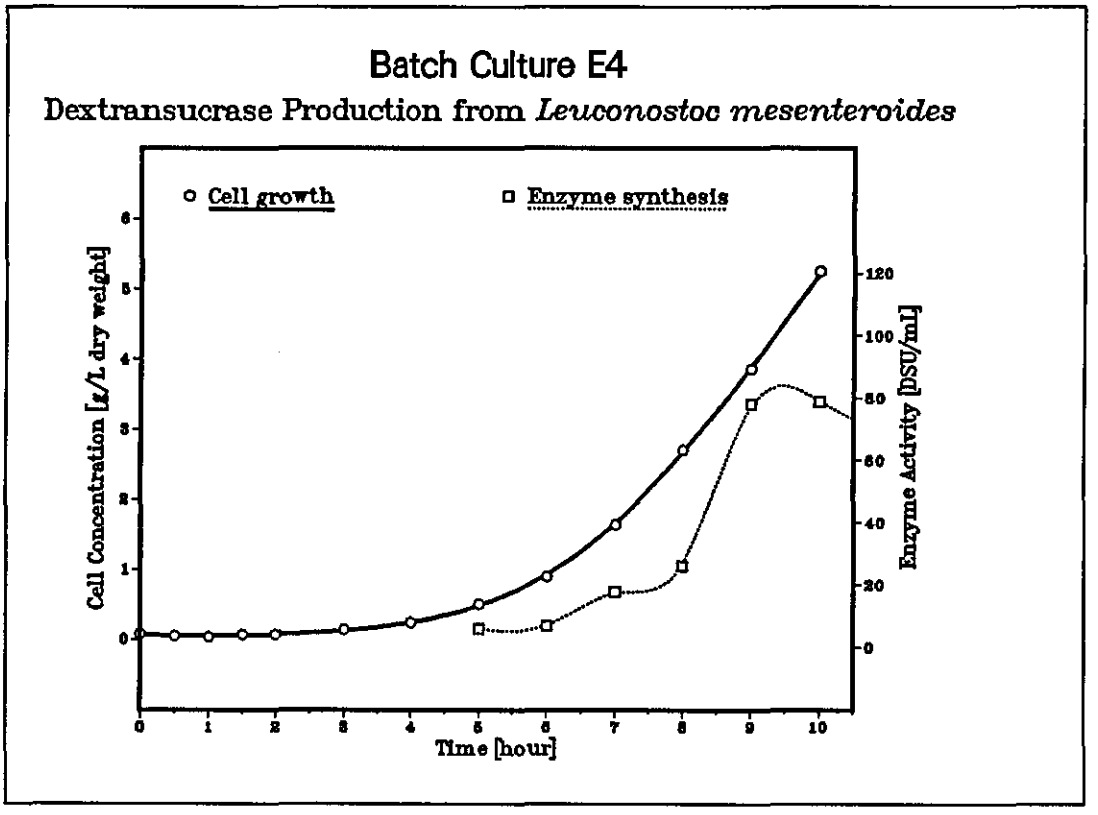

Figure K.8

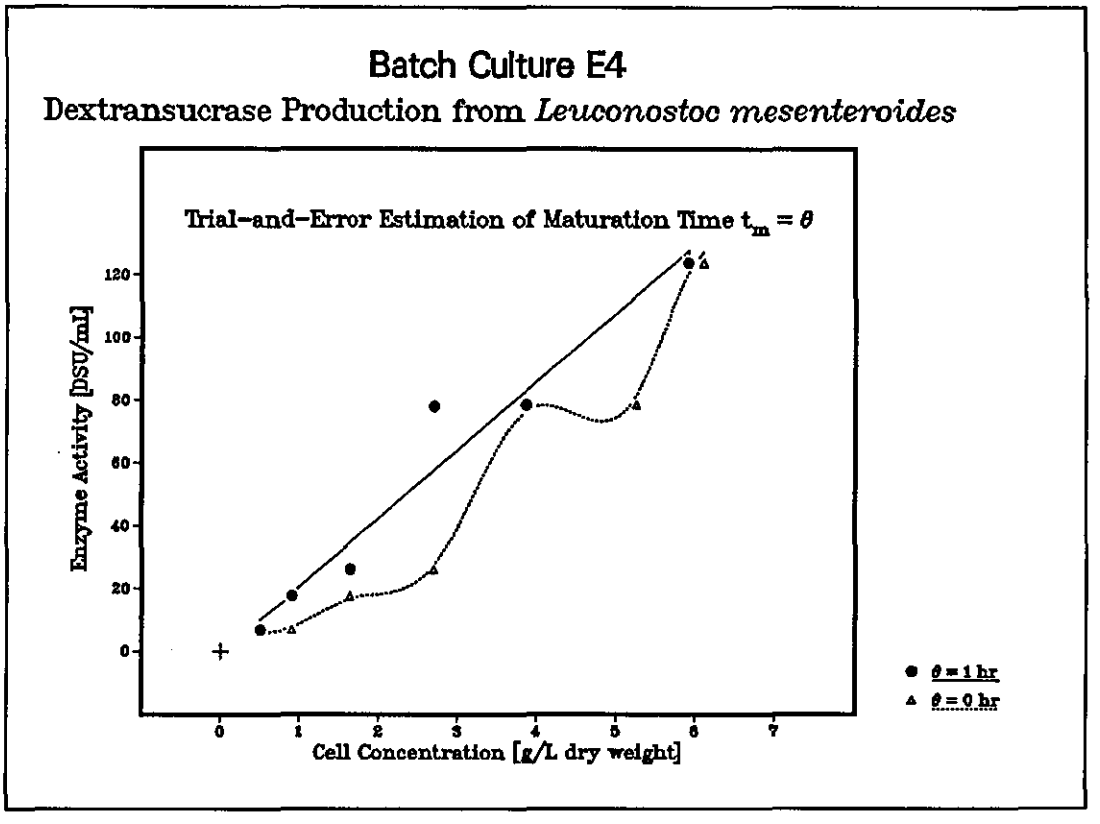

Table K.5

Dextransucrase Production in Batch Culture E5

Initial sucrose concentration = 50.00 g/L

Time (hour)	Cell Concentration (g/L dry weight)
0.00	0.0260
0.50	0.0390
1.00	0.0442
1.50	0.0364
2.00	0.0546
2.50	0.0676
3.00	0.0806
3.50	0.0936
4.00	0.1196
5.00	0.2262
6.00	0.4745
7.00	0.8190
8.00	1.4300
9.00	2.6520
9.50	3.1850
10.00	3.7960

Time (hour)	Enzyme Activity (DSU/mL
3.00	4.4260
4.00	2.8160
5.00	5.4990
6.00	6.6390
7.00	6.7060
8.00	20.9220
9.00	40.2350
10.00	78.3250
24.00	82.1470
25.00	98.5760

Figure K.9

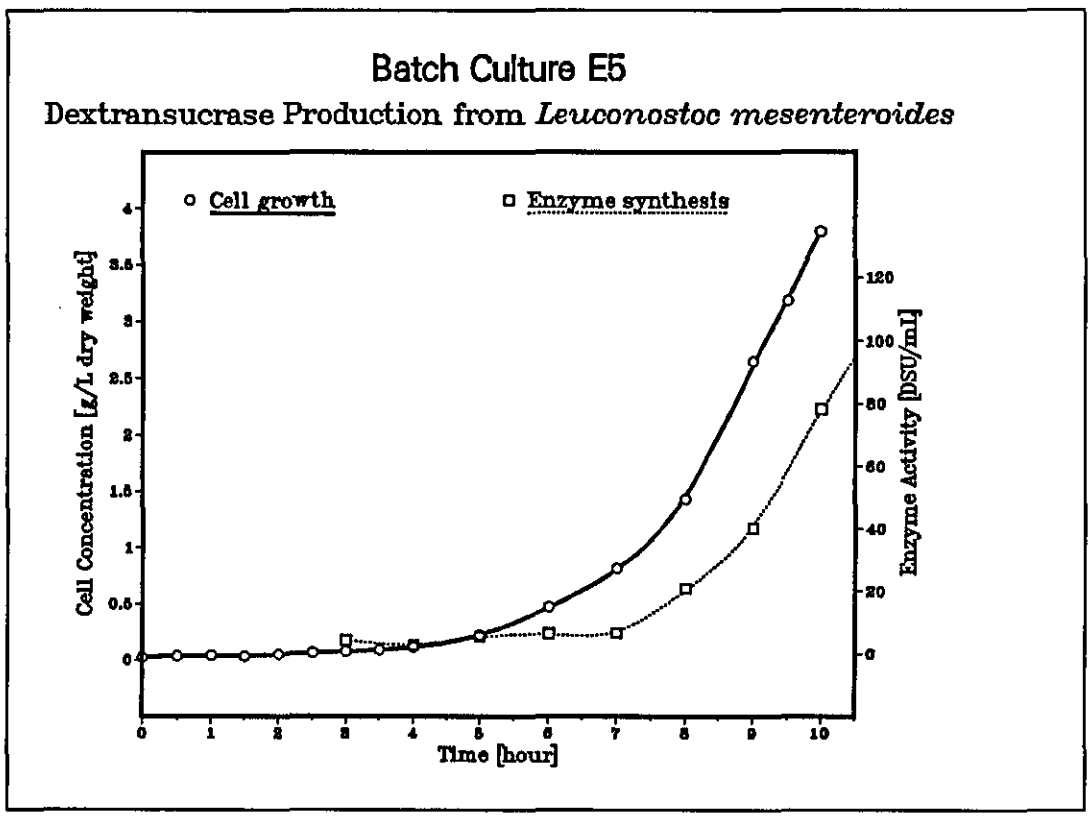

Figure K.10

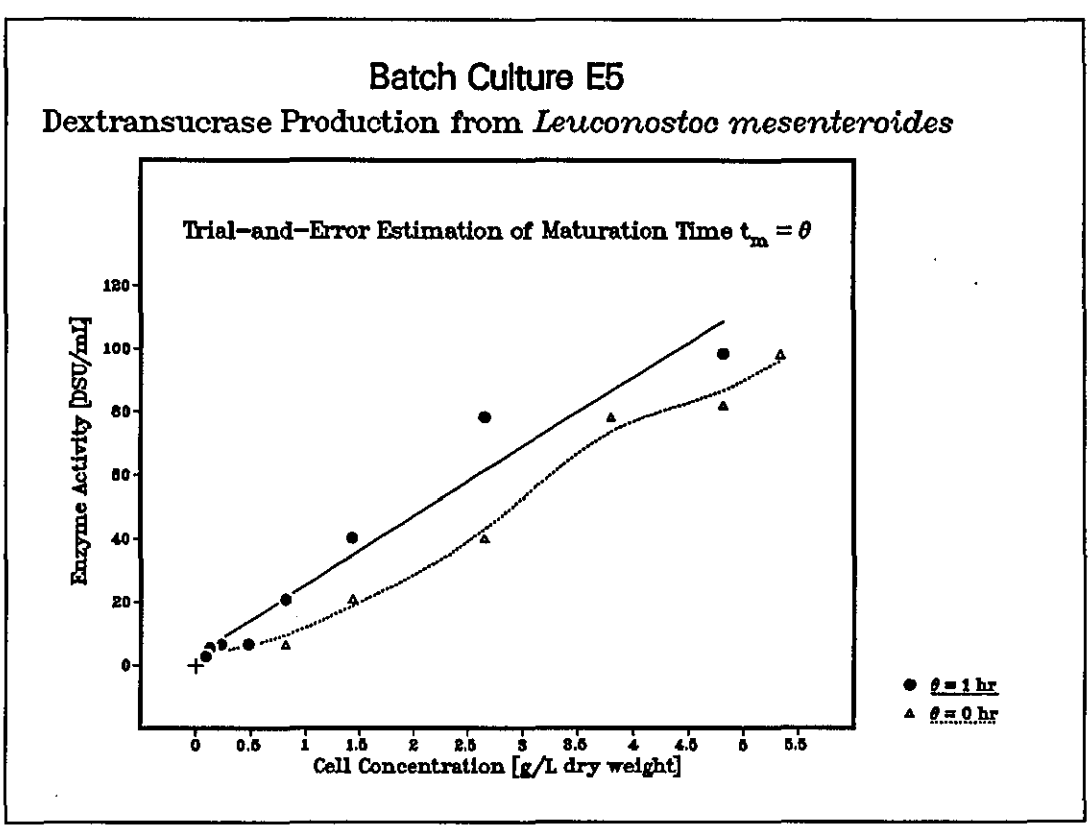

Table K.6
Enzyme Production in Batch Cultures
Analysis of Growth Associated Model

Case	Cell Concentration x (g/L dry weight)	Enzyme Activity p (DSU/mL)
1	0.5421	4.640
2	0.6084	6.840
3	0.8190	6.706
4	0.8970	6.907
5	1.0140	7.953
6	1.1752	14.686
7	1.4300	20.922
8	1.6380	17.771
9	1.7160	15.244
10	1.7940	20.215
11	1.9110	23.135
12	2.2880	29.774
13	2.6000	30.176
14	2.6208	33.802
15	2.6520	40.235
16	2.7040	26.153
17	2.7456	27.174
18	3.6036	72.907
19	3.6725	47.390
20	3.7960	78.325
21	3.8610	78.124
22	4.2120	78.541
23	4.8100	82.147
24	4.8880	66.942
25	5.2520	78.794
26	5.3300	98.576
27	5.9150	126.071
28	5.9800	96.767
29	6.1100	123.925

Correlation of x and p = 0.962

The regression equation is
p = - 13.6 + 20.3 x

Predictor	Coef	Stdev	t-ratio
Constant	-13.626	3.838	-3.55
x	20.280	1.114	18.21

s = 10.33 R-sq = 92.5% R-sq(adj) = 92.2%

Analysis of Variance

SOURCE	DF	SS	MS
Regression	1	35352	35352
Error	27	2879	107
Total	28	38231	

Unusual Observations

Obs.	x	p	Fit	Stdev.Fit	Residual	St.Resid
27	5.92	126.07	106.33	3.78	19.74	2.05R

R denotes an obs. with a large st. resid.

Confidence interval of regression coefficients

Coef	Stdev	Lo_limit	Up_limit	95% C.I.
-13.6256	3.83842	-21.5015	-5.7498	7.87586
20.2804	1.11372	17.9953	22.5656	2.28518

Table K.7
Enzyme Production in Batch Cultures
Analysis of Maturation Time Model

Case	Cell Concentration $x_{(t-1)}$ (g/L dry weight)	Enzyme Activity p_t (DSU/mL)
1	0.0806	2.816
2	0.1196	5.499
3	0.2262	6.639
4	0.3744	6.840
5	0.4576	7.953
6	0.4745	6.706
7	0.5070	6.907
8	0.6084	14.686
9	0.8190	20.922
10	0.8970	17.771
11	1.0140	15.244
12	1.1752	23.135
13	1.4300	40.235
14	1.6380	26.153
15	1.7160	27.174
16	1.7940	33.802
17	1.9110	29.774
18	2.2880	30.176
19	2.6208	72.907
20	2.6520	78.325
21	2.7040	78.124
22	2.7456	47.390
23	3.6036	78.541
24	3.6725	66.942
25	3.8610	78.794
26	4.8100	98.576
27	5.9150	123.925

Correlation of $x_{(t-1)}$ and p_t = 0.960

The regression equation is

$p_t = 21.0\ x_{(t-1)}$

Predictor	Coef	Stdev	t-ratio
Noconstant			
$x_{(t-1)}$	20.9798	0.7612	27.56

s = 9.421

Analysis of Variance

SOURCE	DF	SS	MS
Regression	1	67428	67428
Error	26	2308	89
Total	27	69735	

Unusual Observations

Obs.	$x_{(t-1)}$	p_t	Fit	Stdev.Fit	Residual	St.Resid
20	2.65	78.32	55.64	2.02	22.69	2.47R
21	2.70	78.12	56.73	2.06	21.39	2.33R
26	4.81	98.58	100.91	3.66	-2.34	-0.27 X
27	5.92	123.93	124.10	4.50	-0.17	-0.02 X

R denotes an obs. with a large st. resid.
X denotes an obs. whose $x_{(t-1)}$ value gives it large influence.

Confidence interval of regression coefficient

Coef	Stdev	Lo_limit	Up_limit	95% C.I.
20.9798	0.761151	19.4152	22.5444	1.56459

Table K.8

Analysis of Growth Associated Model

Data of McAvoy

Case	Cell Concentration x (g/L dry weight)	Enzyme Activity p (DSU/mL)
1	0.8688	6.095
2	0.9412	10.294
3	1.0136	22.800
4	1.1584	14.176
5	1.3032	24.805
6	1.3756	36.077
7	1.5928	41.510
8	1.5928	65.347
9	2.2082	40.068
10	2.3892	62.700
11	2.6064	26.989
12	3.1856	56.220
13	3.6200	77.439
14	3.7648	61.752
15	3.9096	69.230
16	4.3440	73.448
17	5.0680	123.691
18	5.2128	79.672
19	5.2128	102.037
20	6.2264	104.754
21	6.3712	93.699
22	6.5160	159.304
23	6.5160	175.149
24	6.6608	97.256
25	7.2400	110.829
26	7.2400	124.639
27	7.3848	185.255
28	7.8192	213.004
29	8.1088	110.829
30	8.3984	199.500
31	8.5432	221.095
32	8.6880	228.000
33	8.8328	216.738
34	9.1224	165.260
35	9.2672	200.705
36	9.5568	255.759
37	9.7016	197.919
38	9.8464	207.413
39	9.9912	283.874
40	10.2084	255.571
41	10.7152	250.652

Correlation of x and p = 0.935

The regression equation is
p = - 13.5 + 23.9 x

Predictor	Coef	Stdev	t-ratio
Constant	-13.457	9.436	-1.43
x	23.913	1.447	16.53

s = 29.11 R-sq = 87.5% R-sq(adj) = 87.2%

Analysis of Variance

SOURCE	DF	SS	MS
Regression	1	231441	231441
Error	39	33046	847
Total	40	264487	

Unusual Observations

Obs.	x	p	Fit	Stdev.Fit	Residual	St.Resid
29	8.1	110.83	180.45	5.71	-69.62	-2.44R
39	10.0	283.87	225.46	7.68	58.41	2.08R

R denotes an obs. with a large st. resid.

Confidence interval of regression coefficients

Coef	Stdev	Lo_limit	Up_limit	95% C.I.
-13.4567	9.43642	-32.5436	5.6302	19.0869
23.9127	1.44688	20.9861	26.8393	2.9266

Table K.9

Analysis of Maturation Time Model

Data of McAvoy

Case	Cell Concentration $x_{(t-1)}$ (g/L dry weight)	Enzyme Activity p_t (DSU/mL)
1	0.8688	10.294
2	0.9412	14.176
3	1.0136	36.077
4	1.1584	24.805
5	1.3032	41.510
6	1.3756	65.347
7	1.5928	40.068
8	1.5928	62.700
9	2.2082	56.220
10	2.3892	77.439
11	2.6064	61.752
12	3.1856	73.448
13	3.6200	102.037
14	3.7648	79.672
15	3.9096	123.691
16	4.3440	104.754
17	5.0680	175.149
18	5.2128	93.699
19	5.2128	159.304
20	6.2264	124.639
21	6.3712	97.256
22	6.5160	185.255
23	6.5160	213.004
24	6.6608	110.829
25	7.2400	110.829
26	7.2400	165.260
27	7.3848	199.500
28	7.8192	228.000
29	8.3984	221.095
30	8.5432	216.738
31	8.6880	255.759
32	9.1224	200.705
33	9.5568	283.874
34	9.9912	255.571
35	10.2084	250.652

Correlation of $x_{(t-1)}$ and p_t = 0.929

The regression equation is

$p_t = 25.2\ x_{(t-1)}$

Predictor	Coef	Stdev	t-ratio
Noconstant			
$x_{(t-1)}$	25.2269	0.8486	29.73

s = 29.50

Analysis of Variance

SOURCE	DF	SS	MS
Regression	1	769023	769023
Error	34	29589	870
Total	35	798612	

Unusual Observations

Obs.	$x_{(t-1)}$	p_t	Fit	Stdev.Fit	Residual	St.Resid
21	6.4	97.26	160.73	5.41	-63.47	-2.19R
25	7.2	110.83	182.64	6.14	-71.81	-2.49R
35	10.2	250.65	257.53	8.66	-6.87	-0.24 X

R denotes an obs. with a large st. resid.

X denotes an obs. whose $x_{(t-1)}$ value gives it large influence.

Confidence interval of regression coefficient

Coef	Stdev	Lo_limit	Up_limit	95% C.I.
25.2269	0.848633	23.5022	26.9515	1.72463

Appendix L Fed-Batch Cultivation and Simulations of Dextransucrase Production

Table L.1
Experimental Data of Enzyme Production in Fed-Batch Culture

Time (hour)	Cell Concentration (*g/L* dry weight)
0.00	0.0728
0.50	0.0728
1.00	0.0780
1.50	0.1014
2.00	0.1040
2.50	0.1300
3.00	0.1716
3.50	0.2652
4.00	0.3536
5.00	0.6240
5.50	0.9152
6.00	1.0920
6.50	1.4820
7.00	1.7550
7.50	2.1840
8.00	2.6000
8.50	3.2825
9.00	4.0950
9.50	4.7840
10.00	5.5250

Time (hour)	Enzyme Activity (DSU/mL)
3.00	4.359
5.00	10.729
6.00	12.406
7.00	26.824
8.00	42.918
9.00	62.029
10.00	77.788

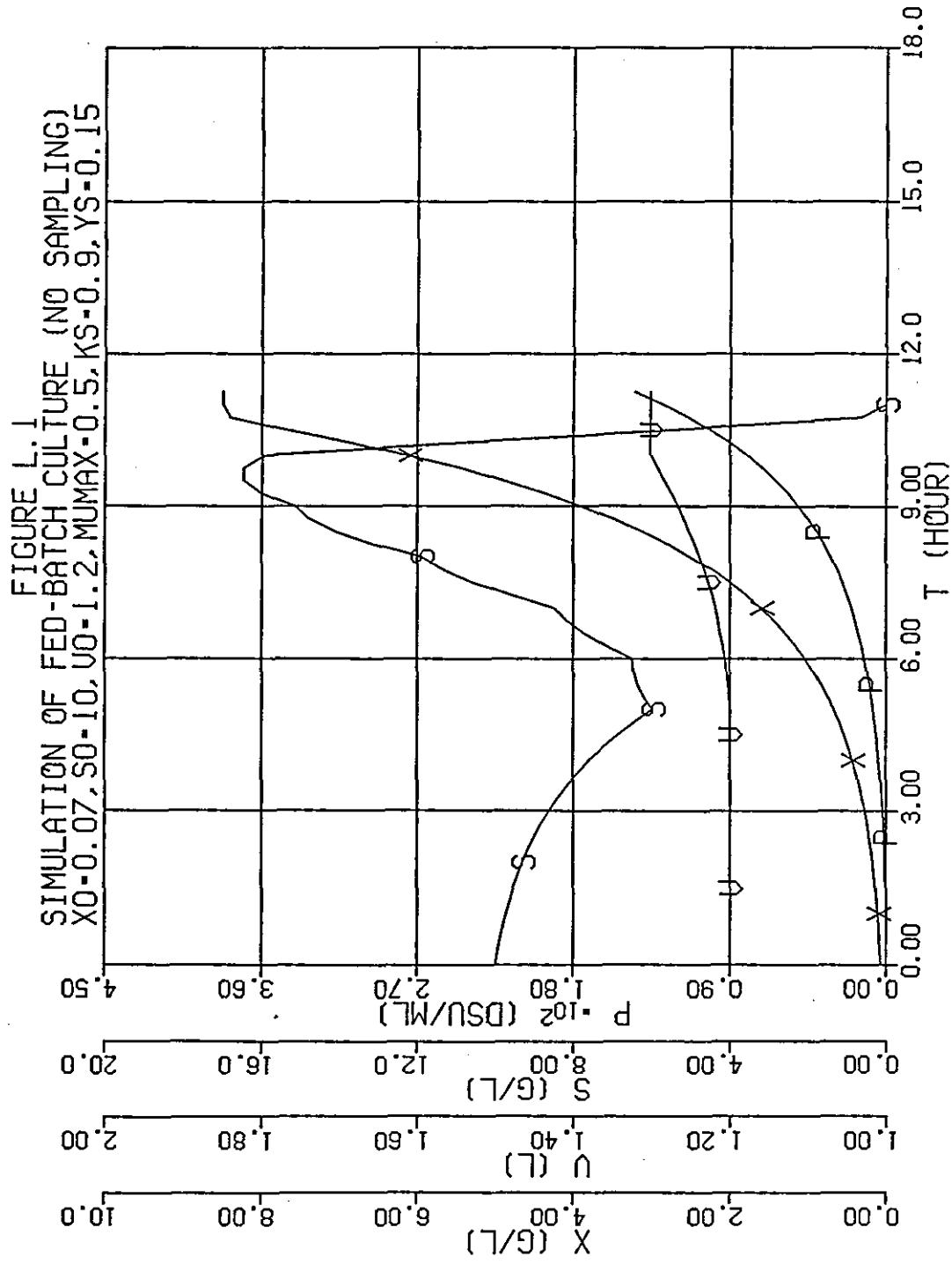
FIGURE L.1
SIMULATION OF FED-BATCH CULTURE (NO SAMPLING)
XO=0.07,SO=10,VO=1.2,MUMAX=0.5,KS=0.9,YS=0.15
T (HOUR)
0.00
3.00
6.00
9.00
12.0
15.0
18.0
P -10² (DSU/ML)
0.00
0.90
1.80
2.70
3.60
4.50
S (G/L)
0.00
4.00
8.00
12.0
16.0
20.0
V (L)
1.00
1.20
1.40
1.60
1.80
2.00
X (G/L)
0.00
2.00
4.00
6.00
8.00
10.0

FIGURE L.2
SIMULATION OF FED-BATCH CULTURE (PULSE SAMPLING)
XO-0.07, SO-10, VO-1.2, MUMAX-0.5, KS-0.9, YS-0.15

FIGURE L.3
SIMULATION OF FED-BATCH CULTURE, IMPULSE SAMPLING
X0=0.07, S0=10, V0=1.2, MUMAX=0.5, KS=0.9, YS=0.15

PLATE 1
The Microcomputer-Controlled Fermentation System

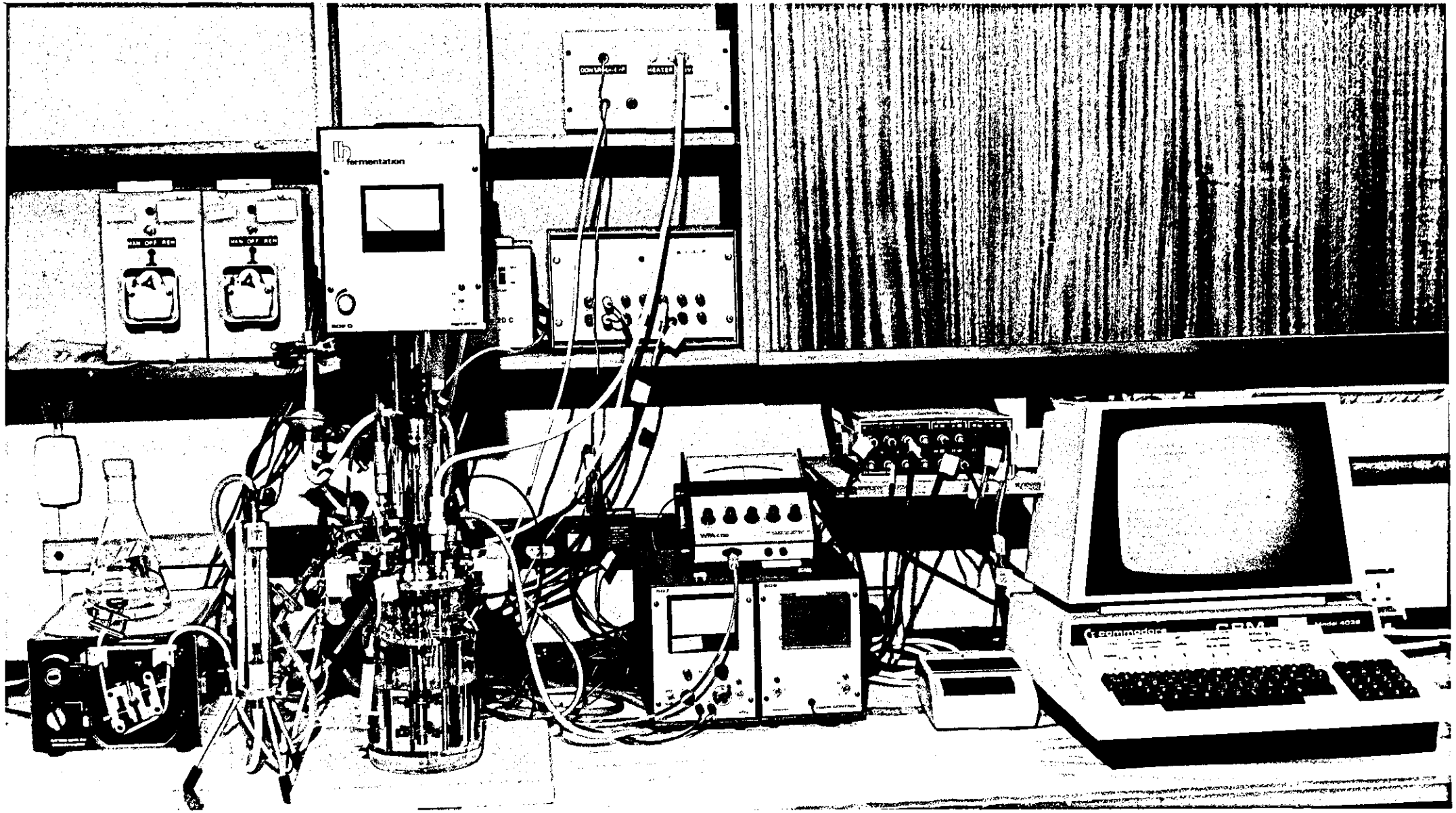
lh
fermentation
Commodore
CBM